

NOVEL DEVELOPMENT TOOLS FOR PROCESSING OF RECOMBINANT VIRUS-LIKE PARTICLES

zur Erlangung des akademischen Grades eines
DOKTORS DER INGENIEURWISSENSCHAFTEN (Dr.-Ing.)

der Fakultät für Chemieingenieurwesen und Verfahrenstechnik des
Karlsruher Instituts für Technologie (KIT)
vorgelegte

genehmigte
DISSERTATION

von
Dipl.-Ing. Christopher Ladd Effio
aus Lima (Peru)

Referent: Prof. Dr. Jürgen Hubbuch
Korreferent: Prof. Dr.-Ing. Udo Reichl
Tag der mündlichen Prüfung: 05.02.2016

Acknowledgments

With all my heart I want to thank the following people who supported me in realizing this project:

- My doctoral advisor Prof. Dr. Jürgen Hubbuch for mentoring, pushing, hiring and inspiring me during the last years. His great lectures literally forced me into joining our Biomolecular Separation Engineering group and it was him who raised my interest in high-throughput screening and virus-like particles. With great discussions, his open mind, his support for conference participations as well as academic and industrial collaborations, he allowed me to expand my horizon and to develop project ideas and this thesis. Thank you for giving me this great opportunity to work as a PhD student in your group.
- Prof. Dr.-Ing. Udo Reichl for being the second referee of my thesis, for taking the long way from Magdeburg to Karlsruhe for my dissertation defense, for giving me the opportunity to give my first conference talk (ENVVP2013) and for great discussions on virus-like particle vaccines.
- Dr.-Ing. Stefan Oelmeier for introducing me to high-throughput experimentation, aqueous two-phase extraction and scientific writing, presenting and working. Without your support and mentoring skills this thesis would probably not exist.
- All project members for their material, financial and scientific support. My special thanks go to Prof Dr. Anton Middelberg for introducing me to the world of virus-like particles and giving me the great opportunity to visit his group in Brisbane. Dr. Heike Schwarz, Dr. Richard Kneusel and Dr. Iris Asen from Diarect for their support on insect cells, parvo-VLPs and inviting me to Freiburg, Kim Erickson and Prof Dr. Robert Garcea from the University of Colorado for their help with protein expression in *E.coli*, Dr. Louis Villain, Katrin Töppner and Dr. Martin Leuthold from Sartorius for their support on membrane chromatography, Dr. Mike Kosinski and Dr. Marc Wenger from Merck for providing information on HPV and inviting me to Philadelphia.
- All members of the Biomolecular Separation Engineering group for the great time, scientific support and so many funny activities (kayaking, sledging, climbing, soccer, handball, etc.). My special thanks go to Dr.-Ing. Tobias Hahn for having enough patience and energy to introduce me to chromatography modeling and his software ChromX, Dr.-Ing. Pascal Baumann for setting up our microbiology laboratory, allowing me to work with frightening virus proteins and for collaborating on a great *E.coli* project. In addition, I would like to thank my colleagues Dipl.-Ing. Frank Hämmerling, Dr.-Ing. Kai Baumgartner and Dr.-Ing Ertan Akgün for having become great friends and for delighting my time in Karlsruhe in the last years.

-
- My students Ozan Ötes, Lukas Wenger, Philipp Vormittag, Sebastian Andris, Claudia Weigel, Julia Seiler, Hannah Brück, Lara Wehrle, Wolfgang Nguyen, Dominik Hümmer and Jan Tobias Weggen for their outstanding work and contributions to this thesis.
 - My parents, brothers, grandparents and friends for believing in me and for supporting me throughout my whole life. Special thanks go to my mother for investing so much of her time and love in me, for pushing and helping me at school and registering me at the soccer team TSG Hechtsheim. Furthermore, I thank my best friends Emrah Karakaya, Sven Sonnack and Farshid Farmandeh who were always there when I needed them and who share my childish sense of humour.
 - The most important person in my life: my wife. Without you, none of this would have been possible. You have supported me when no one else was around, when I again overburdened myself with work, when I failed and when I succeeded, when I needed a timeout and when I needed someone to discuss my (outstanding and revolutionary J) scientific results. Thank you for your endless love and for believing in me. Birgit, you are the best thing that ever happened to me. I love you.

“It’s not what you look at that matters,
it’s what you see.”

-Henry David Thoreau

Abstract

Numerous human drugs have emerged over the last decades by the implementation of biopharmaceutical manufacturing processes. Continuous improvements and innovations in genetic, biomolecular and bioprocess engineering have created versatile prospects for pharmaceutical drug design. Biopharmaceutical processes utilizing recombinant DNA technology have evolved from the production of comparably small biomolecules (antibiotics, hormones, enzymes) into manufacturing of large biomolecules (monoclonal antibodies, virus-like particles, nucleic acids) allowing treatment of cancer as well as infectious, autoimmune and cardiovascular diseases. However, the production in genetically modified organisms requires a long and complex process chain of upstream processing (USP), downstream processing (DSP) and formulation of the desired target molecule. During USP, the biomolecules are produced in bioreactors and are subsequently purified during DSP to remove undesired process- and product-related impurities that might impact drug safety and efficacy. It is evident that an increasing complexity and size of target molecules challenges the design of biopharmaceutical processes. Hence, the scope of this doctoral thesis was to develop novel systematic procedures for the process design of large biomolecular entities. Apart from monoclonal antibodies (mAbs) another fast growing class of biologics represented the key issue of this work: recombinant protein-based virus-like particles (VLPs).

VLPs are highly ordered protein assemblages covering a size range of 20-200 nm. Due to their pathogen-associated molecular patterns and the lack of viral nucleic acids, VLPs represent promising bionanoparticles for vaccine applications, generating new prospects for untreated infectious diseases and emerging pandemic threats. An increasing multitude of VLPs have been developed in different recombinant production systems and were approved for vaccination against cervical cancer, hepatitis B, hepatitis E and malaria. Novel VLP structures and vaccine candidates in clinical studies were reviewed in the first section of this doctoral thesis highlighting current trends, process limitations and state-of-the-art unit operations for purification. With regard to an economic and rapid process, aqueous two-phase extraction (ATPE), precipitation and membrane chromatography were identified as promising DSP unit operations for VLPs. For rapid and robust process development, high-throughput experimentation (HTE) and mechanistic modeling approaches were implemented and applied for industrially relevant biological feedstocks. In general, this doctoral thesis is divided into four major topics aiming at accelerating, innovating and intensifying processing of VLPs. Whereas the first section focuses on the development of HTE-based proceedings for low-cost and rapid VLP processes, the second approach deals with the *in silico* design of a membrane process, the third section covers the HTE-based development of an alternative VLP upstream process and the last section concludes with the development of a high-throughput (HT) assay for the characterization of VLPs.

The evaluation of ATPE for mAbs and VLPs is the first central topic of this thesis. Characterization of polyethylene glycol (PEG)-salt aqueous two-phase systems (ATPSs) and partitioning studies were realized by automated screenings on a robotic liquid handling station. HT-compatible analytics were conducted in microtiter plates by implementing an ultra-high performance liquid chromatography (UHPLC) method and automated protein and DNA assays. More than twenty PEG-salt ATPS phase diagrams were generated

and a variety of system compositions were screened and ranked for mAbs and VLPs in terms of attained recovery, capacity and purity. The ultimate goals were to elucidate optimal design spaces and critical process attributes of an ATPS capture step. The molecular weight of PEG, the pH value and the salt type were identified as main parameters affecting the partitioning of mAbs and VLPs. In order to gain a more profound process understanding, the partitioning patterns were successfully correlated with solubility curves for mAbs, VLPs and host-cell proteins (HCPs) indicating that the distribution was primarily dictated by solubility limitations in ATPS phases. Hence, a systematic solubility-guided screening procedure was followed for the design of ATPS processes. Case studies for several human IgG1 antibodies derived from Chinese hamster ovary (CHO) cells and human B19 parvovirus-like particles derived from *Spodoptera frugiperda* insect cells highlighted the benefit of the solubility-guided HTS-based approach. The proposed capture steps for mAbs and VLPs allowed high loading capacities in the ATPS top phases approaching capacities of chromatographic stationary phases. Regarding VLP purification, the developed process incorporated clearance of cell debris and host-cell DNA while concentrating VLPs in the top phase.

For further optimization of the separation efficiency by ATPE, centrifugal partition chromatography (CPC) was assessed as scalable multi-stage extraction method. A 'Design of Experiments' (DoE) approach was applied for determining the effect of operating and system conditions on the separation of VLPs and mAbs from HCPs. Low flow rates and elevated rotation speeds lead to an increased resolution of target and contaminant components. These findings were successfully correlated with the retention of stationary phase in the CPC. Optimum operating conditions and ATPS compositions were identified for both mAbs and VLPs demonstrating the general feasibility of the CPC technology for purification of biopharmaceuticals. An operation procedure referred to as 'Dual Mode' revealed the best process performance for mAbs by stripping HCPs through inversion of mobile and stationary phases during the run.

In order to meet required purity levels for biopharmaceuticals with more simple purification procedures, alternative two step processes incorporating a combination of ATPE and precipitation were developed for mAbs and VLPs demanding only minimal investments for hardware. Process integration of a single-stage PEG-salt ATPE in accordance with subsequent steps was pursued by precipitation of target molecules from ATPS top phases. For process development, a HTS method was established allowing miniaturized and automated precipitation, solid-liquid separation and resolubilization of biomolecules. Hence, straightforward non-chromatographic downstream processes for mAbs and VLPs were designed by HTE obtaining protein purities in the range of 90 to 98%. In particular, the demonstrated orthogonal separation mechanisms of ATPE and precipitation depicted important findings. Whereas cell debris and host cell DNA were cleared from VLP feedstocks by ATPE, HCPs were depleted by precipitating VLPs with PEG. Results by Fourier transform infrared spectroscopy (FTIR) for mAbs and transmission electron microscopy (TEM) as well as immuno dot blots for VLPs confirmed the preservation of the native protein and particle structure of processed target substances.

The focus of the second topic of this thesis lies on the implementation of a process model for membrane adsorbers allowing *in silico* design of VLP purification procedures with minimal experimental effort. The scope of this approach was to develop a bind-and-elute anion-exchange membrane chromatography step for the isolation of human B19 parvovi-

rus VLPs from a complex insect cell lysate. Hydrodynamic mass transfer in a spiral wound membrane module was modeled using a lumped rate model adapted to radial flow. Modeling of ion-exchange for the complex VLP feedstock was performed with a scaled steric mass action model using UV absorption-based modeling. All process model equations were integrated in the in-house chromatography software package ChromX. The software allowed automation of model parameter estimations and of process optimizations based on evolutionary algorithms. For process simulations the feedstock was virtually split into 17 subcomponents. Model parameters were estimated for each subcomponent based on experimental calibration runs and utilized to generate a design space and process solution for maximum product recovery and purity in a simple salt step elution procedure. Binding conditions for VLPs were optimized by HTE-based approaches using DoE and micro-scale membrane formats. The hybrid approach of HTE and mechanistic modeling resulted in a membrane process with a high dynamic binding capacity and purity.

Major obstacles impairing the performance of VLP processes are the large size and complexity of the bionanoparticles. A method to avoid upstream and downstream processing of such large particles is the production of VLP subunits. The murine polyomavirus (MuPyV) protein VP1 is a capsid protein capable of forming VLPs by *in vitro* self-assembly under controlled buffer conditions. MuPyV VLPs have been evaluated in multiple pre-clinical studies for generation of tailored chimeric vaccines presenting surface-exposed foreign antigenic epitopes. The third section of this thesis deals with the HTE-based optimization of an alternative low-cost microbial production platform for MuPyV VLPs. The development approach included codon optimization of the VP1 insert, strain and vector selection, miniaturized upstream development, HT cell lysis and HT-compatible analytics by capillary gel electrophoresis. During micro-scale cultivations in 48-well format the temperature, shaker speed, pH value and induction conditions were varied according to a DoE set-up. Obtained product titers for the optimum conditions exceeded all so far reported VLP yields at shaker flask scale and reached the highest levels at the optimum growth temperature for *E.coli* (37 °C), decreased pH (pH 6), and low oxygen supply at a shaker speed of 600 rpm. In addition, a scalable purification procedure based on membrane chromatography and size-exclusion chromatography was suggested with a final *in vitro* assembly step creating homogeneous spherical bionanoparticles. In summary, the developed alternative production process comprises a promising and industrially feasible option for tailored VLP vaccines.

The last section of this thesis focuses predominantly on the development of a rapid and generic characterization method for VLPs. Therefore, different commercial size-exclusion chromatography columns were evaluated on a UHPLC system for the separation of VLPs and VLP aggregates. Subsequent to the identification of a promising chromatographic support, the method was accelerated by performing interlaced sample injections. This procedure allowed the establishment of a VLP characterization method with a throughput of 20 samples per hour outperforming traditional analytical VLP methods with one or two samples per hour. The developed assay was successfully applied for the characterization of five VLP vaccine candidates including human papillomavirus (HPV) VLPs, human enterovirus 71 (EV71) VLPs, MuPyV VLPs, human B19 parvovirus VLPs, and chimeric hepatitis B core antigen (HBcAg) VLPs. This highlights the generic applicability of the assay for VLPs. The method was furthermore supported and complemented by dynamic light scattering and TEM measurements. In order to deploy the analytical tool

for HTE case studies, the assay was used to track VLP aggregates during downstream processing and stability studies.

In summary, the HTE methods and process models established in this doctoral thesis represent novel powerful tools for the design of VLP processes and have laid the foundation for an improved understanding and control of the applied unit operations.

Zusammenfassung

In den vergangenen Jahrzehnten wurden weltweit zunehmend mehr Arzneimittel auf Basis von biopharmazeutischen Herstellungsverfahren entwickelt und produziert. Die großtechnische Produktion neuartiger biopharmazeutischer Wirkstoffe beruht dabei vor allem auf Fortschritten in der Entwicklung und Optimierung gentechnischer, molekularbiologischer und verfahrenstechnischer Methoden. Biopharmazeutische Herstellprozesse beschränkten sich in der Vergangenheit zunächst noch auf vergleichsweise kleine Biomoleküle wie Antibiotika, Hormone oder Enzyme. Heutzutage werden rekombinante DNA-Techniken auch zur Produktion großer Biomoleküle wie monoklonaler Antikörper, Virus-ähnlicher Partikel oder Nukleinsäuren eingesetzt. Hierdurch sind unter anderem neue Möglichkeiten zur Therapie und Prävention von Krebs, Infektionskrankheiten, Autoimmunerkrankungen und Herz-Kreislauf-Erkrankungen entstanden. Die Wirkstoffproduktion in gentechnisch veränderten Organismen erfordert jedoch eine lange und komplexe Prozesskette von Kultivierungsverfahren (Upstream Processing), Aufarbeitungs- (Downstream Processing) und Formulierungsschritten bis zum fertigen Produkt. Die Herstellung von Biomolekülen wird über die Kultivierung gentechnisch veränderter Expressionswirte in Bioreaktoren realisiert. Im Anschluss daran werden bei der Aufarbeitung unerwünschte prozess- und produktbedingte Verunreinigungen abgetrennt, die die Arzneimittelsicherheit und Wirksamkeit beeinträchtigen können. Es ist offensichtlich, dass eine zunehmende Komplexität und Größe von Biomolekülen die Auslegung biopharmazeutischer Prozesse zusätzlich erschwert. Das Ziel der vorliegenden Dissertation war es daher die Entwicklung neuer systematischer Verfahren für die Prozessauslegung großer Biomoleküle voranzutreiben. Neben der Betrachtung monoklonaler Antikörper (*engl.* monoclonal antibodies (mAbs)) lag der Fokus dabei vor allem auf einer zunehmend wichtiger werdenden biopharmazeutischen Produktklasse: Virus-ähnliche Partikel (*engl.* virus-like particles (VLPs)).

VLPs sind hochorganisierte Bionanopartikel im Größenbereich von 20-200 nm, die sich aus einer Vielzahl von Proteinuntereinheiten zusammensetzen. Aufgrund ihrer pathogen-assoziierten Struktur und fehlender viraler Nukleinsäuren stellen die Partikel eine vielversprechende Alternative für Impfstoffanwendungen dar. Hierdurch entstehen neue Möglichkeiten für die Prävention bislang nicht oder nur schwer therapierbarer Infektionserkrankungen wie Ebola, HIV oder Malaria. In den letzten Jahren wurde eine Vielzahl an VLP-Strukturen in verschiedenen rekombinanten Systemen hergestellt und teilweise bereits in Vakzinformulierungen zugelassen. Impfstoffe gegen Gebärmutterhalskrebs, Hepatitis B, Hepatitis E und Malaria basieren beispielsweise auf pathogen-assoziierten VLPs. Im ersten Abschnitt der vorliegenden Dissertation wurden neuartige VLPs und VLPs in klinischen Studien genauer betrachtet und aktuelle Trends, Prozesslimitierungen und Verfahrensschritte für die Aufarbeitung von VLPs evaluiert. Dabei wurden die wässrige Zweiphasenextraktion, Präzipitation sowie Membranchromatographie als vielversprechende Verfahren für kostengünstige und schnelle VLP- Prozesse ausgemacht. Für eine schnelle und robuste Prozessentwicklung wurden zwei verschiedene Ansätze implementiert und für industriell relevante biopharmazeutische Produkte angewandt: Hochdurchsatz-Experimente (HTE) sowie die mechanistische Prozessmodellierung.

Die vorliegende Dissertation ist in vier Themenbereiche untergliedert, die darauf abzielen die Prozessierung von VLPs zu beschleunigen, zu intensivieren und innovative Lösungsansätze zu generieren. Im ersten Teil der Arbeit liegt der Fokus auf der Entwick-

lung von HTE-basierten Ansätzen für kostengünstige und schnelle VLP-Aufarbeitungsprozesse. Im zweiten Themenbereich wird die Implementierung mechanistischer Modelle zur *in silico* Auslegung von Membranverfahren für VLPs behandelt. In den letzten beiden Kapiteln werden neuentwickelte Methoden für einen alternativen VLP-Herstellprozess und eine Hochdurchsatz-kompatible Analytikmethode für die Charakterisierung von VLPs vorgestellt.

Das erste zentrale Thema der Dissertation ist die Evaluierung der wässrigen Zweiphasenextraktion für die Aufarbeitung von mAbs und VLPs. Die Charakterisierung von Polyethylenglykol (PEG)-Salz-Systemen sowie Verteilungsstudien wurden hierfür über automatisierte Screenings auf einer Pipettierroboterplattform realisiert. Hochdurchsatzkompatible analytische Verfahren wurden im Mikrotiterplatten-Maßstab durchgeführt. Dabei kamen sowohl Ultra-Hochleistungsflüssigkeitschromatographie (UHPLC)-Methoden als auch automatisierte farbstoffbasierte Methoden für die Gesamtprotein- sowie DNA-Quantifizierung zum Einsatz. Mehr als zwanzig Phasendiagramme für PEG-Salz-basierte wässrige Zweiphasensysteme wurden generiert und eine Vielzahl von Systemzusammensetzungen wurde für die Aufarbeitung von mAbs und VLPs evaluiert. Die Hauptkriterien bei der Auswahl geeigneter Systemzusammensetzungen waren die Ausbeute, Kapazität und Reinheit. Im Vordergrund standen bei der Prozessentwicklung vor allem die Auslegung optimaler Prozessfenster sowie die Identifizierung kritischer Prozessattribute bei der wässrigen Zweiphasenextraktion. Die Hauptparameter, die die Verteilung von mAbs sowie VLPs in wässrigen Zweiphasensystemen beeinflussten, waren das Molekulargewicht des eingesetzten Polymers, der pH-Wert sowie die Salzart. Um ein fundierteres Prozessverständnis zu generieren, wurden die erhaltenen Verteilungsmuster mit Löslichkeitskurven für mAbs, VLPs und Wirtszellproteine (HCPs) korreliert. Die Ergebnisse zeigten deutlich, dass die Verteilung hauptsächlich durch Löslichkeitsgrenzen in den ATPS-Phasen bestimmt wurde. Über ein löslichkeitsbasiertes Screening-Verfahren konnte die Zusammensetzung der wässrigen Zweiphasensysteme daher so optimiert werden, dass in den Oberphasen für mAbs und VLPs sehr hohe Kapazitäten in der Nähe von Bindekapazitäten von Chromatographiematerialien erreicht wurden. Bei der wässrigen Zweiphasenextraktion der VLPs konnten ein Großteil der Zellbruchstücke und Wirtszell-DNA abgetrennt und die VLPs in der Oberphase konzentriert werden.

Eine weitere Optimierung der wässrigen Zweiphasenextraktion wurde über mehrstufige Extraktionen mit Hilfe der zentrifugalen Verteilungschromatographie (*engl.* centrifugal partition chromatography (CPC)) evaluiert. Der Einfluss von Betriebs- sowie Systemparametern auf die Trennung von VLPs und mAbs von HCPs wurde über einen Design of Experiments (DoE) Ansatz untersucht. Dabei wurde festgestellt, dass geringe Flussraten und erhöhte Rotordrehzahlen zu einer verbesserten Trennung von Zielkomponenten und HCPs führten. Die Ergebnisse konnten erfolgreich mit der Retention der stationären Phase in der CPC korreliert werden. Sowohl für mAbs als auch für VLPs wurden optimale Betriebsbedingungen und Zusammensetzungen der wässrigen Zweiphasensysteme entwickelt, die zeigten, dass es sich bei der CPC-Technologie um eine vielversprechende Aufarbeitungsmethode für Biopharmazeutika handelt. Vor allem die Anwendung der 'Dual Mode'-Verfahrensweise, bei der HCPs über den Wechsel von mobiler und stationärer Phase abgereichert wurden, führte bei der Aufarbeitung von mAbs zu der höchsten Reinheit. Um die regulatorischen Reinheitsvorgaben für Biopharmazeutika wie mAbs und VLPs mit möglichst einfachen Prozessen und minimalen Investitionskosten zu erfüllen,

wurde ein zweistufiges Verfahrenskonzept entwickelt. Die Prozessintegration eines Extraktionsschrittes sollte hierfür über die Präzipitation der Zielmoleküle aus der Oberphase umgesetzt werden. Für die Prozessentwicklung wurde eine HTE-basierte Methode entworfen, mit der miniaturisierte und automatisierte Fällungen mit gekoppelter Fest-Flüssig-Trennung und Wiederauflösung präzipitierter Biomoleküle untersucht werden sollten. Die Methodik ermöglichte eine schnelle Entwicklung nicht-chromatographischer hochselektiver Reinigungsprozesse für VLPs sowie mAbs mit erzielten Proteinreinheiten von 90 bis 98%. Insbesondere die gezeigte Orthogonalität der Trennmechanismen der wässrigen Zweiphasenextraktion und Präzipitation stellt eine wichtige Erkenntnis der Arbeit dar. Während Zellbruchstücke und Wirtszell-DNA primär im ersten Verfahrensschritt über die wässrige Zweiphasenextraktion abgetrennt wurden, wurde die Abreicherung von HCPs vor allem über die Präzipitation der VLPs mit PEG erreicht. Untersuchungen basierend auf der Fourier-Transformations-Infrarotspektroskopie (FTIR) für mAbs und der Transmissionselektronenmikroskopie (TEM) sowie Immunoblot-Analyse für VLPs bestätigten in beiden Fällen den Erhalt der nativen Struktur der Zielmoleküle.

Der Schwerpunkt des zweiten Themenbereichs der Arbeit ist die Implementierung eines Prozessmodells für Membranadsorber, das die *in silico* Auslegung chromatographischer Aufbereitungsverfahren für VLPs mit minimalem experimentellen Aufwand ermöglichen soll. Ziel hierbei war die Entwicklung eines Chromatographieverfahrens für die Bindung und Elution humaner Parvovirus B19 VLPs aus einem Insektenzelllysate mittels Anionenaustauscher-Membranadsorbern. Der hydrodynamische Stofftransport in einem spiralförmig gewundenen Membranadsorbermodul wurde unter Verwendung des 'Lumped Rate'-Modells bei radialer Anströmung modelliert. Für die Modellierung der Stofftransportvorgänge von Komponenten aus einem komplexen *Spodoptera frugiperda* Lysat war es notwendig die Modellgleichungen mit UV-Absorptionskoeffizienten so zu modifizieren, dass Berechnungen auf Basis von UV-Signalen möglich wurden. Für die Beschreibung der Adsorption und Desorption über Ionenaustauschvorgänge wurde das Steric-Mass-Action-Modell verwendet. Alle Modellgleichungen wurden in die am Lehrstuhl entwickelte Chromatographiesoftware ChromX integriert. Die Software ermöglicht die automatisierte Schätzung von Modellparametern und optimalen Prozessbedingungen basierend auf genetischen Algorithmen. Für Prozesssimulationen wurde das Ausgangsmaterial basierend auf dem Elutionsverhalten einzelner Spezies in 17 Komponentengruppen unterteilt. Für jede Teilkomponente wurden basierend auf experimentellen Kalibrierungsläufen die Modellparameter geschätzt und im Anschluss verwendet, um Prozessfenster und Lösungen für eine maximale Produktausbeute und Reinheit bei einer stufenweisen Salzelution zu generieren. Bindungsbedingungen für VLPs wurden durch HTE-basierte Ansätze mittels DoE und miniaturisierten Membranformaten optimiert. Der kombinatorische Ansatz von HTE und mechanistischer Prozessmodellierung ermöglichte es in kurzer Zeit und mit minimalem Probenverbrauch einen Membranprozess mit hohen dynamischen Bindekapazitäten und Produktreinheiten auszulegen.

Die Effizienz von VLP-Prozessen wird im Wesentlichen von der Größe und Komplexität der Partikel beeinflusst. Die Produktion von VLP-Untereinheiten stellt einen Ansatz dar, bei dem statt ganzen Partikel einzelne Virusproteine prozessiert werden. Zum Ende des Prozesses hin können die Virusproteine unter definierten Pufferbedingungen dann zu VLPs zusammengebaut werden. Eine vielversprechende VLP-Plattform, die in mehreren präklinischen Studien zur Erzeugung maßgeschneiderter chimärer Impfstoffe

verwendet wurde, ist die Herstellung von murinen Polyomavirus (MuPyV) VLPs. Der dritte Teil dieser Arbeit beschäftigt sich mit der HTE-basierten Optimierung einer alternativen mikrobiellen Produktionsplattform für MuPyV VLPs. Der Entwicklungsansatz umfasste dabei die Codon-Optimierung der Gensequenz des Haupt-Kapsidproteins VP1, die Stamm- und Vektorauswahl, miniaturisierte Kultivierungsexperimente, eine Hochdurchsatz-Zellaufschlussmethode und eine Hochdurchsatz-Analytik mittels Kapillar-Gelelektrophorese. In miniaturisierten Kultivierungsversuchen im 48-Well Format wurden die Temperatur, die Schüttelgeschwindigkeit, der pH-Wert und die Induktionsbedingungen mittels DoE-Ansatz variiert. Die erzielten Produkttiter für die optimalen Expressionsbedingungen übertrafen alle bislang veröffentlichten VLP-Ausbeuten im Schüttelkolbenmaßstab und waren bei der optimalen Wachstumstemperatur für *E. coli* (37°C), einem leicht sauren pH-Wert (pH 6) und einem geringen Sauerstoffeintrag bei einer Schüttlergeschwindigkeit von 600 rpm am höchsten. Nach der Optimierung der Expressionsbedingungen wurde zudem ein Prozess zur Aufarbeitung der Virusproteine entwickelt. Für die Herstellung homogener, kugelförmiger Partikel wurden die Virusproteine zunächst per Membranchromatographie und Größenausschlusschromatographie aufgereinigt und anschließend per *in vitro* Assemblierung zu VLPs zusammengelagert. Insgesamt konnte somit eine vielversprechende und industriell anwendbare Prozessalternative für neuartige VLP-Produkte entwickelt werden.

Der letzte Teil dieser Arbeit konzentriert sich hauptsächlich auf die Entwicklung einer schnellen und generischen Methode zur Qualitätskontrolle von VLPs. Hierfür wurden an einem UHPLC-System verschiedene analytische Größenausschlusschromatographie-Säulen im Hinblick auf die Trennleistung von VLPs und VLP-Aggregaten evaluiert. Die Analysezeit für die vielversprechendste analytische Säule konnte über vorgeschaltete (*engl.* interlaced) Probeninjektionen drastisch verkürzt werden. Dadurch wurde ein analytischer Durchsatz für die Charakterisierung von VLPs mit bis zu 20 Probeninjektionen pro Stunde erreicht. Die entwickelte Methode wurde erfolgreich zur Charakterisierung von fünf VLP-Impfstoff-Kandidaten einschließlich humaner Papillomavirus (HPV) VLPs, humaner Enterovirus 71 (EV71) VLPs, MuPyV VLPs, humaner Parvovirus B19 VLPs und chimärer Hepatitis-B-Core-Antigen (HBcAg) VLPs eingesetzt. Dies unterstreicht die generische Anwendbarkeit der Methode für VLPs. Die Methode wurde weiterhin durch dynamische Lichtstreuungs- und TEM-Messungen gestützt und ergänzt. Die Anwendung in zwei HTE-Fallstudien zeigte, dass mit der Methode VLP-Aggregate während der Entwicklung von Aufarbeitungsprozessen und in Stabilitätsstudien nachverfolgt werden konnten. Zusammenfassend stellen die in dieser Doktorarbeit etablierten Hochdurchsatzmethoden und Modelle neue und wichtige Werkzeuge für die Auslegung von VLP-Prozessen dar und tragen zudem zu einem besseren Prozessverständnis bei.

Contents

1	Introduction	15
1.1	Virus-like Particles (VLPs)	16
1.1.1	Structure of VLPs	16
1.1.2	Bioengineering of VLPs	17
1.1.3	Manufacturing of VLPs	20
1.2	Downstream Processing (DSP) of Large Biomolecules	22
1.3	Membrane Chromatography	22
1.3.1	The Prospects of Large Pores	22
1.3.2	Geometric and Processing Formats of Membrane Adsorbers	23
1.3.3	Mass Transfer in Membrane Adsorbers	23
1.4	Aqueous Two-Phase Extraction (ATPE)	25
1.4.1	The Formation of Aqueous Two-Phase Systems (ATPSs)	26
1.4.2	Partitioning in ATPSs	26
1.4.3	ATPE of Large Biomolecules	27
1.4.4	Multi-stage Extractors for Biopharmaceutical Processes	28
1.4.5	Centrifugal Partition Chromatography	29
1.5	Process Development Tools for Biopharmaceuticals	30
1.5.1	High-throughput Process Development (HTPD)	31
1.5.2	Model-based Process Development	31
2	Research Proposal	33
3	Publications & Manuscripts	35
	Next Generation Vaccines and Vectors: Designing Downstream Processes for Recombinant Protein-based Virus-like Particles	37
	Alternative Separation Steps for Monoclonal Antibody Purification: Combination of Centrifugal Partition Chromatography and Precipitation	65
	Downstream Processing of Virus-like Particles: Single-stage and Multi-stage Aqueous Two-Phase Extraction	85
	Modeling and Simulation of Anion-Exchange Membrane Chromatography for Purification of <i>Sf9</i> Insect Cell-derived Virus-like Particles	111
	High-throughput Process Development of an Alternative Platform for the Production of Virus-like Particles in <i>Escherichia coli</i>	137
	High-throughput Characterization of Virus-like Particles by Interlaced Size-Exclusion Chromatography	163
4	Conclusion & Outlook	183
5	References	185
6	Curriculum Vitae	197

CONTENTS

1 Introduction

Over the last century, the global health infrastructure and pharmaceutical industry have been drastically changing. The average human life span was dramatically increased by improvements in global sanitation and hygiene, and the introduction of antibiotics and vaccines (Cooper *et al.*, 2002). The rise of novel pathogens, cancer, infectious, metabolic, neurodegenerative and cardiovascular diseases represent today's major public health threats. The majority of current pharmaceutical drugs is based on small molecules derived from chemical synthesis or natural material. However, advances in biomolecular, genetic and bioprocess engineering have created essential healthcare prospects in the last decades by enabling the industrial-scale production of larger molecules: biologics. Biologics summarize a large number of therapeutic and prophylactic drugs derived from living organisms including enzymes, hormones, growth factors, blood factors, monoclonal antibodies (mAbs) and vaccines. The molecular variety and tailor-made design of biologics have generated a broad range of target indications such as therapies of cancer, autoimmune diseases, infectious diseases or hormone and enzyme deficiencies. Hence, biopharmaceutical products account for the fastest growing segment in the global pharmaceutical industry (Love *et al.*, 2013) and are steadily creating novel therapy approaches such as gene or cell therapies. Numerous clinical and postlicensing successes of therapies with biopharmaceutical products have heightened the enthusiasm for the future of biologics. Nevertheless, despite these successes, there are a lot of constraints linked to the development and manufacturing of biopharmaceutical products. Especially the high costs of biologics resulting in limited accessibility for developing countries and increasing burdens for global health insurances represent a critical issue. The high expenditure of biopharmaceutical products is predominantly generated by time-intensive product development phases and cost-intensive manufacturing processes.

Manufacturing processes of biologics are generally divided into upstream processing (USP), downstream processing (DSP), formulation, and filling and packaging of a biopharmaceutical drug product. In a typical USP of a biologic drug, eukaryotic or prokaryotic cells expressing the target molecule are cultured in bioreactors. Subsequently, in the DSP, the target molecule is separated from host cell impurities (*process-related impurities*) including host cell proteins (HCPs), endotoxins or DNA and product variants (*product-related impurities*) by a series of unit operations such as centrifugation, chromatography and filtration. Finally, during formulation, the drug substance is transferred into the final buffer at the desired concentration and filled and packaged for administration yielding the drug product. Required capital investments for production facilities, reactors, tanks and all unit operations are accompanied by high operating costs for cell culture media, chromatography media, buffer consumption and facility operation. Hence, it is evident that a reduction of manufacturing costs can only be obtained for a biopharmaceutical drug if the yield of product is increased, if the number of process steps and process time is lowered or if the consumption of raw materials is decreased. The definition, design and optimization of the operating instruments, procedures and conditions is set during process development. This underlines the impact of process development tools and strategies on the overall costs and timelines of biopharmaceutical products.

In the following section, the design and manufacturing of a biopharmaceutical product will be discussed in the case of virus-like particles, which represent the central topic of

this thesis. Subsequently, downstream processing of large biomolecules will be focused, describing theory and concepts of membrane chromatography and aqueous two-phase extraction in the lights of process intensification and process integration. At the end of this section, current process development approaches will be introduced and discussed.

1.1 Virus-like Particles (VLPs)

Virus-like particles (VLPs) comprise non-infectious assemblages of viral structural proteins capable of mimicking viruses and presenting antigen epitopes. Due to the absence of viral nucleic acids, the pathogen-associated molecular patterns, the highly repetitive surfaces and particle sizes from 20 to over 200 nm (Vicente *et al.*, 2011) VLPs combine ideal characteristics for activating T cells and B cells required for cell-mediated and humoral immune responses (Link *et al.*, 2012). The high variety and complexity of VLPs have lead to a vast and steadily increasing number of medical applications. Up to date, the majority of VLPs is used for vaccination against viral pathogens such as hepatitis B virus (Lacson *et al.*, 2005) and human papillomavirus (HPV) (Dochez *et al.*, 2014). Among the top five vaccine manufacturers by 2014 revenue (GlaxoSmithKline, Merck & Co, Novartis, Pfizer, and Sanofi Pasteur), each company has either initiated development or production of VLP vaccines in recent years (Chandramouli *et al.*, 2013, Dochez *et al.*, 2014, Farlow *et al.*, 2015, Fiers *et al.*, 2009, Sharma *et al.*, 2011). In addition, novel target indications have recently advanced enormously such as vaccination against malaria (Vekemans *et al.*, 2009) and bacterial pathogens (Rivera-Hernandez *et al.*, 2013), gene therapy (Keswani *et al.*, 2015, Tegerstedt *et al.*, 2005) as well as immunotherapy of cancer (Klamp *et al.*, 2011), metabolic diseases (Spohn *et al.*, 2014), chronic diseases (Bachmann and Whitehead, 2013) and Alzheimer's disease (Chackerian, 2010, Farlow *et al.*, 2015). This ongoing progress can only be realized by designing adequate VLP structures for the desired application.

1.1.1 Structure of VLPs

In 1982, Valenzuela *et al.* (Valenzuela *et al.*, 1982) were the first reporting the successful production and characterization of recombinant protein-based VLPs using *Saccharomyces cerevisiae* yeast cells. The surface antigen of hepatitis B virus (HBsAg) was expressed and assembled to spherical particles revealing similar structural and functional properties as the 22 nm hepatitis viruses secreted by human cells (Valenzuela *et al.*, 1982). Meanwhile, HBsAg VLPs are licensed as hepatitis B vaccines (Lacson *et al.*, 2005) and the prospects for VLP design have become more diverse than ever before. The phenomenon of particle assembly from proteins to VLPs depends on the applied virus protein structure, the chemical environment and the production host. VLPs of mammalian viruses are usually not assembled in prokaryotic cells and post-translational modifications such as protein glycosylation require expression in eukaryotic hosts. In general, VLPs are classified as non-enveloped and enveloped particles. Fig. 1 gives a schematic overview of different VLP structures. In contrast to non-enveloped capsid-based VLPs, enveloped VLPs consist of proteins enclosed by a lipid layer. The lipid layer is derived from the membrane of the expression host and embeds glycoproteins. Depending on the parental virions and the structural stability, VLPs consist of single or multiple proteins building single or

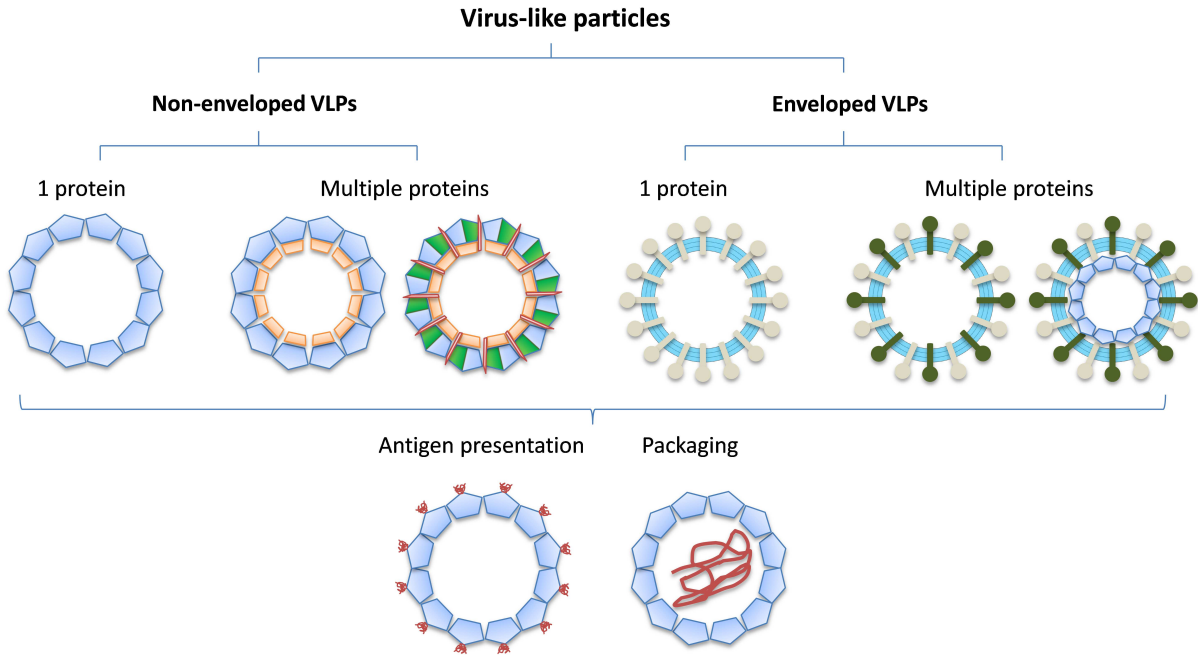


Figure 1: Classification of recombinant protein-virus-like particles (VLPs). Particles are assembled by one or multiple proteins building single or multilayered structures. Both lipid enveloped and non-enveloped VLPs can be used for antigen presentation and packaging of DNA (Keswani *et al.*, 2013), proteins (Kaczmarczyk *et al.*, 2011) or small molecules (Garcea and Gissmann, 2004).

multilayered protein shells. Hence, structurally simple viruses such as non-enveloped HPV can be mimicked by expressing a single capsid protein (e.g. papillomavirus L1 (Neuper *et al.*, 1996)), whereas more complex VLPs composed of four or more proteins such as influenza (Pushko *et al.*, 2011), rotavirus (Palomares and Ramírez, 2009) or cytomegalovirus VLPs (Wellnitz *et al.*, 2014) can be assembled using recombinant protein expression systems. The spherical and highly ordered structure of VLPs is generated by attractive interactions between virus proteins due to hydrophobic as well as charged amino acid groups. For instance the large size of HPV VLPs with a hydrodynamic diameter of 60 nm is based on the assembly of 72 pentameric capsomeres composed of a single virus protein L1 (Zhao *et al.*, 2005). VLPs designed with highly similar structures as their native viruses are mostly used to target molecules based on single or multicomponent capsids. Other designs involve the presentation of foreign antigens or tumor-associated cell line markers on VLP surfaces to target molecules of foreign pathogens or tumor cells. Antigen presentation can be achieved by genetic fusion or chemical conjugation of epitopes to capsid proteins or glycoproteins, or in case of enveloped VLPs also by insertion of foreign glycoproteins (Lua *et al.*, 2014). Moreover, VLPs can be designed as delivery vehicles for packaging of molecules such as nucleic acids (Keswani *et al.*, 2013), proteins (Kaczmarczyk *et al.*, 2011) or small molecules (Garcea and Gissmann, 2004).

1.1.2 Bioengineering of VLPs

Today's diversity of VLP structures could only be realized by the development and optimization of recombinant expression systems, genome sequencing and structure determination of viruses. Designing or 'bioengineering' of VLPs requires primarily a definition

of the desired application: immunization against a specific virus pathogen, immunization against different virus serotypes or non-viral pathogens, targeting of tumor cells, or delivery of drug or gene substances. The application defines the necessitated complexity of the VLP structure and therefore the selection of the production host. VLPs for vaccination purposes against a specific virus are usually designed by expressing the major proteins of the native virus.

Structurally simple VLPs based on a single protein are mostly generated by protein expression in *Escherichia coli* or yeast cells providing high expression yields and easy scalability (Lua *et al.*, 2014). For protein expression, the tailored gene sequence of the desired protein is cloned into a DNA plasmid which is transferred into the production host cell line. During fermentation of transformed *E.coli* or yeast cells virus proteins are expressed and in some cases assembled *in vivo* to VLPs. *In vivo* VLP assembly in yeast cells occurs for instance upon expression of the major HPV capsid protein L1, the basic subunit of Merck & Co.'s cervical cancer vaccine Gardasil[®] (Neeper *et al.*, 1996). Another example for *in vivo* assembly of single protein-based VLPs is the expression of the hepatitis B core antigen (HBcAg) in *E.coli* (Holmes *et al.*, 2015). HBcAg VLPs are currently evaluated for the immunotherapy of chronic hepatitis B (Al-Mahtab *et al.*, 2013), foreign epitope presentation (Karpenko *et al.*, 2000) and drug delivery (Lu *et al.*, 2015). Recombinant expression of HBsAg in yeast cells yields in VLPs budding from cells as lipid enveloped particles which are successfully used as human hepatitis B vaccines (Lacson *et al.*, 2005).

More complex VLPs composed of multiple proteins can be produced in insect or mammalian cells. A widely spread expression system is the baculovirus expression vector (BEVS)/insect cell (IC) system. The system relies on recombinant baculoviruses with inserted gene sequences for the desired virus proteins. The baculoviruses carrying single or multiple foreign genes infect the insect cells during the exponential cell growth phase (Vicente *et al.*, 2011), and induce both expression and *in vivo* assembly of virus proteins to corresponding VLPs. The BEVS/IC system is for instance used for the production of several non-enveloped VLP-based vaccine candidates consisting of multiple proteins such as human B19 parvovirus VLPs (Bernstein *et al.*, 2011), human enterovirus 71 VLPs (Lin *et al.*, 2015), and human rotavirus VLPs (Palomares and Ramírez, 2009).

Enveloped VLPs such as bilayered influenza VLPs (Hahn *et al.*, 2013), HIV-1 gag VLPs (Cervera *et al.*, 2013) or filamentous ebola-VLPs Sun *et al.* (2009) are produced either in insect or mammalian cells allowing appropriate protein folding and glycosylation. Mimicking of complex viruses with a high architectural consistency can be realized using insect or mammalian cell culture systems. However, scalability, yields, process time and costs represent major challenges and bottlenecks in comparison to bacterial or yeast cell processes. Therefore, another more flexible VLP class has attracted increased attention in recent years: chimeric VLPs.

Chimeric VLPs are tailor-made nanocarriers presenting foreign epitopes or antigens on their surfaces to elicit immune responses against foreign pathogens or cells. Several chimeric VLP platforms have been developed and evaluated in preclinical and clinical phases: the bacteriophage Q β (Bachmann and Whitehead, 2013, Riviere *et al.*, 2014), HBcAg (Fiers *et al.*, 2009, Klamp *et al.*, 2011), HBsAg (Bouchie, 2013, Vekemans *et al.*, 2009), the woodchuck hepadnavirus core protein (WHcAg) (Whitacre *et al.*, 2010), the murine polyoma virus protein VP1 (Middelberg *et al.*, 2011) or the papaya mosaic virus

(PapMV) system (Baz *et al.*, 2008). Table 1 gives an overview of chimeric VLPs generated for vaccination and immunotherapy. While feasible antigen length and complexity vary for each chimeric VLP platform, all carrier systems rely on a single virus protein and a simple production host using either *E.coli* or *S.cerevisiae* cells. Apart from genetic engineering, epitopes can also be fused to VLPs by chemical conjugation (Smith *et al.*, 2013). This covalent binding approach was for instance used for the fusion of the influenza peptide M2e to cowpea chlorotic mottle virus (CCMV) VLPs by conjugation to surface exposed cysteines and lysines (Cantin *et al.*, 2011). Major advantages of chimeric VLPs are the rapid adaptability of processes for novel antigens, the simple production hosts, and the possibility to create artificial pathogen-like particles for non-viral pathogens or viruses incapable of forming VLPs. Hence, this approach constitutes a powerful tool for the generation of future vaccine platforms based on peptide design as demonstrated recently by the approval of a chimeric VLP-based malaria vaccine (RTS,S/ MOSQUIRIX[®]) (Umeh *et al.*, 2014).

Table 1: Overview of chimeric vaccines generated by epitope presentation on VLP-based nanocarriers. A β : amyloid β ; Claudin18: gastric epithelium-associated lineage marker; CS: Malaria *P. falciparum* circumsporozoite protein; GH1: globular head domain of hemagglutinin (HA); HBcAg: hepatitis B core antigen; HBsAg: hepatitis B surface antigen; Her2: human epidermal growth factor receptor 2; M2e: ectodomain of influenza matrix protein 2; J8i: Group A streptococcus peptide antigen; MuPyV: murine polyomavirus; PapMV: papaya mosaic virus; WHcAg: woodchuck hepadnavirus core protein.

Status	Vaccine	Platform	Epitope	Reference
Preclinical	Group A streptococcus	MuPyV (E.coli)	VLP J8i	(Rivera-Hernandez <i>et al.</i> , 2013)
	Influenza	MuPyV (E.coli)	VLP M2e	(Anggraeni <i>et al.</i> , 2013, Middelberg <i>et al.</i> , 2011)
	Breast cancer	MuPyV (E.coli)	VLP Her2 fragment	(Tegerstedt <i>et al.</i> , 2007)
	Lung cancer	HBc Ag (E.coli)	Claudin18	(Klamp <i>et al.</i> , 2011)
	Malaria	WHcAg (E.coli)	CS fragment	(Billaud <i>et al.</i> , 2005)
	Influenza	PapMV (E.coli)	M2e	(Baz <i>et al.</i> , 2008)
Phase I	Influenza	HBs Ag (Yeast)	VLP M2e	(Fiers <i>et al.</i> , 2009)
	Influenza	bacterio-phage Qbeta (E.coli)	VLPs GH1	(Low <i>et al.</i> , 2014)
Phase II	Alzheimer (CAD106)	bacterio-phage Qbeta (E.coli)	VLPs A β fragment	(Farlow <i>et al.</i> , 2015)
Approved	Malaria (MOSQUIRIX [®])	HBs Ag (Yeast)	VLP CS fragment	(Umeh <i>et al.</i> , 2014)

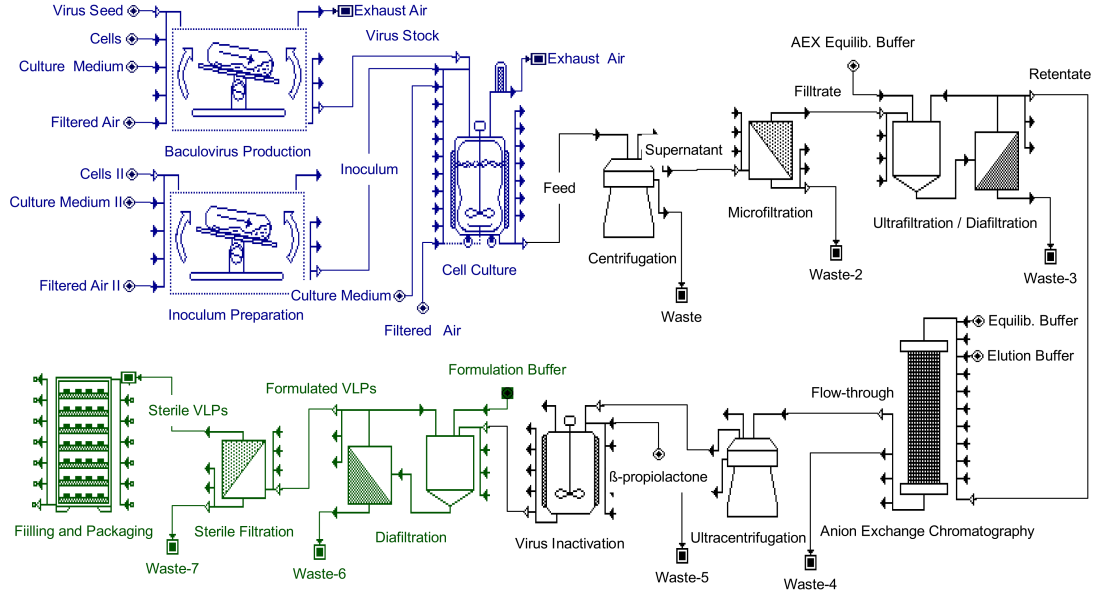
In addition, Table 1 demonstrates that chimeric VLPs are moving towards applications beyond vaccination against infectious diseases such as therapy of cancer and Alzheimer’s disease. However, constraints remain due to possible carrier specific immune responses, limited length and number of fused surface epitopes, and epitope dependent biophysical stability and process fluctuations. Another promising application, VLPs as vectors for packaging and delivery, can be realized by exploiting the assembly and disassembly mechanism of VLPs. This approach was for instance implemented in *in vivo* studies for the delivery of small molecules, proteins and nucleic acids using MuPyV VLPs produced in insect cells (Tegerstedt *et al.*, 2005). An advantage of MuPyV VLPs as delivery vehicles is the lack of human pre-existing immunity. In contrast to vaccines, gene vector agents need to fulfill requirements such as increased bioavailability, reduced immunogenicity, and efficient targeted cell delivery. Hybrid delivery vectors consisting of retrovirus VLPs produced in mammalian cells and synthetic lipid or polymer layers have shown promising results for gene delivery to human embryonic kidney cells and human oral carcinoma cells (Keswani *et al.*, 2015, 2013). Increased bioavailability and reduced immunogenicity were achieved by retarded dissociation of lipids or polymers and the absence of retroviral envelope proteins. Using VLPs as vehicles for gene therapy avoids the potential danger of activating viral oncogenes and offers novel prospects for the prevention, treatment and elimination of diseases.

1.1.3 Manufacturing of VLPs

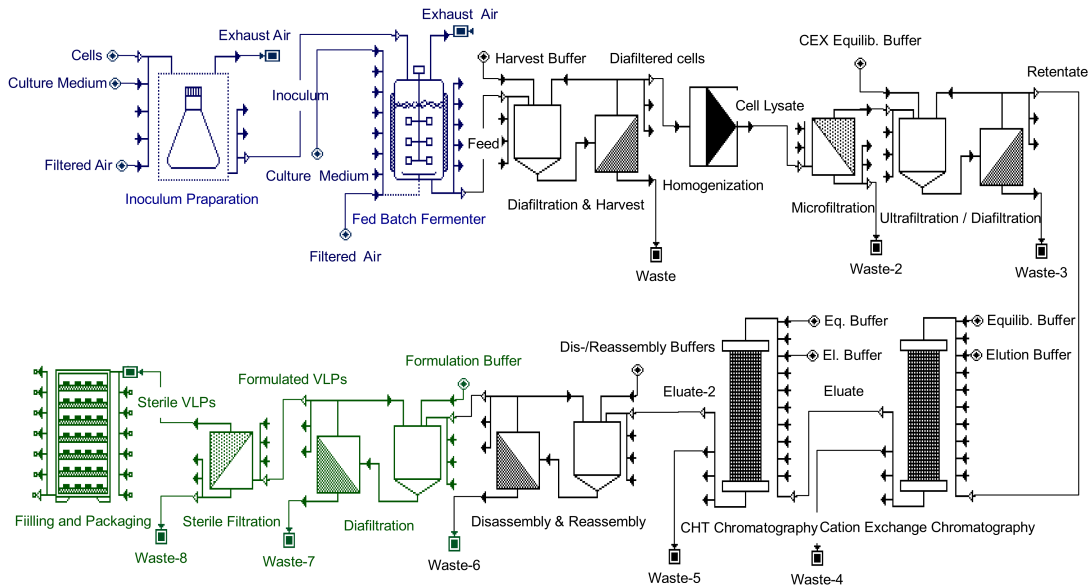
Manufacturing conditions for VLPs are tied to the definition of the product and the required degree of VLP complexity. Processes and production sites should be designed following ‘current good manufacturing practice’ (cGMP) guidelines given by regulatory agencies such as the US Food and Drug Administration (FDA) and the European Medicines Agency (EMA) to ensure safe and effective products in humans (Marshall and Baylor, 2011). In contrast to viral vaccines, a major advantage of VLP processes is the lower biosafety risk elicited by non-infectious recombinant virus proteins (Grabherr and Reichl, 2015). The utilization of recombinant protein expression systems generates different manufacturing process schemes than the production of viral vaccines.

Fig. 2 depicts process schemes of two manufacturing processes for VLP-based vaccines. In Fig. 2a the production of enveloped influenza A (H7N9) VLPs at Novavax is illustrated. *In vivo* assembled VLPs are expressed with the BEVS/IC culture system, purified by a series of chromatography, ultracentrifugation and filtration steps, formulated into the final formulation buffer and filled into glass vials. In contrast to traditional biopharmaceutical manufacturing, the entire process applies single use technologies allowing more flexible production facilities and reduced contamination risks (Nestola *et al.*, 2015). The reported total batch production time was three months from virus genomic sequences to the release of the first vaccine doses (Hahn *et al.*, 2013). In comparison, Fig. 2b shows the manufacturing process of the multivalent cervical cancer vaccine Gardasil[®] based on non-enveloped HPV VLPs. VLPs are produced in *S. cerevisiae* cells in stainless steel fermenters, purified by a series of filtration and chromatography steps and a controlled *in vitro* disassembly and re-assembly step before formulation of the drug substance including adsorption to an aluminium-containing adjuvant (Cook, 2003, Josefsberg and Buckland,

2012, Zhao *et al.*, 2012). To obtain multivalent vaccines each HPV serotype VLP is produced according to the presented process scheme and merged in the final formulation steps yielding the drug product Gardasil®.



(a) Influenza A (H7N9) VLP vaccine process



(b) Human papilloma VLP vaccine process

Figure 2: Process schemes of manufacturing processes for virus-like particle vaccines. Process flow-sheets were designed in SuperPro Designer® 8.5 (Intelligen Inc., Scotch Plains, NJ, USA). Processes are classified into upstream processing ('blue'), downstream processing ('black') and formulation ('green'). a) Production process of an insect-cell derived enveloped VLP vaccine against avian influenza A (H7N9) virus according to Hahn *et al.* (2013). b) Production of the yeast-cell derived non-enveloped VLP vaccine Gardasil® against cervical cancer with subsequent purification and formulation steps according to Cook (2003) and Zhao *et al.* (2012).

1.2 Downstream Processing (DSP) of Large Biomolecules

Downstream processing (DSP) of human protein or vaccine products can be subdivided into four process steps: clarification, capturing, intermediate purification, and polishing of the target molecule. A variety of unit operations are available for these process steps to remove process- and product-related contaminants and to ensure safe and effective drug products. The most prevalent technique for capturing, intermediate purification and polishing steps in biopharmaceutical manufacturing processes is liquid chromatography (Close *et al.*, 2014). However, the large size of complex therapeutic targets such as VLPs, viruses, plasmid DNA or stem cells represents a challenge for DSP design affecting the economic feasibility of novel vaccine candidates as well as gene and cell therapy products (Willoughby, 2009). Two promising approaches for purification of larger biomolecules have attracted increased attention in recent years: membrane chromatography and aqueous two-phase extraction (ATPE).

1.3 Membrane Chromatography

Membrane processes are widely used as separation techniques in pharmaceutical, food and chemical industry. In recent years, novel membrane designs have been steadily developed for adsorptive separations entailing new prospects for bioprocesses as cost-effective alternatives to column chromatography (Orr *et al.*, 2013). Membrane chromatography represents an integrated process combining filtration and chromatography in a single unit operation. Support matrices of commercial membranes are mostly based on regenerated cellulose due to lower costs and reduced non-specific protein binding in comparison to synthetic polymers such as nylon or polyethersulfone (PES) (Orr *et al.*, 2013). Adsorptive membrane interactions with biomolecules can be realized by surface immobilization of basically all ligand chemistries that are used in packed bed chromatography: cation-exchange, anion-exchange, hydrophobic interaction, mixed-mode or affinity ligands. Additional spacer arms (e.g. polypeptide, polyamine, polyether, etc.) are often included between support matrix and ligand molecules to ensure a good ligand accessibility (Suen *et al.*, 2003).

1.3.1 The Prospects of Large Pores

Membrane pore structures are typically designed in the micrometer range to allow high flow rates with a reduced pressure drop and decreased mass transfer resistance. Since large pore sizes imply a reduced surface and binding capacity in comparison to porous chromatography resins, membranes are most often used towards the end of protein downstream processes for polishing and flow-through procedures. On the other hand, membranes generate unique prospects for processing of large biomolecules such as VLPs. Major advantages are the large pore sizes, reduced diffusional path lengths, ease of scale-up, avoidance of column packing, and the operation in ready-to-use disposable devices. Membrane adsorbers have been successfully applied for purification of numerous large biomolecules including plasmid DNA, adenoviruses, influenza viruses, retroviruses, rotavirus-like particles and modified vaccinia ankara virus (McNally *et al.*, 2014, Nestola *et al.*, 2014, Opitz *et al.*, 2007, Orr *et al.*, 2013, Vicente *et al.*, 2008, Wolff and Reichl,

2008, Wolff *et al.*, 2010). Reported utilization of membranes as capture step from biological feedstocks, for product concentration or in flow-through mode at small and large scales underline the relevance of this technique for integrated processing of VLPs.

1.3.2 Geometric and Processing Formats of Membrane Adsorbers

Several geometries of membrane chromatography devices have been developed and commercialized in recent years. Fig. 3 shows an overview of the most prevalent designs according to Ghosh (2002) and Suen *et al.* (2003). The most widely-used modules for membrane chromatography are based on stacked flat-sheet or spiral wound geometries (Ghosh, 2002). While the mobile phase in stacked flat-sheet membranes is introduced in axial flow direction normal to the membrane surface, the liquid in spiral wound membranes flows in radial direction. The two flow patterns have different effects on mass transport phenomena of membrane processes as presented in the subsequent passage.

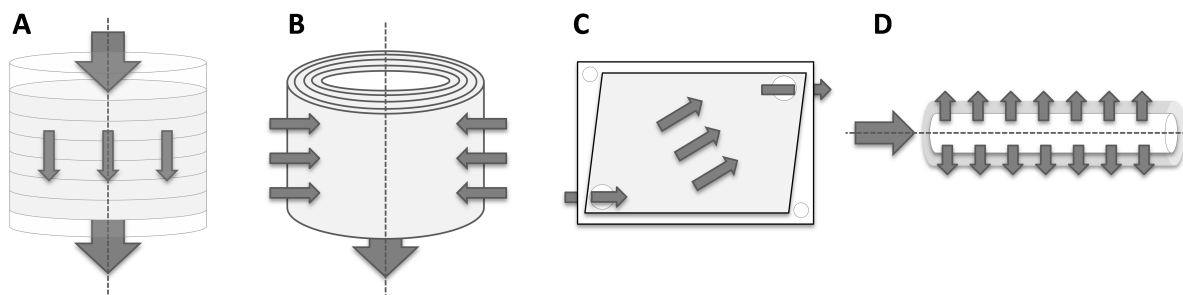


Figure 3: Schematic illustration of membrane chromatography modules adapted from Ghosh (2002) and Suen *et al.* (2003). (A) Stacked flat-sheet, (B) spiral wound, (C) tangential flow flat-sheet, and (D) hollow-fiber geometry.

1.3.3 Mass Transfer in Membrane Adsorbers

Similar to packed bed chromatography, the following mechanisms describe the molecular transport within membrane adsorbers (van Beijeren *et al.*, 2013):

- Convection within the mobile phase
- Axial dispersion within the mobile phase
- Film diffusion from the mobile phase into the stationary phase
- Pore diffusion within the stationary phase
- Surface diffusion along the membrane surface
- Adsorption and desorption kinetics at the membrane surface

Several models with different levels of complexity have been developed for mass balances of molecules in the mobile and stationary phase. Hydrodynamic models are usually one-dimensional neglecting effects normal to the flow direction and assuming homogeneous

membranes and fluids. The most detailed model incorporating all above mentioned transport phenomena is the general rate model (Gu *et al.*, 1991, van Beijeren *et al.*, 2013). The following description of the general rate model for membrane adsorbers is based on the research article of van Beijeren *et al.* (2013).

The calculation of the interstitial linear velocity u in a stacked flat-sheet module is identical to axial chromatography columns given the volumetric flow rate F , the membrane porosity ε_{pores} and the frontal area A_{front} (Eq.(1)):

$$u(x) = \frac{F}{\varepsilon_{pores}A_{front}} \quad (1)$$

In contrast, the frontal area A_{front} for a spiral wound geometry is defined by the radial position x and the membrane height H . Hence, the interstitial velocity u increases towards the center of the membrane adsorber for inward flow (Eq.(2)):

$$u(x) = \frac{F}{\varepsilon_{pores}A_{front}(x)} = \frac{F}{\varepsilon_{pores}2\pi xH} \quad (2)$$

The continuity equation for the mobile phase in a stacked flat sheet module in axial direction x can be written as (Eq.(3)):

$$\frac{\partial c_i}{\partial t} = -u \frac{\partial c_i}{\partial x} + D_{ax} \frac{\partial^2 c_i}{\partial x^2} - \frac{(1 - \varepsilon_{pores})}{\varepsilon_{pores}} k_{L,i} a_v (c_i - c_{p,i}) \quad i = 1 \dots N \quad (3)$$

The change of the concentration c_i of component i within the mobile phase is modeled by three terms. The first term considers convective transport affected by the interstitial velocity u . The middle term describes the hydrodynamic dispersion determined by the dispersion coefficient D_{ax} . The last term incorporates the transport of component i between bulk and membrane pore volume $c_i - c_{p,i}$ for the membrane porosity ε_{pores} , the liquid film diffusion coefficient $k_{L,i}$ and the specific surface area a_v .

The continuity equation for the mobile phase in a spiral wound module in radial direction x can be written as (Eq.(4)):

$$\frac{\partial c_i}{\partial t} = \left(\pm u + \frac{D_{ax}}{x} \right) \frac{\partial c_i}{\partial x} + D_{ax} \frac{\partial^2 c_i}{\partial x^2} - \frac{(1 - \varepsilon_{pores})}{\varepsilon_{pores}} k_{L,i} a_v (c_i - c_{p,i}) \quad i = 1 \dots N \quad (4)$$

The algebraic sign of the convective transport term is positive for inward flow and negative for outward flow. Modeling of mass transport phenomena in the stationary phase requires information of the membrane structure and the adsorption mechanism. The majority of membrane adsorbers is modified with grafted polymer layers to increase the specific surface areas. These hydrogels are incorporated in model equations by assuming a homogeneous layer present on the pore walls with a porosity $\varepsilon_{hydrogel}$. Hence, the mass balance for the stationary phase considering accumulation and mass transport within membrane pores and solid phase at a hydrogel position y can be written as (Eq.(5)) and (Eq.(6)):

$$\frac{\partial c_{p,i}}{\partial t} = k_{p,i} \frac{\partial^2 c_{p,i}}{\partial y^2} - \frac{(1 - \varepsilon_{hydrogel})}{\varepsilon_{hydrogel}} \times \left[k_{ads,i} c_{p,i} \left(q_{max,i} - \sum_{i=1}^N q_i \right) - k_{des,i} q_i \right] \quad i = 1 \dots N \quad (5)$$

$$\frac{\partial q_i}{\partial t} = k_{S,i} \frac{\partial^2 q_i}{\partial y^2} + \left[k_{ads,i} c_{p,i} \left(q_{max,i} - \sum_{i=1}^N q_i \right) - k_{des,i} q_i \right] \quad i = 1 \dots N \quad (6)$$

The first term in Eq.(5) describes the pore diffusion within the stationary phase influenced by the pore diffusion coefficient $k_{p,i}$, while the second terms in Eq.(5) and Eq.(6) consider the accumulation in the solid volume of the stationary phase due to binding on immobilized ligands. The binding mechanism is characterized by an adsorption coefficient $k_{ads,i}$, a desorption coefficient $k_{des,i}$, an accumulated concentration q_i and a maximum binding capacity $q_{max,i}$. The diffusion at the membrane surface is described by the solid film diffusion coefficient $k_{S,i}$. The adsorption of biomolecules on membrane adsorbents can be characterized with different models depending on the driving interaction forces and the desired complexity. In this thesis, ion-exchange (IEX) membranes were used for purification of biomolecules. Adsorption models for IEX interactions are for instance the Freundlich (Freundlich, 1906), Langmuir (Langmuir, 1916), Brunauer-Emmett-Teller (Brunauer *et al.*, 1938), and steric mass-action (SMA) isotherm (Brooks and Cramer, 1992). The steric mass action model which is applied in this thesis is a semi-mechanistic approach that considers stoichiometric ion-exchange reactions of biomolecules with multiple binding sites on a chromatographic solid phase. The isotherm accounts the competition between salts and proteins for available binding places limited by the total ionic capacity Λ , and incorporates a component specific characteristic charge ν_i and a shielding factor σ_i . The kinetic form of the SMA isotherm describes the accumulation in the solid volume of the stationary phase q_i and can be written as (Eq.(7)) (Hahn *et al.*, 2014):

$$\frac{\partial q_i}{\partial t} = k_{ads,i} \left(\Lambda - \sum_{j=1}^N (\nu_j + \sigma_j) q_j \right)^{\nu_i} c_{p,i} - k_{des,i} c_{p,salt}^{\nu_i} q_i \quad i = 1 \dots N \quad (7)$$

Eq. (8) describes the mass balance for salt ions attached to the IEX adsorbent:

$$q_{salt} = \Lambda - \sum_{j=1}^N \nu_j q_j \quad (8)$$

1.4 Aqueous Two-Phase Extraction (ATPE)

A unit operation that has gained increased attention in recent years for downstream processing of large biomolecules such as monoclonal antibodies, nucleic acids, viruses and cells is aqueous two-phase extraction (ATPE) (Jue *et al.*, 2014, Kepka *et al.*, 2009, Richter *et al.*, 2014, Rosa *et al.*, 2013a, Tsukamoto *et al.*, 2009, Vijayaragavan *et al.*, 2014). While liquid extraction processes have been widely used for decades in the pharmaceutical industry for isolation and separation of small molecules such as natural drug products, antibiotics, vitamins, and other active pharmaceutical ingredients (APIs) (Crowell, 1997, Hanson, 2013, Voeste *et al.*, 2012), the ATPE technique has hardly been implemented for large scale purifications of biopharmaceutical products. In contrast to traditional biphasic systems (e.g. organic-aqueous systems) used for extraction processes, aqueous two-phase systems (ATPSs) provide mild process conditions for biologics using hydrophilic solutes such as polymers or salts. However, current major drawbacks of ATPSs impeding industrial applications are attributed to the high experimental effort during process development, limited mechanistic understanding, low loading capacities, unfavourable physical

properties for scale-up, and unknown compatibility with preceding or subsequent unit operations. The scope of this section is to introduce the basic concept of ATPS, depict strategies for process integration and present scalable options for multi-stage extraction.

1.4.1 The Formation of Aqueous Two-Phase Systems (ATPSs)

ATPSs can be formed by a variety of polymers, salts, ionic liquids or non-ionic surfactants (Albertsson, 1971, Fischer *et al.*, 2013). The most common ATPSs considered for biopharmaceutical processes contain polyethylene glycol (PEG) and inorganic salts (Reschke *et al.*, 2014). Fig. 4 shows the illustration of a typical binary phase diagram for a PEG-salt ATPS. Similar to traditional biphasic systems, ATPSs are characterized by equilibrium *binodal* curves and *tie-lines*. Binodal curves reflect the components' critical transition concentrations for the formation of two immiscible aqueous phases (Hatti-Kaul, 2000). Systems with concentrations above the binodal curve separate into a PEG-rich top phase and a salt-rich bottom phase. The exact phase compositions are given by the intersection points of binodal curve and tie-line. Along the same tie-line coordinates compositions of top and bottom phases remain constant. In contrast, volume ratios of top to bottom phases change for different system compositions along the tie-line as illustrated in Fig. 4.

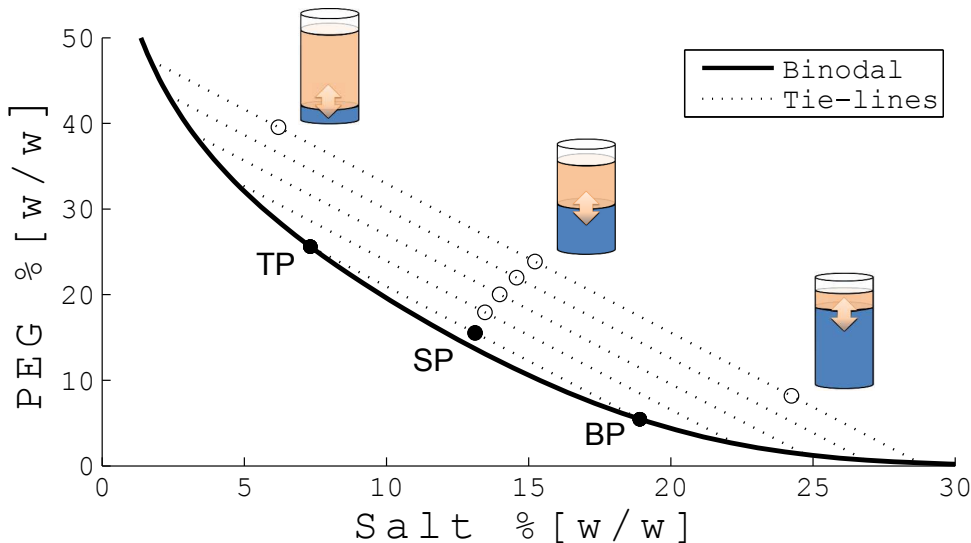


Figure 4: Schematic phase diagram of a PEG-salt aqueous two-phase system (ATPS). The system point *SP* separates into a PEG-rich top phase *TP* and a salt-rich bottom phase *BP*.

1.4.2 Partitioning in ATPSs

Purification of biomolecules by ATPE can be realized by exploiting differences in partitioning trends of the target component and contaminants. A characteristic value to rank partitioning trends of molecules is the ratio of top phase to bottom phase concentration, referred to as partition coefficient k (Eq. (9)):

$$k = \frac{c_{TP,i}}{c_{BP,i}} \quad (9)$$

Several model approaches have been developed to correlate the partition coefficient of proteins with ATPS phase properties and molecular descriptors such as molecular weight, surface charge, and hydrophobicity (Albertsson, 1971, Andrews and Asenjo, 2010, Andrews *et al.*, 2005, Asenjo, 1994). Models focused on hydrophobic properties of proteins revealed the most promising correlations using either hydrophobicities calculated from the primary amino acid sequence, surface hydrophobicities derived from molecular dynamic simulations of three dimensional protein structures or experimentally determined hydrophobicity values (Andrews and Asenjo, 2010, Dismer *et al.*, 2013). Incorporation of ATPS phase properties in model approaches was for instance accomplished by characterization with solvatochromic dyes (Madeira *et al.*, 2013, Nuno *et al.*, 2015), by molecular dynamic simulations of PEG and salt molecules (Dismer *et al.*, 2013, Oelmeier *et al.*, 2012a) or by description with the electrolyte fluid theory (ePC-SAFT) developed by Gross and Sadowski (2001) (Reschke *et al.*, 2014). Nevertheless, reliable mechanistic modeling of ATPSs has not yet been realized since current model approaches fail to include effects of varying biomolecule concentrations, saturation of phases and three-dimensional structures of large biomolecules such as antibodies, viruses or VLPs. An alternative empirical approach to shorten development times for ATPS selection is solubility-guided process development that was for instance implemented for the pre-selection of promising ATPSs for industrial mAbs (Oelmeier *et al.*, 2012b). The approach is based on the correlation of solubility curves of biomolecules for increasing phase component concentrations with ATPS compositions in top and bottom phases.

1.4.3 ATPE of Large Biomolecules

Regarding the size effect of large biomolecules on partitioning in ATPSs, Luechau *et al.* (2010) developed a model for interfacial partitioning combining the theory of Brownian motion (Boltzmann constant k ($1.381 \times 10^{-23} JK^{-1}$), absolute temperature T), the cross-sectional area of a bioparticle $\pi/4d_p^2$ and the surface tension γ_{TP} between top and bottom phase. The theory assumes that a particle can only adsorb to the interface between top and bottom phase if the particle motion from one phase to the other decreases the interfacial tension (Eq. (10)):

$$kT < \gamma_{TP} \frac{\pi}{4} d_p^2 \quad (10)$$

Hence, the critical particle diameter at which interfacial adsorption might occur can be estimated with Eq. (11):

$$d_p > \left(\frac{4kT}{\pi\gamma_{TP}} \right)^{1/2} \quad (11)$$

According to calculations from Luechau *et al.* (2010), bioparticles with diameters above 50 nm have a high tendency to adsorb to ATPS interfaces and can hardly be distributed into top or bottom phases. Interfacial adsorption of particles was for instance observed for cells, cell debris, nanoparticles, protein aggregates, and viruses and offers the possibility to integrate both a capture and solid-liquid separation into one unit operation (Oelmeier *et al.*, 2012b, Rito-Palomares and Lyddiatt, 2002, Selvakumar *et al.*, 2010, Targovnik

et al., 2012, Tsukamoto *et al.*, 2009). This highlights the suitability of ATPE for the initial purification of biomolecules from crude cell culture broths (Builder *et al.*, 1995, Hayenga and Valex, 2002, Tran *et al.*, 2011, Van *et al.*, 2011). Apart from solid-liquid separation and capturing, interfacial partitioning has also been used for concentrating biomolecules such as viruses (Jue *et al.*, 2014). However, interfacial adsorption of target molecules is undesirable for capture processes aiming at separating cells, and is furthermore linked to the precipitation of biomolecules (Guo *et al.*, 2012). Vijayaragavan *et al.* (2014) pointed out that top phase partitioning of large biomolecules can only be realized if hydrophobic forces promoting partitioning into PEG-rich phases outperform the surface tension of ATPSs.

Since ATPE is not considered as high-resolution separation technique, subsequent purification procedures are needed to meet required purity levels for biopharmaceuticals. For direct processing of PEG-rich or salt-rich phases, precipitation, filtration, hydrophobic interaction (HIC) and mixed-mode (MM) chromatography have been evaluated for mAbs, and other proteins (Azevedo *et al.*, 2008, Diederich *et al.*, 2015, Tran *et al.*, 2011). The main obstacle impeding direct processing by chromatographic unit operations is the high viscosity of ATPSs causing diffusive limitations, pumping difficulties, and compression of packed chromatography beds. Hence, integration of ATPS into an overall manufacturing process is easier to realize using micro- or macroporous chromatographic supports such as membranes or monoliths (Lee *et al.*, 1995, Vargas *et al.*, 2015). A reduction of viscosity is obtained by buffer exchange separating polymers by means of precipitation or diafiltration procedures. Another procedure to increase the separation efficiencies of ATPS processes is multi-stage extraction.

1.4.4 Multi-stage Extractors for Biopharmaceutical Processes

The goal of multi-stage ATPE is to increase the number of theoretical stages for a separation problem. The number of theoretical stages obtainable with a multi-stage extractor depends on operating conditions, physical properties of the biphasic system, and the design of the apparatus. In general, extractor configurations and types are classified into three main groups: mixer-settler units, column contactors, and liquid-liquid chromatography systems. Fig. 5 shows an overview of different extraction instruments. Mixer-settler units possess the most simple apparatus design consisting of multiple units of mixing stages coupled to settling and separating units (Espitia-Saloma *et al.*, 2014). An accelerated mass transfer and phase separation for large scale applications is obtained with centrifugal extractors as demonstrated by Richter *et al.* (2014) at Boehringer Ingelheim for industrial scale purification of monoclonal antibodies. In column contactors top and bottom phases are pumped in vertical direction using two separate inlets and outlets for the lighter and heavier phase. Thus, the phase separation is realized by gravity, while the mass transfer between the phases can be promoted by diverse mechanisms such as spray mechanisms, rotating vanes or discs, pulsed caps, packing material or mixers (Espitia-Saloma *et al.*, 2014). A benefit making multi-stage extractors attractive for the biopharmaceutical industry is the compatibility with continuous processes (Rosa *et al.*, 2013b).

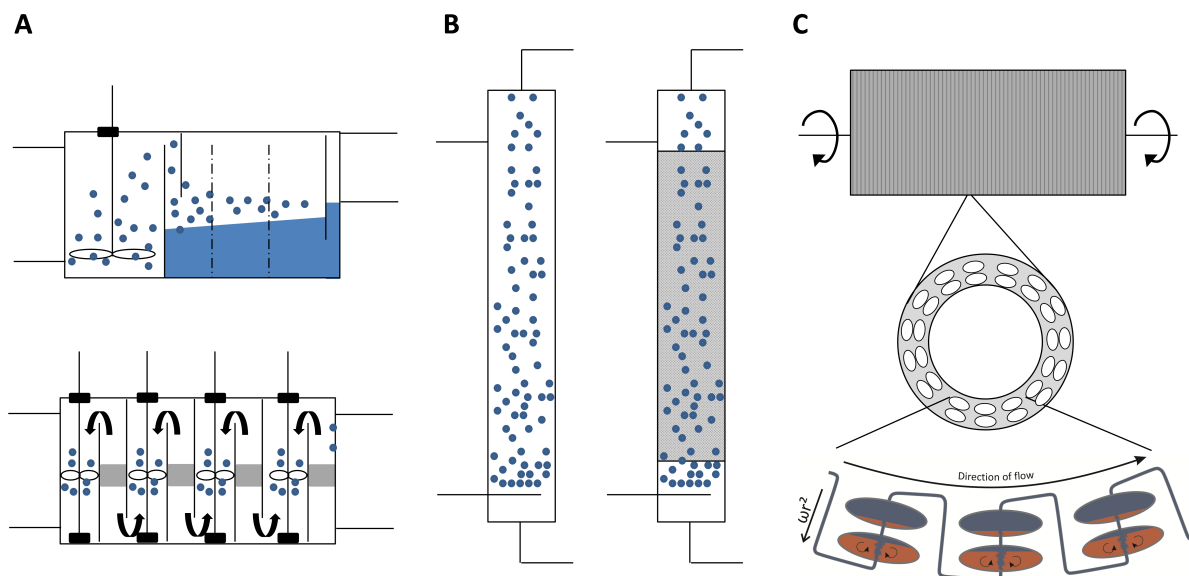


Figure 5: Illustration of multi-stage extraction instruments: (A) Mixer-settler units, (B) Column extractors, (C) Centrifugal partition chromatography.

1.4.5 Centrifugal Partition Chromatography

An adaptation of extraction processes to a more chromatography-like unit operation and to common chromatography periphery set-ups is feasible with liquid-liquid chromatography devices. There are two types of centrifugal liquid-liquid chromatography systems: hydrodynamic and hydrostatic counter-current chromatography (CCC). In both set-ups one phase of an ATPE is used as stationary phase while the other phase is pumped through the column as mobile phase. The retention of the stationary phase is achieved by different mechanisms. The equilibrium in hydrodynamic CCC is based on the Archimedean Screw effect generated by a combination of a coiled tube configuration and a rotating force field with planetary motion. The technique is termed hydrodynamic since the phases redistribute to the ends of the coil if the flow is stopped (Sutherland, 2007).

The first hydrodynamic CCC was designed in the 1960s by Ito *et al.* (1966). Since then, the technology has been steadily advanced with novel designs such as the 'J' type coil planet centrifuge, multilayer toroidal coil chromatography, and centrifugal partition chromatography (CPC) (Ito and Bowman, 1977, Sumner, 2011, Sutherland *et al.*, 2011, Sutherland, 2007). In this thesis, CPC was evaluated for purification of large biomolecules. Phase mixing and separation in CPC is implemented by the design of serially interconnected chambers mounted circumferentially on rotating disks. Due to the centrifugal force field, the heavier phase is distributed to the bottom while the lighter phase is moved towards the top of each chamber. To minimize backmixing effects, the top of one chamber is always connected to the bottom of the next by capillaries. CPC is also referred to as hydrostatic CCC since the phases remain in the chambers if the flow is stopped (Sutherland, 2007). CPC can be operated in *ascending mode* with the heavier phase as stationary phase or in *descending mode* using the lighter phase as stationary phase and the heavier as mobile phase. A third operation procedure is *dual mode*, a combination of *ascending* and *descending mode*, that is realized by switching the di-

rection of flow during the process. Up to date, only few CPC case studies have been published on the purification of proteins and other large biomolecules from cell culture broths (Grudzien *et al.*, 2013, Oelmeier *et al.*, 2012b). Most reported studies on ATPS-based CPC dealt with the separation of model proteins (Bezold *et al.*, 2015, Chen *et al.*, 1999, Schwienheer *et al.*, 2014, Sutherland *et al.*, 2008). However, due to centrifugally aided phase separation and a high number of theoretical stages of 200-600 (Hopmann and Minceva, 2012), CPC is considered as an ideal extraction instrument for challenging separations in biphasic systems with low interfacial tension, low density differences and high viscosities such as ATPSs (Adelmann and Schembecker, 2011, Schwienheer *et al.*, 2014). In general, the resolution in CPC predominantly depends on the retention of stationary phase which is influenced by operating conditions and system properties Sutherland (2007). A higher volume of stationary phase creates narrower peaks and higher peak resolution as demonstrated in hydrodynamic CPC models and case studies (de Folter and Sutherland, 2009, Oelmeier *et al.*, 2012b). Critical process parameters affecting the stationary phase retention are the flow rate, the centrifugal speed, the chamber geometry and the operation mode (Adelmann and Schembecker, 2011).

1.5 Process Development Tools for Biopharmaceuticals

According to Pronker *et al.* (2011) the average development period for a biopharmaceutical product from idea to market launch is 12 years generating research and development costs of US\$ 200-800 million (Andre, 2002, DiMasi *et al.*, 2003). Along this development time line molecular design, process design, preclinical *in vivo* studies, clinical phase studies and ongoing process optimizations are realized. Process development for manufacturing of a novel drug candidate is already initiated in the discovery phase in order to supply enough material for preclinical and clinical tests. The final process scheme for full manufacture must be set before start of phase III clinical trials (Rathore and Winkle, 2009, Werner, 2004). At this stage, production processes such as those presented in section 1.1.3 for VLP vaccines are not allowed to be changed substantially according to FDA and EMA requirements (Yu, 2008). This applies especially to production hosts, unit operations and process buffer solutions (Werner, 2004). In the light of 'time-to-market' demands in the pharmaceutical industry, this circumstance enhances additional time pressure on the process development of drug candidates. Hence, strategies for supporting manufacturing and process development of biologics should provide systematic, rapid and flexible tools. Traditionally, biopharmaceutical processes were designed and optimized by one-factor-at-a time approaches and heuristic or knowledge-based approaches. Considering the diversity and high number of drug candidates in preclinical and early-stage clinical phases, such development strategies prolong pharmaceutical development times and result in suboptimal process conditions, which remain critical at later development stages due to regulatory obstacles for process adjustments (Nfor *et al.*, 2009).

The introduction of 'Quality by Design' (QbD) in the biopharmaceutical industry has recently changed the requirements for process development (Herwig *et al.*, 2015, Rathore and Winkle, 2009). The basic tenet of QbD is to assess the effect of deviations in manufacturing processes on product quality attributes. For robust and rapid identification of critical process parameters and definition of process design spaces, novel development approaches rely on statistical methodologies, high-throughput experimentation (HTE)

and mechanistic modeling. An ongoing trend has been initiated moving from rules of thumb to improved understanding and sophisticated characterization of processes (Nfor *et al.*, 2009).

1.5.1 High-throughput Process Development (HTPD)

Automation, parallelization and miniaturization of unit operations and entire manufacturing processes by HTE approaches facilitate and accelerate the generation of a wide range of experimental data enormously (Bhambure *et al.*, 2011, Hubbuch, 2012). In recent years, the majority of downstream process unit operations such as chromatography, filtration, precipitation and aqueous two-phase extraction have been implemented on robotic liquid handling stations at microtiter-plate scale (Berg *et al.*, 2012, Bhambure *et al.*, 2011, Gibson *et al.*, 2011, Wiendahl *et al.*, 2008, 2007, 2009). Many biopharmaceutical companies have already established HTE routines for upstream and downstream process development and couple the screening methods to statistical tools such as Design of Experiments (DoE) or evolutionary search algorithms (Coffman *et al.*, 2008, Hansen and Oelmeier, 2012, Treier *et al.*, 2012). While the throughput for robotic screenings of single unit operations has been reduced to a couple of hours, novel bottlenecks arise in analytics and data handling (Hubbuch, 2012).

1.5.2 Model-based Process Development

Further reduction of sample consumption and experimental effort is obtained by applying mathematical models and numerical simulations for process development and optimizations (Close *et al.*, 2014, Nfor *et al.*, 2009). Predictive model approaches rely either on empirical correlations or fundamental mathematical descriptions of physico-chemical processes. Molecular dynamics (MD) simulations and quantitative structure-property relationship (QSPR) are for instance development tools used for prediction of process behaviour based on structural properties of biomolecules under defined buffer conditions (Dismar *et al.*, 2013, Ladiwala *et al.*, 2005, Schaller *et al.*, 2014, Zhang and Sun, 2010). For liquid chromatography processes, several hydrodynamic and mechanistic models have been developed as depicted in section 1.3.3 for membrane adsorbers. Thermodynamic models describing ion-exchange, hydrophobic interaction and mixed-mode chromatography have been implemented and applied for modeling of protein separations (Huuk *et al.*, 2014, Mollerup, 2008, Mollerup *et al.*, 2008, Osberghaus *et al.*, 2012). The development of chromatography modeling software packages (Hahn *et al.*, 2015a, Mehay and Gu, 2014) incorporating hydrodynamic models, adsorption models and algorithms has moved model-based approaches further towards industrial process development (Hahn *et al.*, 2015b). However, the estimation of model parameters in the presence of crude material such as cell debris, complex feedstocks including HCPs, DNA or cell culture medium components represents a challenge for predicting processes and defining design spaces *in silico*.

In this thesis the application and development of HTE-based and model-based development tools for processing of VLPs will be presented addressing above-mentioned challenges and bottlenecks.

2 Research Proposal

Virus-like particles (VLPs) have recently gained increased attention as innovative molecular entities for vaccination and gene therapy. Due to the large size and complexity, the design of recombinant protein-based VLP products represents a challenge for upstream, downstream and analytical process development. This research work is part of the project 'Optimization of an industrial process for the production of cell-culture-based seasonal and pandemic influenza vaccines'. Within the scope of future influenza vaccines, VLPs are assessed as alternative vaccine platforms in collaboration with project partners from academia and industry. The entire research consortium addresses four core areas dealing with the design of vaccine processes: Process integration, development of novel methods, continuous processing and aggregation (Fig. 6).

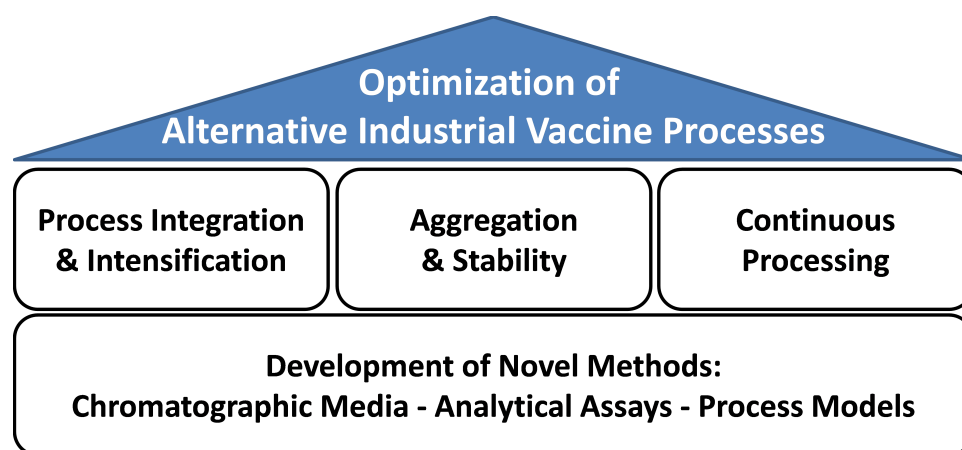


Figure 6: Overview of the project 'Optimization of an industrial process for the production of cell-culture-based seasonal and pandemic influenza vaccines'.

The focus of this thesis is laid on the implementation of integrated bioprocesses and the development of novel methods. In contrast to protein therapeutics such as mAbs, production and purification procedures, chromatographic supports and analytical assays have not yet been adapted and standardized for VLPs. Rational development strategies based on high-throughput experimentation, statistical design and model approaches are rarely applied. Current process development predominantly relies on heuristic approaches. The selection of suboptimal unit operations and process conditions during DSP has led to dramatically low process yields and high manufacturing costs for VLP vaccines. To counteract this status, the scope of this thesis is to provide process solutions with respect to three overall objectives:

- Economic design
- Process innovation
- Process acceleration

For realization of an economic design of future VLP processes, DSP unit operations requiring minimal investment for hardware such as aqueous two-phase extraction (ATPE), precipitation and membrane chromatography will be assessed for purification. The huge

number of process parameters in ATPE depicts a major obstacle hindering industrial implementation. The lack of mechanistic models drives process development for ATPE into heuristic or trial-and-error experimentation. Within the scope of this thesis, accelerated process development and improved process understanding for ATPE of large biomolecules will be sought by coupling robotic HTE with heuristics, solubility correlations, design of experiments and HTS-compatible analytical methods. The aim of this development strategy will be to identify critical process parameters for the ATPE of mAbs and VLPs and to define robust design spaces for purification. Another approach to reduce costs of VLP processes will focus on the upstream part using a low-cost microbial production host: *Escherichia coli*. The goal will be to optimize the process of an alternative carrier platform for antigens based on the murine polyoma virus protein VP1. The murine polyoma VLP platform is currently evaluated in preclinical trials for presentation of pathogen epitopes, but lacks an economic and industrially feasible production process.

As a second focus, implementation of innovative process concepts will be aspired by evaluation and integration of alternative unit operations. While the industrial purification of mAbs is based on so called platform processes incorporating multiple chromatography steps, VLPs are most often purified by ultracentrifugation. VLP or mAb purification by a single ATPE step will not provide a sufficient purity for clinical applications. Hence, one key aspect will be to develop a simple procedure for process integration of ATPE. With regards to industrial relevance, the integrated process should start with a crude mAb or VLP feedstock and end with a purified target under compatible process conditions for subsequent steps. The realization of this approach will be attempted by evaluating precipitation and centrifugal partition chromatography (CPC) in combination with ATPE. The development of adequate miniaturized methods and a systematic process procedure will first of all be established in a case study on mAbs derived from mammalian cell culture.

As a third focus, several approaches will be implemented to accelerate process development and overall process time for VLP products. A reduction of upstream process time is intended by using microbial cells for VLP production, while the downstream process time is planned to be minimized by reducing the number of intermediate unit operations and applying ATPE and precipitation for purification. Concerning speed-up of process development and analytics, novel HTS and model-based design tools are required. HTS tools need to be developed for miniaturized precipitation and resolubilization screenings, automated binding screenings with membrane adsorbers, cell lysis and process analytical techniques for VLPs.

In summary, this thesis aims to generate straightforward production, purification and analytical procedures for VLPs by adapting and advancing rational design tools for large biomolecules.

3 Publications & Manuscripts

1. Next Generation Vaccines and Vectors: Designing Downstream Processes for Recombinant Protein-based Virus-like Particles

C. Ladd Effio, J. Hubbuch

Biotechnol. J. (2015), doi:10.1002/biot.201400392

Virus-like particles are protein assemblages produced in recombinant systems and represent a new platform for vaccines and gene vectors requiring robust purification processes. In this review article, recent advances in the design of downstream processes and unit operations for recombinant based virus-like particles are presented. A special focus is placed on regulatory requirements, and novel strategies for reducing manufacturing costs and development times for VLP-based products.

2. Alternative Separation Steps for Monoclonal Antibody Purification: Combination of Centrifugal Partition Chromatography and Precipitation

S. A. Oelmeier, C. Ladd Effio, J. Hubbuch

J. Chrom. A (2013), doi:10.1016/j.chroma.2013.10.043

This article discusses the purification of the most prominent class of large biomolecules: monoclonal antibodies. A column-free process for human IgG1 is presented combining ATPE and precipitation. HTS methods were implemented to identify optimal conditions for ATPE, precipitation and re-dissolution of antibodies. For multi-stage ATPE, scale-up to a 500 mL centrifugal partition chromatography system was performed investigating the effect of sample, system and operating conditions on the isolation of antibodies from a Chinese hamster ovary supernatant. For integration into a traditional protein purification process, antibodies were precipitated and re-dissolved incorporating a virus inactivation step. Preservation of the native secondary protein structure was demonstrated by Fourier transform infrared spectroscopy (FTIR).

3. Downstream Processing of Virus-like Particles: Single-stage and Multi-stage Aqueous Two-Phase Extraction

C. Ladd Effio, L. Wenger, O. Oetes, S. A. Oelmeier, R. Kneusel, J. Hubbuch

J. Chrom. A (2015), doi:10.1016/j.chroma.2015.01.007

This article describes the design of an ATPE process for human B19 parvo VLPs derived from insect cells. Reversed-phase ultra-high performance chromatography (RP-UHPLC) was established as high-throughput analytical tool for tracking VLPs and host-cell proteins (HCPs). Promising ATPS conditions for VLP capturing, and separation of host-cell DNA and cell debris were identified using HTS methods. A systematic approach for VLP partitioning trends was developed by correlation with solubility curves. HCP separation was realized by multi-stage extraction with a centrifugal partition chromatography instrument. Gel electrophoresis, transmission

electron microscopy (TEM) and binding assays with human patient sera demonstrated the purity, homogeneity and antigen reactivity of processed VLPs.

4. **Modeling and Simulation of Anion-Exchange Membrane Chromatography for Purification of *Sf9* Insect Cell-derived Virus-like Particles**

C. Ladd Effio, T. Hahn, J. Seiler, S. A. Oelmeier, I. Asen, C. Silberer, L. Villain, J. Hubbuch

J. Chrom. A (2015), doi:10.1016/j.chroma.2015.12.006

This article deals with the application of a hybrid development approach combining high-throughput experimentation and mechanistic modeling for the design of an anion-exchange membrane chromatography process. Optimal binding conditions for VLPs derived from insect cells were identified by membrane binding screenings using design of experiments. A model for radial flow membrane chromatography was implemented, calibrated and applied for simulating a bind-and-elute process. Using UV absorption-based modeling a design space for an optimized salt elution step of VLPs was developed *in silico* enhancing yield and purity.

5. **High-throughput Process Development of an Alternative Platform for the Production of Virus-like Particles in *Escherichia coli***

C. Ladd Effio[‡], P. Baumann[‡], C. Weigel, P. Vormittag, A. Middelberg and J. Hubbuch ([‡]: Contributed equally)

J. Biotechnol. (2016), doi:10.1016/j.jbiotec.2015.12.018

This article describes the development of an upstream and downstream process for murine polyoma VLPs in *Escherichia coli*. USP development was realized by codon optimization for the major capsid protein VP1 and a HTS procedure consisting of high-throughput cultivations in 48-well format, HTS cell disruption and capillary gel electrophoresis as HTS-compatible analytical tool. A simple two-step purification process was developed using membrane and size-exclusion chromatography. Analysis of assembled VLPs by TEM revealed the presence of homogeneous spherical particles.

6. **High-throughput Characterization of Virus-like Particles by Interlaced Size-Exclusion Chromatography**

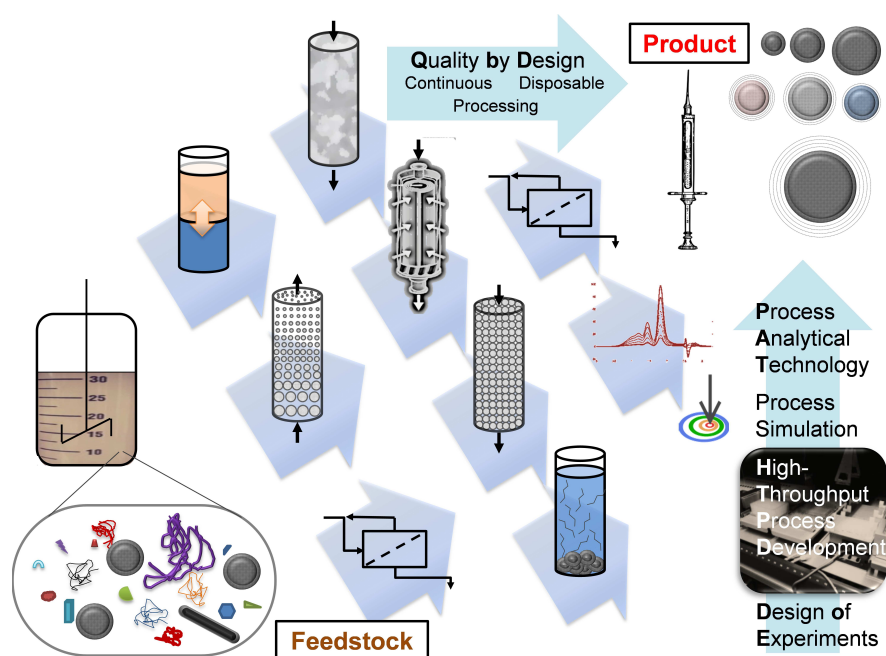
C. Ladd Effio, S. A. Oelmeier, J. Hubbuch

Vaccine (2016), doi:10.1016/j.vaccine.2016.01.035

This article depicts the development of a rapid analytical tool for virus-like particles. A size-exclusion UHPLC method was designed for assessing the dispersity of VLPs. Assay time was reduced to a few minutes by performing interlaced sample injections. The final method was applied for characterization of five VLP vaccine candidates and allowed tracking of VLP aggregates during DSP development and stability studies.

Next Generation Vaccines and Vectors: Designing Downstream Processes for Recombinant Protein-based Virus-like Particles

C. Ladd Effio and J. Hubbuch*



Institute of Process Engineering in Life Sciences, Section IV: Biomolecular Separation Engineering, Karlsruhe Institute of Technology, Engler-Bunte-Ring 1, 76131 Karlsruhe, Germany

* : Corresponding author. *E-mail address:* juergen.hubbuch@kit.edu (J. Hubbuch)

Biotechnol. J. (2015), doi:10.1002/biot.201400392

Abstract

In recent years, the development of novel recombinant virus-like particles (VLPs) has been generating new perspectives for the prevention of untreated and arising infectious diseases. However, cost-reduction and acceleration of manufacturing processes for VLP-based vaccines or vectors are key challenges for the global health system. In particular, the design of rapid and cost-efficient purification processes is a critical bottleneck. In this review, we describe and evaluate new concepts, development strategies and unit operations for the downstream processing of VLPs. A special focus is placed on purity requirements and current trends, as well as chances and limitations of novel technologies. The discussed methods and case studies demonstrate the advances and remaining challenges in both rational process development and purification tools for large biomolecules. The potential of a new era of VLP-based products is highlighted by the progress of various VLPs in clinical phases.

Keywords: High-throughput screening, Modeling, Purification, Vaccine, VLP

1 Introduction

Virus-like particles (VLPs) represent new molecular toolboxes for the control and containment of infectious diseases[1]. VLPs are protein assemblages composed of one or several types of viral proteins. Lacking viral nucleic acids, they mimic the virus they are derived from in size and morphology. In recent years, the assemblies of numerous virus-like structures have been realized using recombinant VLP technology approaches. In addition, VLPs have been used as carrier systems for the presentation of foreign antigen epitopes to design new tailored vaccine candidates. Examples are the development of VLP-based vaccine candidates against malaria [2, 3], diseases attributed to group A *Streptococcus* infections [4], Alzheimer’s disease [5, 6, 7], asthma [8, 9], diabetes [10], tumor growth [11, 12] and the design of packaged VLPs for the delivery of anti-cancer reagents [13]. Thus, VLP technology paves new ways for further medical applications such as immunotherapy of cancer, Alzheimer’s disease, metabolic and chronic diseases [14].

The production of VLPs is achieved by recombinant protein expression. Viral structural proteins are expressed in systems such as bacteria, yeast, mammalian, insect or plant cells. In eukaryote cells the assembly into empty capsids occurs *in vivo*, while upstream processes with prokaryotic cells require most often an *in vitro* assembly step [15]. More complex VLPs composed of several viral proteins and a lipid envelope require a eukaryotic host. A detailed overview and comparison of expression systems for VLPs has been reviewed elsewhere [16, 17, 18, 19, 20]. The advances in virus structure determination, genetic engineering, and bioengineering have generated a high and steadily increasing number of VLP-based vaccine candidates which are now evaluated in preclinical and clinical studies [16, 17]. VLP-based vaccines have contributed significantly to the prevention of cervical cancer and hepatitis B [21, 22]. Table 1 gives an overview of some vaccine candidates in clinical phases, and licensed products using the VLP technology approach.

A challenge slowing down manufacturing processes and the development of new VLP-based products is the design and scale-up of downstream processes. Purification of VLPs produced in genetically modified cells is essential for the generation of safe human vaccines. Host cell impurities have shown to increase reactogenicity, induce secondary immune responses, and thus generate preventable risks for human patients [51, 52, 42]. Classical chromatography devices and matrices for downstream processing of biopharmaceuticals were initially developed for smaller biomolecules such as peptides and proteins. Therefore, the most widely used technique for VLP purification is still ultracentrifugation. For decades, this technique has proven to be a valuable platform technology for purifying and concentrating all kinds of VLPs or viruses in lab scale. Drawbacks arise due to low product yields, limited separation efficiencies, difficult scalability, and long process times [15]. The purpose of this review paper is to sum up new technologies, trends, and approaches for purification of VLPs at different stages of a downstream process. Guidelines, challenges, and strategies for the design of a VLP downstream process are presented.

2 Purity Guidelines for Virus-like Particles

VLP production in recombinant systems comes along with the generation of numerous impurities which are summarized into two subgroups: process-related and product-related contaminants [53]. Process-related contaminants are predominantly attributed to host cell impurities such as cells, cell debris, host cell proteins (HCPs), DNA, proteases, endotoxins, polysaccharides, and lipids. Further impurities dedicated to the production process are media components, anti-foam reagents, and other potential hazards supplemented during upstream or downstream processing such as stabilizers, excipients, proteases, and nucleases. A list of inactive ingredients allowed in final drug formulations is provided by the Food and Drug Administration

3 PUBLICATIONS & MANUSCRIPTS

Table 1 Development stages of virus-like particle based vaccines.

Development stage	Virus/ pathogen/ disease
Preclinical	Chikungunyavirus [23], Coxsackievirus B3 [24], Cytomegalovirus [25], Denguevirus [26], Enterovirus 71 [27, 28], Group A Streptococcus [4], Human B19 parvovirus [29], Human immunodeficiency virus [30, 31], Human papillomavirus [32], Rotavirus [33]
Phase 1	Allergic rhinitis/ Asthma (anti IgE Q β -VLP), Chikungunyavirus [34], Ebolavirus ^a [35], Influenza H1N1 [36, 37], Influenza H7N9 [38], Respiratory syncytial virus [39]
Phase 2	Alzheimer disease (amyloid Q β -VLP) [14, 40, 41], Human B19 parvovirus [42], Influenza H1N1 [43], Influenza H5N1 [37], Norovirus [44],
Phase 3	Human papillomavirus [45, 46], Malaria <i>P. falciparum</i> (RTS,S) [47]
Licensed	Human papillomavirus (Gardasil [®] , Cervarix [®]) [48], Hepatitis B virus (Recombivax HB [®] , Engerix-B [®]) [49], Hepatitis E virus (Hecolin [®]) [50]

^a Novavax initiated phase-1 clinical trials with Ebola-VLPs in Feb 2015

(<http://ir.novavax.com/phoenix.zhtml?c=71178&p=irol-newsArticle&ID=2016192>).

(FDA) (<http://www.accessdata.fda.gov/scripts/cder/iig/index.cfm>). According to the World Health Organization (WHO), quality monitoring of final VLP-based vaccine bulks should include, among others [54]:

- Testing for sterility (bacteria, fungi);
- Testing for virus clearance;
- Summary of vaccine composition (protein, lipid, polysaccharides);
- Control of residual DNA, protein and endotoxin content;
- Determination of protein purity (by SDS-PAGE or similar); and
- Description of residual chemicals.

Industry is required to set specifications for contaminants during the process of product development. Residual contaminant levels should not exceed values found in vaccine lots shown to be safe in clinical trials [55]. The US Food and Drug Administration provides guidelines concerning acceptable ranges of DNA content in vaccine doses and recommends to measure the amount and size distribution of residual DNA. Residual host cell or viral DNA might be a risk due to oncogenicity and infectivity potentials. Therefore, maximum residual amounts of DNA depend on the host system, but should be below 10 ng per dose, with the DNA size being below 200 base pairs for parenterally administered vaccines [56].

Furthermore, residual HCPs and endotoxins strongly affect the safety of human vaccines and can elicit immunogenic responses and reactogenicity in humans [51, 52]. Recently, the WHO recommended a protein purity of at least 95% for the late-stage VLP-based malaria vaccine candidate RTS,S (GlaxoSmithKline plc) [55, 57]. Vaccine manufacturers do not release their

lot specifications on DNA, HCP, and endotoxin levels. However, Brito et al. [58] from Novartis Vaccines and Diagnostics recommended an endotoxin level below 20 EU/mL for recombinant subunit vaccines. Purity data for a patented VLP downstream process developed by Merck Research Laboratories was reported by Cook et al.[59]: protein purity according to SDS-PAGE was 98% and residual DNA content was 0.84 ng/mL in the final human papilloma-VLP vaccine bulk. For comparison, acceptable HCP and DNA levels for therapeutic biopharmaceutical products such as monoclonal antibodies are usually set below 100 ppm HCPs and 100 pg DNA, respectively [60].

Product-related contaminants result from product alterations during upstream and downstream processing and include aggregated, misfolded, deformed, and disassembled particles or subunits. VLP size and homogeneity are commonly assessed by electron microscopy and dynamic light-scattering techniques. The quality of in vivo-assembled VLPs in recombinant systems depends on several factors such as the host system, the cell environment, the expression of all required viral structural proteins, and the virus subtype [61]. Since not all of the mentioned conditions can be controlled sufficiently during in vivo VLP assembly, in vitro disassembly and reassembly processes were developed and optimized for several VLPs [62, 63, 64, 65, 66]. VLP disassembly and re-assembly enable the removal of encapsulated host cell impurities and have shown to increase the homogeneity, stability, and reactivity of VLPs [67, 68]. New tools, such as molecular dynamic simulations, have helped to improve understanding of the assembly mechanism and to predict the quality of new designed VLP constructs [69, 70]. Further product-related contaminants are VLP aggregates formed during both upstream and downstream processing even after VLP disassembly and re-assembly [71, 72, 73]. Hence, downstream processing of VLPs should not only include the separation of process-related contaminants but also the reduction and control of potential reactogenic product-related contaminants.

3 Downstream Process Unit Operations for Virus-like Particles

Several purification steps are required to meet the desired purity criteria for recombinant VLPs. These include unit operations for clarification, capturing, intermediate purification, and polishing of the molecule of interest. Figure 1 gives an overview of downstream process unit operations used for the purification of VLPs. Process-related contaminants should be separated particularly at the beginning of the process while product-related contaminants and residual process-related impurities should be removed in the final polishing steps. In recent years, the rapidly growing field of large biomolecule products has enlarged the purification toolbox for VLPs. New alternative and integrated downstream process unit operations are summarized in Figure 2.

3.1 Clarification of Cell Feedstocks

The first step in a VLP downstream process is the solidliquid separation of the cell culture broth. VLPs in recombinant systems are either produced intra- or extracellularly depending on host and viral proteins. If the VLPs are not secreted into the extracellular medium, a cell lysis step is required before clarification. Large-scale lysis of cells for VLP recovery is commonly done by high-pressure homogenization [59, 74, 75, 76]. The addition of protease inhibitors and stabilizing agents is essential at this process stage. A popular, but expensive method for DNA digestion can be carried out at such an early downstream process stage by the addition of nucleases such as Benzonase[®] endonuclease.

The actual clarification step, i.e. separation of cells, cell debris, and insoluble aggregates, is usu-

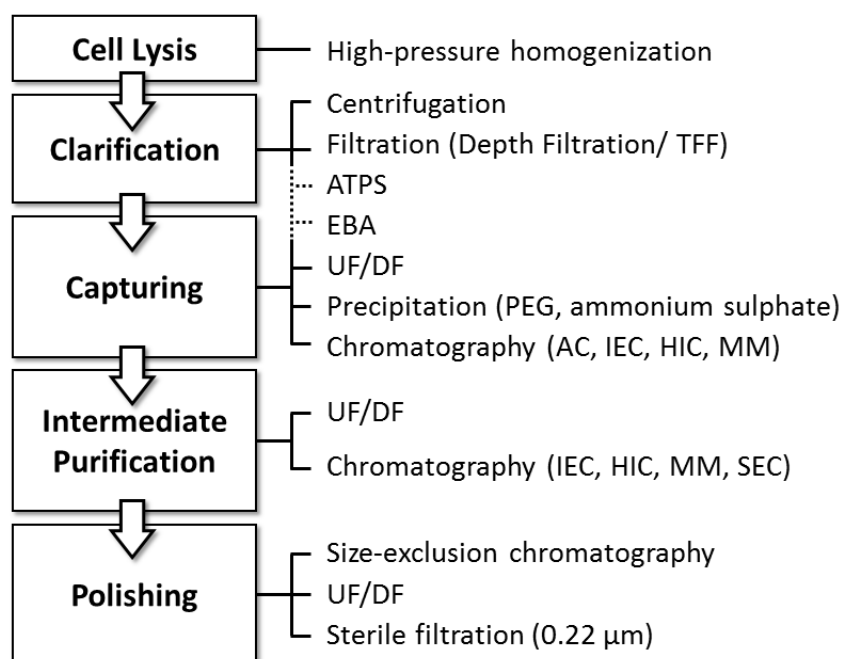


Figure 1 Overview of downstream process scheme and state-of-the-art unit operations for the purification of virus-like particles. The process scheme on the left shows the different steps of a downstream process ranging from the initial product isolation out of cells to concentration, intermediate and polishing unit operations. The methods of choice for these process stages are presented on the right side pointing out several chromatography, filtration and integrating purification techniques. (Abbreviations: AC, affinity chromatography; ATPS, aqueous two-phase system; DF, diafiltration; EBA, expanded bed adsorption; HIC, hydrophobic interaction chromatography; IEC, ion exchange chromatography; MM, mixed mode chromatography; PEG, polyethylene glycol; SEC, size-exclusion chromatography; TFF, tangential flow filtration; UF, ultrafiltration.)

ally performed by centrifugation and filtration steps [15]. Depending on the used host system the final cell density and viability are critical factors affecting the performance of subsequent purification steps [77]. Cell lysis during clarification increases the contaminant level and is therefore especially critical for secreted VLPs. Centrifugation in batch or continuous mode has been the method of choice for decades. However, the trend of incorporating cleaning- and validation-free disposable technologies into manufacturing processes has forwarded the development of new membrane formats. Membrane processes are easily scalable and offer an easier control of shear stress during operation [15, 31]. High shear stress is not only critical for cells but also for VLPs due to an increased risk of aggregation and particle deformation or disassembly [78, 71]. Negrete et al. demonstrated the potential of tangential flow filtration (TFF) with $0.45\ \mu\text{m}$ hollow fibers for the rapid clarification of shear-sensitive extracellular HIV gag-VLPs derived from insect cells [31]. Hollow fiber microfiltration in diafiltration mode was also used for the clarification of yeast cell lysates containing human papillomaVLPs with $0.45\ \mu\text{m}$ or $0.65\ \mu\text{m}$ pores [59, 75]. Peixoto et al. used disposable dead-end depth filters with $3\ \mu\text{m}$ pores for the clarification of insect cell lysate containing rota-virus-like particles [79]. An advantage of using depth filters for clarification can be the adsorption of HCPs and DNA [80, 81]. Further promising technologies for the initial clarification step are rotating or vibrating dynamic cross-flow filter membranes [82] and the flocculation of cell debris with borax before centrifugation [74].

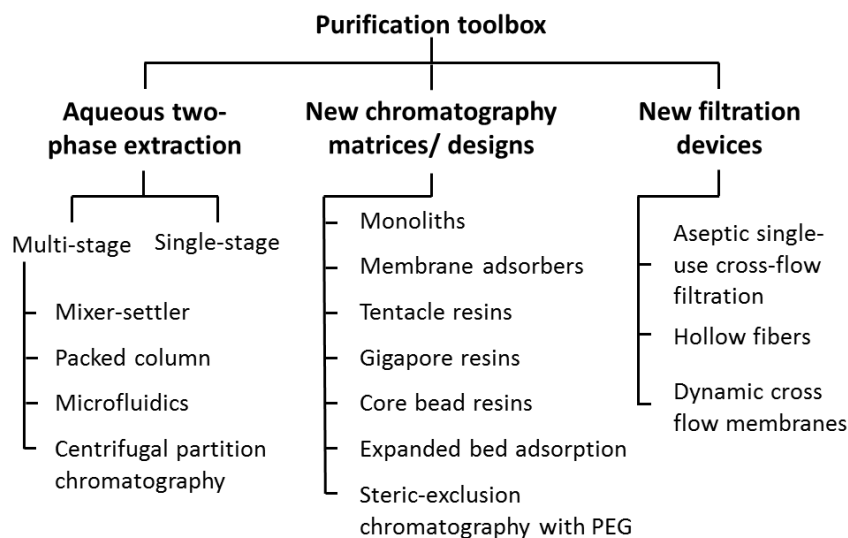


Figure 2 New technologies for the purification of virus-like particles. The majority of novel purification tools for large biomolecules can be divided into three groups: Aqueous two-phase extraction, chromatography matrices and filtration designs. New chromatography materials entail either large pore sizes (e.g. monoliths or membranes) accessible for bionano - particles or smaller pore sizes (e.g. core bead resins) for the steric exclusion and flow through purification of viral particles.

3.2 Capturing and Concentration of Virus-like Particles

An efficient capture step should predominantly reduce the bulk volume and increase the concentration ratio of VLPs to host cell impurities. Appropriate methods, new techniques and devices for this process step can be found in the fields of filtration, precipitation, chromatography, and extraction. Ultra- and diafiltration (UF/DF) with large pore membranes is a common platform unit operation for separating small host cell contaminants, digested DNA, and media components from all kinds of VLPs. TFF with membranes or hollow fibers has been applied for concentrating and purifying HIV gag-VLPs with 300 or 500 kDa cut-offs [78, 31], rota-VLPs with 750 kDa cut-off [79, 83], cytomegalo-VLPs with 750 kDa cut-off [25] and enterovirus 71 VLPs with 1000 kDa cut-off [27]. Interestingly, the largest nominal molecular weight cut-off (NMWC) was used successfully for capturing the smallest VLPs (entero-VLPs) with a diameter of 25-30 nm. A general rule of thumb for the selection of NMWC is to choose a value of 0.2 to 0.3 of the product molecular weight [84]. However, NMWC values are typically determined using protein or dextran markers and must be evaluated in small scale for each VLP. Typical membrane materials used for UF/DF of VLPs are polysulfone and regenerated cellulose [84]. UF/DF is often needed as an essential preliminary step before chromatographic purifications. An alternative method is the precipitation of the target component followed by a re-dissolution in the desired buffer. Typical precipitants for large biomolecules are ammonium sulfate and polyethylene glycol (PEG) [19]. PEGs with molecular weights ranging from 4,000 to 8,000 Da have been used in the past for concentrating numerous viruses [85, 86, 87] and VLPs such as cowpea mosaic VLPs, noro-VLPs, and chikungunya-VLPs [88, 89, 90]. Tsoka et al. purified VLPs derived from *Saccharomyces cerevisiae* by PEG-induced precipitation and scaled up the process to pilot scale in a 100 L stirred tank [74]. They reported a purification factor of 1.6 for VLPs with a product recovery of 90 %. Recently, precipitation with PEG has been revised for the purification of monoclonal antibodies and proved to be native and reversible [91], highly selective [92, 93], scalable in combination with hollow fiber TFF [94] and ready to integrate into manufacturing processes [94, 95]. Several researchers have shown that the mechanism and efficiencies

of PEG induced precipitation are predominantly linked to the hydrodynamic radius of PEG and protein [85, 96, 97, 98]. This explains the high selectivity observed for large biomolecules. However, drawbacks of the technique are the co-precipitation of other large biomolecules such as baculoviruses, nucleic acids [99], batch variances due to varying feed-stream concentrations and buffer compositions, and the risk of irreversible aggregation and product alterations [89]. Chromatography is undoubtedly the workhorse of downstream processes in the biopharmaceutical industry. Affinity, ion exchange, hydrophobic and mixed mode chromatography are powerful interaction modes for capturing VLPs in bind-and-elute mode. A good accessibility of ligands is an essential requirement for adsorptive interactions. Recently, chromatography suppliers have developed numerous new matrices for large biomolecules such as monoliths [100], gigapore resins [101], tentacle resins [102] or membrane adsorbers [103] with pore sizes in the micrometer region. The most popular purification method for biomolecules is affinity chromatography, because it enables the separation of a large number of contaminants in a single process step by taking advantage of highly selective interactions. However, affinity chromatography is only an option for few VLPs. The method requires either a specific antibody, which can be fused to a chromatography matrix, or a protein or peptide fusion tag on the VLP surface such as glutathion-S-transferase, biotin or polyhistidine [104, 105, 106]. Drawbacks in both cases arise due to high process costs, slow binding kinetics, low capacities, product alterations and in case of protein tags the need for separating the tag as a process-related contaminant in subsequent purification steps. A novel promising pseudo affinity interaction mode is cellulose sulfate (CS) chromatography with sulphated cellulose as ligand. Ohtaki et al. captured West Nile-VLPs from a mammalian cell culture supernatant using a CS column with a dynamic binding capacity of 3 mg/mL and a product recovery of 93% [107]. Using the heparin analogue suramin as competitive eluent, they demonstrated that the binding mechanism can be attributed to heparin groups on the VLP surface. Heparin chromatography has also been used for purifying human papillomaVLPs and nervous necrosis VLPs derived from *Saccharomyces Cerevisiae* [108, 109]. However, impurities such as HCPs and baculoviruses may also bind to CS and must be separated either by optimizing the elution conditions or by using subsequent purification steps [110].

Ion exchange chromatography (IEC) is the most prevalent chromatography method for biomolecules. IEC in bind-and-elute mode requires a low ionic strength and, therefore, mostly a preliminary buffer exchange step to remove media or cell lysis buffer components. Almost all large-scale downstream processes for VLPs include an IEC step at some point of the process. Examples of VLPs captured by anion exchange chromatography (AEC) in bind-and-elute mode are the purification of hepatitis B surface antigen (HBsAg) VLPs [111], Adenovirus type 3 dodecahedral (Ad3) VLPs [112], rota-VLPs [83], noro-VLPs [113] and human B19 parvoVLPs [29]. Quaternary amine (Q), diethylamine (DEAE) and ethylenediamine (EDA) were used as ligands with product recoveries ranging from 23% to 74%. Perfusion chromatography with sulfopropyl cation-exchange ligands has been applied at Merck Research Laboratories for recovering up to 45% of human papillomaVLPs from clarified yeast cell lysate [59, 114]. A novel chromatography technique incorporating the selectivity of PEG induced precipitation was developed by the Gagnon group [115, 116, 117, 118]: This technique is referred to as steric exclusion chromatography. Hydroxylated monoliths and starch-coated magnetic nanoparticles were used as stationary phases for capturing bacteriophages, IgM, and IgG with very high capacities of up to 58 g IgG per mL nanoparticles. The molecules of interest were retained in the stationary phase by steric exclusion of PEG at high PEG concentrations and eluted by lowering the PEG concentration, recovering about 70% product and separating more than 99% of HCPs and aggregates.

Other options for the initial purification step from clarified VLP feed streams are hydrophobic interaction (HIC) and mixed-mode chromatography. An advantage of these techniques is the

direct application of clarified cell culture feedstreams without preliminary buffer exchange steps [119, 120]. In a monolith case study on HBsAg-VLPs, Burden et al. determined higher recoveries for binding and elution on weakly hydrophobic hydroxyl ligands than on stronger hydrophobic butyl ligands. However, yeast cell lipids decreased the dynamic capacity drastically and induced column fouling [120]. Thus, an additional lipid removal step is advisable when using HIC for capturing VLPs from crude cell feedstocks.

3.3 Integrated Unit Operations for Process Intensification

Increasing the number of process steps in a downstream process triggers a decline of the overall product recovery. Hence, the integration of several process steps into one unit operation is an interesting feature of alternative separation technologies such as aqueous two-phase extraction (ATPE) and expanded bed adsorption. Aqueous two-phase systems (ATPSs) provide mild conditions for the extraction of biomolecules and have been applied for small and large scale purifications of numerous biopharmaceutical products [121, 122, 123, 124]. The number of new biocompatible devices for multi-stage extractions such as mixer-settler-systems [125], packed columns [126], centrifugal partition chromatography [127] and microfluidic platforms [128] is steadily increasing. ATPE enables rapid capturing of biomolecules from crude cell feedstocks incorporating clarification, concentration and purification with high selectivity [129, 130]. Proof of concept has been shown for the purification of rota-VLPs [131], human B19 parvoVLPs [132] and human papillomavirus protein L1 [133]. Nevertheless, low VLP capacities in the range of 0.005 to 0.6 mg/mL, low separation efficiencies, and limited mechanistic understanding underline the need of further research before getting a robust alternative unit operation for the purification of VLPs.

Expanded-bed adsorption (EBA) chromatography [134] is another promising integrated method for industrial-scale clarification, concentration, and purification of biomolecules. The interaction modes can be selected from traditional chromatography by using affinity, ion exchange, hydrophobic or mixed mode ligands. The fluidized bed allows the separation of cell debris in the flow-through by capturing the molecule of interest in bind and elute mode. EBA has been applied for the initial purification of hepatitis B core antigen (HBcAg) VLPs with DEAE and immobilized metal affinity ligands from unclarified *Escherichia coli* homogenate. Obtained recoveries were about 50%, and purity factors of 3.6 similar to those found for density gradient ultracentrifugation [135, 136]. Moreover, Cabrera et al. have developed and patented an EBA method in collaboration with Medicago Inc. using DEAE ligands for capturing influenza VLPs from plant cells [137].

3.4 Intermediate Purification of Virus-like Particles

Further purification after capturing is mostly achieved by a subsequent chromatographic separation step such as IEC or HIC. Separation of residual HCPs or DNA is often done by anion exchange chromatography (AEC) in flowthrough or bind-and-elute mode. A promising concept for flow-through applications is the core bead technology comprising size exclusion and ion exchange chromatography. An industrial example is the purification of influenza VLPs derived from insect cells at Novavax Inc [138]. Whereas VLPs were recovered at elevated ionic strength in the flow-through, baculoviruses and DNA bound to Q ligands were found in the core bead particles. Recoveries were ranging from 70% in the laboratory scale to 40% in the pilot scale [139]. The same method was also used for intermediate purification of HIV gag-VLPs [31]. In addition, there is also a tendency to use anion exchange membrane adsorbers for flow-through

purification of large biomolecules [140, 141]. Flow-through chromatography is especially suitable for the purification of lipid-enveloped and less stable VLPs because the risk of product alterations by binding and elution is reduced. However, a drawback is the need for processing of large volumes necessitating several extra concentration steps.

A common two-step process reducing the bulk volume is the combination of precipitation with PEG and AEC in bind-and-elute mode. Koho et al. purified noro- VLPs derived from insect cells by precipitation with PEG 6000 and a step gradient elution on a Q AEC column with a final purity of 95% [89]. A similar method was applied by the group for purifying Coxsackievirus B3 VLPs using a monolithic Q column [24]. Although successful purification was achieved in both case studies, no information was given on actual recovery values. More detailed performance data for the two-step process was reported by Phelps et al.: only 22% of cowpea mosaic VLPs could be purified from a plant cell feedstock. Precipitation with PEG 6000 and perfusion chromatography media with a strong Q ligand yielded in a final purity of 95% [88]. In contrast, Venkatachalam et al. recovered 55% of Enterovirus VLPs derived from insect cells by using a weak DEAE ligand on a monolithic column after VLP precipitation with PEG 8000 [87]. Thus, a weaker ion exchange ligand and larger pore sizes promoted higher VLP recoveries.

Kim et al. applied precipitation by ammonium sulphate for capturing and preparing human papillomaVLPs for a subsequent chromatography step by CEC or heparin chromatography [142]. The method separated HCPs in both chromatography processes with recoveries of 63% and demonstrated that the mechanism, elution profile, and selectivity of heparin chromatography correlated well with a CEC step. VLPs captured by IEC at high ionic strength can be directly processed by HIC or ceramic hydroxyapatite (CHT) chromatography. Kim et al. purified HBsAg-VLPs subsequent to AEC by bind-and-elute on a butyl HIC column with a recovery of 70% for the HIC step. Industrial intermediate purification of e.g., human papilloma-VLPs has been performed with CHT chromatography subsequent to a CEC capture step [143, 114]. CHT chromatography is a mixed mode chromatography method often used for large biomolecules with typical pore sizes of 80 to 100 nm [144].

3.5 Polishing and Formulation of Virus-like Particles

In the final polishing steps of a downstream process, all product-related contaminants, residual and encapsulated process-related contaminants need to be removed. Final purification of VLPs is mostly done by size-exclusion chromatography (SEC) [138], UF/DF [145], and sterile filtration. VLPs are transferred into the final formulation buffer and concentrated to the desired concentration for administration. Residual baculoviruses can be inactivated with e.g. β -propiolactone [138]. As mentioned at the beginning, removal of encapsulated contaminants and an increase in particle homogeneity can be accomplished by VLP disassembly and re-assembly. Disassembly of capsids can be triggered by adding reducing agents such as β -mercaptoethanol or dithiothreitol at elevated pH values [61, 146]. Thereafter, virus proteins can be further purified in the presence of reducing or chaotropic agents and are finally reassembled to VLPs by diafiltration removing reducing agents [62, 147]. The homogeneity of the final VLP bulk can be controlled by varying pH, ionic strength and adding divalent cations [72, 148]. For long-term stability excipients such as sucrose, trehalose, sorbitol, glycine, chitosan glutamate or mannitol can be added to the formulation buffer. A detailed review of formulation and stabilization of VLP-based vaccines was recently published by Jain et al. summarizing excipients, adjuvants and new routes of administration [149]. Prior to filling VLPs are sterile filtered with 0.22 μ m filter membranes.

4 Challenges and Bottlenecks of Purification Processes

The described examples of unit operations for VLPs illustrate the challenges and bottlenecks associated with the processing of large biomolecules. Table 2 summarizes dynamic binding capacities reported for VLPs captured from clarified feed streams by chromatographic methods. It is evident that capacities for VLPs are still far away from the capacity range of 50-200 mg/mL usually observed for proteins in affinity chromatography, IEC or HIC. In addition, the reported VLP recoveries in bind-and-elute mode were mostly in the range of 30 to 60% due to product alterations caused by interactions with stationary phases. While chromatography separations suffer from poor recoveries, filtration methods fail at removing larger process-related contaminants such as baculoviruses and DNA. Another process challenge occurs at the final sterile filtration step: VLPs are often retained in the filter by unspecific interactions or due to large particle sizes approximating the mean filter pore size of 0.22 μm . Alternative downstream unit operations such as ATPE, EBA, and precipitation are valuable purification tools for VLPs, but require much time and effort for process development. Although ultracentrifugation processes have been replaced in industrial-scale purifications, there is still a lack of straightforward ready-to-use processes for material supply during early-stage development. Ultracentrifugation remains the method of choice during preclinical studies [27, 152, 90, 29]. Moreover, process development is often delayed by laborious offline analytical methods such as gel electrophoresis, Western blotting or electron microscopy. Rapid technologies are especially needed for the control and characterization of product-related contaminants such as VLP aggregates.

5 Strategies and Tools for Future Downstream Process Development

In the past, process development and optimization of downstream processes were mostly based on empirical approaches conducting trial-and-error experiments. By virtue of a more global industry and numerous new emerging technologies, the FDA has forwarded the implementation of 'quality by design' (QbD) and 'process analytical technology' (PAT) for biopharmaceutical products. The idea of these approaches is the development of a better knowledge and control of products and manufacturing processes by using PAT methods and rational development strategies. PAT methods include, for instance, online high-performance liquid chromatography (HPLC) systems or light-scattering techniques which enable process surveillance and control of unit operations in realtime [153, 150]. New rational development strategies for biopharmaceutical products involve the approaches of design of experiments (DoE), scale-down, high-throughput experimentation, and process modeling. Promising concepts have already been suggested for VLPs to obtain a more rational downstream process development. Vicente et al. predicted the elution profile of rota-VLPs on a DEAE membrane adsorber by implementing hydrodynamics and steric mass-action (SMA) model developed by Brooks and Cramer [154] into a software package for process modeling [83]. Prediction of chromatography elution profiles generates a profound process understanding and enables *in silico* optimization and estimation of process fluctuations during chromatographic separations [155, 156]. A scale-down model of chromatographic separations was implemented by Wenger et al. on a robotic liquid handling station. Column chromatography was miniaturized 1000-fold from laboratory scale to micropipette columns and allowed the establishment and assessment of a whole industrial HPV-VLP vaccine downstream process at the microscale [114]. Such microscale processes enable rapid

Table 2 Dynamic binding capacities and recoveries of chromatographic methods applied for the purification of VLPs. Ad3: adenovirus type 3 dodecahedral; CHT: ceramic hydroxyapatite; CS: cellulose sulfate; DBC: dynamic binding capacity; DEAE: diethylamine; EBA: expanded bed adsorption; HBcAg: hepatitis B core antigen; HBsAg: hepatitis B surface antigen; HPV: human papillomavirus; IDA: iminodiacetic acid; IEC: ion exchange chromatography; NDV: newcastle disease virus; OH: hydroxyl; WNV: west Nile virus.

Mode (ligand)	Matrix	VLP	Recovery [%]	DBC [mg/mL]	Reference
IEC (DEAE)	Cross-linked agarose gel	HBsAg	24.06	0.38	[150]
IEC (DEAE)	Cross-linked agarose gel with dextran surface extenders	HBsAg	31.88	0.97	[150]
IEC (DEAE)	Agarose coated gigaporous polystyrene resin (120 nm pore size)	HBsAg	43.18	1.87	[150]
IEC (DEAE)	Agarose coated gigaporous polystyrene resin (280 nm pore size)	HBsAg	68.33	3.03	[150]
IEC-EBA (DEAE)	Cross-linked agarose with stainless steel core material	HBcAg	52.43	0.5	[135]
IEC (Q)	Methacrylate monolith	Ad 3	52	1.38×10^{16} VLP/ mL	[112]
HIC (OH)	Methacrylate monolith	HBsAg	85	0.25	[120]
HIC (Butyl)	Cross-linked agarose gel	HBsAg	90	0.08	[120]
MM (CHT)	Ceramic hydroxyapatite resin	HPV	82	2.9	[143]
AC (CS)	sulfated cellulose resin	WNV	93	3.0	[107]
AC -EBA (IDA)	Cross-linked agarose with stainless steel core material	HBcAg	56	5.6	[136]
AC -EBA (IDA)	Cross-linked agarose with stainless steel core material	NDV	9.6	2.94	[151]

downstream process development for product subtypes as well as new constructs at early development stages and improve the overall process and product understanding[157, 158, 159]. In order to improve recoveries and dynamic capacities in chromatographic processes, the influences of matrices, pore sizes, ligands, ligand densities, and stabilizers need to be further addressed for VLPs. Inverse size exclusion chromatography, confocal laser scanning microscopy, miniaturized bind-and-elute studies, and tracer experiments with dextrans are powerful tools for understanding and designing chromatography processes. For instance, Wu et al. demonstrated by confocal laser scanning microscopy that adsorption of HPV-VLPs is limited to a thin layer on the particle surface of perfusion resins due to steric exclusion from the particles' micropores[160]. The development of new PAT methods for the quantitative characterization of VLPs has been forwarded in recent years with new technologies such as asymmetrical flow field-flow fractionation (AF4), electrospray differential mobility analysis, native mass spectrometry, and in-line or at-line light-scattering techniques [161, 150, 162, 163, 164]. Further rapid analytical techniques have been applied for the characterization of viruses such as flow cytometry, tunable resistive pulse sensing and nanoparticle tracking analysis [165, 166]. A tool for selective in-line quantification of biomolecules has recently been described by our group using spectral data from diode array detectors [167].

Concluding the findings of all described approaches for bind-and-elute chromatography, the authors suggest to: (i) avoid the use of chromatography media with small pore sizes; (ii) avoid the use of very strong ligands; and (iii) add stabilizers such as glycerol or PEG to the mobile phase to counteract the risk of product alteration during adsorption and desorption processes [112, 111]. The large size and complexity of VLPs are challenges to the downstream processing. However, these characteristics can be utilized by size-dependent purification tools such as filtration, flow-through or size-exclusion chromatography. A straightforward process scheme possibly applicable to various VLPs could be designed as follows:

1. Clarification by TFF with 0.45 μm hollow fibers/ membranes;
2. UF/DF by TFF with 1000 kDa hollow fibers/ membranes for removal of small process-related contaminants and media components;
3. IEC in flow-through mode for removal of large charged process-related contaminants;
4. UF/DF by TFF with 1000 kDa hollow fibers/ membranes for concentration and formulation; and
5. Sterile filtration.

A possible option for avoiding the sterile filtration of very large VLPs is to design the whole manufacturing process with aseptic single-use unit operations [25]. Such disposable technologies are available for a variety of unit operations such as centrifugation, filtration, and chromatography, and enable the design of flexible ready-to-use process solutions [168]. Another important strategy for increasing the productivity while reducing overall costs is to switch manufacturing from batch to continuous processing. Promising results were obtained in case studies for the purification of influenza- and adenoviruses by simulated moving bed chromatography with multiple SEC columns [169, 170].

6 Conclusion and Outlook

Responding faster to emerging pathogens, increasing the safety of vaccines, and accelerating material supply during clinical phases are key issues affected by the downstream processing of

VLPs. New technologies and strategies for VLP purification and process control have arisen in recent years, representing the basis for future manufacturing processes. The reported methods and case studies demonstrate the progressive replacement of ultracentrifugation steps in both industry and science by scalable chromatography and filtration unit operations. Promising new stationary phases have underlined their potential for VLP processing, and alternative methods such as aqueous two-phase extraction, precipitation, and expanded-bed adsorption chromatography are gaining increasing attention. Similar to monoclonal antibody processing, the implementation of QbD and PAT in VLP processing will standardize downstream processes used for future manufacturing and development phases. Downstream processes slowly move towards a scalable platform process scheme with tangential flow filtration and anion exchange matrices as the most prevalent unit operations. It is the turn of industry, process scientists, and life science suppliers to take advantage of the size and complexity of VLPs for designing simple, scalable, and efficient platform processes for all kinds of small and large VLPs. The foundation of such generic processes has been laid in the case studies reviewed in here.

Acknowledgements

The authors gratefully acknowledge funding from the **German Federal Ministry of Education and Research** (Grant agreement 0315640B).

Conflict of Interest

The authors declare no financial or commercial conflict of interest.

References

- [1] C. Ludwig, R. Wagner, Virus-like particles-universal molecular toolboxes., *Curr. Opin. Biotechnol.* 18 (6) (2007) 537–45. doi:10.1016/j.copbio.2007.10.013.
- [2] J. Vekemans, A. Leach, J. Cohen, Development of the RTS,S/AS malaria candidate vaccine., *Vaccine* 27 Suppl 6 (2009) G67–71. doi:10.1016/j.vaccine.2009.10.013.
- [3] D. Rodríguez, G. González-Aseguinolaza, J. R. Rodríguez, A. Vijayan, M. Gherardi, P. Rueda, J. I. Casal, M. Esteban, Vaccine efficacy against malaria by the combination of porcine parvovirus-like particles and vaccinia virus vectors expressing CS of Plasmodium., *PLoS One* 7 (4) (2012) e34445. doi:10.1371/journal.pone.0034445.
- [4] Y. P. Chuan, N. Wibowo, N. K. Connors, Y. Wu, F. K. Hughes, M. R. Batzloff, L. H. L. Lua, A. P. J. Middelberg, Microbially synthesized modular virus-like particles and capsomeres displaying group A streptococcus hypervariable antigenic determinants., *Biotechnol. Bioeng.* doi:10.1002/bit.25172.
- [5] B. Chackerian, Virus-like particle based vaccines for Alzheimer disease, *Hum. Vaccin.* 6 (11) (2010) 926–930. doi:10.4161/hv.6.11.12655.
- [6] A. Graf, M. Staufienbiel, T. Blaettler, P. Paganetti, Composition comprising vlp and amyloid beta peptide, uS Patent 8,617,566 (Dec. 31 2013).
URL <https://www.google.com/patents/US8617566>

-
- [7] H. Jin, W. Wang, S. Zhao, W. Yang, Y. Qian, N. Jia, G. Feng, $A\beta$ -HBc virus-like particles immunization without additional adjuvant ameliorates the learning and memory and reduces $A\beta$ deposit in PDAPP mice, *Vaccine* 32 (35) (2014) 4450–4456. doi:10.1016/j.vaccine.2014.06.051.
- [8] S. Sharma, A. Whalley, J. McLaughli, F. Brello, B. Bishop, A. Banerjee, Fermentation process technology transfer for production of a recombinant vaccine component, *BioPharm International* 24 (7) (2011) 30–39.
- [9] A. Brown, B. Champion, C. Christy, D. Gervais, L. Jones, A. Kjerrstrom, D. Pryde, L. Roberts, D. Wyatt, Ige ch3 peptide vaccine, uS Patent 8,475,801 (Jul. 2 2013). URL <https://www.google.com/patents/US8475801>
- [10] G. Spohn, C. Schori, I. Keller, K. Sladko, C. Sina, R. Guler, K. Schwarz, P. l. Johansen, G. T. Jennings, M. F. Bachmann, Preclinical efficacy and safety of an anti-IL-1 β vaccine for the treatment of type 2 diabetes, *Mol. Ther. - Methods Clin. Dev.* 1 (April) (2014) 14048. doi:10.1038/mtm.2014.48.
- [11] T. Klamp, J. Schumacher, G. Huber, C. Kühne, U. Meissner, A. Selmi, T. Hiller, S. Kreiter, J. Markl, O. Türeci, U. Sahin, Highly specific auto-antibodies against claudin-18 isoform 2 induced by a chimeric HBcAg virus-like particle vaccine kill tumor cells and inhibit the growth of lung metastases., *Cancer Res.* 71 (2) (2011) 516–27. doi:10.1158/0008-5472.CAN-10-2292.
- [12] M. R. Sheen, P. H. Lizotte, S. Toraya-Brown, S. Fiering, Stimulating antitumor immunity with nanoparticles, *Wiley Interdisciplinary Reviews: Nanomedicine and Nanobiotechnology* 6 (5) (2014) 496–505. doi:10.1002/wnan.1274.
- [13] M. Zochowska, A.-C. Piguet, J. Jemielity, J. Kowalska, E. Szolajska, J.-F. Dufour, J. Chroboczek, Virus-like particle-mediated intracellular delivery of mRNA cap analog with in vivo activity against hepatocellular carcinoma., *Nanomedicine* (2014) 1–10doi:10.1016/j.nano.2014.07.009.
- [14] M. F. Bachmann, P. Whitehead, Active immunotherapy for chronic diseases., *Vaccine* 31 (14) (2013) 1777–84. doi:10.1016/j.vaccine.2013.02.001.
- [15] T. Vicente, A. Roldão, C. Peixoto, M. J. T. Carrondo, P. M. Alves, Large-scale production and purification of VLP-based vaccines., *J. Invertebr. Pathol.* 107 Suppl (2011) S42–8. doi:10.1016/j.jip.2011.05.004.
- [16] A. Roldão, A. C. Silva, M. C. M. Mellado, I. D. Tecnologia, U. N. D. Lisboa, 1 . 47 Viruses and Virus-Like Particles in Biotechnology : Fundamentals and Applications, second edi Edition, Vol. 1, Elsevier B.V., 2011. doi:10.1016/B978-0-08-088504-9.00072-6.
- [17] N. Kushnir, S. J. Streatfield, V. Yusibov, Virus-like particles as a highly efficient vaccine platform: diversity of targets and production systems and advances in clinical development., *Vaccine* 31 (1) (2012) 58–83. doi:10.1016/j.vaccine.2012.10.083.
- [18] P. Pushko, P. Pumpens, E. Grens, Development of virus-like particle technology from small highly symmetric to large complex virus-like particle structures., *Intervirology* 56 (3) (2013) 141–65. doi:10.1159/000346773.
- [19] A. Zeltins, Construction and characterization of virus-like particles: a review., *Mol. Biotechnol.* 53 (1) (2013) 92–107. doi:10.1007/s12033-012-9598-4.

- [20] L. H. L. Lua, N. K. Connors, F. Sainsbury, Y. P. Chuan, N. Wibowo, A. P. J. Middelberg, Bioengineering virus-like particles as vaccines., *Biotechnol. Bioeng.* 111 (3) (2014) 425–40. doi:10.1002/bit.25159.
- [21] M. Brisson, M. Drolet, T. Malagón, Inequalities in Human Papillomavirus (HPV)-associated cancers: implications for the success of HPV vaccination., *J. Natl. Cancer Inst.* 105 (3) (2013) 158–61. doi:10.1093/jnci/djs638.
- [22] C. Harrison, H. Britt, S. Garland, L. Conway, A. Stein, M. Pirotta, C. Fairley, Decreased management of genital warts in young women in Australian general practice post introduction of national HPV vaccination program: results from a nationally representative cross-sectional general practice study., *PLoS One* 9 (9) (2014) e105967. doi:10.1371/journal.pone.0105967.
- [23] S. W. Metz, B. E. Martina, P. van den Doel, C. Geertsema, A. D. Osterhaus, J. M. Vlak, G. P. Pijlman, Chikungunya virus-like particles are more immunogenic in a lethal AG129 mouse model compared to glycoprotein E1 or E2 subunits., *Vaccine* 31 (51) (2013) 6092–6. doi:10.1016/j.vaccine.2013.09.045.
- [24] T. Koho, M. R. L. Koivunen, S. Oikarinen, L. Kummola, S. Mäkinen, A. J. Mähönen, A. Siiofy-Khojine, V. Marjomäki, A. Kazmertsuk, I. Junntila, M. S. Kulomaa, H. Hyöty, V. P. Hytönen, O. H. Laitinen, Coxsackievirus B3 VLPs purified by ion exchange chromatography elicit strong immune responses in mice., *Antiviral Res.* 104 (2014) 93–101. doi:10.1016/j.antiviral.2014.01.013.
- [25] T. Vicente, S. Burri, S. Wellnitz, K. Walsh, S. Rothe, J. Liderfelt, Fully aseptic single-use cross flow filtration system for clarification and concentration of cytomegalovirus-like particles, *Eng. Life Sci.* 14 (3) (2014) 318–326. doi:10.1002/elsc.201300093.
- [26] J. Schmitz, J. Roehrig, A. Barrett, J. Hombach, Next generation dengue vaccines: a review of candidates in preclinical development., *Vaccine* 29 (42) (2011) 7276–84. doi:10.1016/j.vaccine.2011.07.017.
- [27] C.-Y. Chung, C.-Y. Chen, S.-Y. Lin, Y.-C. Chung, H.-Y. Chiu, W.-K. Chi, Y.-L. Lin, B.-L. Chiang, W.-J. Chen, Y.-C. Hu, Enterovirus 71 virus-like particle vaccine: improved production conditions for enhanced yield., *Vaccine* 28 (43) (2010) 6951–7. doi:10.1016/j.vaccine.2010.08.052.
- [28] Z. Ku, Q. Liu, X. Ye, Y. Cai, X. Wang, J. Shi, D. Li, X. Jin, W. An, Z. Huang, A virus-like particle based bivalent vaccine confers dual protection against enterovirus 71 and coxsackievirus A16 infections in mice., *Vaccine* 32 (34) (2014) 4296–303. doi:10.1016/j.vaccine.2014.06.025.
- [29] S. Chandramouli, A. Medina-Selby, D. Coit, M. Schaefer, T. Spencer, L. a. Brito, P. Zhang, G. Otten, C. W. Mandl, P. W. Mason, P. R. Dormitzer, E. C. Settembre, Generation of a parvovirus B19 vaccine candidate., *Vaccine* 31 (37) (2013) 3872–8. doi:10.1016/j.vaccine.2013.06.062.
- [30] L. Buonaguro, M. Tagliamonte, M. L. Visciano, H. Andersen, M. Lewis, R. Pal, M. L. Tornesello, U. Schroeder, J. Hinkula, B. Wahren, F. M. Buonaguro, Immunogenicity of HIV virus-like particles in rhesus macaques by intranasal administration., *Clin. Vaccine Immunol.* 19 (6) (2012) 970–3. doi:10.1128/CVI.00068-12.

-
- [31] A. Negrete, A. Pai, J. Shiloach, Use of hollow fiber tangential flow filtration for the recovery and concentration of HIV virus-like particles produced in insect cells., *J. Virol. Methods* 195 (2014) 240–6. doi:10.1016/j.jviromet.2013.10.017.
- [32] L. Gissmann, HPV vaccines: preclinical development., *Arch. Med. Res.* 40 (6) (2009) 466–70. doi:10.1016/j.arcmed.2009.07.002.
- [33] T. Li, H. Lin, Y. Zhang, M. Li, D. Wang, Y. Che, Y. Zhu, S. Li, J. Zhang, S. Ge, Q. Zhao, N. Xia, Improved characteristics and protective efficacy in an animal model of E. coli-derived recombinant double-layered rotavirus virus-like particles., *Vaccine* 32 (17) (2014) 1921–31. doi:10.1016/j.vaccine.2014.01.093.
- [34] L.-J. Chang, K. a. Dowd, F. H. Mendoza, J. G. Saunders, S. Sitar, S. H. Plummer, G. Yamshchikov, U. N. Sarwar, Z. Hu, M. E. Enama, R. T. Bailer, R. a. Koup, R. M. Schwartz, W. Akahata, G. J. Nabel, J. R. Mascola, T. C. Pierson, B. S. Graham, J. E. Ledgerwood, Safety and tolerability of chikungunya virus-like particle vaccine in healthy adults: a phase 1 dose-escalation trial., *Lancet* 6736 (14) (2014) 25–27. doi:10.1016/S0140-6736(14)61185-5.
- [35] D. Mohammadi, International community ramps up Ebola vaccine effort, *Lancet* 384 (9955) (2014) 1658–1659. doi:10.1016/S0140-6736(14)61788-8.
- [36] J. G. H. Low, L. S. Lee, E. E. Ooi, K. Ethirajulu, P. Yeo, A. Matter, J. E. Connolly, D. a. G. Skibinski, P. Saudan, M. Bachmann, B. J. Hanson, Q. Lu, S. Maurer-Stroh, S. Lim, V. Novotny-Diermayr, Safety and immunogenicity of a virus-like particle pandemic influenza A (H1N1) 2009 vaccine: results from a double-blinded, randomized Phase I clinical trial in healthy Asian volunteers., *Vaccine* 32 (39) (2014) 5041–8. doi:10.1016/j.vaccine.2014.07.011.
- [37] B. J. Ward, N. Landry, S. Trépanier, G. Mercier, M. Dargis, M. Couture, M.-A. D’Aoust, L.-P. Vézina, Human antibody response to N-glycans present on plant-made influenza virus-like particle (VLP) vaccines., *Vaccine* 32 (46) (2014) 6098–106. doi:10.1016/j.vaccine.2014.08.079.
- [38] L. F. Fries, G. E. Smith, G. M. Glenn, A recombinant viruslike particle influenza a (h7n9) vaccine, *New England Journal of Medicine* 369 (26) (2013) 2564–2566, PMID: 24224560. doi:10.1056/NEJMc1313186.
- [39] G. M. Glenn, G. Smith, L. Fries, R. Raghunandan, H. Lu, B. Zhou, D. N. Thomas, S. P. Hickman, E. Kpamegan, S. Boddapati, P. a. Piedra, Safety and immunogenicity of a Sf9 insect cell-derived respiratory syncytial virus fusion protein nanoparticle vaccine., *Vaccine* 31 (3) (2013) 524–32. doi:10.1016/j.vaccine.2012.11.009.
- [40] M.-E. Riviere, A. Caputo, N. Laurent, I. Vostiar, N. Andreasen, S. Cohen, R. W. Kressig, J. M. Ryan, A. Graf, Active Ab Immunotherapy Cad106 Phase Ii Dose-Adjuvant Finding Study: Immune Response, *Alzheimer’s Dement.* 10 (4) (2014) P447–P448. doi:10.1016/j.jalz.2014.05.606.
- [41] A. Caputo, A. Graf, M.-E. Riviere, G. Alva, E. Balaguer, A. Zacharias, R. P. Maguire, J. Sovago, J. M. Ryan, Active Ab Immunotherapy Cad106 Phase Ii Dose-Adjuvant Finding Study: Amyloid Pet, *Alzheimer’s Dement.* 10 (4) (2014) P445–P446. doi:10.1016/j.jalz.2014.05.602.

- [42] D. I. Bernstein, H. M. El Sahly, W. a. Keitel, M. Wolff, G. Simone, C. Segawa, S. Wong, D. Shelly, N. S. Young, W. Dempsey, Safety and immunogenicity of a candidate parvovirus B19 vaccine., *Vaccine* 29 (43) (2011) 7357–63. doi:10.1016/j.vaccine.2011.07.080.
- [43] C. López-Macías, E. Ferat-Osorio, A. Tenorio-Calvo, A. Isibasi, J. Talavera, O. Arteaga-Ruiz, L. Arriaga-Pizano, S. P. Hickman, M. Allende, K. Lenhard, S. Pincus, K. Connolly, R. Raghunandan, G. Smith, G. Glenn, Safety and immunogenicity of a virus-like particle pandemic influenza A (H1N1) 2009 vaccine in a blinded, randomized, placebo-controlled trial of adults in Mexico., *Vaccine* 29 (44) (2011) 7826–34. doi:10.1016/j.vaccine.2011.07.099.
- [44] A. Sundararajan, M. Y. Sangster, S. Frey, R. L. Atmar, W. H. Chen, J. Ferreira, R. Bargatze, P. M. Mendelman, J. J. Treanor, D. J. Topham, Robust mucosal-homing antibody-secreting B cell responses induced by intramuscular administration of adjuvanted bivalent human norovirus-like particle vaccine, *Vaccine* (2014) 1–9doi:10.1016/j.vaccine.2014.09.073.
- [45] B. K. Erickson, E. E. Landers, W. K. Huh, Update on vaccination clinical trials for HPV-related disease., *Clin. Ther.* 36 (1) (2014) 8–16. doi:10.1016/j.clinthera.2013.11.003.
- [46] A. Hildesheim, S. Wacholder, G. Catteau, F. Struyf, G. Dubin, R. Herrero, Efficacy of the HPV-16/18 vaccine: final according to protocol results from the blinded phase of the randomized Costa Rica HPV-16/18 vaccine trial., *Vaccine* 32 (39) (2014) 5087–97. doi:10.1016/j.vaccine.2014.06.038.
- [47] R. Umeh, S. Oguche, T. Oguonu, S. Pitmang, E. Shu, J.-T. Onyia, C. a. Daniyam, D. Shwe, A. Ahmad, E. Jongert, G. Catteau, M. Lievens, O. Ofori-Anyinam, A. Leach, Immunogenicity and safety of the candidate RTS,S/AS01 vaccine in young Nigerian children: A randomized, double-blind, lot-to-lot consistency trial., *Vaccine* 32 (48) (2014) 6556–6562. doi:10.1016/j.vaccine.2014.07.067.
- [48] C. Dochez, J. J. Bogers, R. Verhelst, H. Rees, HPV vaccines to prevent cervical cancer and genital warts: an update., *Vaccine* 32 (14) (2014) 1595–601. doi:10.1016/j.vaccine.2013.10.081.
- [49] E. Lacson, M. Teng, J. Ong, L. Vienneau, N. Ofsthun, J. M. Lazarus, Antibody response to Engerix-B[®] and Recombivax-HB[®] hepatitis B vaccination in end-stage renal disease, *Hemodial. Int.* 9 (2005) 367–375.
- [50] X. Zhang, M. Wei, H. Pan, Z. Lin, K. Wang, Z. Weng, Y. Zhu, L. Xin, J. Zhang, S. Li, N. Xia, Q. Zhao, Robust manufacturing and comprehensive characterization of recombinant hepatitis E virus-like particles in Hecolin[®]., *Vaccine* 32 (32) (2014) 4039–50. doi:10.1016/j.vaccine.2014.05.064.
- [51] M. F. Wilson, R. Blum, P. Dandona, S. A. Mousa, Effects in humans of intravenously administered endotoxin on soluble cell-adhesion molecule and inflammatory markers: a model of human diseases., *Clin. Exp. Pharmacol. Physiol.* 28 (2001) 376–380.
- [52] M. Duchene, J. Descamps, I. Pierard, Immunogenicity of impurities in cell-derived vaccines, in: *Medicines from Animal Cell Culture*, John Wiley & Sons, Ltd, 2007, pp. 491–496. doi:10.1002/9780470723791.ch25.

-
- [53] U.S. Food and Drug Administration, CBER, Guidance for Industry Information and Establishment Description Information for a Vaccine (1999).
- [54] World Health Organization, Guidelines to Assure the Quality, Safety and Efficacy of Recombinant Human Papillomavirus Virus-Like Particle Vaccines (October) (2006) 23–27.
- [55] World Health Organization, Guidelines on the quality , safety and efficacy of recombinant malaria vaccines targeting the pre-erythrocytic and blood stages of *Plasmodium falciparum*.
- [56] U.S. Food and Drug Administration, CBER, FDA Guidance for Industry Characterization and Qualification of Cell Substrates and Other Guidance for Industry Characterization and Qualification of Cell Substrates and Other Biological Materials Used in the Production of Viral Vaccines for Infectious Disease Indications. (2007).
- [57] R. C. T. Partnership, Efficacy and Safety of the RTS,S/AS01 Malaria Vaccine during 18 Months after Vaccination: A Phase 3 Randomized, Controlled Trial in Children and Young Infants at 11 African Sites, *PLoS Med.* 11 (7) (2014) e1001685. doi:10.1371/journal.pmed.1001685.
- [58] L. a. Brito, M. Singh, Acceptable Levels of Endotoxin in Vaccine Formulations During Preclinical Research, *J. Pharm. Sci.* 100 (1) (2011) 34–37. doi:10.1002/jps.
- [59] J. C. Cook, J. G. Joyce, H. a. George, L. D. Schultz, W. M. Hurni, K. U. Jansen, R. W. Hepler, C. Ip, R. S. Lowe, P. M. Keller, E. D. Lehman, Purification of virus-like particles of recombinant human papillomavirus type 11 major capsid protein L1 from *Saccharomyces cerevisiae*., *Protein Expr. Purif.* 17 (3) (1999) 477–84. doi:10.1006/prep.1999.1155.
- [60] T. Wolter, A. Richter, Assays for Controlling Host-Cell Impurities in Biopharmaceuticals, *Bioprocess Int.*
- [61] H. Mach, D. B. Volkin, R. D. Troutman, B. E. I. Wang, Disassembly and Reassembly of Yeast-Derived Recombinant Human Papillomavirus Virus-like Particles (HPV VLPs), *J. Pharm. Sci.* 95 (10) (2006) 2195–2206. doi:10.1002/jps.
- [62] M. P. M. C. McCarthy, W. I. White, F. Palmer-hill, S. Koenig, J. A. Suzich, Quantitative Disassembly and Reassembly of Human Papillomavirus Type 11 Viruslike Particles In Vitro, *J. Virol.* 72 (1) (1998) 32–41.
- [63] Y. Ren, S.-M. Wong, L.-Y. Lim, In vitro-reassembled plant virus-like particles for loading of polyacids., *J. Gen. Virol.* 87 (Pt 9) (2006) 2749–54. doi:10.1099/vir.0.81944-0.
- [64] L. Xing, T.-C. Li, N. Mayazaki, M. N. Simon, J. S. Wall, M. Moore, C.-Y. Wang, N. Takeda, T. Wakita, T. Miyamura, R. H. Cheng, Structure of hepatitis E virion-sized particle reveals an RNA-dependent viral assembly pathway., *J. Biol. Chem.* 285 (43) (2010) 33175–83. doi:10.1074/jbc.M110.106336.
- [65] A. Link, F. Zabel, Y. Schnetzler, A. Titz, F. Brombacher, M. F. Bachmann, Innate immunity mediates follicular transport of particulate but not soluble protein antigen., *J. Immunol.* 188 (8) (2012) 3724–33. doi:10.4049/jimmunol.1103312.

- [66] A. Roldão, M. C. M. Mellado, J. C. Lima, M. J. T. Carrondo, P. M. Alves, R. Oliveira, On the effect of thermodynamic equilibrium on the assembly efficiency of complex multi-layered virus-like particles (VLP): the case of rotavirus VLP., *PLoS Comput. Biol.* 8 (2) (2012) e1002367. doi:10.1371/journal.pcbi.1002367.
- [67] Q. Zhao, M. J. Allen, Y. Wang, B. Wang, N. Wang, L. Shi, R. D. Sitrin, Disassembly and reassembly improves morphology and thermal stability of human papillomavirus type 16 virus-like particles., *Nanomedicine* 8 (7) (2012) 1182–9. doi:10.1016/j.nano.2012.01.007.
- [68] Q. Zhao, Y. Modis, K. High, V. Towne, Y. Meng, Y. Wang, J. Alexandroff, M. Brown, B. Carragher, C. S. Potter, D. Abraham, D. Wohlpart, M. Kosinski, M. W. Washabaugh, R. D. Sitrin, Disassembly and reassembly of human papillomavirus virus-like particles produces more virion-like antibody reactivity., *Viol. J.* 9 (1) (2012) 52. doi:10.1186/1743-422X-9-52.
- [69] L. Zhang, R. Tang, S. Bai, N. K. Connors, L. H. L. Lua, Y. P. Chuan, A. P. J. Middelberg, Y. Sun, Molecular energetics in the capsomere of virus-like particle revealed by molecular dynamics simulations., *J. Phys. Chem. B* 117 (18) (2013) 5411–21. doi:10.1021/jp311170w.
- [70] L. Zhang, R. Tang, S. Bai, N. K. Connors, L. H. L. Lua, Y. P. Chuan, A. P. J. Middelberg, Y. Sun, Energetic changes caused by antigenic module insertion in a virus-like particle revealed by experiment and molecular dynamics simulations., *PLoS One* 9 (9) (2014) e107313. doi:10.1371/journal.pone.0107313.
- [71] L. Shi, G. Sanyal, A. Ni, Z. Luo, S. Doshna, B. Wang, T. L. Graham, N. Wang, D. B. Volkin, Stabilization of human papillomavirus virus-like particles by non-ionic surfactants., *J. Pharm. Sci.* 94 (7) (2005) 1538–51. doi:10.1002/jps.20377.
- [72] Y. Ding, Y. P. Chuan, L. He, A. P. J. Middelberg, Modeling the competition between aggregation and self-assembly during virus-like particle processing., *Biotechnol. Bioeng.* 107 (3) (2010) 550–60. doi:10.1002/bit.22821.
- [73] S. P. Sánchez-rodríguez, L. Münch-anguiano, O. Echeverría, G. Vázquez-nin, M. Morapale, J. S. Dordick, I. Bustos-jaimés, Human parvovirus B19 virus-like particles : In vitro assembly and stability, *Biochimie* 94 (3) (2012) 870–878. doi:10.1016/j.biochi.2011.12.006.
- [74] S. Tsoka, O. C. Ciniawskyj, O. R. Thomas, N. J. Titchener-Hooker, M. Hoare, Selective flocculation and precipitation for the improvement of virus-like particle recovery from yeast homogenate., *Biotechnol. Prog.* 16 (4) (2000) 661–7. doi:10.1021/bp0000407.
- [75] Z. Jiang, G. Tong, B. Cai, Y. Xu, J. Lou, Purification and immunogenicity study of human papillomavirus 58 virus-like particles expressed in *Pichia pastoris*., *Protein Expr. Purif.* 80 (2) (2011) 203–10. doi:10.1016/j.pep.2011.07.009.
- [76] H. Lünsdorf, C. Gurramkonda, A. Adnan, N. Khanna, U. Rinas, Virus-like particle production with yeast: ultrastructural and immunocytochemical insights into *Pichia pastoris* producing high levels of the hepatitis B surface antigen., *Microb. Cell Fact.* 10 (1) (2011) 48. doi:10.1186/1475-2859-10-48.
- [77] M. Iammarino, J. Nti-gyabaah, M. Chandler, D. Roush, K. Göklen, Impact of Cell Density and Viability on Primary Clarification of Mammalian Cell Broth, *Bioprocess Int.*

-
- [78] P. E. Cruz, C. C. Peixoto, K. Devos, L. Moreira, E. Saman, M. J. T. Carrondo, Characterization and downstream processing of HIV-1 core and virus-like-particles produced in serum free medium, *Enzyme Microb. Technol.* 26 (2000) 61–70.
- [79] C. Peixoto, M. F. Q. Sousa, a. C. Silva, M. J. T. Carrondo, P. M. Alves, Downstream processing of triple layered rotavirus like particles., *J. Biotechnol.* 127 (3) (2007) 452–61. doi:10.1016/j.jbiotec.2006.08.002.
- [80] Y. Yigzaw, R. Piper, M. Tran, A. a. Shukla, Exploitation of the adsorptive properties of depth filters for host cell protein removal during monoclonal antibody purification., *Biotechnol. Prog.* 22 (1) (2006) 288–96. doi:10.1021/bp050274w.
- [81] E. B. Schirmer, M. Kuczewski, K. Golden, B. Lain, C. Bragg, J. Chon, M. Cacciuttolo, G. Zarbis-papastoitsis, Primary Clarification of Very High-Density Cell Culture Harvests By Enhanced Cell Settling, *Bioprocess Int.*
- [82] M. Y. Jaffrin, Dynamic filtration with rotating disks, and rotating and vibrating membranes: an update, *Curr. Opin. Chem. Eng.* 1 (2) (2012) 171–177. doi:10.1016/j.coche.2012.01.002.
- [83] T. Vicente, M. F. Sousa, C. Peixoto, J. P. Mota, P. M. Alves, M. J. Carrondo, Anion-exchange membrane chromatography for purification of rotavirus-like particles, *J. Memb. Sci.* 311 (1-2) (2008) 270–283. doi:10.1016/j.memsci.2007.12.021.
- [84] A. A. Shukla, M. R. Etzel, S. Gadam, *Process Scale Bioseparations for the Biopharmaceutical Industry*, Taylor & Francis Group, 2007.
- [85] I. R. M. Juckes, C. Town, Fractionation of proteins and viruses with polyethylene glycol, *Biochim. Biophys. Acta* 229 (1971) (1971) 535–546.
- [86] M. Summa, C.-H. von Bonsdorff, L. Maunula, Evaluation of four virus recovery methods for detecting noroviruses on fresh lettuce, sliced ham, and frozen raspberries., *J. Virol. Methods* 183 (2) (2012) 154–60. doi:10.1016/j.jviromet.2012.04.006.
- [87] A. R. Kattur Venkatachalam, M. Szyporta, T. K. Kiener, P. Balraj, J. Kwang, Concentration and purification of enterovirus 71 using a weak anion-exchange monolithic column., *Virol. J.* 11 (1) (2014) 99. doi:10.1186/1743-422X-11-99.
- [88] J. P. Phelps, N. Dang, L. Rasochova, Inactivation and purification of cowpea mosaic virus-like particles displaying peptide antigens from *Bacillus anthracis*., *J. Virol. Methods* 141 (2) (2007) 146–53. doi:10.1016/j.jviromet.2006.12.008.
- [89] T. Koho, T. Mäntylä, P. Laurinmäki, L. Huhti, S. J. Butcher, T. Vesikari, M. S. Kulomaa, V. P. Hytönen, Purification of norovirus-like particles (VLPs) by ion exchange chromatography., *J. Virol. Methods* 181 (1) (2012) 6–11. doi:10.1016/j.jviromet.2012.01.003.
- [90] S. W. Metz, J. Gardner, C. Geertsema, T. T. Le, L. Goh, J. M. Vlak, A. Suhrbier, G. P. Pijlman, Effective chikungunya virus-like particle vaccine produced in insect cells., *PLoS Negl. Trop. Dis.* 7 (3) (2013) e2124. doi:10.1371/journal.pntd.0002124.
- [91] S. Matheus, W. Friess, D. Schwartz, H.-C. Mahler, Liquid high concentration IgG1 antibody formulations by precipitation., *J. Pharm. Sci.* 98 (9) (2009) 3043–57. doi:10.1002/jps.21526.

- [92] C. Knevelman, J. Davies, L. Allen, N. J. Titchener-Hooker, High-throughput screening techniques for rapid peg-based precipitation of igg4 mab from clarified cell culture supernatant., *Biotechnol. Prog.* 26 (3). doi:10.1002/btpr.357.
- [93] R. Sommer, A. Tscheliessnig, P. Satzer, H. Schulz, B. Helk, A. Jungbauer, Capture and intermediate purification of recombinant antibodies with combined precipitation methods, *Biochem. Eng. J.* 93 (2015) 200–211. doi:10.1016/j.bej.2014.10.008.
- [94] M. Kuczewski, E. Schirmer, B. Lain, G. Zarbis-Papastoitis, A single-use purification process for the production of a monoclonal antibody produced in a PER.C6 human cell line., *Biotechnol. J.* 6 (1) (2011) 56–65. doi:10.1002/biot.201000292.
- [95] S. Oelmeier, C. Ladd-Effio, J. Hubbuch, Alternative separation steps for monoclonal antibody purification: Combination of centrifugal partitioning chromatography and precipitation, *J. Chromatogr. A* 1319 (2013) 118–126.
- [96] D. H. Atha, K. C. Ingham, Mechanism of Precipitation of Proteins by Polyethylene Glycols, *J. Biol. Chem.* 256 (23) (1981) 12108–12117.
- [97] T. Odijk, Depletion theory and the precipitation of protein by polymer., *J. Phys. Chem. B* 113 (12) (2009) 3941–6. doi:10.1021/jp806722j.
- [98] S.-L. Sim, T. He, A. Tscheliessnig, M. Mueller, R. B. H. Tan, A. Jungbauer, Protein precipitation by polyethylene glycol: a generalized model based on hydrodynamic radius., *J. Biotechnol.* 157 (2) (2012) 315–9. doi:10.1016/j.jbiotec.2011.09.028.
- [99] J. T. Lis, R. Schleif, Size fractionation of double -stranded DNA by precipitation with polyethylene glycol, *Nucleic Acids Res.* 2 (3) (1975) 383–389.
- [100] A. Jungbauer, R. Hahn, Polymethacrylate monoliths for preparative and industrial separation of biomolecular assemblies., *J. Chromatogr. A* 1184 (1-2) (2008) 62–79. doi:10.1016/j.chroma.2007.12.087.
- [101] J.-B. Qu, X.-Z. Wan, Y.-Q. Zhai, W.-Q. Zhou, Z.-G. Su, G.-H. Ma, A novel stationary phase derivatized from hydrophilic gigaporous polystyrene-based microspheres for high-speed protein chromatography., *J. Chromatogr. A* 1216 (37) (2009) 6511–6. doi:10.1016/j.chroma.2009.07.059.
- [102] H. Thomas, B. Coquebert de Neuville, G. Storti, M. Morbidelli, M. Joehnck, M. Schulte, Role of tentacles and protein loading on pore accessibility and mass transfer in cation exchange materials for proteins., *J. Chromatogr. A* 1285 (2013) 48–56. doi:10.1016/j.chroma.2013.01.104.
- [103] V. Orr, L. Zhong, M. Moo-Young, C. P. Chou, Recent advances in bioprocessing application of membrane chromatography., *Biotechnol. Adv.* 31 (4) (2013) 450–65. doi:10.1016/j.biotechadv.2013.01.007.
- [104] P. O. Michel, A. R. Mäkelä, E. Korhonen, J. Toivola, L. Hedman, M. Söderlund-Venermo, K. Hedman, C. Oker-Blom, Purification and analysis of polyhistidine-tagged human parvovirus B19 VP1 and VP2 expressed in insect cells., *J. Virol. Methods* 152 (1-2) (2008) 1–5. doi:10.1016/j.jviromet.2008.06.006.

-
- [105] D. I. Lipin, A. Raj, L. H. L. Lua, A. P. J. Middelberg, Affinity purification of viral protein having heterogeneous quaternary structure: modeling the impact of soluble aggregates on chromatographic performance., *J. Chromatogr. A* 1216 (30) (2009) 5696–708. doi:10.1016/j.chroma.2009.05.082.
- [106] Y. Nishimura, K. Takeda, J. Ishii, C. Ogino, A. Kondo, An affinity chromatography method used to purify His-tag-displaying bio-nanocapsules., *J. Virol. Methods* 189 (2) (2013) 393–6. doi:10.1016/j.jviromet.2013.03.008.
- [107] N. Ohtaki, H. Takahashi, K. Kaneko, Y. Gomi, T. Ishikawa, Y. Higashi, M. Todokoro, T. Kurata, T. Sata, A. Kojima, Purification and concentration of non-infectious West Nile virus-like particles and infectious virions using a pseudo-affinity Cellufine Sulfate column., *J. Virol. Methods* 174 (1-2) (2011) 131–5. doi:10.1016/j.jviromet.2011.03.021.
- [108] H. J. Kim, S. J. Lim, H.-L. Kwag, H.-J. Kim, The choice of resin-bound ligand affects the structure and immunogenicity of column-purified human papillomavirus type 16 virus-like particles., *PLoS One* 7 (4) (2012) e35893. doi:10.1371/journal.pone.0035893.
- [109] Y. R. Choi, H. J. Kim, J. Y. Lee, H. A. Kang, H.-J. Kim, Chromatographically-purified capsid proteins of red-spotted grouper nervous necrosis virus expressed in *Saccharomyces cerevisiae* form virus-like particles., *Protein Expr. Purif.* 89 (2) (2013) 162–8. doi:10.1016/j.pep.2013.03.007.
- [110] P. Guo, Y. El-Gohary, K. Prasadana, C. Shiota, X. Xiao, J. Wiersch, J. Paredes, S. Tulachan, G. K. Gittes, Rapid and simplified purification of recombinant adeno-associated virus., *J. Virol. Methods* 183 (2) (2012) 139–46. doi:10.1016/j.jviromet.2012.04.004.
- [111] W. Zhou, J. Bi, J.-C. Janson, A. Dong, Y. Li, Y. Zhang, Y. Huang, Z. Su, Ion-exchange chromatography of hepatitis B virus surface antigen from a recombinant Chinese hamster ovary cell line., *J. Chromatogr. A* 1095 (1-2) (2005) 119–25. doi:10.1016/j.chroma.2005.08.006.
- [112] L. Urbas, B. L. Jarc, M. Barut, M. Zochowska, J. Chroboczek, B. Pihlar, E. Szolajska, Purification of recombinant adenovirus type 3 dodecahedral virus-like particles for biomedical applications using short monolithic columns., *J. Chromatogr. A* 1218 (17) (2011) 2451–9. doi:10.1016/j.chroma.2011.01.032.
- [113] J. Tomé-Amat, L. Fleischer, S. a. Parker, C. Bardliving, C. Batt, Secreted production of assembled Norovirus virus-like particles from *Pichia pastoris*., *Microb. Cell Fact.* 13 (1) (2014) 134. doi:10.1186/s12934-014-0134-z.
- [114] M. D. Wenger, P. Dephillips, C. E. Price, D. G. Bracewell, An automated microscale chromatographic purification of virus-like particles as a strategy for process development., *Biotechnol. Appl. Biochem.* 47 (Pt 2) (2007) 131–9. doi:10.1042/BA20060240.
- [115] P. Gagnon, B. Godfrey, D. Ladd, Method for obtaining unique selectivities in ion-exchange chromatography by addition of organic polymers to the mobile phase, *J. Chromatogr. A* 743 (1) (1996) 51–55. doi:10.1016/0021-9673(96)00125-2.
- [116] M. a. Snyder, P. Ng, H. Mekosh, P. Gagnon, PEG enhances viral clearance on ceramic hydroxyapatite., *J. Sep. Sci.* 32 (23-24) (2009) 4048–51. doi:10.1002/jssc.200900156.
- [117] J. Lee, H. T. Gan, S. M. A. Latiff, C. Chuah, W. Y. Lee, Y.-S. Yang, B. Loo, S. K. Ng, P. Gagnon, Principles and applications of steric exclusion chromatography., *J. Chromatogr. A* 1270 (2012) 162–70. doi:10.1016/j.chroma.2012.10.062.

- [118] P. Gagnon, P. Toh, J. Lee, High productivity purification of immunoglobulin G monoclonal antibodies on starch-coated magnetic nanoparticles by steric exclusion of polyethylene glycol., *J. Chromatogr. A* 1324 (2014) 171–80. doi:10.1016/j.chroma.2013.11.039.
- [119] F. Oehme, J. Peters, Mixed-mode chromatography in downstream process development, *BioPharm Int.*
- [120] C. S. Burden, J. Jin, A. Podgornik, D. G. Bracewell, A monolith purification process for virus-like particles from yeast homogenate., *J. Chromatogr. B* 880 (1) (2012) 82–9. doi:10.1016/j.jchromb.2011.10.044.
- [121] P. a. J. Rosa, I. F. Ferreira, a. M. Azevedo, M. R. Aires-Barros, Aqueous two-phase systems: A viable platform in the manufacturing of biopharmaceuticals., *J. Chromatogr. A* 1217 (16) (2010) 2296–305. doi:10.1016/j.chroma.2009.11.034.
- [122] J. Benavides, M. Rito-Palomares, J. A. Asenjo, *Aqueous Two-Phase Systems*, second Edition, Vol. 1, Elsevier B.V., 2011. doi:10.1016/B978-0-08-088504-9.00124-0.
- [123] M. Wiendahl, S. a. Oelmeier, F. Dismer, J. Hubbuch, High-throughput screening-based selection and scale-up of aqueous two-phase systems for pDNA purification., *J. Sep. Sci.* 35 (22) (2012) 3197–207. doi:10.1002/jssc.201200310.
- [124] J. Muendges, I. Stark, S. Mohammad, A. Górak, T. Zeiner, Fluid Phase Equilibria Single stage aqueous two-phase extraction for monoclonal antibody purification from cell supernatant, *Fluid Phase Equilib.* 385 (2015) 227–236. doi:10.1016/j.fluid.2014.10.034.
- [125] J. K. Eggersgluess, M. Richter, M. Dieterle, J. Strube, Multi-Stage Aqueous Two-Phase Extraction for the Purification of Monoclonal Antibodies, *Chem. Eng. Technol.* 37 (4) (2014) 675–682. doi:10.1002/ceat.201300604.
- [126] P. a. J. Rosa, a. M. Azevedo, S. Sommerfeld, W. Bäcker, M. R. Aires-Barros, Continuous aqueous two-phase extraction of human antibodies using a packed column., *J. Chromatogr. B. Analyt. Technol. Biomed. Life Sci.* 880 (1) (2012) 148–56. doi:10.1016/j.jchromb.2011.11.034.
- [127] I. Sutherland, P. Hewitson, R. Siebers, R. van den Heuvel, L. Arbenz, J. Kinkel, D. Fisher, Scale-up of protein purifications using aqueous two-phase systems: comparing multilayer toroidal coil chromatography with centrifugal partition chromatography., *J. Chromatogr. A* 1218 (32) (2011) 5527–30. doi:10.1016/j.chroma.2011.04.013.
- [128] D. F. C. Silva, a. M. Azevedo, P. Fernandes, V. Chu, J. P. Conde, M. R. Aires-Barros, Design of a microfluidic platform for monoclonal antibody extraction using an aqueous two-phase system., *J. Chromatogr. A* 1249 (2012) 1–7. doi:10.1016/j.chroma.2012.05.089.
- [129] K. Schügerl, J. Hubbuch, Integrated bioprocesses., *Curr. Opin. Microbiol.* 8 (3) (2005) 294–300. doi:10.1016/j.mib.2005.01.002.
- [130] P. Diederich, S. Amrhein, F. Hämmerling, J. Hubbuch, Evaluation of PEG/phosphate aqueous two-phase systems for the purification of the chicken egg white protein avidin by using high-throughput techniques, *Chem. Eng. Sci.* 104 (2013) 945–956. doi:10.1016/j.ces.2013.10.008.

-
- [131] J. Benavides, J. a. Mena, M. Cisneros-Ruiz, O. T. Ramírez, L. a. Palomares, M. Rito-Palomares, Rotavirus-like particles primary recovery from insect cells in aqueous two-phase systems., *J. Chromatogr. B. Analyt. Technol. Biomed. Life Sci.* 842 (1) (2006) 48–57. doi:10.1016/j.jchromb.2006.05.006.
- [132] F. Luechau, T. C. Ling, A. Lyddiatt, Recovery of B19 virus-like particles by aqueous two-phase systems, *Food Bioprod. Process.* 89 (4) (2011) 322–327. doi:10.1016/j.fbp.2010.10.008.
- [133] M. Rito-Palomares, A. P. Middelberg, Aqueous two-phase systems for the recovery of a recombinant viral coat protein from *Escherichia coli*, *J. Chem. Technol. Biotechnol.* 77 (9) (2002) 1025–1029. doi:10.1002/jctb.673.
- [134] a. Arpanaei, a. Heebø ll Nielsen, J. J. Hubbuch, O. R. T. Thomas, T. J. Hobley, Critical evaluation and comparison of fluid distribution systems for industrial scale expanded bed adsorption chromatography columns., *J. Chromatogr. A* 1198–1199 (2008) 131–9. doi:10.1016/j.chroma.2008.05.044.
- [135] M. Y. T. Ng, W. S. Tan, N. Abdullah, T. C. Ling, B. T. Tey, Effect of different operating modes and biomass concentrations on the recovery of recombinant hepatitis B core antigen from thermal-treated unclarified *Escherichia coli* feedstock., *J. Biotechnol.* 138 (3–4) (2008) 74–9. doi:10.1016/j.jbiotec.2008.08.004.
- [136] W. B. Yap, B. T. Tey, N. B. M. Alitheen, W. S. Tan, Purification of His-tagged hepatitis B core antigen from unclarified bacterial homogenate using immobilized metal affinity-expanded bed adsorption chromatography., *J. Chromatogr. A* 1217 (21) (2010) 3473–80. doi:10.1016/j.chroma.2010.03.012.
- [137] R. Cabrera, A. Lihme, K. Oishi, I. Vaarst, Methods for capturing virus like particles from plants using expanded bed chromatography, wO Patent App. PCT/EP2011/068,919 (2012).
URL <http://www.google.com/patents/WO2012055986A9?cl=en>
- [138] S. Pincus, S. Boddapati, J. Li, T. Sadowski, Release and stability testing programs for a novel virus-like particle vaccine, *BioPharm Int.*
- [139] GE Healthcare, Removal of DNA and baculovirus from influenza virus-like particles using CaptoTM Q (2011).
- [140] G. Iyer, S. Ramaswamy, D. Asher, U. Mehta, A. Leahy, F. Chung, K.-S. Cheng, Reduced surface area chromatography for flow-through purification of viruses and virus like particles., *J. Chromatogr. A* 1218 (26) (2011) 3973–81. doi:10.1016/j.chroma.2011.04.086.
- [141] G. Iyer, S. Ramaswamy, K.-S. Cheng, N. Sisowath, U. Mehta, A. Leahy, F. Chung, D. Asher, Flow-Through Purification of Viruses- A Novel Approach to Vaccine Purification, *Procedia Vaccinol.* 6 (2012) 106–112. doi:10.1016/j.provac.2012.04.015.
- [142] H. J. Kim, S. Y. Kim, S. J. Lim, J. Y. Kim, S. J. Lee, H.-J. Kim, One-step chromatographic purification of human papillomavirus type 16 L1 protein from *Saccharomyces cerevisiae*., *Protein Expr. Purif.* 70 (1) (2010) 68–74. doi:10.1016/j.pep.2009.08.005.
- [143] J. C. Cook III, Process for purifying human papillomavirus virus-like particles, uS Patent 6,602,697 (Aug. 5 2003).

- [144] E. Schmoeger, C. Paril, R. Tscheliessnig, A. Jungbauer, Adsorption of plasmid DNA on ceramic hydroxyapatite chromatographic materials., *J. Sep. Sci.* 33 (20) (2010) 3125–36. doi:10.1002/jssc.201000318.
- [145] J. M. Wagner, J. D. Pajerowski, C. L. Daniels, P. M. McHugh, J. a. Flynn, J. W. Balliet, D. R. Casimiro, S. Subramanian, Enhanced production of Chikungunya virus-like particles using a high-pH adapted *Spodoptera frugiperda* insect cell line., *PLoS One* 9 (4) (2014) e94401. doi:10.1371/journal.pone.0094401.
- [146] B. C. Bundy, J. R. Swartz, Efficient disulfide bond formation in virus-like particles., *J. Biotechnol.* 154 (4) (2011) 230–9. doi:10.1016/j.jbiotec.2011.04.011.
- [147] S. Mukherjee, M. V. Thorsteinsson, L. B. Johnston, P. a. DePhillips, A. Zlotnick, A quantitative description of in vitro assembly of human papillomavirus 16 virus-like particles., *J. Mol. Biol.* 381 (1) (2008) 229–37. doi:10.1016/j.jmb.2008.05.079.
- [148] M. W. O. Liew, Y. P. Chuan, A. P. J. Middelberg, Reactive diafiltration for assembly and formulation of virus-like particles, *Biochem. Eng. J.* 68 (2012) 120–128. doi:10.1016/j.bej.2012.07.009.
- [149] N. K. Jain, N. Sahni, O. S. Kumru, S. B. Joshi, D. B. Volkin, C. Russell Middaugh, Formulation and stabilization of recombinant protein based virus-like particle vaccines, *Adv. Drug Deliv. Rev.* doi:10.1016/j.addr.2014.10.023.
- [150] Z. Yu, J. C. Reid, Y.-P. Yang, Utilizing dynamic light scattering as a process analytical technology for protein folding and aggregation monitoring in vaccine manufacturing., *J. Pharm. Sci.* 102 (12) (2013) 4284–90. doi:10.1002/jps.23746.
- [151] Y. P. Tan, T. C. Ling, W. S. Tan, K. Yusoff, B. T. Tey, Purification of recombinant nucleocapsid protein of Newcastle disease virus from unclarified feedstock using expanded bed adsorption chromatography., *Protein Expr. Purif.* 46 (1) (2006) 114–21. doi:10.1016/j.pep.2005.06.015.
- [152] F.-S. Quan, M.-C. Kim, B.-J. Lee, J.-M. Song, R. W. Compans, S.-M. Kang, Influenza M1 VLPs containing neuraminidase induce heterosubtypic cross-protection., *Virology* 430 (2) (2012) 127–35. doi:10.1016/j.virol.2012.05.006.
- [153] A. S. Rathore, H. Winkle, Quality by design for biopharmaceuticals, *Nat. Biotechnol.* 27 (1).
- [154] C. a. Brooks, S. M. Cramer, Steric mass-action ion exchange: Displacement profiles and induced salt gradients, *AIChE J.* 38 (12) (1992) 1969–1978. doi:10.1002/aic.690381212.
- [155] T. Hahn, A. Sommer, A. Osberghaus, V. Heuveline, J. Hubbuch, Adjoint-based estimation and optimization for column liquid chromatography models, *Comput. Chem. Eng.* 64 (2014) 41–54. doi:10.1016/j.compchemeng.2014.01.013.
- [156] T. C. Huuk, T. Hahn, A. Osberghaus, J. Hubbuch, Model-based integrated optimization and evaluation of a multi-step ion exchange chromatography, *Sep. Purif. Technol.* 136 (2014) 207–222. doi:10.1016/j.seppur.2014.09.012.
- [157] M. Bensch, P. Schulze Wierling, E. von Lieres, J. Hubbuch, High Throughput Screening of Chromatographic Phases for Rapid Process Development, *Chem. Eng. Technol.* 28 (11) (2005) 1274–1284. doi:10.1002/ceat.200500153.

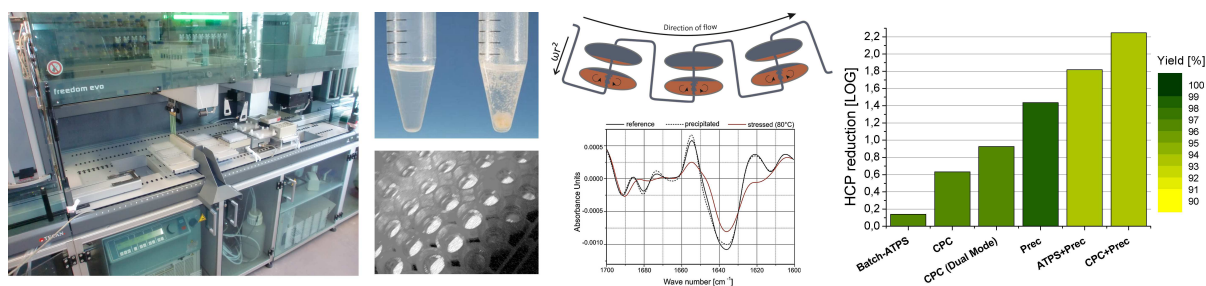
-
- [158] M. Wiendahl, P. Schulze Wierling, J. Nielsen, D. Fomsgaard Christensen, J. Krarup, a. Staby, J. Hubbuch, High Throughput Screening for the Design and Optimization of Chromatographic Processes - Miniaturization, Automation and Parallelization of Breakthrough and Elution Studies, *Chem. Eng. Technol.* 31 (6) (2008) 893–903. doi:10.1002/ceat.200800167.
- [159] S. A. Oelmeier, C. Ladd Effio, J. Hubbuch, High throughput screening based selection of phases for aqueous two-phase system-centrifugal partitioning chromatography of monoclonal antibodies, *J. Chromatogr. A* 1252 (2012) 104–114.
- [160] Y. Wu, J. Simons, S. Hooson, D. Abraham, G. Carta, Protein and virus-like particle adsorption on perfusion chromatography media., *J. Chromatogr. A* 1297 (2013) 96–105. doi:10.1016/j.chroma.2013.04.062.
- [161] L. F. Pease, D. I. Lipin, D.-H. Tsai, M. R. Zachariah, L. H. L. Lua, M. J. Tarlov, A. P. J. Middelberg, Quantitative characterization of virus-like particles by asymmetrical flow field flow fractionation, electrospray differential mobility analysis, and transmission electron microscopy., *Biotechnol. Bioeng.* 102 (3) (2009) 845–55. doi:10.1002/bit.22085.
- [162] J. Mohr, Y. P. Chuan, Y. Wu, L. H. L. Lua, A. P. J. Middelberg, Virus-like particle formulation optimization by miniaturized high-throughput screening., *Methods* 60 (3) (2013) 248–56. doi:10.1016/j.ymeth.2013.04.019.
- [163] G. K. Shoemaker, E. van Duijn, S. E. Crawford, C. Uetrecht, M. Baclayon, W. H. Roos, G. J. L. Wuite, M. K. Estes, B. V. V. Prasad, A. J. R. Heck, Norwalk virus assembly and stability monitored by mass spectrometry., *Mol. Cell. Proteomics* 9 (2010) 1742–1751. doi:10.1074/mcp.M900620-MCP200.
- [164] C. Uetrecht, I. M. Barbu, G. K. Shoemaker, E. van Duijn, A. J. R. Heck, Interrogating viral capsid assembly with ion mobility-mass spectrometry., *Nat. Chem.* 3 (2011) 126–132. doi:10.1038/nchem.947.
- [165] C. Ladd Effio, J. Hubbuch, Virus-like particle and nano-particle vaccines 2014 - session 10 technology, *Human Vaccines & Immunotherapeutics* doi:10.4161/hv.29840.
- [166] S. Heider, C. Metzner, Quantitative real-time single particle analysis of virions., *Virology* 462-463 (2014) 199–206. doi:10.1016/j.virol.2014.06.005.
- [167] N. Brestrich, T. Briskot, A. Osberghaus, J. Hubbuch, A tool for selective inline quantification of co-eluting proteins in chromatography using spectral analysis and partial least squares regression., *Biotechnol. Bioeng.* 111 (7) (2014) 1365–73. doi:10.1002/bit.25194.
- [168] B. T. J. Hahn, D. Courbron, M. Hamer, M. Masoud, J. Wong, K. Taylor, J. Hatch, M. Sowers, E. Shane, M. Nathan, H. U. A. Jiang, Z. Wei, J. Higgins, K.-h. Roh, J. Burd, D. Chinchilla-olszar, M. Malou-williams, D. P. Baskind, G. E. Smith, Rapid Manufacture and Release of a GMP Batch of Avian Influenza A(H7N9) Virus-Like Particle Vaccine Made Using Recombinant Baculovirus-Sf9 Insect Cell Culture Technology, *Bioprocess. J.* 12 (2013) 1–10.
- [169] T. Kröber, M. W. Wolff, B. Hundt, a. Seidel-Morgenstern, U. Reichl, Continuous purification of influenza virus using simulated moving bed chromatography, *J. Chromatogr. A* 1307 (2013) 99–110. doi:10.1016/j.chroma.2013.07.081.

3 PUBLICATIONS & MANUSCRIPTS

- [170] P. Nestola, R. J. S. Silva, C. Peixoto, P. M. Alves, M. J. T. Carrondo, J. P. B. Mota, Adenovirus purification by two-column, size-exclusion, simulated countercurrent chromatography., *J. Chromatogr. A* 1347 (2014) 111–21. doi:10.1016/j.chroma.2014.04.079.

Alternative Separation Steps for Monoclonal Antibody Purification: Combination of Centrifugal Partition Chromatography and Precipitation

S. A. Oelmeier^{1, 2,*}, C. Ladd Effio¹ and J. Hubbuch¹



¹ : Institute of Process Engineering in Life Sciences, Section IV: Biomolecular Separation Engineering, Karlsruhe Institute of Technology, Engler-Bunte-Ring 1, 76131 Karlsruhe, Germany

² : Boehringer Ingelheim Pharma GmbH & Co. KG, Birkendorfer Str. 65, 88400 Biberach an der Riß, Germany

* : Corresponding author. *E-mail address:* stefan.oelmeier@kit.edu (S. A. Oelmeier)

J. Chrom. A (2013), doi:10.1016/j.chroma.2013.10.043

Abstract

Protein drugs continue to grow both in medicinal importance as in scale of their production. This fur- thers the interest in separation technologies that have the potential to replace chromatographic steps in a protein purification process. Two such unit operations that are employed in large scale in the chemical industry are extraction and precipitation. Their usefulness for the purification of proteins has been demonstrated, but the integration of such unit operations in a way that generate an output stream of high protein concentration and low process related impurities was missing. In this work, we employ centrifugal partition chromatography (CPC) in combination with precipitation of the protein of interest to purify a cell culture supernatant of a monoclonal antibody producing cell line. Centrifugal partition chromatography was used as means of multi-step extraction using aqueous two-phase systems and was able to remove up to 88.2% of host cell protein (HCP). The following PEG driven precipitation and resolubilization of the protein of interest was use to condition the CPC output stream to suit subsequent chromatographic steps, to increase mAb concentration, remove the phase forming polymer, further improve HCP clearance, and integrate a low pH hold step for viral clearance. The entire process reduced HCP content by 99.4% while recovering 93% of the protein of interest. High throughput screening techniques were extensively employed during the development of the process.

Keywords: Aqueous two-phase partitioning, Centrifugal partition chromatography, Precipitation, Monoclonal antibody, Biopurification process design

1 Introduction

Proteinaceous drugs are continually increasing in importance both economically and medically. All protein drugs are produced in a process that can roughly be divided into three steps: fermentation of the product (“upstream process”), purification of the product (“downstream process”) and the creation of a commercial product by final formulation and filling. With a single molecule class (monoclonal antibodies) gaining utmost importance over the recent decade the pharmaceutical industry has centered and matured around these molecules. While fermentation was optimized to yield increasingly more product, the downstream process was standardized into platform processes fitting most new molecules of this class. As fermentation titers increase an inevitable need to scale or number up the purification unit operations arises as downstream processes scale by mass rather than volume. Current plant footprints and chromatography skid sizes are finite. Thus, two options to reduce processing cost and footprint have recently been come into focus: alternative separations steps operating at high concentrations and (semi-)continuous processing. Two alternative unit operations amenable to semi-continuous processing are precipitation and extraction [1, 2]. However, the application of these process steps to pharmaceutical products is still very limited. There is hardly any experience with these process steps in large scale, neither on their application than on the reaction of regulatory agencies to such non chromatographic purification steps. The preparative purification of proteins by precipitation or aqueous two-phase extraction is widely acknowledged as simple and easily scalable process step. Precipitation has been demonstrated to be applicable to monoclonal antibody (mAb) solutions both at the very beginning and very end of a process. Matheus *et. al* [3] demonstrated the use of precipitation by either PEG or salts for the purpose of creating highly concentrated mAb solutions during drug formulation. Knevelman *et. al* [4] demonstrated the use of PEG precipitation as initial process step in the recovery of IgG₄ from cell culture supernatants. The application of aqueous two-phase extraction to mAb purification has recently been extensively studied by Aires-Barros and coworkers. They initially demonstrated the application of single stage ATPS [5] to mAb-HCP separation. They continued in demonstrating the integration of an ATPS step into a traditional chromatography based purification train by either loading the salt rich bottom phase onto a HIC column [6] or the polymer rich top phase onto a cation exchange resin [7]. Finally, multi-step cross-current extractions using a polymer-polymer ATPS were evaluated by Rosa *et. al* [8]. Our group has contentiously worked on implementing small scale screening methods for both ATPS [9, 10] and precipitation [11]. Building on the work of Sutherland *et. al* [12, 13] and Ito *et. al* [14] we have recently combined the established high throughput screenings for both ATPS and precipitation conditions in order to facilitate the selection of conditions for centrifugal partition chromatography [15]. It was shown that such multi-step extraction methods can readily be applied to protein separation, also in the context of pharmaceutical production. The remaining major practical obstacle to the application of precipitation and aqueous two-phase extraction is creating an output stream from these unit operations that is high in protein concentration and low in conductivity and polymer content so that the integration into a whole purification process can be readily achieved. In this work, we demonstrate how aqueous two-phase extraction in the form of centrifugal partition chromatography can be combined with precipitation and resolubilization of the target protein to yield a highly pure and concentrated product stream. The resulting output stream can also be directly applied to subsequent chromatographic purification steps thus resulting in a seamless process integration of the investigated unit operations.

2 Materials & Methods

2.1 Disposables

For spectroscopic measurements Greiner Bio-One (Kremsmünster, Austria) 350 μL -UV-Star plates were used. Precipitation studies were conducted in 350 μL -AcroPrepTM 96 Filter Plates (Pall Corporation, Port Washington, NY) containing a Bio-Inert[®] (modified low protein-binding Nylon) 0.2 μm membrane. ATPS were prepared in 1 mL-96 Deep Well plates (Nalgen Nunc International, Rochester, NY, USA). For all other purposes Greiner Bio-One 350 μL -polypropylene flat bottom MTPs were used.

2.2 Chemicals & Stock Solutions

PEG 400, PEG 600, and PEG 1000 were obtained from Merck KGaA (Darmstadt, Germany). PEG 1450 and Trisodium citrate were purchased from Sigma-Aldrich (St. Louis, MO). Citric acid was obtained from Merck KGaA (Darmstadt, Germany). Stock solutions were prepared in dH_2O as follows: 70% (w/w) PEG 400, 70% (w/w) PEG 600, 60% (w/w) PEG 1000, 60% (w/w) PEG 1450, 40% (w/w) PEG 4000, 35% (w/w) citric acid, 35% (w/w) trisodium citrate. Citrate stock solutions for ATPS were combined as follows: 96.43 g trisodium citrate solution and 3.57 g citric acid solution to yield pH 6.0. All other chemicals were obtained from Merck KGaA (Darmstadt, Germany).

2.3 Protein Solutions

Three monoclonal antibodies ('mAb1', 'mAb2', 'mAb4') and a corresponding HCP pool were supplied by Boehringer Ingelheim Pharma GmbH & Co. KG (Ingelheim am Rhein, Germany). All mAbs were derived from CHO cell culture and were of the same subtype IgG1. The mAbs were supplied as active pharmaceutical ingredient (API). If needed, protein concentration in the API solutions was increased by ultrafiltration using a 30 kDa MWCO membrane as described earlier [10]. Protein stock solutions used for precipitation and ATPS ranged in concentration from 4 to 25 mg/mL. The mAb free flow-through obtained from a Protein A chromatography step of clarified cell culture fluid (CCF) of a mAb producing cell line was used as HCP pool. This host cell protein (HCP) solution was concentrated by a factor of 10 to yield the HCP stock. UV absorption gave a HCP concentration of 4.1 g/L for the 10x solution.

2.4 Liquid Handling Station

In this study, a Tecan Freedom Evo 200 system (Tecan, Crailsheim, Germany) was used as liquid handling platform. Liquid handling calibration and set-up were described earlier [10]. Solid-liquid-separation by filtration was accomplished by using an integrated vacuum station "Te-Vacs" (Tecan, Crailsheim, Germany).

2.5 Software

Excel 2007 (Microsoft, Redmond, WA) files were used as import format and for data storage. All calculations, evaluation, and visualization of data were done using Matlab R2011a (The Mathworks, Natick, ME) and OriginPro[®]8.1G (OriginLab Corporation, Northampton). The robotic workstation was controlled using Evoware 2.3 (Tecan, Crailsheim, Germany). The spectrophotometer was controlled using Magellan 6.4 (Tecan, Crailsheim, Germany). The CPC column was controlled by Armen glider CPC software (Armen Instrument, Vannes, France).

2.6 High-throughput Screening Methods

2.6.1 Automated Precipitation Procedure

In order to find applicable precipitants for the separation of proteins as well as an explanation for partitioning in ATPS, protein solubility curves provide important information. Hence, solubility of 1 mg/mL mAb1, mAb2, mAb4 and 0.41 mg/mL HCP were analyzed separately for different concentrations of PEG 400, PEG 600, PEG 1000, PEG 1450, PEG 4000 and Citrate pH 6.0. Due to the high experimental demand a precipitation screening on the liquid handling station was used. Each data point was measured at least in triplicates. First, systems of 300 μL total volume were put together in filter plates: water and precipitant were dispensed and after an intermediate mixing step on an orbital shaker (1000 rpm, 2 min) protein solution was added followed by another mixing step (1000 rpm, 5 min). All liquids were pipetted using the system's fixed tips with the appropriate deposited calibration curves for the stock solutions. To ensure equilibrium, systems were incubated for 30 minutes. At last, systems were filtrated (700 mbar pressure difference, 15 min) to remove aggregates and 30 μL permeate samples were diluted with 270 μL dH₂O before UV-measurement. Protein concentration was finally determined by UV280 absorption comparing samples to a reference with known concentration (external standard).

2.6.2 Automated Precipitation and Redissolving Procedure

Re-dissolution of precipitates in an appropriate buffer was accomplished by an extension of the described precipitation screening. The method consisted basically upon three process steps, each followed by filtration: precipitation, washing and re-dissolution. After precipitation the protein precipitates were washed by dispensing 300 μL of a washing buffer containing the same precipitant concentration as during the precipitation step. Washing was achieved by first mixing precipitate and washing buffer (1000 rpm, 5 min) and second filtering the mixture (700 mbar, 15 min). The last process step was the re-dissolution of the protein precipitates in citrate buffer. 300 μL of either 20 mM Citrate pH 6 or 0.1 M Citrate pH 3 were dispensed and mixed with the protein precipitates (1000 rpm, 30 min). Finally systems were again filtrated and the permeate samples analyzed as in the precipitation procedure. All precipitate-re-dissolution screenings were done with PEG 4000 in 50 mM Citrate pH 6 and each data point was measured at least in triplicates.

2.6.3 Binodal and Tie Line Determination

Binodal curves and tie lines were measured to select reasonable screening ranges. Semi-automated binodal determination was done using the "cloud point method" as described previously [10]. Systems were put together and mixed in UV-plates on the liquid handling station and phase separation was determined by visual inspection. While one-phase systems stay clear, two-phase systems become opaque after mixing. In a series of increasing phase forming component concentration, one point on the binodal was identified as the mean of adjacent data points between which phase separation was observed. Systems containing a dye known to partition exclusively into the upper phase (methylviolet) were used to determine phase volumes as described before [16]. Tie lines were then calculated by the lever arm rule. The average tieline slope was calculated based on five to ten different system compositions. Binodals and tie lines were determined for four different ATPS. All ATPS were composed of PEG (molecular weights: 400, 600, 1000 and 1450 Da) and citrate buffer with a pH of 6.0. Binodal data was fitted to equation 1 as described by Merchuk *et al.* [17].

$$[PEG] = a * \exp(b * [Citrate]^{0.5} + c * [Citrate]^3) \quad (1)$$

2.6.4 Automated ATPE Procedure

As binodals, tie lines and solubility curves of mAbs and HCP were determined, adequate data points with a volume ratio of 1 were selected for analyzing protein partitioning. The method used for ATPS screening was established and described earlier by our group [16, 10]. Distribution and recovery of 1 mg/mL mAb1, mAb2, mAb4 and 0.41 mg/mL HCP were determined by UV280 absorption comparing samples to external standards. Based on the average tieline slope, five total system compositions (termed 'systems points' throughout this manuscript (SPs)) were selected for each of the four PEG molecular weights for increasing tieline lengths (table 1). Protein distribution and phase volumes were measured at least in triplicate, blank values at least in duplicate. Mean values of protein distribution and recovery are reported throughout this manuscript. Distribution coefficients were calculated as the ratio of protein concentration in the upper phase to the concentration in the lower phase. Promising system points were further investigated by increasing antibody concentration from 1 up to 8 mg/mL.

Table 1 The five total system compositions of PEG400-citrate systems used in this study. The term 'system point' ('SP') is used throughout this study to refer to the compositions given in this table.

SP#	% PEG 400 [w/w]	% Citrate [w/w]
SP1	19.26	18.84
SP2	19.74	18.85
SP3	21.02	18.99
SP4	22.18	19.22
SP5	23.26	19.51

2.7 Centrifugal Partition Chromatography

Centrifugal partition chromatography ('CPC') experiments were performed on an Armen 500 mL CPC column (Armen Instrument, Vannes, France). It is equipped with one 500 mL rotor containing 42 stacked discs with a total of 1008 bipartite chambers or 24 per disc. Each chamber has a volume of 424 μ L. An Armen Instruments HPLC pump delivered solvent flow to the column. An Äkta prime (GE Healthcare) system was used for online UV and conductivity signals as well as fraction collection.

CPC experiments were conducted with either the upper or lower phase of an ATPS as mobile phase. Prior to each run ATPS (SP3: 21.02 w% PEG 400, 18.99 w% citrate) was prepared in 2.5 kg scale by dissolving 525.5 g PEG 400, 521.73 g trisodium citrate dihydrate and 18.55 g citric acid monohydrate in dH₂O. Thereafter the system was incubated for 30 min in a separating funnel. For protein purification 40 mL CCF ATPS with the same composition as the 2.5 kg ATPS were prepared in standard beaker glass. Stock solutions of phase forming components and dH₂O were combined as required and the systems mixed on a magnetic stirrer. After this initial mixing step, protein stock solution was added as last component followed by another mixing step. The obtained systems were then incubated in a separating funnel for 30 min. Samples of both phases were taken, diluted 1:10 and analyzed for mAb and HCP content by ProteinA-HPLC and ELISA.

A basic requirement for an efficient separation of two components in CPC is the stability of the inserted two phase system, i.e. the retention of the stationary phase Sf. The CPC was operated in Ascending Mode using the upper phase as mobile phase. Before adding proteins the goal was to find ideal operating conditions yielding in a high retention of the stationary

phase Sf. Hence, using a Design of Experiments approach five operating points with different flow rates from 5 to 15 mL/min and rotational speeds from 1500 to 2500 rpm were selected for describing ATPS behavior in CPC. For column equilibration with the stationary phase, the column was operated at 500 rpm and 1.5 CV lower phase were pumped into the column displacing distilled storage water with a flow rate of 50 mL/min. Successful displacement of water was checked by conductivity measurements. Fraction collection and UV and conductivity measurement were started together with delivery of mobile phase to the column. Fraction size was 10 mL. The elution was conducted for at least 90 minutes. Samples were analyzed for stationary phase content using graduated fraction containers to determine column composition and stability. The operating point inducing the highest retention of the stationary phase was then used for a purification experiment with 5 mg/mL mAb2 and 0.41 mg/mL HCP. 10 mL upper phase of the appropriate CCF-ATPS were injected in a sample loop of the CPC. 10 minutes after starting the elution with upper phase the sample was injected onto the column by allowing the mobile phase to flow through the loop before entering the column. Protein fractions were identified by UV signals and mAb and HCP contents were analyzed as described below. For further optimization mAb2 was processed again at the same operating point, but in Dual Mode, i.e. switching between upper and lower phase as mobile phase. Dual Mode [18, 19] is a CPC operating mode that prevents continuous backmixing of components extracted by one phase with those from the opposed phase. Thus, it was assumed to increase resolution and simultaneously decrease product dilution. After 10 mL sample loading as described above 1.2 CV lower phase were pumped through the column in order to extract contaminants. Finally, the purified sample was eluted with the upper phase as mobile phase.

2.8 Analytical Methods

2.8.1 Protein Quantification

In high throughput screenings, the protein content was measured by UV-absorption at 280 nm with appropriate blanks subtracted and by comparison to a reference sample with known concentration (external standard). CPC fractions were analyzed by ProteinA-HPLC for mAb concentration. HCP content in CPC fractions and after precipitation and re-dissolution were measured using a proprietary ELISA-like assay. The assay relies on the binding of host cell proteins by specific antibodies and the subsequent quantification of the host cell protein - antibody complexes.

2.8.2 Fourier Transform Infrared Spectroscopy (FTIR)

Preservation of the native secondary protein structure is a major requirement in the development of alternative purification techniques for therapeutic proteins. Thus, infrared spectra of 2 mg/mL mAb solutions after precipitation and re-dissolution and reference samples were recorded using a Confocheck FTIR-system (Bruker Optik GmbH, Ettlingen, Germany) equipped with a BioATR II cell (Attenuated Total Reflectance). Prior to FTIR-analysis all samples were diafiltered with Vivaspin-filters (30.000 MWCO PES, Sartorius Stedim Biotech, Gttingen, D) into 20 mM citrate pH 6.0. 20 μ L of each sample were measured with the BioATR-cell automatically subtracting the signal of the buffer solution. Recorded infrared spectra were displayed by Bruker Software Opus as vector-normalized second derivative amide I spectra.

3 Results

3.1 Precipitation & Redissolving

Precipitations of the monoclonal antibodies used in this study and the appropriate HCP pool were performed for two reasons. First, the selection of suitable ATPS conditions for centrifugal partition chromatography at a preparative scale was done using the solubility guided process development approach previously described [15]. Second, precipitation was evaluated as a possible alternative purification methods. Figure 1 shows selected results from these precipitation experiments. In figure 1(a) the recovery of mAb2 and HCP is plotted against the weight percent of PEG used for precipitation. A clear influence of the molecular weight of the PEG can be seen. The antibody stayed in solution up to 36 % [w/w] of PEG 400. The last PEG concentration at which full recovery was observed was reduced to 24 % [w/w] for PEG 600, 18 % [w/w] for PEG 1000, 12 % [w/w] for PEG 1450, and 4% [w/w] for PEG 4000. The other two antibodies investigated showed very similar results (data not shown). While the mAbs were prone to precipitation, HCP stayed in solution with an average recovery of 77 % at 42% [w/w] PEG. HCP recovery was influenced less strongly by changes in the molecular weight of PEG and for easier illustration of the data, the average recovery of HCP when precipitated with all but PEG 4000 is shown in figure 1(a). The data clearly indicated that HCP depletion through precipitation of the antibody was likely. Figure 1(b) shows the recoveries of mAb1, mAb2, mAb4, and HCP when precipitated with PEG 4000. It can be seen that all antibodies follow a similar trend while showing slight differences in their susceptibility for precipitation. With HCP recoveries of at least 75% in the permeate, a PEG 4000 concentration of 15% [w/w] was deemed most promising, as no antibody was recoverable in the supernatant at this PEG concentration for all three mAbs tested.

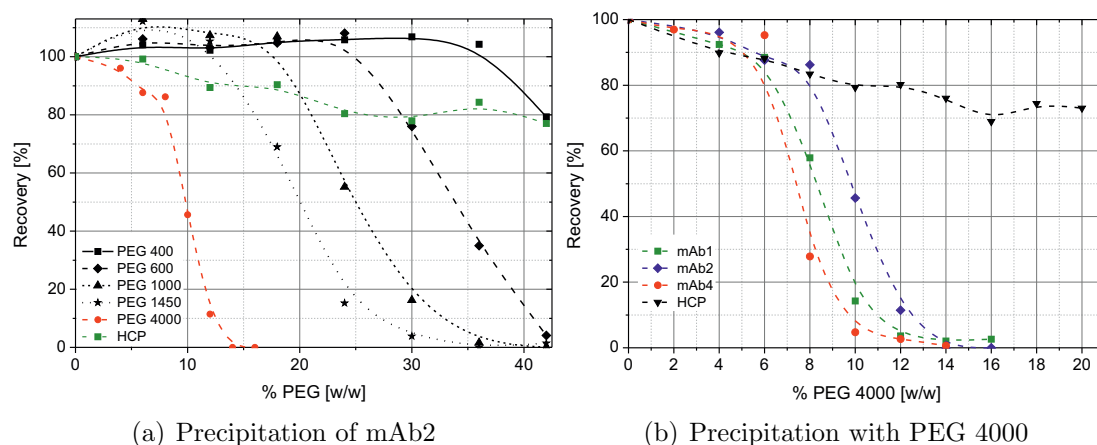


Figure 1 Selected results from the precipitation screenings. Datapoints represent the mean value of triplicates, lines are interpolations to guide the eye. **(a):** Precipitation of the most soluble mAb used in this study with PEGs of different molecular weight. Precipitations were performed at 1 g/L mAb concentration, 0.41 g/L HCP concentration and pH 6.0. Results shown for HCP represent the average recovery of precipitations performed with PEG 400, 600, 1000, and 1450. **(b):** Precipitation of all mAbs used in this study and an appropriate HCP pool with PEG4000. Precipitations were performed at protein concentrations of 1 g/L for mAbs and 0.41 g/L for HCP at pH 6.0.

In order to use precipitation of the target protein as a process step, the precipitate needs to be readily redissolvable and the protein needs to stay in its active conformation. Two conditions to redissolve mAb precipitates were tested. The buffer in which the protein had initially been pre-

precipitated and a citrate buffer at pH 3.0. The latter was chosen to incorporate into the process a low pH hold viral inactivation step as the one incorporated into the standard mAb process after ProteinA elution. Table 2 show the results of these experiments. Recoveries above 93% and reductions of HCP by more than 89% were found under all conditions. With recoveries close to 100% and HCP depletions above 96.4% results were better when redissolving the precipitate at pH 3.0 than at pH 6.0.

Table 2 HCP reduction and mAb recovery after precipitation of a mixture of 1 g/L mAb and 0.41 g/l HCP in 50 mM citrate buffer at pH 6.0 with 15 %[w/w] PEG4000 and subsequent redissolving of the precipitated protein in either 20 mM citrate buffer at pH 6.0 or 100 mM citrate buffer at pH 3.0.

Protein	pH	HCP-Reduction [%]	Recovery [%]
mAb1	pH 6	90.6	94.0
	pH 3	96.4	100
mAb2	pH 6	89.1	96.2
	pH 3	96.4	98.4
mAb4	pH 6	90.9	93.3
	pH 3	97.6	99.3

FT-IR spectroscopy measurement of the mAbs before and after the precipitation and redissolving procedure were performed to check for significant structural changes. The raw absorption spectrum and its second derivative of mAb2 are shown in figure 2(a) and 2(b). To illustrate the difference in FT-IR spectra caused by denaturation, a heat treated sample of mAb2 was added to the analysis. From figure 2 it can be seen that the spectra and their second derivative of mAb2 before and after precipitation and redissolving differ only insignificantly compared to the heat treated sample. It should be noted that the results from mAb2 were chosen as an illustration, as the observed spectral difference was largest for this protein. Additionally, the redissolved protein was investigated for ProteinA binding by ProteinA-HPLC. No significant change in ProteinA binding was observed.

3.2 Batch Partitioning in PEG400/Citrate-Systems

Prior to batch partitioning of proteins, binodal and tieline data of the PEG-citrate systems were obtained. Figure 3 shows the resulting binodals and gives the average tieline slope determined for PEG 400, 600, 1000, and 1450-citrate systems. Additionally, the three fit-factors for equation 1 are given. The binodals showed the expected trend of shifting towards the origin of the plot with increasing PEG molecular weight. Average tieline slopes also showed the expected trend of decreasing with increasing PEG molecular weight. For the further progress in the solubility guided process development it is important to note that for all PEG molecular weights except of PEG 400, the concentration of the non-dominating phase forming component was (Citrate in the upper phase, PEG in the lower phase) significantly below 5% in both phases. Accordingly, only in PEG400 systems the influence of the non-dominating phase forming component were taken into account in the solubility measurements by adding 5% PEG400 to the precipitant.

Batch ATPS distribution experiments were performed for three monoclonal antibodies and a corresponding HCP pool. The results for PEG 400-citrate systems are plotted in figure 4, with

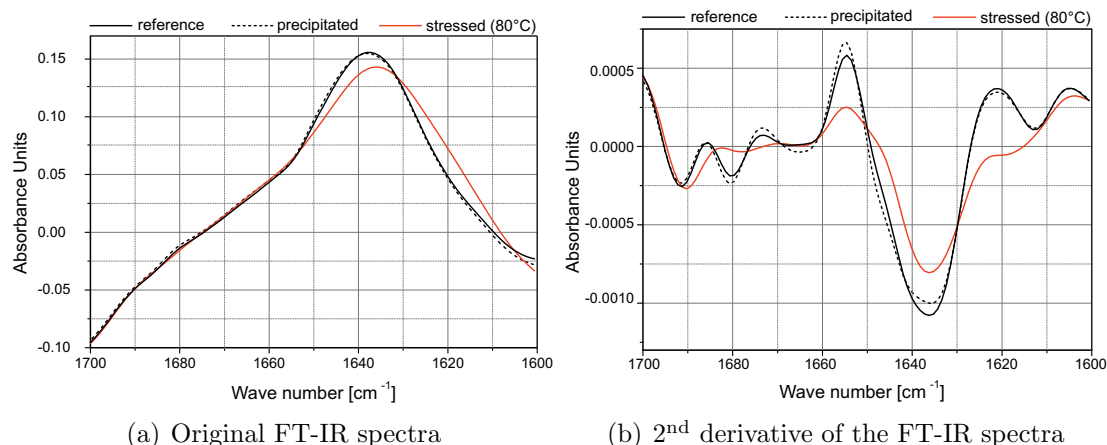


Figure 2 FT-IR spectra of mAb2 at 2 g/L and pH 6.0. 'Reference': unprocessed mAb2, 'Precipitated': mAb2 precipitated by 15 % PEG4000 at 2 g/L, pH 6.0 and redissolved in 20 mM citrate buffer pH 6.0, 'stressed': mAb2 at 2 g/L subjected to 80°C for 10 minutes.

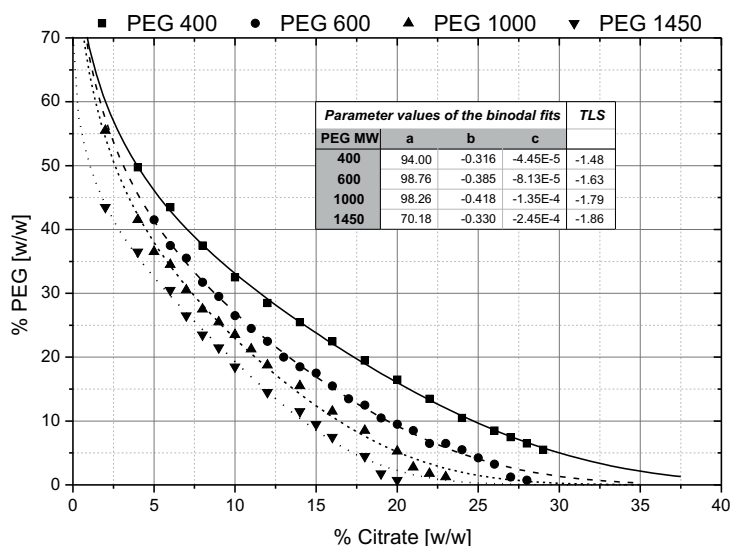


Figure 3 Binodals of PEG-Citrate aqueous two-phase systems measured by the automated turbidity methods. Data was fitted to equation 1 as described by Merchuk *et al.* [17]. The parameter values of the resulting fit are given in the table included in the graph. The column headed 'TLS' in the table gives the average tieline slope determined for the corresponding PEG MW using phase volume determination and the lever arm rule.

figures 4(a) to 4(c) showing results of mAb1, mAb2, and mAb4 respectively, and figure 4(d) the results of HCP. The concentration of the phase forming components is plotted on the axes. Along the axes, bar plots show the recoveries that resulted of the precipitation experiments. The binodal and the tielines of the systems used is plotted, with a dot plot representing the protein recovery in each of the two phases. The distribution coefficient can be inferred from the recoveries in the top and bottom phase. As can be seen from figure 4, the precipitation experiments show a good qualitative correlation to the distribution of the proteins. mAbs showed a strong distribution into the upper phase with distribution coefficients in the range of 60 to 200. The HCP pool showed a significantly differed distribution with distribution coefficients of 1.6 to 2.0. While the mass balance for HCP was closed within the experimental certainty, recovery of mAbs decreased with increasing tieline length. The effect was different for all mAbs with

mAb4 showing the strongest (100% down to 11%) and mAb2 showing the weakest influence (100% down to 90%).

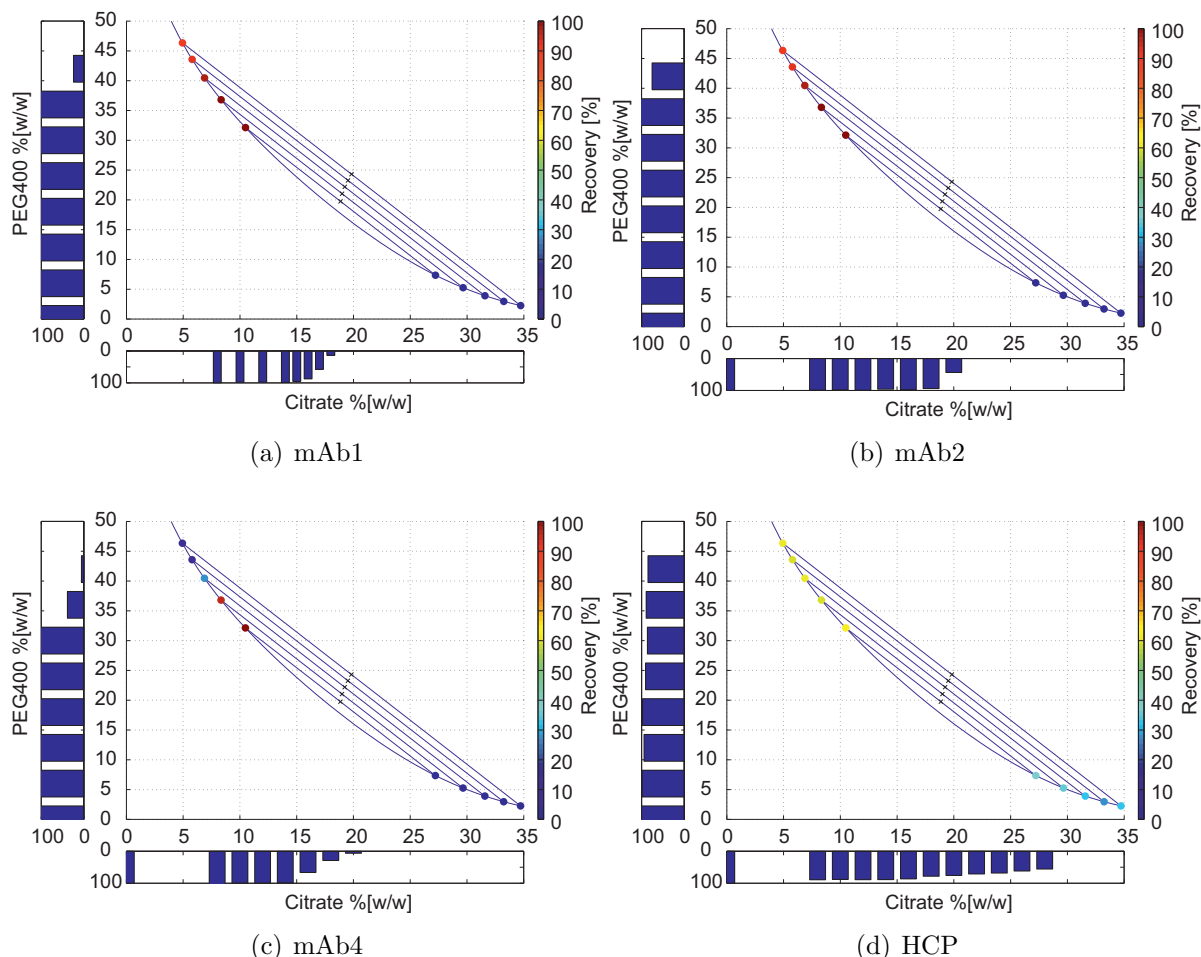


Figure 4 Results of the batch ATPS screenings using PEG400-Citrate systems. Bar plots along the axes show results of precipitation experiments with the phase forming components. Binodal and tielines are shown. 'x' corresponds to the total system composition. The recoveries in top and bottom phase are shown as color coded dots at the composition of the respective top and bottom phase. The distributions coefficient can be deduced from the shown recoveries. Protein concentrations were at 1.0 g/L for all experiments with mAbs and at 0.41 g/L for all experiments with HCP.

The correlation between precipitation data and ATPS distribution of the mAbs suggested that there was an influence of the total protein concentration in the system on the measured distribution coefficient. In order to evaluate this influence and to determine the maximum capacity of the system, the most soluble mAb, mAb2, was distributed in PEG 400 SP3 systems at different total protein concentrations. Figure 5 shows the resulting mAb2 concentrations in the top and bottom phase as a function of the total protein concentration in the systems. For all concentrations shown, the mass balance was closed within the experimental certainty. The top phase concentration showed an approximate linear correlation to the total system concentration, the bottom phase concentration increased only slightly with increasing total system concentration. Total protein concentrations of 8 g/L, resulting in top phase concentrations of approximately 13 g/L, could be accommodated in the system without loss of product. As can be seen in 5 a slight downwards curvature can be seen in the top phase concentrations. This could be a sign of a

beginning capacity limitation of the top phase. As no significant loss of product was observed, capacity limitation in the tested range seem negligible. Additionally, the decrease in top phase concentration relative to the total system concentration might also be a result of slight changes in the volume ratio of the phases in reaction to the changes in protein content. Higher mAb concentrations were not tested due to limitations in the available stock solution concentration and mAb mass.

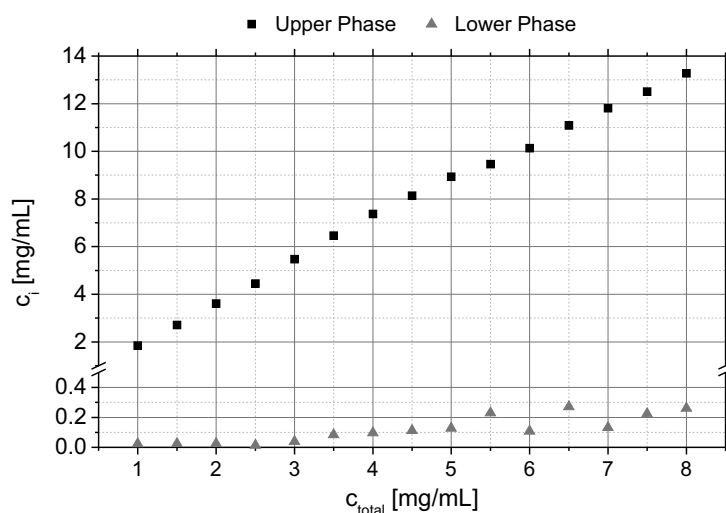


Figure 5 Top and bottom phase concentration of mAb2 in batch PEG400 SP3 systems as a function of total system concentration of mAb2.

3.3 Centrifugal Partition Chromatography

For the CPC experiments the combination of mAb2 and SP3 of the PEG 400 citrate systems were chosen. This system point in combination with this protein had shown a high capacity and the highest distribution coefficient. Additionally, SP3 is the longest tieline for which full recovery in the top phase was observed. Longer tielines were considered more robust in terms of the CPC process, as small changes in system composition carry less risk of shifting the system into the single-phase region. The amount of stationary phase retained in the column and the column back pressure generated under different operating conditions were evaluated in a standard two level full factorial designed experiment. Figure 6 shows the results of these experiments as contour plots. From figure 6(a) it can be seen that the stationary phase ratio S_f was more strongly influenced by the flow-rate than by the rotational speed. S_f declined with increasing flow-rate from 0.53 at 5 mL/min to 0.29 at 15 mL/min. S_f values were slightly higher at higher rotational speed. Column back-pressure in contrast was influence strongly by both parameters with higher flow-rates and lower rotational speed causing less back-pressure. At low RPMs, the effect of flow-rate was less pronounced than at higher RPMs. Highest back-pressure, 4 MPa, was observed at 2500 RPM and 5 mL/min. Lowest back-pressure, 1.5 to 1.6 MPa, was observed at 1500 RPMs and 5 to 15 mL/min respectively. Based on these observations, operating conditions of 5 mL/min and 1500 RPM were chosen for the purification of mAb2. Figure 7 shows resulting elution profiles of SP3 systems run in the CPC at 5 mL/min and 2500 RPM both in regular injection-elution mode as well as in dual mode as described in the methods section. Figure 7(a) shows the elution profile of mAb2 and HCP from a 10 mL injection of an SP3 top phase. While the antibody eluted in one comparably narrow peak between fractions

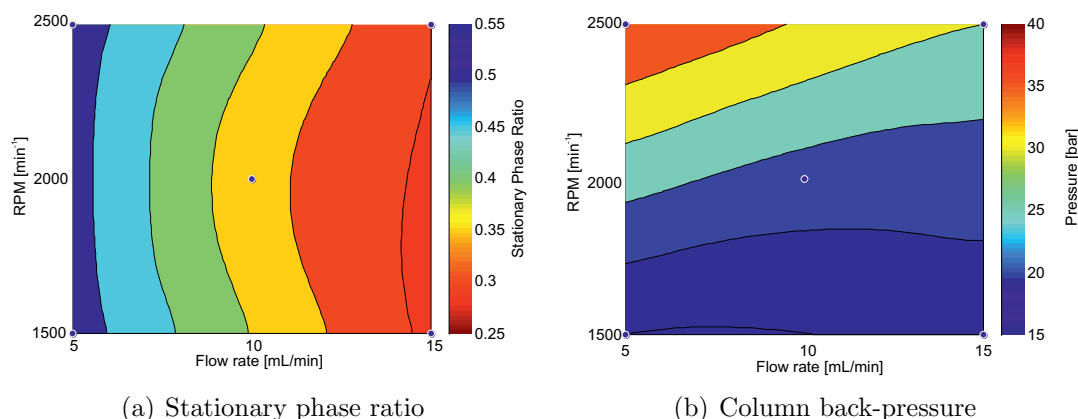


Figure 6 Evaluation of CPC operating conditions on the stationary phase ratio and column back-pressure using a PEG400 SP3 system. Contour plot were generated using cubic interpolation. **(a):** Stationary phase ratio S_f , **(b):** Column back-pressure

37 and 41, the HCP elution showed two distinct peaks. One of the HCP peaks co-eluted with the antibody, while the second one stretched from fraction 42 to 47. It should be noted that the mass balance for mAb2 was closed considering the single elution peak and that the mAb2 concentration was reduced fourfold by the process step. Mass balance for HCP was not closed even when taking into account both elution peaks. 67.9 % of the injected HCP was not found within the analyzed fractions. Figure 7(b) shows the online conductivity and UV280 traces recorded in a dual mode run, using an SP3 system and a sample volume of 10 mL. Data shown start directly after switching to the bottom phase as mobile phase. With the bottom phase being the mobile phase, a steep increase in conductivity was observed. After approximately one column volume, an increase in UV280 was observed. The fractions were tested and were found to contain HCP but no mAb2. After elution with 620 mL bottom phase, the mobile phase was switched back to the top phase. mAb2 co-eluted with the mobile phase after 850 mL. An HCP reduction of 88.2% was reached. The dilution of the mAb2 after elution was 2.3 fold while the mass balance for the mAb closed within the experimental certainty.

3.4 Combination of Process Steps

ATPS and CPC separation of mAb2 from HCP was combined with mAb2 precipitation and re-dissolving in order to increase mAb2 concentration and reduce polymer concentration in the solution. Table 3 shows both HCP reduction and mAb2 recoveries of the combination of process steps.

While a single batch ATPS step only yielded 27.4 % HCP reduction, switching from batch mode to CPC increased the HCP reduction to 76.7% in regular mode and 88.2% in dual mode while not changing the mAb2 recovery of 96.9%. A single precipitation step reduced HCP by 96.3% with mAb2 recovery at 98.4%. Combining ATPS either in batch mode or in CPC mode with a precipitation and re-dissolving step gave HCP clearances of 98.5% and 99.4% respectively while reducing the mAb2 recovery slightly to 93.4 and 93.0%.

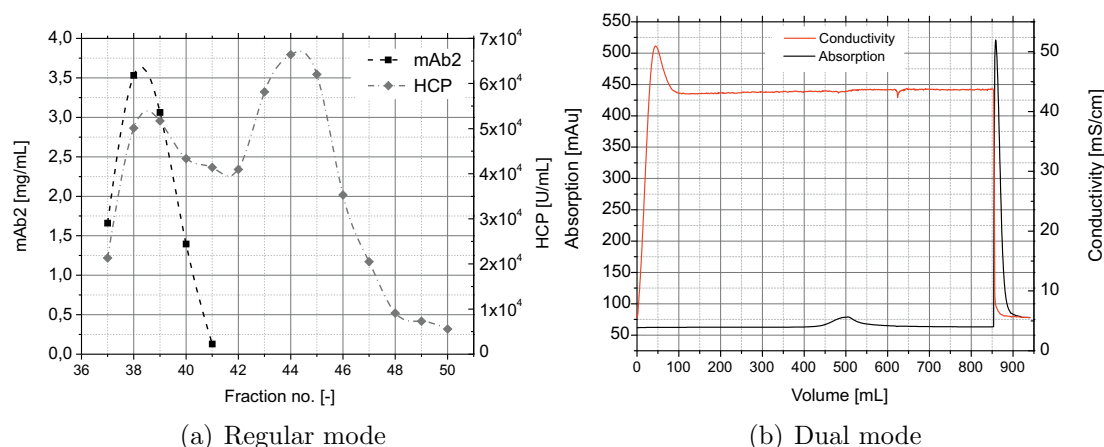


Figure 7 (a): Elution profile of a CPC run performed with SP3 of PEG400. Operating conditions were: 5 mL/min, 2500 RPM. Sample volume: 10 mL. Sample composition: top phase of an SP3 system with total concentrations of 5 g/L mAb2 and 0.41 g/L HCP. **(b):** UV280 and conductivity trace of a CPC run performed in dual mode using an SP3 system and 10 mL load. Elution of HCP after 500 mL was clearly resolved from the elution of mAb after 850 mL.

Table 3 HCP reductions and mAb2 recoveries of different process steps and combinations thereof. Batch ATPS was performed in PEG400-Citrate SP3 systems - results of batch-ATPS are given for the top phase. Precipitation & re-dissolving was performed using 15% [w/w] PEG4000 at pH 6.0 to precipitate and 100 mM citric acid buffer at pH 3.0 to redissolve. Precipitation after CPC was done using 20% [w/w] PEG4000. The mAb2 concentration in these experiments was 1 g/L.

Process step	HCP-Reduction [%]	mAb-Recovery [%]
Batch-ATPS	27.4	96.9
CPC (Ascending Mode)	76.7	96.9
CPC (Dual Mode)	88.2	96.9
Precipitation & Re-dissolving	96.4	98.4
Batch ATPS & Precipitation & Re-dissolving	98.5	93.4
CPC (Ascending Mode) & Precipitation & Re-dissolving	99.4	93.0

4 Discussion

4.1 Precipitation & Resolubilization

Precipitations and re-dissolving of the process solutions were successfully implemented in a 96 well high-throughput screening scale. Using PEG as precipitant, the target protein was more prone to precipitation as the impurities. Thus, purification by bringing the target protein out of solution and subsequently redissolving it was evaluated and showed high HCP separation. Precipitating the target protein rather than the impurities has certain advantages and disadvantages. Clear advantages are the possibility of increasing the target protein concentration, the incorporation of a low-pH virus inactivation step and the high selectivity when precipitating one certain protein rather than a pool of unknown proteins. Disadvantages might be the need to show that the target protein is not adversely influenced by the procedure and the removal of residual precipitant from the precipitate. In the case presented here, no adverse effect on the

target protein was found. Both FT-IR and a functional assay (ProteinA-binding) showed no effect of the procedure. While these assays cannot confirm the biological functionality of the molecule, they are strong indicators, that no significant structural changes have occurred. The remaining PEG 4000 in the precipitant could not be quantified. Re-dissolving of the mAbs was successful both at pH 6.0 and at pH 3.0 with HCP depletion higher at the lower pH. This might be a result of HCP proteins not re-dissolving at the lower pH. As the re-dissolved protein was passed through a filter, HCP still in a precipitate would be removed by the filtration. While the three mAbs tested in this study showed very similar behavior, and while it is likely that other mAbs might also show this behavior, molecules other than mAbs will most likely show a different behavior. For such molecules, this approach would have to be reevaluated. With the current knowledge on the mechanism behind the precipitation of proteins by PEG [20, 21, 22], it is likely that proteins of large molecular weight will react similar to the mAbs tested herein.

4.2 Batch Partitioning in PEG400/Citrate-Systems

Batch partitioning of monoclonal antibodies has been shown to be a promising approach for HCP removal for both PEG-PO₄ and PEG-Citrate systems. [23, 5]

High throughput screening processes to evaluate PEG-Citrate systems were successfully employed in this study. The phase selection theme, guided by solubility data, was performed as previously described [15]. The entire work-flow, from precipitation data, to binodal and tieline determination, to ATPS evaluation was performed in 96 well format as described in [16, 10]. The validity of the solubility guided phase selection scheme under preparative conditions was again shown. The precipitation data suggested a significantly lower solubility of the mAbs in the citrate rich bottom phase. Consequently, the bottom phase contained only minimal amounts of mAb. In contrast, the PEG 400 concentrations in the upper phases of the shorter tielines allowed for the mAb to stay in solution. With increasing tieline, the recovery of mAb decreased in the case of mAb4, the target molecule that had shown the lowest solubility throughout the study.

4.3 Centrifugal Partition Chromatography

The CPC setup as used in this study was also used by Sutherland *et. al* [13]. They showed that by using a PEG1000-PO₄ system in a CPC, two model proteins having partition coefficients of 0.59 and 1.91 could be baseline separated over a CPC. While the separation power of this process step was demonstrated, the shortcomings, dilution of the target molecules and low capacity, also became obvious. We have addressed these shortcomings in the present manuscript by applying a different phase selection scheme and optimizing capacity both via phase selection and operation in dual mode.

Multi-step extraction for HCP removal from antibody solutions has also been successfully implemented both using an extraction column [24] or using mixer-settler batteries [25]. Including a subsequent back-extraction step, the output stream was compatible with HIC. However, the need for a back-extraction necessitated the use of high amount of NaCl in the initial ATPS, thus severely limiting the capacity of the system.

4.4 Combination of Process Steps

Finally, combinations of batch ATPS, CPC, and precipitation were evaluated. It was shown, that the combination of an extraction step with a subsequent precipitation of the protein of interest can be highly advantageous. The precipitations step not only removed a significant

amount of HCP, but also counteracted the dilution introduced by the CPC and made the incorporation of a virus inactivation step and polymer removal step possible. Additionally, it is important to note that the combination of process steps yielded more than the simple sum of HCP clarification of the two steps. Different populations of HCP are removed by the two steps and as a result, they worked in a cooperative manner. The entire process would start with a cell culture supernatant. Cells might be removed either by regular means (centrifugation, depth filtration) or it might be left to the subsequent batch ATPS to remove cells. Second, a batch ATPS would be created either to use it as single partitioning step, or to create a sample for a CPC run. If a CPC run was performed, it would be run in dual mode, stripping HCP from the mAb containing upper phase. After the extraction step (either batch or CPC), the mAb would be precipitated by the addition of PEG4000. The precipitate would be washed and re-dissolved in a standard citrate buffer at pH 3.0. A viral hold step might be included into the process at this time. The final output stream of the entire procedure would end with a higher concentration of the mAb than the input stream, a 2.2 log step clearance of HCP, and an overall mAb recovery of 93%. This output stream could, after slight adjustments to pH and conductivity be used directly as a feed stream to a following chromatographic separation. In a review article Przybycien *et. al* [2] discussed the merits of various alternative separation steps. ATPS was classified as having higher resolution but less industry maturity than precipitation. In the investigation presented herein, we found precipitation to have a higher resolution than ATPS. This might be due to the specific class of molecule investigated as explained above. One of the most severe challenges impeding implementation of alternative separations for biopharmaceuticals is their integration into a chromatography based process. This was also pointed out by Przybycien *et. al* [2] who concluded that currently none of the alternative process steps were easily integrable. The presented approach however yield a process stream that can be readily combined with subsequent chromatographic steps. While the implementation of a CPC in a GMP surrounding might yet be a challenging task, using batch extraction in combination with precipitation could be implemented in a pharmaceutical process plant with little effort. Process economics might necessitate the recycling of the polymer to reduce cost of goods and cost of disposal. Several ways to recycle the polymer have been suggested [26, 27]. These include electrophoretic separation of proteins from the polymer solution with subsequent removal of water by ultrafiltration, which would be the most appropriate approach under the given circumstances.

5 Conclusion & Outlook

In this work, we have demonstrated how an alternative separation step in the form of aqueous two-phase extraction in combination with precipitation and resolubilization can be developed using high throughput screening techniques. The combination of these unit operations were developed in small scale and the results shown to be transferable to larger scale systems. The combination of these unit operations resulted in a high HCP clearance while providing and output stream that is both high in target protein concentration and low in process related impurities that might impede subsequent steps.

6 Acknowledgments

The authors gratefully acknowledge supply of the CPC equipment by **Armen Instrument** and material supply and financial support by **Boehringer Ingelheim Pharma GmbH & Co. KG**

References

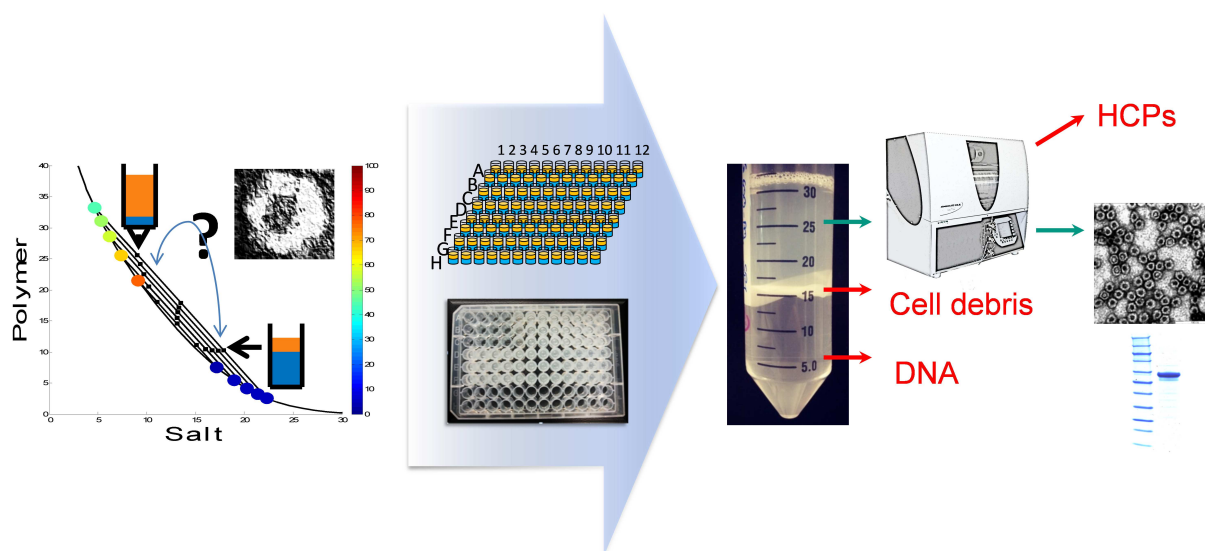
- [1] J. Thömmes, M. Etzel, Alternatives to chromatographic separations., *Biotechnol. Progr.* 23 (1) (2007) 425. doi:10.1021/bp0603661.
- [2] T. M. Przybycien, N. S. Pujar, L. M. Steele, Alternative bioseparation operations: life beyond packed-bed chromatography., *Curr. Opin. Biotechnol.* 15 (5) (2004) 469–78. doi:10.1016/j.copbio.2004.08.008.
- [3] S. Matheus, W. Friess, D. Schwartz, H.-c. Mahler, Liquid high concentration igg1 antibody formulations by precipitation., *J. Pharm. Sci.* 98 (9) (2009) 304357. doi:10.1002/jps.21526.
- [4] C. Knevelman, J. Davies, L. Allen, N. J. Titchener-Hooker, High-throughput screening techniques for rapid peg-based precipitation of igg4 mab from clarified cell culture supernatant., *Biotechnol. Progr.* 26 (3) (2009) 697705. doi:10.1002/btpr.357.
- [5] A. M. Azevedo, P. A. J. Rosa, I. F. Ferreira, M. R. Aires-Barros, Optimisation of aqueous two-phase extraction of human antibodies., *J. Biotechnol.* 132 (2) (2007) 20917. doi:10.1016/j.jbiotec.2007.04.002.
- [6] A. M. Azevedo, P. A. J. Rosa, I. F. Ferreira, M. R. Aires-Barros, Integrated process for the purification of antibodies combining aqueous two-phase extraction, hydrophobic interaction chromatography and size-exclusion chromatography., *J. Chromatogr. A* 1213 (2) (2008) 15461. doi:10.1016/j.chroma.2008.09.115.
- [7] A. M. Azevedo, P. A. J. Rosa, I. F. Ferreira, J. d. Vries, T. J. Visser, M. R. Aires-Barros, Downstream processing of human antibodies integrating an extraction capture step and cation exchange chromatography., *J. Chromatogr. B* 877 (1-2) (2009) 508. doi:10.1016/j.jchromb.2008.11.014.
- [8] P. A. J. Rosa, A. M. Azevedo, I. F. Ferreira, S. Sommerfeld, W. Bäcker, M. R. Aires-Barros, Downstream processing of antibodies: single-stage versus multi-stage aqueous two-phase extraction., *J. Chromatogr. A* 1216 (50) (2009) 87419. doi:10.1016/j.chroma.2009.02.024.
- [9] M. Wiendahl, P. Schulze Wierling, J. Nielsen, D. Fomsgaard Christensen, J. Krarup, A. Staby, J. J. Hubbuch, High throughput screening for the design and optimization of chromatographic processes miniaturization, automation and parallelization of breakthrough and elution studies, *Chem. Eng. Technol.* 31 (6) (2008) 893903. doi:10.1002/ceat.200800167.
- [10] S. A. Oelmeier, F. Dimer, J. J. Hubbuch, Application of an aqueous two-phase systems high-throughput screening method to evaluate mab hcp separation., *Biotech. Bioeng.* 108 (1) (2011) 69–81. doi:10.1002/bit.22900.
- [11] M. Wiendahl, C. Völker, I. Husemann, J. Krarup, A. Staby, S. Scholl, J. J. Hubbuch, A novel method to evaluate protein solubility using a high throughput screening approach, *Chem. Eng. Sci.* 64 (17) (2009) 37783788. doi:10.1016/j.ces.2009.05.029.
- [12] I. A. Sutherland, Recent progress on the industrial scale-up of counter-current chromatography., *J. Chromatogr. A* 1151 (1-2) (2007) 6–13. doi:10.1016/j.chroma.2007.01.143.

- [13] I. A. Sutherland, G. Audo, E. Bourton, F. Couillard, D. Fisher, I. Garrard, P. Hewitson, O. Intes, Rapid linear scale-up of a protein separation by centrifugal partition chromatography., *J. Chromatogr. A* 1190 (1-2) (2008) 57–62. doi:10.1016/j.chroma.2008.02.092.
- [14] Y. Ito, Centrifugal precipitation chromatography: Novel fractionation method for biopolymers, based on their solubility, *J. Liq. Chromatogr. Related Technol.* 25 (13-15) (2002) 2039–2064. doi:10.1081/JLC-120013994.
- [15] S. A. Oelmeier, C. Ladd-Effio, J. Hubbuch, High throughput screening based selection of phases for aqueous two-phase system-centrifugal partitioning chromatography of monoclonal antibodies, *J. Chromatogr. A* 1252 (2012) 104 – 114. doi:10.1016/j.chroma.2012.06.075.
- [16] M. Bensch, B. Selbach, J. J. Hubbuch, High throughput screening techniques in downstream processing: Preparation, characterization and optimization of aqueous two-phase systems, *Chem. Eng. Sci.* 62 (7) (2007) 2011–2021. doi:10.1016/j.ces.2006.12.053.
- [17] J. C. Merchuk, B. A. Andrews, J. A. Asenjo, Aqueous two-phase systems for protein separation. studies on phase inversion., *J. Chromatogr. B* 711 (1-2) (1998) 285–93.
- [18] M. Agnely, D. Thiébaud, Dual-mode high-speed counter-current chromatography: retention, resolution and examples, *J. Chromatogr. A* 790 (1-2) (1997) 17–30. doi:10.1016/S0021-9673(97)00742-5.
- [19] E. Delannay, A. Toribio, L. Boudesocque, J.-M. Nuzillard, M. Zèches-Hanrot, E. Dardennes, G. Le Dour, J. Sapi, J.-H. Renault, Multiple dual-mode centrifugal partition chromatography, a semi-continuous development mode for routine laboratory-scale purifications., *J. Chromatogr. A* 1127 (1-2) (2006) 45–51. doi:10.1016/j.chroma.2006.05.069.
- [20] D. H. Atha, K. C. Ingham, Mechanism of precipitation of proteins by polyethylene glycols. analysis in terms of excluded volume., *J. Biol. Chem.* 256 (23) (1981) 12108–17.
- [21] S.-L. Sim, T. He, A. Tscheliessnig, M. Mueller, R. B. H. Tan, A. Jungbauer, Protein precipitation by polyethylene glycol: A generalized model based on hydrodynamic radius., *J. Biotechnol.* 157 (2) (2012) 315–9. doi:10.1016/j.jbiotec.2011.09.028.
- [22] R. Bhat, S. N. Timasheff, Steric exclusion is the principal source of the preferential hydration of proteins in the presence of polyethylene glycols., *Protein Sci.* 1 (9) (1992) 1133–43. doi:10.1002/pro.5560010907.
- [23] P. A. J. Rosa, A. M. Azevedo, M. R. Aires-Barros, Application of central composite design to the optimisation of aqueous two-phase extraction of human antibodies., *J. Chromatogr. A* 1141 (1) (2007) 5060. doi:10.1016/j.chroma.2006.11.075.
- [24] P. A. J. Rosa, A. M. Azevedo, S. Sommerfeld, W. Bäcker, M. R. Aires-Barros, Continuous aqueous two-phase extraction of human antibodies using a packed column., *J. Chromatogr. B* 880 (1) (2012) 14856. doi:10.1016/j.jchromb.2011.11.034.
- [25] M. R. Aires-Barros, Aqueous two-phase systems for antibodies purification: From macro to micro-scale, in: *Recovery of Biological Products XV*, 2012.
- [26] P. Å. Albertsson, Partition of cell particles and macromolecules: distribution and fractionation of cells, mitochondria, chloroplasts, viruses, proteins, nucleic acids, and antigen-antibody complexes in aqueous polymer two-phase systems, Wiley-Interscience, 1971.

-
- [27] R. Hatti-Kaul, *Aqueous Two-phase Systems: Methods and Protocols*, *Methods in biotechnology*, Humana Press, 2000.

Downstream Processing of Virus-like Particles: Single-stage and Multi-stage Aqueous Two-Phase Extraction

C. Ladd Effio ¹, Lukas Wenger ¹, Ozan Ötes ¹, S. A. Oelmeier ^{1,2}, R. Kneusel ³ and
J. Hubbuch ^{1,*}



¹ : Institute of Process Engineering in Life Sciences, Section IV: Biomolecular Separation Engineering, Karlsruhe Institute of Technology, Engler-Bunte-Ring 1, 76131 Karlsruhe, Germany

² : Boehringer Ingelheim Pharma GmbH & Co. KG, Birkendorfer Str. 65, 88400 Biberach an der Riß, Germany

³ : Diarect AG, Bötzingen Str. 29B, 79111 Freiburg im Breisgau, Germany

* : Corresponding author. *E-mail address:* juergen.hubbuch@kit.edu (J. Hubbuch)

J. Chrom. A (2015), doi:10.1016/j.chroma.2015.01.007

Abstract

The demand for vaccines against untreated diseases has enforced the research and development of virus-like particle (VLP) based vaccine candidates in recent years. Significant progress has been made in increasing VLP titres during upstream processing in bacteria, yeast and insect cells. Considering downstream processing, the separation of host cell impurities is predominantly achieved by time-intensive ultracentrifugation processes or numerous chromatography and filtration steps. In this work, we evaluate the potential of an alternative separation technology for VLPs: aqueous two-phase extraction (ATPE). The benefits of ATPE have been demonstrated for various biomolecules, but capacity and separation efficiency were observed to be low for large biomolecules such as VLPs or viruses. Both performance parameters were examined in detail in a case study on human B19 parvovirus-like particles derived from *Spodoptera frugiperda* Sf9 insect cells. A solubility-guided approach enabled the design of polyethylene (PEG) salt aqueous two-phase systems with a high capacity of up to 4.1 mg/mL VLPs. Unique separation efficiencies were obtained by varying the molecular weight of PEG, the pH value and by using neutral salt additives. Further improvement of the separation of host cell impurities was achieved by multi-stage ATPE on a centrifugal partition chromatography (CPC) device in 500 mL scale. While single-stage ATPE enabled a DNA clearance of 99.6%, multi-stage ATPE improved the separation of host cell proteins (HCPs). The HPLC purity ranged from 16.8% (100% VLP recovery) for the single-stage ATPE to 69.1% (40.1% VLP recovery) for the multi-stage ATPE. An alternative two-step downstream process is presented removing the ATPS forming polymer, cell debris and 99.77% DNA with a HPLC purity of 90.6% and a VLP recovery of 63.9%.

Keywords: VLP, Aqueous two-phase systems, Centrifugal Partition Chromatography, High-throughput screening, DNA removal, Parvovirus

1 Introduction

Virus-like particles (VLPs) represent a new class of bionanoparticles incorporating unique features for medical applications. VLPs are composed of one or several viral structural proteins capable of spontaneously self-assembling into capsids. Thus, they can either mimic the pathogens they derived from [1] or present antigen epitopes of foreign pathogens [2] or tumor cells [3]. Apart from diagnostic applications VLPs show increasing importance as vaccine candidates against unsolved or emerging infectious diseases and as new "designer vaccine platforms" [4, 5]. Currently, there are five VLP-based products licensed for vaccination: two cervical cancer vaccines (Gardasil[®], Merck & Co. and Cervarix[®], GlaxoSmithKline), two hepatitis B vaccines (Recombivax HB[®], Merck & Co. and Engerix-B[®], GlaxoSmithKline) and a hepatitis E vaccine (Hecolin[®], Xiamen Innovax Biotech Co., Ltd.). About 10 candidates entered clinical phases II or III [6] for indications such as influenza, gastroenteritis and malaria. Further research studies focus on using VLPs as vectors for targeted delivery of small molecules [7] or nucleic acids [8]. Hence, there is an increasing demand for pure clinical grade VLPs in both pharmaceutical industry and research centres for infectious diseases. Purity guidelines for human VLP-based vaccines are given by the U.S. Food and Drug Administration and the World Health Organization: DNA concentrations should be below 10 ng per dose and protein purities above 95% [9, 10]. The production of VLPs has been optimized in recent years for a number of different VLPs enabling the choice between varieties of recombinant systems such as bacteria, yeast, insect, mammalian or plant cells [11]. In contrast, downstream processing of VLPs predominantly relies on time-consuming and hardly scalable ultracentrifugation steps [2].

Vaccine manufacturers have recently focused on replacing ultracentrifugation by chromatography or filtration steps [12, 13, 11]. Although this approach has significantly improved the scalability of VLP processes, low binding capacities [14, 15], product loss due to irreversible interactions and process-related product alterations [16, 17], long process times and high process costs [18] remain major challenges. Making vaccines more available to the developing world, responding faster to pandemics and accelerating research, development and clinical studies are main issues to be solved. An alternative unit operation for biomolecules avoiding interactions with solid phases is aqueous two-phase extraction (ATPE). ATPE has proven to be a rapid [19], low-cost [20], scalable [21], selective [22] and integrated [23] bioprocess unit operation. A high and steadily increasing number of publications has underlined the applicability of aqueous two-phase systems (ATPSs) for the purification of antibiotics, enzymes, therapeutic proteins, monoclonal antibodies and viruses [20, 22, 24, 25, 26, 19]. ATPSs have beneficial characteristics, especially for capturing products from crude cell feedstocks [27]. Drawbacks arise due to high experimental effort during process development, limited mechanistic understanding and low capacities.

High-throughput screenings on liquid handling stations have proven to be a valuable tool for rapid selection of adequate ATPSs for separation tasks and for improving the mechanistic understanding of protein partitioning [28, 29]. This study focuses on the effect of different ATPS characteristics on the partitioning of human B19 parvo-VLPs derived from *Spodoptera frugiperda* Sf9 insect cells and the removal of host cell contaminants such as cell debris, host cell proteins (HCPs) and DNA. Human B19 parvo-VLPs are currently investigated as prophylactic vaccine candidates against diseases attributed to parvovirus infections [30, 31]. This virus infects human erythroid precursor cells in the bone marrow and may cause aplastic anemia. An infection during pregnancy can lead to fetal anemia, often resulting in fetal congestive heart failure (hydrops fetalis) and miscarriage. Hence, there is a need for a vaccine, a diagnostic immunoreagent and a scalable purification process with a high VLP recovery. Recent studies evaluating ATPSs for the purification of VLPs have shown that such large biomolecules can be partitioned in a stable form

in either polymer- or salt-rich phases. Benavides et al. [32] observed the partitioning of human rota-VLPs derived from *Sf9* cells into the top phase of a PEG400-phosphate system achieving an HPLC purity of 11%. Partitioning of human B19 parvo-VLPs in PEG1000-magnesium sulphate systems was investigated by Luechau et al. [33]. The outcome was either a partitioning of VLPs and the majority of host cell proteins (HCPs) in the bottom phase or the interfacial attachment of VLPs separating HCPs into top and bottom phase. Since one of the major advantages of ATPSs is the incorporation of a solid-liquid separation step the latter result of Luechau et al. using clarified cell lysate would not be a desired process design for an integrated capture step. Moreover, Luechau et al. used low pH values throughout their study, which can entail disassembly and aggregation of VLPs [34, 35]. While ATPSs might have unique advantages for capturing products from crude cell lysates, separation efficiency depends predominantly on the type of operation. Multi-stage ATPE provides mostly higher separation efficiencies than single-stage ATPE due to improved concentration profiles and a higher number of theoretical plates. A promising technique for multi-stage and large scale extraction of biopharmaceutical products is centrifugal partition chromatography (CPC). CPC systems have been optimized to achieve high stationary phase retentions for ATPSs and optimized mixing between stationary and mobile phases [36]. CPC case studies with ATPSs have been performed in the past for high-resolution separations of model proteins [37], and for the purification of monoclonal antibodies [38]. In this work, we demonstrate how capacity, recovery and purity of VLPs can be optimized in an integrated ATPE step. The resulting ATPS can be easily implemented as single-step process in any laboratory scale with basic equipment or as a multi-stage process with proper extraction devices. In addition, an alternative purification process for human B19 parvoVLPs is suggested.

2 Materials & Methods

2.1 Disposables

All solubility screenings on the liquid handling station were conducted in 96 well Half Area polystyrene flat-bottom plates by Greiner Bio-One (Kremsmünster, Austria). ATPSs were prepared in 1 mL-96 Deep Well polypropylene plates (Thermo Fisher Scientific Inc., Waltham, Massachusetts, USA). All UV absorbance measurements were carried out in Greiner Bio-One 350 μ L-polystyrene UV Star[®] plates. All fluorescence measurements were conducted in black Nunc[®] MicroWell[™] polystyrene plates (Sigma-Aldrich, St. Louis, MO, USA). For all other purposes Greiner Bio-One 350 μ L-polypropylene flat bottom MTPs were used. ATPS scale-up was done in BD Falcon[™] 50 mL Conical Centrifuge Tubes (Becton, Dickinson and Company (BD), Franklin Lakes, New Jersey, USA).

2.2 Chemicals & Stock Solutions

PEG 200 and PEG 1450 were purchased from Sigma-Aldrich (St. Louis, MO, USA). K_2HPO_4 and $NaH_2PO_4 \cdot H_2O$ were obtained from VWR BDH Prolabo (Radnor, Pennsylvania, USA). All other chemicals were purchased from Merck KGaA (Darmstadt, Germany). All buffer and stock solutions were prepared with ultra pure water drawn from a water purification system from Sartorius (Goettingen, Germany). Polymer and salt stock solutions were used as follows: 70% [w/w] PEG 400, 70% [w/w] PEG 600, 70% [w/w] PEG 1000, 60% [w/w] PEG 1450, 40% [w/w] PEG 4000, 40% [w/w] NaH_2PO_4 , 40% K_2HPO_4 [w/w], 35% [w/w] citric acid, 35% [w/w] trisodium citrate, 40% [w/w] ammonium sulfate, 30% [w/w] sodium carbonate. Mono- and dibasic phosphate and citrate stock solutions were combined to yield the desired pH-values: e.g.

22.73 g NaH_2PO_4 solution and 77.27 g K_2HPO_4 solution yield pH 7.4. pH values of all other stock solutions and buffer solutions were titrated with hydrochloric acid and sodium hydroxide solutions.

2.3 Human B19 Parvovirus-like Particles

VLPs were derived from *Spodoptera frugiperda Sf9* insect cells. Recombinant production of human B19 parvovirus-like particles and material supply was done by the industrial partner Diarect AG (Freiburg, Germany). VLPs composed of the major capsid protein VP2 and the minor capsid protein VP1 (VP1/VP2-VLP) and VLPs assembled by solely VP2 (VP2-VLP) were used throughout this study. All experiments were performed with *Sf9* insect cell lysates prepared according to the following procedure: Frozen (-80°C) pellets containing 8×10^8 *Sf9* cells were resuspended in 20 mL lysis buffer (10 mM Tris pH 7.4, 15 mM MgCl_2 , 250 mM NaCl, 0.5% [v/v] polysorbate 80, 10% [v/v] glycerol) by shaking the suspension for 30 min on an overhead shaker. Thereafter, cells were lysed on ice by sonication with a Branson Sonicator 450D equipped with a 1/2 inch microtip horn (Branson Ultrasonics, Danbury, CT, USA): 8x 15 s sonication at 80%, with 59 s cooling steps in between. Protein degradation by proteases was counteracted by adding EDTA-free SIGMAFASTTM protease inhibitor cocktail tablets (Sigma-Aldrich, St. Louis, MO, USA) to the lysis buffer. Clarification of cell lysates was carried out by centrifugation for 30 min at 10.000 g and filtration with 0.1 μm cellulose acetate filters (Sartorius AG, Goettingen, Germany). Aliquoted cell lysates were stored frozen at -30°C . VLPs purified by several ultracentrifugation steps were supplied by the industrial partner and served as reference material for analytics.

2.4 Liquid Handling Station

A Tecan Freedom EVO[®]200 system (Tecan, Crailsheim, Germany) was used as liquid handling platform. Liquid handling calibration, solid-liquid separation and set-up were described earlier [26]. The robotic workstation was controlled using Evoware 2.3 (Tecan, Crailsheim, Germany). Data import and output were done with Excel 2010 (Microsoft, Redmond, WA) files. Matlab R2013a (The Mathworks, Natick, ME) was used for data calculations and visualizations.

2.4.1 Solubility Screening

A solubility guided approach was chosen to select suitable aqueous two-phase components for VLPs. Solubility screenings for 0.5 mg/mL VP2-VLP were conducted with different concentrations of PEG 200, PEG 400, PEG 600, PEG 1000, PEG 1450, PEG 4000 and phosphate at pH 7.4. Screenings were performed on the liquid handling station in 150 μL total volume with each data point measured in triplicate. The automated procedure was described in detail earlier [38]. Briefly, stock solutions of polymers, salts and *Sf9* cell lysates containing VLPs were pipetted into 96 well Half Area plates, incubated on an orbital shaker and centrifuged. Supernatant samples were taken and analyzed for soluble VLP content. Solubility screenings were also used to evaluate the performance of a VLP precipitation step with PEG 4000 after a single-stage ATPE.

2.4.2 Automated ATPE Procedure

Binodals and tie lines for seventeen different ATPSs were determined according to automated methods established and described by our group [29, 26]. Binodal data points were identified

using the cloud point method [38] and fitted to Eq. (1) given by Merchuk *et al.* [39].

$$x_{\text{PEG}} = a * \exp(b * x_{\text{salt}}^{0.5} + c * x_{\text{salt}}^3) \quad (1)$$

Tie-lines were determined with the lever arm rule using volume ratios (V_r) calculated from mass balances with a dye as described before [29, 26]. Automated ATPE experiments were conducted according to Oelmeier *et al.* [26]. Subsequent to the solubility screenings promising ATPSs with volume ratios near 1 were selected for investigating partitioning of VLPs. Parameters such as molecular weight of PEG, salt type, pH, additive concentration and tie-line length were varied to evaluate the effect on VLP separation from total protein and DNA. 650 μL ATPSs with a concentration 0.5 mg/mL VP2-VLP were built by adding stock solutions of phase components, cell lysates with known VP2-VLP concentrations and water into 96 Deep Well plates. ATPSs were mixed, incubated and centrifuged for phase separation. Samples of top and bottom phases were taken and analyzed for VLP, total protein and DNA content. Phase volumes, VLP, DNA and total protein partitioning were measured at least in triplicate, blank values at least in duplicate. Partitioning in top and bottom phases was determined by multiplying the measured solute concentrations with the respective phase volumes. Mean values of recoveries of VLP, total protein and DNA are reported throughout this manuscript. For a detailed analysis of the pH effect, ratios of monobasic NaH_2PO_4 stock solution and dibasic K_2HPO_4 stock solution were varied to yield the desired pH values in a range between pH 5.5 and 8.5. Prior to performing pH screenings with VLP samples system compositions were tested in 10 mL scale for two-phase separation. All actual system pH values of the bottom phases were checked and showed standard deviations below 0.5% from the desired pH value.

2.5 Physical Characterization of ATPS

ATPSs with a promising performance for multi-stage extractions were further characterized measuring viscosities and densities of top and bottom phases. ATPSs were built, mixed and incubated in 50 mL scale. Phase separation was accelerated by centrifugation at 10.000 g for 10 min. Viscosity was determined using a cone-plate rheometer HAAKE RheoScope 1 (Thermo Fisher Scientific, Waltham, Massachusetts, USA). The rheometer was controlled by HAAKE RheoWin 4.30 (Thermo Fisher Scientific, Waltham, Massachusetts, USA). Viscosities of top and bottom phases were measured with a C50/1° cone increasing shear stress from 0.1 to 10 Pa. Phase densities were measured with calibrated standard 5 mL Blaubrand® pycnometers (BRAND GMBH + CO KG, Wertheim, Germany) using an analytical balance (Sartorius AG, Goettingen, Germany). Viscosity and density measurements were conducted at least in duplicate with standard deviations below 5%.

2.6 Centrifugal Partition Chromatography

Multi-stage extractions were conducted by Centrifugal Partition Chromatography (CPC) on an Armen 500 mL CPC column (Armen Instrument, Vannes, France). The CPC column consists of 42 stacked discs with 24 twin chambers. Set-up including HPLC pump, ÄKTA prime (GE Healthcare) for UV and conductivity detection as well as detailed proceeding of operation modes were described earlier [38]. For each run a 3 kg ATPS was prepared by dissolving polymer and salts in ultra pure water: e.g. 422.4 g PEG 400, 458.26 g K_2HPO_4 , 34.67 g $\text{NaH}_2\text{PO}_4 \cdot \text{H}_2\text{O}$ and 225 g NaCl (system point (SP) 1*: 14.08 % [w/w] PEG400, 16.28 % [w/w] phosphate pH 8.5, 7.5 % [w/w] NaCl). Phase settling was done in a separating funnel. CPC columns can be run either in Ascending Mode using the top phase as mobile phase and the bottom as stationary phase or in Descending Mode using bottom phase as mobile and the top as stationary

phase. Ascending and Dual operation mode were tested for PEG 400- and PEG 600-phosphate systems. In Ascending Mode the CPC column was at first filled with bottom phase at 50 mL/min and 500 rpm replacing residual distilled water present in the system. Complete filling was assured by continuing bottom phase flow until the outlet conductivity signal remained constant. Subsequently, the column was equilibrated by pumping the mobile phase at the desired operating flow rate and rotational speed. Stationary phase retention was determined by collecting the displaced bottom phase during the whole run. Column equilibration was monitored by the change from high conductivity (salt phase) to a constant low conductivity signal (polymer phase). Following the described procedure the stationary phase retention of four PEG 400-phosphate systems and one PEG 600-phosphate system was studied at flow rates from 3 to 10 mL/min and a rotational speed of 2500 rpm. System and operating points inducing a stationary phase retention above 35% were utilized for purification experiments with a total system concentration of 0.5 mg/mL VLP. Purification experiments were performed by injecting 10 mL top phase of a separately prepared ATPS containing crude *Sf9* cell lysate into the CPC sample loop. Sample injection was done after column equilibration. Eluting proteins were identified by UV measurements, fractionated and analyzed for VLP, HCP and DNA content as described below.

2.7 Combination of ATPE & Precipitation

A combination of single-stage ATPE and precipitation was performed in 50 mL scale. ATPSs were built by mixing 22.06% [w/w] PEG 400, 6.8% [w/w] phosphate pH 8.5, 7.5% [w/w] NaCl and crude *Sf9* cell lysate containing human B19 parvoVLPs and cell debris. Purifications of both VP2- and VP1/VP2-VLPs were tested for process evaluation. ATPSs were mixed for 30 min on a rotating shaker and centrifuged at 6.000 g for 15 min. The top phase was mixed in 50 mL scale with PEG 400 and NaCl stock solutions to attain a mixture of 13% [w/w] PEG 400 and 9% [w/w] NaCl. The mixture was incubated for 30 min and centrifuged at 6.000 g for 15 min. After a washing step with 13% [w/w] PEG 4000 in 50 mM Tris pH 9.0, 0.8 M arginine the precipitate was redissolved in PBS at pH 7.4 on a rotating shaker for 2 h and filtrated with a 0.1 μ m cellulose acetate filter (Sartorius AG, Goettingen, Germany). The process was conducted in triplicate.

2.8 Analytical Methods

2.8.1 VP2 & HCP Quantification

Quantification of the major virus protein VP2 and HCPs was done by reversed-phase ultra-high-performance-liquid chromatography (RP-UHPLC) using an UltiMate[®]3000 RSLC x 2 Dual system from Thermo Fisher Scientific (Waltham, Massachusetts, USA). Sample analysis was performed on a Waters Acquity BEH300 C4 1.7 μ m column (diameter x length = 2.1 mm x 50 mm) at a flow rate of 0.5 mL/min and a column temperature of 75°C. Mobile phase buffers were ultra pure water containing 0.5% [v/v] trifluoroacetic acid (TFA) (solvent A) and acetonitrile containing 0.4% [v/v] TFA (solvent B). Protein analysis was conducted as follows: Column was equilibrated with 8% B for 1.4 min, followed by an increase to 45 % B in 0.35 min, held for 0.35 min, followed by a gradient of 45-50% over 2.15 min and an increase to 95% in 0.35 min, held for 0.7 min. Thus, the total analysis time was 5.4 min per sample. Prior to RP-UHPLC analysis VLPs were disassembled. Disassembly was performed by diluting samples 1:4 with an adapted dissociation buffer suggested by Yuan *et al.* [40]: 8 M guanidine-HCl/ 50 mM Tris pH 8.0, 60 mM DTT and an incubation at 55°C for 15 min. Due to the dissociation effect on VLPs and HCPs the sample preparation method minimized the risk of column blockage by protein precipitation

upon contact with acetonitrile and enabled the analysis of whole cell lysates. A calibration for VP2 with purified reference samples with known VP2-VLP (and VP1/VP2-VLP) concentration enabled the quantification of VP2 in cell lysates and ATPS samples. Samples of ATPS top and bottom phases with lysis buffer instead of cell lysate were subtracted from chromatograms as blank systems. A chromatogram of a *Sf9* cell lysate sample containing VP2-VLP is shown in Fig.1 a. Fig. 1 b displays the RP chromatogram of the purified VP2-VLP standard.

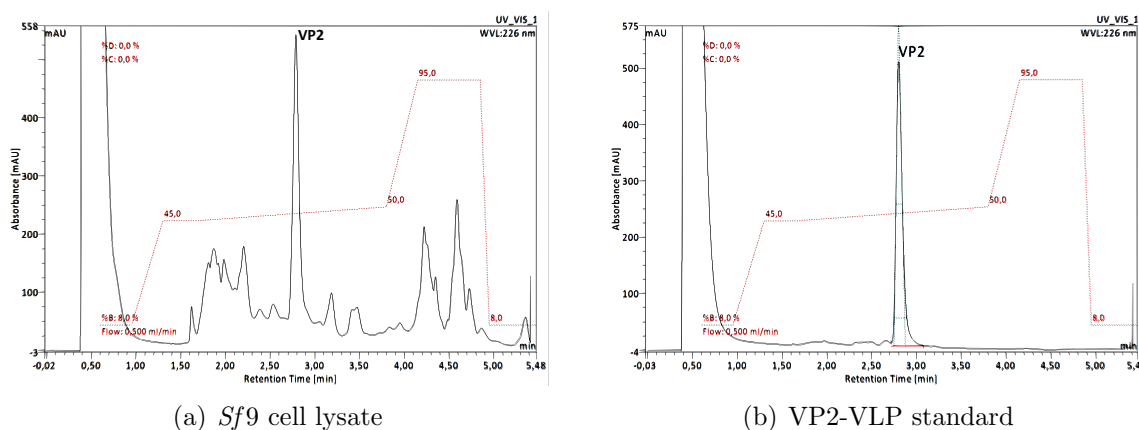


Figure 1 Selected chromatograms from Reversed Phase UHPLC runs. UV-signals at 226 nm are plotted against the retention time. The major peak VP2 is marked in the chromatograms at a retention time of 2.799 min. (a) Analysis of *Spodoptera frugiperda Sf9* insect cell lysate containing human B19 parvo-VP2-VLPs. (b) Analysis of 5 μ g human B19 parvo-VP2-VLPs (external standard)

For HCP measurements total peak areas of substances eluting at lower (HCP group 1) and at higher (HCP group 2) acetonitrile concentrations than VP2 were integrated and summarized into sub-HCP-populations for the evaluation of VLP purity. HPLC purity (P) was defined as the ratio of chromatogram peak areas at a UV wavelength of 226 nm:

$$P = \frac{Area_{VP2}}{Area_{Total}} \quad (2)$$

2.8.2 SDS-PAGE Analysis

The electrophoresis was performed using XCell SureLock Mini-Cell (Invitrogen, Paisley, United Kingdom) with NuPage 12% Bis-Tris gel and MES buffer according to the manufacturer's instructions. The VLP amount in each gel lane was kept constant for all analyzed samples at 5 μ g VP2-VLP. Gels were stained applying a coomassie blue staining.

2.8.3 Total Protein Quantification

Total protein was quantified by UV measurements at 562 nm using a BCA assay kit (Thermo Fisher Scientific Inc., Waltham, Massachusetts, USA) according to the manufacturer's instructions. ATPS samples were diluted tenfold prior to analysis to minimize interference by polymers and salts.

2.8.4 DNA Quantification

Determination of dsDNA concentrations was carried out using the PicoGreen[®] dsDNA assay kit (Invitrogen, Paisley, United Kingdom) in 96-well plates according to the manufacturer's

instructions. ATPS samples were diluted three hundredfold (two dilution steps) prior to analysis to minimize interference by polymers and salts. All other samples were diluted tenfold. The detection limit of the PicoGreen[®] dsDNA assay kit is 25 pg/mL DNA.

2.8.5 Examination of VLP structure and Activity

The detection of virus proteins via RP-UHPLC or SDS-PAGE does not necessarily imply the presence of assembled and active VLPs. Therefore, shape and structure of purified VLP samples were monitored by transmission electron microscopy (TEM). Samples were applied on carbon-coated grids at room temperature and dried for two minutes. Residual salt was washed off with distilled water. Particles were stained with 2% [w/w] uranyl acetate and analyzed on a Philips CM 200 FEG/ST transmission electron microscope at 200 kV. Activity of purified VLP samples was examined by the industrial partner with human patient sera containing VP2-binding antibodies.

3 Results

3.1 Solubility-guided Selection of ATPS Phase Components

The selection of ATPS phase components for VLPs was performed following the strategy of a solubility-guided approach [28]: The solubility of 0.5 mg/mL VP2-VLPs was investigated at increasing concentrations of different polyethylene glycols and phosphate at pH 7.4. In Fig. 2 the recovery of VP2-VLPs is plotted against the precipitant concentration given in weight percent. Fig. 2 shows a strong influence of the molecular weight of the polymer on the solubility of the VLPs. While PEG 4000 induced precipitation of VLPs at low polymer concentrations, VLPs remained in solution over a broader concentration range in the presence of smaller polymers such as PEG 200. A decrease of the VLP concentration in the soluble fraction occurred at a concentration of 39 % [w/w] PEG 200, 27 % [w/w] PEG 400, 16% [w/w] PEG 600, 12 % [w/w] PEG 1000, 10% [w/w] PEG 1450, 3 % [w/w] PEG 4000 and 12 % [w/w] phosphate pH 7.4. These concentrations are important for the ATPS selection process, because higher phase component concentrations may cause loss of product recovery [28, 38]. At a concentration of 60 % [w/w] PEG 200 more than 0.35 mg/mL VP2-VLP were still present in the soluble fraction. There were no VLPs detected in the supernatant at precipitant concentrations of 42% [w/w], PEG 400, 26% [w/w] PEG 600, 24% [w/w] PEG 1000, 16% [w/w] PEG 1450, 7% [w/w] PEG 4000 and 16% [w/w] phosphate pH 7.4. Moreover, the absolute value of the slope of the solubility curves in the decreasing segment, defined as the precipitation efficiency β by Sim et al. [41], increases with the chain length of the polymer. The highest β -values were obtained for PEG 4000 and phosphate.

3.2 Single-stage ATPE: Partitioning of VLPs & Contaminants

3.2.1 ATPS Phase Diagrams

Prior to VLP partitioning studies, ATPSs were characterized on the liquid handling station. Binodals and tie-lines of different PEG-phosphate systems at pH 7.4 were determined. Fig. 3 shows the binodals of PEG 200-, PEG 400-, PEG 600-, PEG 1000-, PEG 1450- and PEG 4000-phosphate systems at pH 7.4. The PEG concentration in weight percent is plotted against the phosphate concentration in weight percent. All determined binodal plot coefficients and average tie-line slopes are summarized in Table 1. In accordance to literature [24] binodals shift towards the origin of the plot with increasing PEG molecular weight. Furthermore, increasing

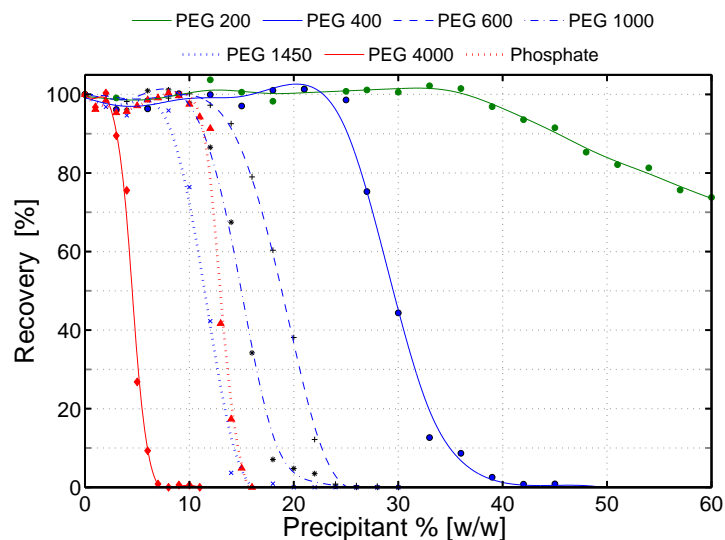


Figure 2 Solubility curves for human B19 parvo-VP2-VLPs determined in 96-well format by automated solubility screenings. The recovery of 0.5 mg/mL VP2-VLP is plotted against the concentration of different precipitants in weight percent. Screenings were conducted with *Spodoptera frugiperda Sf9* insect cell lysate containing VP2-VLPs. Datapoints represent the mean value of triplicate measurements, lines are interpolations to guide the eye.

the PEG molecular weight increased the absolute value of the tie-line slope for PEG-salt ATPSs. The determined phase diagrams illustrate the difficulty of realizing salt concentrations below 12% [w/w] phosphate in the ATPS bottom phase. Such concentration ranges were required to minimize the risk of VLP precipitation in the bottom phase.

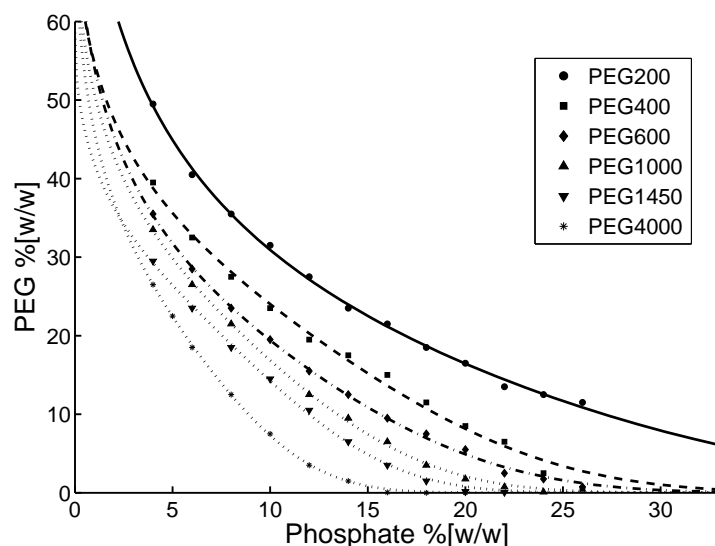


Figure 3 Binodals of PEG-phosphate aqueous two-phase systems at pH 7.4 measured by automated turbidity methods. Data was fitted to equation 1 as described by Merchuk *et al.* [39]. The parameter values of the resulting fit are given in Table 1.

Table 1 Binodal coefficients and tie-line slopes (TLS) of PEG-salt aqueous two-phase systems determined by automated turbidity and dye methods. Data was fitted to equation 1 as described by Merchuk *et al.* [39].

Salt	PEG MW [Da]	pH	a	b	c	TLS
Phosphate	200	7.4	106.63	-0.386	-0.00002	-1.46
	400	7.4	75.87	-0.333	-0.00009	-1.42
	600	7.4	82.17	-0.419	-0.00012	-1.37
	1000	7.4	76.37	-0.408	-0.00022	-1.70
	1450	7.4	58.73	-0.337	-0.00035	-1.79
	4000	7.4	76.6	-0.508	-0.00075	-2.17
	400	8.5	73.70	-0.312	-0.00011	-1.50
Phosphate & 7.5% [w/w] NaCl	600	8.5	79.83	-0.400	-0.00014	-1.74
	1000	8.5	81.18	-0.434	-0.00025	-1.84
Magnesium Sulphate	400	8.5	44.71	-0.264	-0.00018	-1.26
	400	3	66.96	-0.288	-0.00013	-2.04
	400	8.5	66.96	-0.288	-0.00013	-2.04
	8000	3	72.06	-0.695	-0.00221	-2.53
Ammonium Sulphate	8000	8.5	74.43	-0.725	-0.00201	-2.50
	400	7	93.86	-0.32	-0.00006	-1.74
Carbonate	400	11	71.27	-0.386	-0.00043	-2.63
Citrate	400	7.4	93.83	-0.320	-0.00004	-1.65

3.2.2 PEG 200- & PEG 4000-phosphate ATPSs

The VLP solubility screenings have demonstrated that VP2-VLPs were soluble over a broad concentration range for low PEG molecular weights. Hence, initial batch ATPS partitioning studies aimed at inducing top phase VLP partitioning by using the smallest PEG tested in the solubility screenings. On the other hand the largest PEG was investigated for evaluating the potential of bottom phase VLP partitioning. Fig. 4 shows the results obtained for these experiments with 0.5 mg/mL VP2-VLPs. Concentrations of phase forming components are marked on the axes. Binodals and tie-lines of the systems are plotted, with a coloured dot plot representing the VLP recovery in each of the two phases. In all ATPS experiments with VLP or total protein loss a thick interphase layer was observed between top and bottom phase. Hence, if the mass balance for VLPs or other components was not closed for top and bottom phases within the experimental uncertainty, interfacial partitioning due to precipitation was assumed to be the causation. A trend of top phase partitioning of VLPs for PEG 200 ATPS and bottom phase partitioning for the PEG 4000 ATPS was observed. The plots point out that high VLP recoveries above 90 % were obtained for all tested PEG 200 top phases with minimal loss of recovery for increasing tie-line lengths. There were no VLP nor total protein trace amounts detected in the lower ATPS phase of the PEG 200 phosphate systems. In PEG 4000-phosphate systems the highest VLP recovery obtained in the bottom phase was 74.5% for the shortest tie-line. Increasing the tie-line length resulted in a strongly decreasing recovery of VP2-VLPs, indicating precipitation. No separation of DNA was achieved for neither PEG 200-

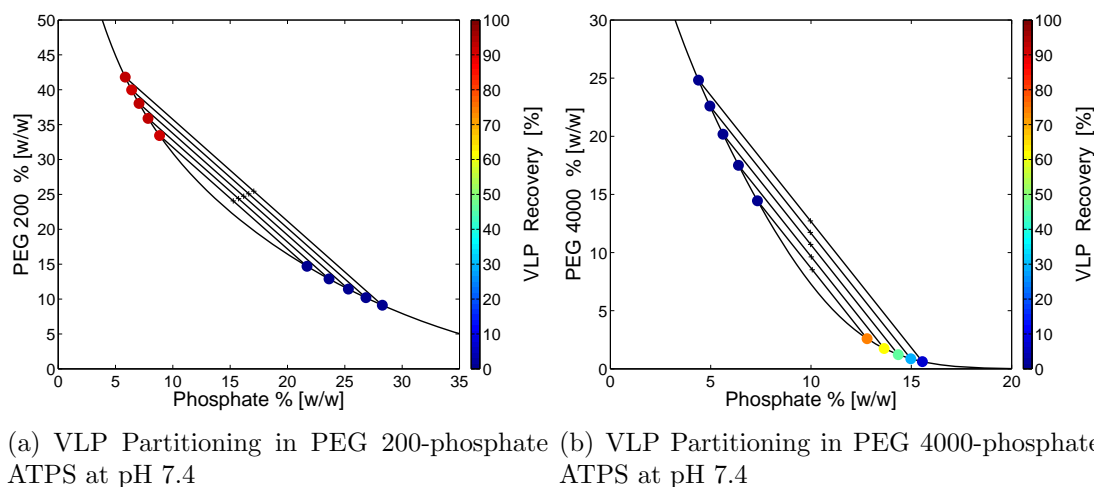


Figure 4 Selected results from the aqueous two phase single-stage extraction screenings. Binodals and tie-lines are shown. Colour coded dots at the composition of the respective top and bottom phases illustrate the recoveries of human B19 parvoVLPs. 'x' corresponds to the system compositions of the ATPSs containing 0.5 mg/mL VP2-VLP. Each data point represents the mean value of triplicate partitioning experiments. Experiments were conducted with *Spodoptera frugiperda Sf9* insect cell lysate containing VP2-VLPs.

nor PEG 4000-phosphate systems. A major drawback of PEG 4000-phosphate ATPS was the settling of cell debris in the bottom phases (data not shown). This characteristics would further complicate the design of an integrated ATPS capture step in comparison with a system with interfacial cell debris partitioning such as a PEG 200 ATPS. High product recoveries and an integrated removal of cells or cell debris as with the PEG 200 ATPS are important requirements for developing a VLP capture step from complex feedstocks. Therefore, further optimization studies with ATPSs built of small PEG molecules focused on improving the separation of HCPs and DNA and identifying promising ATPSs for multistage ATPE. For process optimizations the effect of pH, molecular weight of PEG, salt type and additives on top phase recovery of VLPs, total protein and DNA were investigated.

3.2.3 The Effect of System pH

System pH was varied between pH 5.5 and 8.5 for a defined PEG 400-phosphate system point (15.3% [w/w] PEG 400, 16.9% [w/w] phosphate). PEG 400 was preferred to PEG 200 in order to increase the separation of HCPs or DNA by lowering phosphate concentrations in the bottom phases. Although binodals and tie-lines change slightly for different pH values, all system compositions were found to lie in the two-phase region. Detailed information on binodal and tie-line drifts caused by pH or ionic strength changes can be found in Table 1: increasing pH values and sodium chloride concentrations lead to a shift of the two-phase region to lower PEG and salt concentrations. Fig. 5 shows the effect of the system pH on the partitioning of VLPs, total proteins and DNA. The recoveries for a VP2-VLP concentration of 0.5 mg/mL are plotted against the pH value. It is evident that high pH values induced high VLP-, but also high total protein and DNA recoveries in the top phase. While total protein content remained above 50% in the top phase over the entire pH range, VLPs precipitated and partitioned to the interphase below pH 7.0. A decrease in VLP yield was observed from 79% at pH 7.0 to 15% at pH 6.7. By decreasing the system pH towards the acidic region the partitioning of DNA can be switched from top phase towards bottom phase partitioning. DNA recovery in the bottom

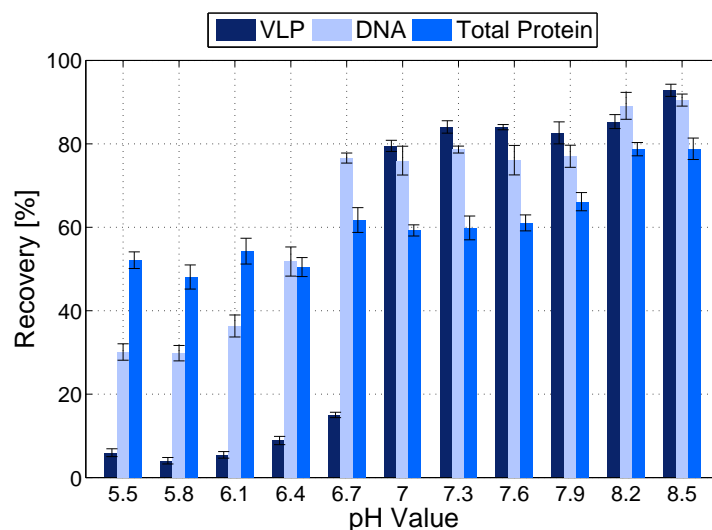


Figure 5 Effect of the ATPS pH value on the top phase partitioning of VLP feedstock components for a PEG 400 phosphate system (15.3% [w/w] PEG 400, 16.9% [w/w] phosphate). Experiments were conducted with *Spodoptera frugiperda* Sf9 insect cell lysate containing human B19 parvo-VP2-VLPs. A concentration of 0.5 mg/mL VP2-VLP was set in each ATPS. Each data point represents the mean value of triplicate partitioning experiments.

phase increased from 17% at pH 6.4 to 78% at pH 5.5. The highest VLP recovery of 92.9% in the PEG-rich top phase was achieved at pH 8.5 coming along with a total protein reduction of 21.1%, a DNA removal of 9.5% and an HPLC purity of 15.9%.

3.2.4 The Effect of PEG Molecular Weight and Salt Type

In the next step the influence of molecular weight of PEG and salt types was studied for improving the separation of host cell contaminants by top phase VLP partitioning. Four different PEG-phosphate systems at pH 8.5 (PEG 200, PEG 400, PEG 600 and PEG 1000) each with five different tie-line lengths were screened for VLP, total protein and DNA recovery. Binodal and tie-line data is appended in Table 1. While the performance of the PEG 200 ATPS showed the same trend for pH 8.5 and 7.4, VLPs were hardly soluble in PEG 1000 ATPSs (data not shown). In Fig. 6 a and 6 b VLP recoveries are plotted again as coloured dot plots in the phase diagrams of a PEG 400- and PEG 600-phosphate system at pH 8.5. It can be seen that VLPs partitioned exclusively to the top phases and an increase of the tie-line length lead to a loss of VLP recovery for both PEG 400- and PEG 600-phosphate systems. The highest recovery in the PEG 600 phosphate systems was 78% VLP at a concentration of 0.5 mg/mL VP2-VLP for the shortest evaluated tie-line and an HPLC purity of 18.9%. There was no decrease of VLP recovery observed for the PEG 400 system points on the two shortest tested tie-lines. It was noticed that larger PEG molecules lead to an increased partitioning of total protein to the bottom phases, but at the same time VLP solubility in the top phase was reduced and lead to precipitation.

For further optimizations of the PEG 400 system, ATPS salt screenings were performed. Apart from phosphate a number of salts such as citrate, sulphate or carbonate can be used for creating ATPSs. In all studies performed with PEG 400-magnesium sulphate (pH 3.0, pH 7.4, pH 8.5 tested) and PEG 400-ammonium sulphate (pH 7.0) systems, precipitation and interfacial partitioning was observed for both VP2- and VP1/VP2-VLPs (data not shown). More promising results were obtained with PEG 400-citrate and PEG 400-carbonate ATPSs and are illustrated

in Fig. 6 c and 6 d. The highest top phase VLP recovery achieved with a PEG 400-citrate system was 57.5% for the shortest tie-line and 58 % with a PEG 400-carbonate system. The corresponding HPLC purities in the PEG 400-citrate and PEG 400-carbonate ATPSs were 17.7% and 22.3% respectively.

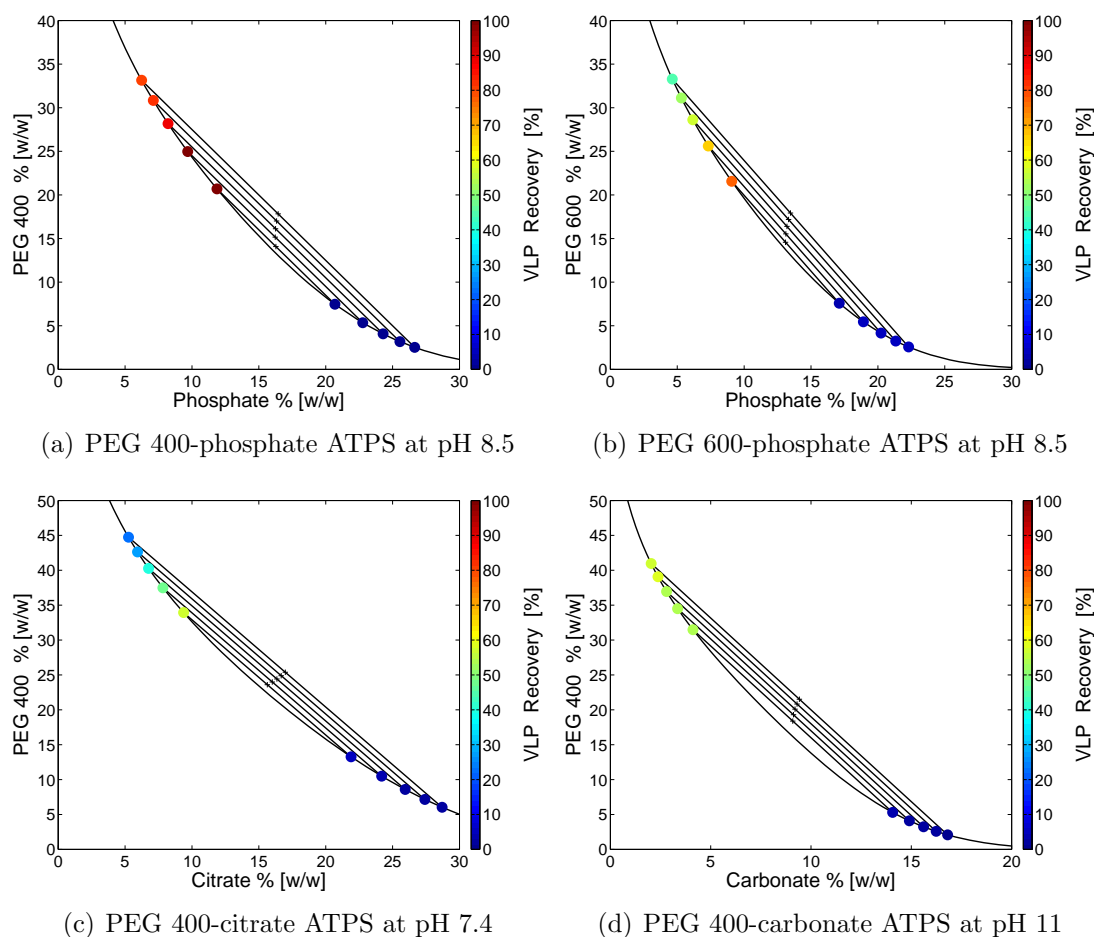
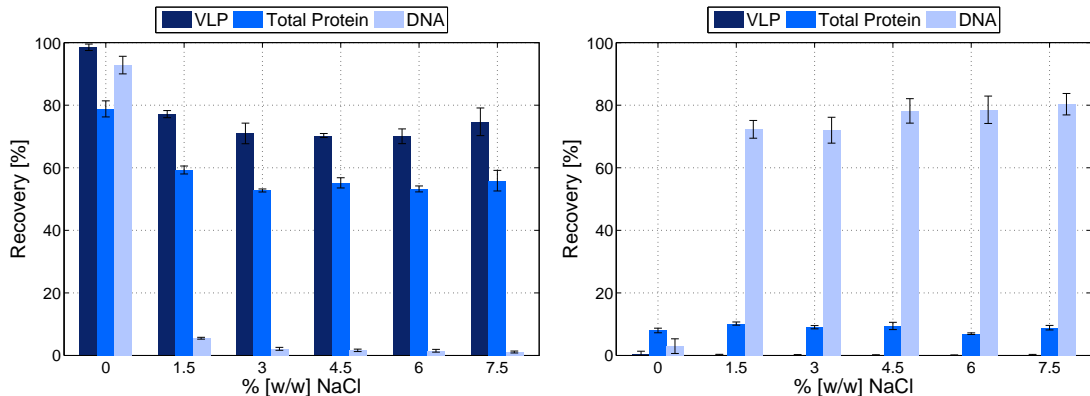


Figure 6 Selected results from the aqueous two-phase single-stage extraction screenings. Binodals and tie-lines are shown. Colour coded dots at the composition of the respective top and bottom phases illustrate the recoveries of human B19 parvoVLPs. 'x' corresponds to the system compositions of the ATPSs containing 0.5 mg/mL VP2-VLP. Each data point represents the mean value of triplicate partitioning experiments. Experiments were conducted with *Spodoptera frugiperda Sf9* insect cell lysate containing VP2-VLPs.

3.2.5 The Effect of Sodium Chloride

Another way of changing partitioning in two-phase systems is to add a neutral salt as modifier. Sodium and potassium chloride were tested as additives for the PEG 400-phosphate system with the highest VLP recovery and capacity (SP1). In Fig. 7 a and 7 b the VLP, total protein and DNA recoveries for top and bottom phases are plotted against the concentration of sodium chloride given in weight percent. A drastic change in partitioning can be observed for DNA from top phase to bottom phase partitioning upon addition of sodium chloride. Since VLPs were recovered in the top phases at all tested sodium chloride concentrations, a separation of up to 99% of DNA was achieved in one step. Furthermore, it is noticeable that upon addition



(a) Top phase recovery of VLP feedstock components at varying NaCl concentrations (b) Bottom phase recovery of VLP feedstock components at varying NaCl concentrations

Figure 7 Effect of sodium chloride on the partitioning of VLP feedstock components for a PEG 400-phosphate system (14.08% [w/w] PEG 400, 16.28% [w/w] phosphate pH 8.5). Experiments were conducted with *Spodoptera frugiperda* Sf9insect cell lysate containing human B19 parvo-VP2-VLPs. A concentration of 0.5 mg/mL VP2-VLP was set in each ATPS. Each data point represents the mean value of triplicate partitioning experiments.

of sodium chloride about 20% of the VP2-VLPs precipitate and partition to the interphase. Nevertheless, the VLP recovery does not decrease further for increasing sodium chloride concentrations. The same partitioning trends for VLPs, total protein and DNA were achieved by adding potassium chloride instead of sodium chloride to the PEG 400-phosphate ATPS (data not shown).

3.3 Multi-stage ATPE: Centrifugal Partition Chromatography

CPC experiments were conducted with three PEG 400-phosphate ATPSs, one PEG 400-phosphate ATPS with 7.5% [w/w] NaCl and one PEG 600-phosphate ATPS at pH 8.5. Detailed information on the exact system composition, viscosities and densities of top and bottom phases are summarized in Table 2. Regarding the physical characteristics it can be seen that increasing the tie-line length for the PEG 400-phosphate system increased both the viscosity ratio between top and bottom phase from 3.12 to 4.05 and the density difference from 0.095 to 0.15 g/mL. The highest density difference of 0.161 g/mL was obtained by addition of 7.5% [w/w] sodium chloride to the PEG 400-phosphate system (SP1). Top and bottom phases of the tested PEG 600-phosphate system showed the lowest density difference of 0.063 g/mL and the lowest viscosity ratio of 2.22. In the CPC the ATPSs were at first tested for stationary phase retention (S_f) and stability against column bleeding (loss of stationary phase during the run). Rotor speed was set at 2500 rpm as suggested by Oelmeier et al. [28] and flow rate was varied from 5 to 10 mL/min. The PEG 600 system with the lowest density difference proved to be unsuitable for CPC extractions. The S_f -value was only 9% at 5 mL/min and column bleeding was observed. The amount of stationary phase retained in the column for the PEG 400 phosphate system was evaluated in a standard two-level full factorial designed experiment varying flow rate and tie-line length. Fig. 8 shows the result of the experiments. S_f -values increased from 26% for tie-line 1 (TL1) at 10 mL/min to 67% for TL5 at 5 mL/min.

Based on these observations, operating conditions of 3 and 5 mL/min and 2500 rpm were chosen for the purification of VP2-VLPs. Purification runs were performed in duplicate with three PEG 400-phosphate ATPSs: SP1 (TL1), SP5 (TL5), SP1* (with 7.5% [w/w] NaCl). Promising

Table 2 Physical properties of ATPS phases tested in CPC stability experiments: Viscosities (η) and densities (ρ) are summarized for PEG 400-phosphate ATPS for varying tie-line lengths, for a PEG 600-phosphate system and for a PEG 400-phosphate system with additional NaCl.

PEG % [w/w]	PO4 % [w/w]	TL [-]	η_{TP} [mPas]	η_{BP} [mPas]	η_r [-]	ρ_{TP} [g/mL]	ρ_{BP} [g/mL]	$\Delta\rho$ [g/mL]
14.08 ^a	16.28	1	5.994	1.920	3.12	1.11	1.205	0.095
16.13 ^a	16.25	3	6.560	1.858	3.53	1.099	1.225	0.125
17.83 ^a	16.45	5	7.086	1.751	4.05	1.098	1.291	0.15
14.08 ^{a,b}	16.28 ^b	1 ^b	7.322	2.848	2.57	1.131	1.292	0.161
14.58 ^c	13.1	1	5.647	2.548	2.22	1.102	1.165	0.063

^a PEG 400.

^b With 7.5% w/w NaCl.

^c PEG 600.

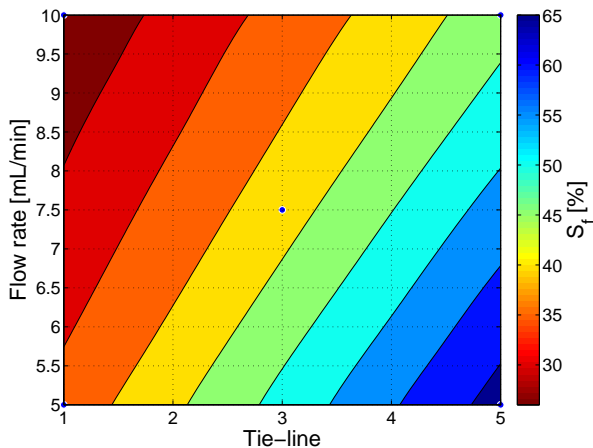


Figure 8 Evaluation of operating and system conditions on the stationary phase retention (S_f) in CPC for PEG 400-phosphate systems. The rotor speed was set to 2500 rpm. Additional information regarding the evaluated tie-lines (TL) is summarized in Table 2. Contour plot was generated using cubic interpolation. Each data point represents the mean value of duplicate CPC experiments.

separations were limited to the PEG 400-phosphate ATPS with sodium chloride (SP1*). The results from the 3 mL/min run with an S_f -value of 70% are shown in Fig. 9. In Fig. 9 a the UV absorption at 280 nm in mAU is plotted against the process time in minutes. The chromatogram shows three sections: (I.) column loading with bottom phase replacing CPC storage solution at 50 mL/min, (II.) column equilibration with mobile top phase displacing bottom phase and (III.) injection and elution of VLP feedstock components at 3 mL/min. Components with a high affinity to the mobile top phase elute at an earlier point than components which interact with the stationary bottom phase. The chromatogram in section III. shows two partially overlapping main peaks. The first peak is narrower and higher than the second peak. Fig. 9 b displays the results from the analyzed CPC fractions. The VP2-VLP concentration and RP chromatogram areas of HCP-group 1 and HCP-group 2 are plotted against the volume. The first UV main peak in Fig. 9 a contains mainly HCPs. VLPs elute at a higher retention volume than host cell impurities, mainly in the second UV peak of the chromatogram in Fig. 9 a. Total VLP recoveries in the CPC runs were 98.2% for SP1, 79.3% for SP5 and 64.4 % for SP1*.

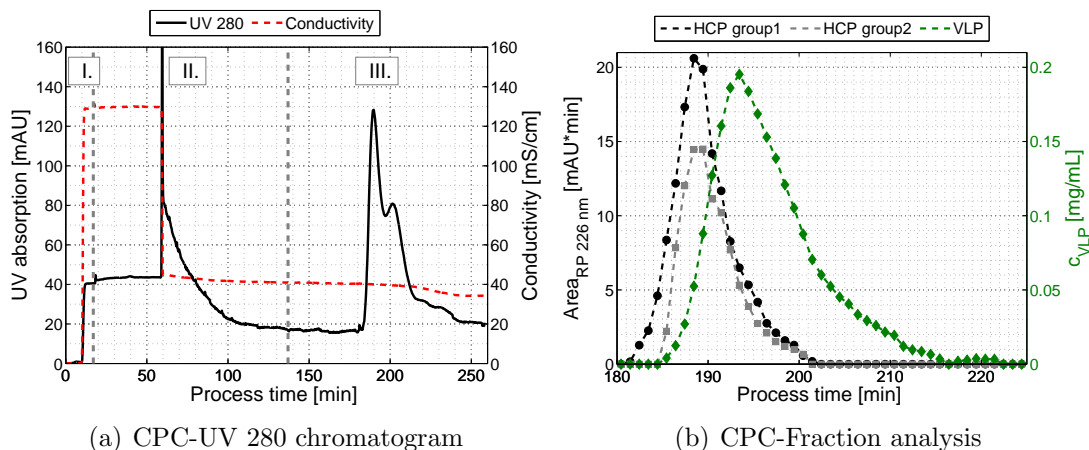


Figure 9 CPC purification run performed with *Spodoptera frugiperda Sf9* insect cell lysate containing human B19 parvo-VP2-VLPs. Operating conditions were: 3 mL/min, 2500 rpm. Sample volume: 10 mL. Sample composition: top phase of a PEG 400 SP1* system (14.08% [w/w] PEG 400, 16.28% [w/w] phosphate pH 8.5, 7.5% [w/w] NaCl) with a total concentration of 0.5 mg/mL VP2-VLP. (a) Chromatogram of a CPC purification run with human B19 parvoVLPs: I. Bottom Phase Loading; II. Equilibration; III. Sample Injection & Elution. (b) CPC Elution profile of VLP feedstock components.

3.4 Evaluation of Process Performance

The evaluation of single- and multi-stage ATPE methods was done by addressing several criteria: VLP recovery, HPLC purity, DNA removal, DNA concentration, VLP structure and antigen reactivity. The data is summarized in Table 3. One of the major challenges hindering implementation of ATPE into manufacturing processes for biopharmaceuticals is the presence of high polymer and salt concentrations. One strategy for removing ATPS components is precipitating the molecule of interest. A common and mild precipitant for large biomolecules is PEG 4000 [42, 43, 44]. Hence, Table 3 includes also process performance data on a combination of a single-stage ATPE (SP1*, $V_r=0.2$), a subsequent precipitation (13 % [w/w] PEG 4000, 9% [w/w] NaCl) followed by re-dissolution in PBS and a sterile filtration. While a high DNA removal of 99% was achieved with a single-stage ATPE, HPLC purities above 69% could only be realized with a subsequent multi-stage ATPE or a precipitation step. The most promising ATPS for an integrated one step purification incorporating solid-liquid-separation (removal of cells & cell debris), VLP concentration up to 3.4 mg/mL VP2-VLPs, separation of 99.6% DNA and 16.8% HPLC purity consisted of 22.05% [w/w] PEG 400, 6.8 % [w/w] phosphate pH 8.5 and 7.5 % [w/w] NaCl. Fig. 10 illustrates the characteristics of the used ATPS in a phase diagram with the binodal curve and system compositions for varying volume ratios (Fig. 10 a), and in a photograph visualizing the interfacial partitioning of cells & cell debris in the ATPS.

Antigen binding of purified VP2-VLPs was confirmed for ATPS and precipitation samples by the industrial partner. TEM images of purified samples and the corresponding SDS-gel lanes are summarized in Fig.11. The TEM image of the filtrated *Sf9* cell lysate reveals the presence of baculoviruses and other particulates apart from VLPs. There were no baculoviruses discovered in the TEM images of neither CPC fractions nor of the process combination sample. An icosahedral structure and an average particles size of 28 nm was observed in all TEM images. Fig. 11 c demonstrates the homogeneity of human B19 parvo-VP2-VLPs produced in *Sf9* cells and purified by the alternative two-step downstream process combining ATPE and precipitation.

Table 3 Process performance data of alternative purification methods for human B19 parvoVLPs.

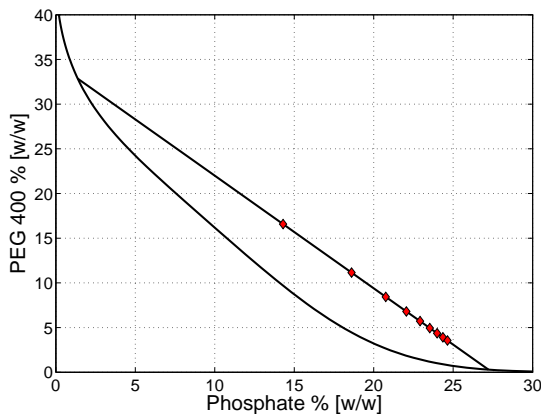
Purification Method	VLP Recovery [%]	HPLC Purity [%]	DNA Depletion [%]	x_{DNA} [ng/ μg VLP]	VLP Capacity [g/L]
Filtrated Cell Lysate	100.0%	5.3%	0.0%	10.668	-
Batch-ATPE ^a	98.5%	15.9%	9.1%	9.693	4.1
Batch-ATPE with NaCl ^b	74.7%	16.3%	98.9%	0.1163	3.4
Batch-ATPE with NaCl ^c	102.1%	16.8%	99.6%	0.0395	3.4
CPC	64.4%	31.4%	100.0%	0	-
CPC ^d	40.1%	69.1%	100.0%	0	-
Batch ATPE ^c & Precipitation	63.9%	90.6%	99.8%	0.0246	-

^a PEG 400-phosphate system (14.08% [w/w] PEG 400, 16.28%[w/w] phosphate pH 8.5)

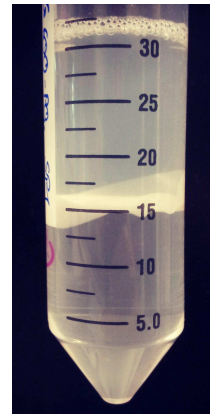
^b PEG 400-phosphate system (14.08% [w/w] PEG 400, 16.28%[w/w] phosphate pH 8.5, 7.5% [w/w] NaCl)

^c PEG 400-phosphate system with $V_r=0.2$ (22.06% [w/w] PEG 400, 6.8%[w/w] phosphate pH 8.5) and crude *Sf9* cell lysate as starting material.

^d Data for pooled CPC fractions of VLPs eluting after 194.4 min.



(a) Phase diagram



(b) Solid-liquid separation

Figure 10 PEG 400-phosphate APTS at pH 8.5 with 7.5% NaCl. (a) Phase diagram with binodal curve and system compositions in red for volume ratios from 1 to 0.1. (b) APTS conducted with crude *Spodoptera frugiperda Sf9* insect cell lysate containing 0.5 mg/mL human B19 parvo-VP2-VLPs at a phase volume ratio near one (14.08% (w/w) PEG 400, 16.28% (w/w) phosphate pH 8.5, 7.5% (w/w) NaCl). Cell debris and precipitate partitioned to the interphase after centrifugation.

4 Discussion

4.1 Batch Partitioning in PEG Salt APTSs

Solubility curves for VLPs, APTS phase diagrams and APTS partitioning trends were successfully determined in 96-well high-throughput screening scale. Screenings pointed out that the solubility of human B19 parvoVLPs in PEG solutions is predominantly a function of the PEG molecular weight. The low solubility of VLPs in PEG and salt solutions is the main issue im-

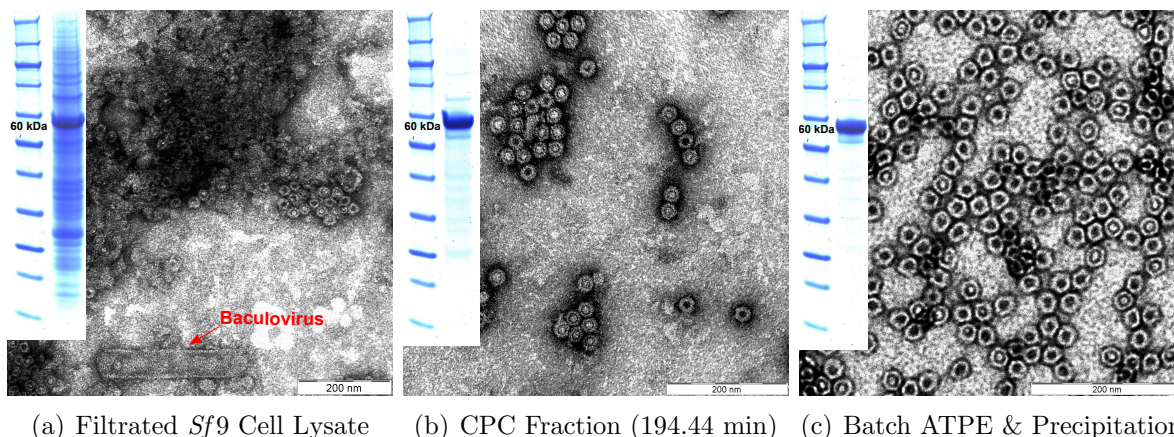


Figure 11 TEM images and SDS-PAGE gels of human B19 parvo-VP2-VLPs derived from *Spodoptera frugiperda* *Sf9* insect cells at different process steps.

peding the development of a robust and selective ATPE step. Larger PEG molecules cause VLP precipitation at lower PEG concentrations. Sim et al. [41] have demonstrated that protein precipitation by polymers is mainly a function of the hydrodynamic radius of protein and polymer, which explains the high precipitation efficiency obtained for PEG 4000 as this declines from high to low PEG molecular weights. Similar to previous studies [28, 38] solubility curves for biomolecules could again be correlated with good accordance to the partitioning behaviour in ATPSs. This was for instance shown for the PEG 200- and PEG 4000-phosphate ATPSs: VLPs partitioned according to the solubility curve in the PEG-rich or salt-rich phase. A stepwise optimization strategy was performed to separate host cell impurities. Low PEG molecular weights were chosen for top phase partitioning and removal of cell debris. High pH values increased the recoveries of VLPs in ATPS top phases and a PEG molecular weight of 400 Da improved the separation of HCPs in the bottom phase compared to a PEG 200 ATPS. DNA removal was achieved by adding sodium chloride to the PEG 400-phosphate ATPS. The DNA depletion from top to bottom phase was accompanied by a loss of a constant VLP fraction which may be attributed to the separation of VLP-DNA complexes in the interphase. Virus proteins are known to bind DNA [45, 46]. Such VLP-DNA-complexes might have a higher tendency for interfacial partitioning if they vary in size, surface charge and hydrophobicity from a single unit VLP. The constant percentage of VLP recovery loss for a broad sodium chloride concentration range and for higher VLP feed concentrations underline the assumption of an inhomogeneous VLP particle size distribution in the *Sf9* cell lysate. Further characterization by Asymmetrical Flow Field Flow Fractionation (AF4) would help determining the structure and homogeneity of human B19 parvoVLPs produced by the Baculovirus/*Sf9* cell system [47]. Remarkably, if the ATPS was built with crude cell lysate, the recovery for VLPs was improved to 102% (compared to a clarified cell lysate). An explanation for this is the top phase recovery of VLPs attached to cell debris or cells. These VLPs get lost in a clarification process by centrifugation or filtration. Furthermore, the batch partitioning studies showed that the performance could not be optimized, but rather deteriorated when changing the dominant salt from phosphate to citrate, carbonate or sulphate.

In summary, the partitioning of human B19 parvoVLPs in PEG salt ATPSs could be controlled or switched solely by modifying two parameters: (I) the PEG molecular weight and (II) the system pH. Short PEG molecules induced top phase partitioning, long PEG molecules induced bottom phase partitioning. System pH values above the isoelectric point of the product strengthened top phase partitioning and recovery. For improving the separation efficiency of a

single-stage ATPE the PEG molecular weight could be varied stepwise or a neutral salt could be added. Sodium chloride drastically changed the partitioning of DNA. This finding paves new ways for ATPS applications in bioprocesses and could be ascribed to a change in electrostatic properties of the two phases. Andrews et al. [48] suggested that higher concentrations of NaCl result in a more negative PEG-rich phase due to an increase in the concentration of chloride ions. Negatively charged components such as DNA might be excluded from the top phase to the bottom phase by a change in electrostatic interactions.

4.2 Centrifugal Partition Chromatography

Chromatograms and stationary phase retentions for different ATPSs have once again proven the applicability of CPC for biomolecule purification by multi-stage ATPE. High stationary phase retention was always linked to a high density difference between top and bottom phase. Since the density difference is predominantly a function of the salt concentration in the bottom phase, system compositions of longer tie-lines lead to higher S_f -values. Nevertheless, the results demonstrated that high stationary phase retention did not imply a good separation of components. For a good chromatographic resolution the components' partitioning coefficients (k) should not assume extreme values ($k \gg 1$ or $k \ll 1$) [37, 49], which is difficult to realize for large biomolecules due to the solubility issues mentioned above. Hence, past multi-stage extractions for biomolecules have focused on using extractor devices for stripping impurities by washing steps using counter current extraction [50] or CPC Dual Mode [38]. In case of the tested PEG 400-phosphate ATPSs this procedure hardly optimized the performance for the VLP purification. An important finding was the effect of sodium chloride on the stationary phase retention and on the separation of HCPs and VLPs. In the ATPS batch experiments there were no changes measured in the partitioning coefficients of neither HCPs nor VLPs upon addition of sodium chloride. Hence, the explanation for the observed separation must be a change in physical properties of the ATPS. Adding sodium chloride increased the density differences between top and bottom phase strongly and decreased the viscosity ratio between the two phases. A higher S_f -value and a lower viscosity ratio improve the mass transfer between mobile and stationary phase [51, 52]. A prolonged retention of VLPs could occur due to an increase in electrostatic repulsion or in interfacial tension upon addition of NaCl. As suggested by Luechau et al. [53] and demonstrated in this work for cell debris and precipitate, the adsorption of particles on the ATPS interphase depends on the interfacial tension of the system and the particle size. Interfacial tensions are usually low for PEG-salt ATPSs with short PEG molecules and can mostly be neglected for very small particles below 50 nm [53, 54]. However, the big interfacial areas generated in the CPC at high centrifugal speed and at a low viscosity ratio probably intensified the interaction of VLPs with the interphase. Since all HCPs were smaller in size than the VLPs, the separation mechanism was probably related to the size of the molecules. Further studies correlating interfacial tension, interfacial area and particle size with the CPC retention time are needed to get a better understanding of the separation mechanism observed inhere for VLPs. The findings can strike a new path in the development of an alternative platform technology for size-dependent particle fractionation.

4.3 Evaluation of ATPE for the Purification of VLPs

The obtained results demonstrate the benefits of ATPE for the downstream processing of human B19 parvoVLPs. The single-stage ATPE allowed the removal of cell debris, the clearance of above 99% DNA and a decrease in HCP content. High VLP recoveries above 60% were obtained for all evaluated purification methods and VLP capacities between 3.4 and 4.1 mg/mL in the

ATPS top phases could be used for concentrating feedstreams with low product concentrations by varying the volume ratio of the ATPS. Two methods were investigated for the separation of HCPs from the top phase of a single-stage ATPS. A separation of HCPs by CPC was shown to be possible and should be evaluated with other CPC devices for an optimization of peak resolution. Drawbacks observed for the purification method were the strong dilution of the biomolecules and the recovery loss of 35% VLPs. The decrease in recovery might be attributed to long process times increasing the risk of product aggregation. The other method suggested inhere was the precipitation of VLPs with PEG 4000 in the presence of NaCl. Since NaCl counteracted the co-precipitation of HCPs by shielding electrostatic attraction, the method was highly selective for the purification of VLPs. In addition, the VLP concentration of the output stream could be set by adapting the volume of the re-dissolution buffer. Antigen reactivity and particle morphology were preserved for both multi-stage ATPE and the redissolved VLP precipitates. VLP preparations were shown to be uniform in size with particles around 28 nm. DNA trace amounts after purification with the suggested alternative downstream processes lay below acceptable threshold values (10 ng per dose [9]) for doses below 400 μ g VLP.

5 Conclusion & Outlook

In this work, we have shown the potential of ATPE for the purification of VLPs. PEG-salt systems were optimized on a high-throughput screening platform for the isolation of human B19 parvoVLPs from crude *Sf9* insect cell lysate. A new alternative VLP downstream process was developed integrating a product concentration, solid-liquid separation and DNA removal step into one unit separation. Intact VLPs were concentrated in the top phase with a high capacity separating cell debris and almost all DNA in the inter- and bottom phase. Further purification of the top phase was demonstrated by multi-stage ATPE using CPC and by precipitation with PEG. A proof of concept of multi-stage ATPE was shown for the first time for such large biomolecules as VLPs. Unique selectivities were obtained for both single- and multi-stage ATPE by the addition of sodium chloride. The combination of ATPE and precipitation resulted in a high HPLC purity, icosahedral and reactive VLPs, the removal of ATPS phase components and an adjustable concentration of the product of interest. The proposed two-step downstream process is rapid, easily scalable [55, 56], requires only a very basic laboratory equipment and can be a valuable addition to the VLP purification toolbox.

Acknowledgments

The authors gratefully acknowledge material supply by **Diarect AG** and financial support from the **German Federal Ministry of Education and Research** (Grant agreement 0315640B). Furthermore, we thank Gregoire Audo from Armen Instrument for support and assistance and Mohammad Fotouhi from the KIT Laboratory for Electron Microscopy for acquisition of transmission electron micrographs.

References

- [1] R. L. Garcea, L. Gissmann, Virus-like particles as vaccines and vessels for the delivery of small molecules., *Curr. Opin. Biotechnol.* 15 (6) (2004) 513–7. doi:10.1016/j.copbio.2004.10.002.

- [2] L. H. L. Lua, N. K. Connors, F. Sainsbury, Y. P. Chuan, N. Wibowo, A. P. J. Middelberg, Bioengineering virus-like particles as vaccines., *Biotechnol. Bioeng.* 111 (3) (2014) 425–40. doi:10.1002/bit.25159.
- [3] T. Klamp, J. Schumacher, G. Huber, C. Kühne, U. Meissner, A. Selmi, T. Hiller, S. Kreiter, J. Markl, O. Türeci, U. Sahin, Highly specific auto-antibodies against claudin-18 isoform 2 induced by a chimeric HBcAg virus-like particle vaccine kill tumor cells and inhibit the growth of lung metastases., *Cancer Res.* 71 (2) (2011) 516–27. doi:10.1158/0008-5472.CAN-10-2292.
- [4] P. Roy, R. Noad, Virus-like particles as a vaccine delivery system: myths and facts., *Adv. Exp. Med. Biol.* 655 (2009) 145–58. doi:10.1007/978-1-4419-1132-2\11.
- [5] H. Joshi, K. Lewis, A. Singharoy, P. J. Ortoleva, Epitope engineering and molecular metrics of immunogenicity: a computational approach to VLP-based vaccine design., *Vaccine* 31 (42) (2013) 4841–7. doi:10.1016/j.vaccine.2013.07.075.
- [6] N. Kushnir, S. J. Streatfield, V. Yusibov, Virus-like particles as a highly efficient vaccine platform: diversity of targets and production systems and advances in clinical development., *Vaccine* 31 (1) (2012) 58–83. doi:10.1016/j.vaccine.2012.10.083.
- [7] C. Goldmann, N. Stolte, T. Nisslein, G. Hunsmann, W. Lüke, H. Petry, Packaging of small molecules into VP1-virus-like particles of the human polyomavirus JC virus., *J. Virol. Methods* 90 (1) (2000) 85–90.
- [8] R. K. Keswani, I. M. Pozdol, D. W. Pack, Design of hybrid lipid/retroviral-like particle gene delivery vectors., *Mol. Pharm.* 10 (5) (2013) 1725–35. doi:10.1021/mp300561y.
- [9] CBER guidelines 2007, US Food and Drug Administration, Center for Biologics Evaluation and Research.
- [10] World Health Organization, Guidelines on the quality , safety and efficacy of recombinant malaria vaccines targeting the pre-erythrocytic and blood stages of *Plasmodium falciparum*.
- [11] T. Vicente, A. Roldão, C. Peixoto, M. J. T. Carrondo, P. M. Alves, Large-scale production and purification of VLP-based vaccines., *J. Invertebr. Pathol.* 107 Suppl (2011) S42–8. doi:10.1016/j.jip.2011.05.004.
- [12] J. Cook, Process for purifying human papillomavirus virus-like particles, uS Patent 6,602,697 (Aug. 5 2003).
- [13] M. D. Wenger, P. Dephillips, C. E. Price, D. G. Bracewell, An automated microscale chromatographic purification of virus-like particles as a strategy for process development., *Biotechnol. Appl. Biochem.* 47 (Pt 2) (2007) 131–9. doi:10.1042/BA20060240.
- [14] N. Willoughby, Too big to bind? Will the purification of large and complex therapeutic targets spell the beginning of the end for column chromatography?, *J. Chem. Technol. Biotechnol.* 84 (2) (2009) 145–150. doi:10.1002/jctb.2020.
- [15] M. Yu, Y. Li, S. Zhang, X. Li, Y. Yang, Y. Chen, G. Ma, Z. Su, Improving stability of virus-like particles by ion-exchange chromatographic supports with large pore size: advantages of gigaporous media beyond enhanced binding capacity., *J. Chromatogr. A* 1331 (2014) 69–79. doi:10.1016/j.chroma.2014.01.027.

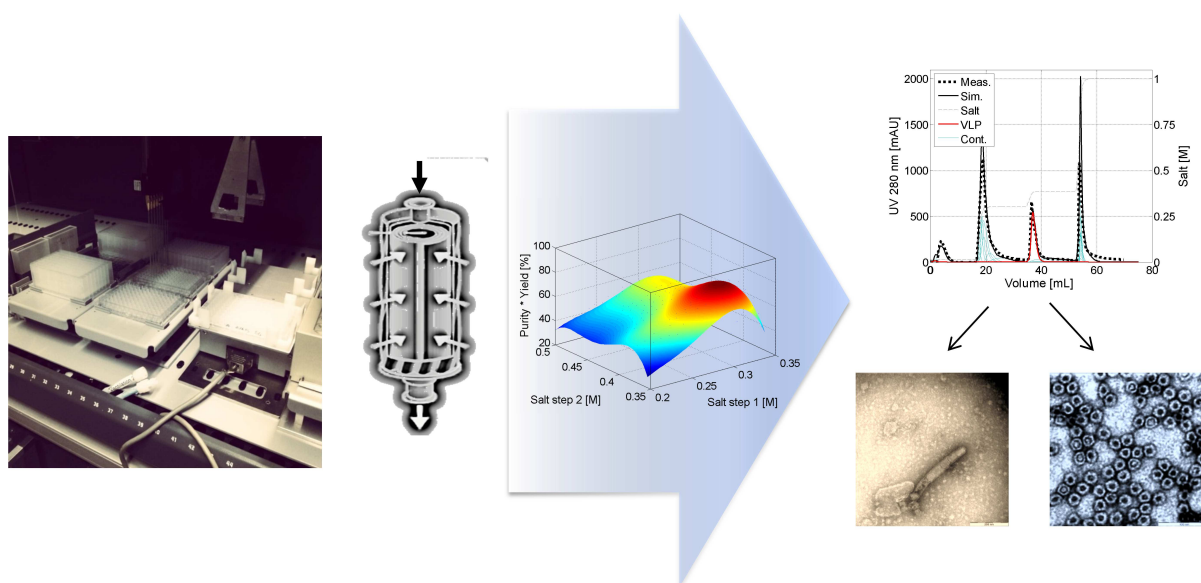
-
- [16] Y. Huang, J. Bi, W. Zhou, Y. Li, Y. Wang, G. Ma, Z. Su, Improving recovery of recombinant hepatitis B virus surface antigen by ion-exchange chromatographic supports with low ligand density, *Process Biochem.* 41 (11) (2006) 2320–2326. doi:10.1016/j.procbio.2006.06.004.
- [17] Y. Li, J. Bi, W. Zhou, Y. Huang, L. Sun, A.-P. Zeng, G. Ma, Z. Su, Characterization of the large size aggregation of Hepatitis B virus surface antigen (HBsAg) formed in ultrafiltration process, *Process Biochem.* 42 (3) (2007) 315–319. doi:10.1016/j.procbio.2006.08.016.
- [18] L. Schädlich, T. Senger, C. J. Kirschning, M. Müller, L. Gissmann, Refining HPV 16 L1 purification from *E. coli*: reducing endotoxin contaminations and their impact on immunogenicity., *Vaccine* 27 (10) (2009) 1511–22. doi:10.1016/j.vaccine.2009.01.014.
- [19] P. Guo, Y. El-Gohary, K. Prasad, C. Shiota, X. Xiao, J. Wiersch, J. Paredes, S. Tulachan, G. K. Gittes, Rapid and simplified purification of recombinant adeno-associated virus., *J. Virol. Methods* 183 (2) (2012) 139–46.
- [20] M. Rito-Palomares, Practical application of aqueous two-phase partition to process development for the recovery of biological products., *J. Chromatogr. B. Analyt. Technol. Biomed. Life Sci.* 807 (1) (2004) 3–11. doi:10.1016/j.jchromb.2004.01.008.
- [21] P. a. J. Rosa, I. F. Ferreira, a. M. Azevedo, M. R. Aires-Barros, Aqueous two-phase systems: A viable platform in the manufacturing of biopharmaceuticals., *J. Chromatogr. A* 1217 (16) (2010) 2296–305. doi:10.1016/j.chroma.2009.11.034.
- [22] P. Diederich, S. Amrhein, F. Hämmerling, J. Hubbuch, Evaluation of PEG/phosphate aqueous two-phase systems for the purification of the chicken egg white protein avidin by using high-throughput techniques, *Chem. Eng. Sci.* 104 (2013) 945–956. doi:10.1016/j.ces.2013.10.008.
- [23] M. Rito-palomares, A. Lyddiatt, Process integration using aqueous two-phase partition for the recovery of intracellular proteins, *Chem. Eng. J.* 87 (2002) 313–319.
- [24] P. Albertsson, Partition of cell particles and macromolecules: distribution and fractionation of cells, mitochondria, chloroplasts, viruses, proteins, nucleic acids, and antigen-antibody complexes in aqueous polymer two-phase systems, Wiley-Interscience, 1971.
- [25] R. Hatti-Kaul, *Aqueous Two-phase Systems: Methods and Protocols*, Methods in biotechnology, Humana Press, 2000.
- [26] S. a. Oelmeier, F. Dismer, J. Hubbuch, Application of an aqueous two-phase systems high-throughput screening method to evaluate mAb HCP separation., *Biotechnol. Bioeng.* 108 (1) (2011) 69–81. doi:10.1002/bit.22900.
- [27] a.M. Targovnik, O. Cascone, M. Miranda, Extractive purification of recombinant peroxidase isozyme c from insect larvae in aqueous two-phase systems, *Sep. Purif. Technol.* 98 (2012) 199–205. doi:10.1016/j.seppur.2012.08.004.
- [28] S. A. Oelmeier, C. Ladd Effio, J. Hubbuch, High throughput screening based selection of phases for aqueous two-phase system-centrifugal partitioning chromatography of monoclonal antibodies, *J. Chromatogr. A* 1252 (2012) 104–114.
- [29] M. Bensch, B. Selbach, J. Hubbuch, High throughput screening techniques in downstream processing: Preparation, characterization and optimization of aqueous two-phase systems, *Chem. Eng. Sci.* 62 (7) (2007) 2011–2021. doi:10.1016/j.ces.2006.12.053.

- [30] D. I. Bernstein, H. M. El Sahly, W. a. Keitel, M. Wolff, G. Simone, C. Segawa, S. Wong, D. Shelly, N. S. Young, W. Dempsey, Safety and immunogenicity of a candidate parvovirus B19 vaccine., *Vaccine* 29 (43) (2011) 7357–63. doi:10.1016/j.vaccine.2011.07.080.
- [31] S. Chandramouli, A. Medina-Selby, D. Coit, M. Schaefer, T. Spencer, L. a. Brito, P. Zhang, G. Otten, C. W. Mandl, P. W. Mason, P. R. Dormitzer, E. C. Settembre, Generation of a parvovirus B19 vaccine candidate., *Vaccine* 31 (37) (2013) 3872–8. doi:10.1016/j.vaccine.2013.06.062.
- [32] J. Benavides, J. a. Mena, M. Cisneros-Ruiz, O. T. Ramírez, L. a. Palomares, M. Rito-Palomares, Rotavirus-like particles primary recovery from insect cells in aqueous two-phase systems., *J. Chromatogr. B. Analyt. Technol. Biomed. Life Sci.* 842 (1) (2006) 48–57. doi:10.1016/j.jchromb.2006.05.006.
- [33] F. Luechau, T. C. Ling, A. Lyddiatt, Recovery of B19 virus-like particles by aqueous two-phase systems, *Food Bioprod. Process.* 89 (4) (2011) 322–327. doi:10.1016/j.fbp.2010.10.008.
- [34] S. Mukherjee, M. V. Thorsteinsson, L. B. Johnston, P. a. DePhillips, A. Zlotnick, A quantitative description of in vitro assembly of human papillomavirus 16 virus-like particles., *J. Mol. Biol.* 381 (1) (2008) 229–37. doi:10.1016/j.jmb.2008.05.079.
- [35] S. P. Sánchez-Rodríguez, L. Münch-Anguiano, O. Echeverría, G. Vázquez-Nin, M. Mora-Pale, J. S. Dordick, I. Bustos-Jaimes, Human parvovirus B19 virus-like particles: In vitro assembly and stability., *Biochimie* 94 (3) (2012) 870–8. doi:10.1016/j.biochi.2011.12.006.
- [36] I. Sutherland, P. Hewitson, R. Siebers, R. van den Heuvel, L. Arbenz, J. Kinkel, D. Fisher, Scale-up of protein purifications using aqueous two-phase systems: comparing multilayer toroidal coil chromatography with centrifugal partition chromatography., *J. Chromatogr. A* 1218 (32) (2011) 5527–30. doi:10.1016/j.chroma.2011.04.013.
- [37] I. a. Sutherland, G. Audo, E. Bourton, F. Couillard, D. Fisher, I. Garrard, P. Hewitson, O. Intes, Rapid linear scale-up of a protein separation by centrifugal partition chromatography., *J. Chromatogr. A* 1190 (1-2) (2008) 57–62. doi:10.1016/j.chroma.2008.02.092.
- [38] S. Oelmeier, C. Ladd-Effio, J. Hubbuch, Alternative separation steps for monoclonal antibody purification: Combination of centrifugal partitioning chromatography and precipitation, *J. Chromatogr. A* 1319 (2013) 118–126.
- [39] J. C. Merchuk, B. a. Andrews, J. a. Asenjo, Aqueous two-phase systems for protein separation. Studies on phase inversion., *J. Chromatogr. B. Biomed. Sci. Appl.* 711 (1-2) (1998) 285–93.
- [40] Y. Yuan, E. Shane, C. N. Oliver, Reversed-phase high-performance liquid chromatography of virus-like particles., *J. Chromatogr. A* 816 (1) (1998) 21–8.
- [41] S.-L. Sim, T. He, A. Tscheliessnig, M. Mueller, R. B. H. Tan, A. Jungbauer, Protein precipitation by polyethylene glycol: a generalized model based on hydrodynamic radius., *J. Biotechnol.* 157 (2) (2012) 315–9. doi:10.1016/j.jbiotec.2011.09.028.
- [42] W. Hönig, M. R. Kula, Selectivity of protein precipitation with polyethylene glycol fractions of various molecular weights., *Anal. Biochem.* 72 (1976) 502–12.

-
- [43] D. H. Atha, K. C. Ingham, Mechanism of Precipitation of Proteins by Polyethylene Glycols, *J. Biol. Chem.* 256 (23) (1981) 12108–12117.
- [44] S. Matheus, W. Friess, D. Schwartz, H.-C. Mahler, Liquid high concentration IgG1 antibody formulations by precipitation., *J. Pharm. Sci.* 98 (9) (2009) 3043–57. doi:10.1002/jps.21526.
- [45] G. Gallinella, Parvovirus B19 Achievements and Challenges, *ISRN Virol* 2013. doi:10.5402/2013/898730.
- [46] M. Pawlita, M. Müller, M. Oppenländer, H. Zentgraf, M. Herrmann, M. Oppenla, M. Pawlita, M. Mu, DNA encapsidation by viruslike particles assembled in insect cells from the major capsid protein VP1 of B-lymphotropic papovavirus . DNA Encapsidation by Viruslike Particles Assembled in Insect Cells from the Major Capsid Protein VP1 of B-Lymphotropic Pap, *J. Virol.* 70 (11) (1996) 7517–7526.
- [47] L. F. Pease, D. I. Lipin, D.-H. Tsai, M. R. Zachariah, L. H. L. Lua, M. J. Tarlov, A. P. J. Middelberg, Quantitative characterization of virus-like particles by asymmetrical flow field flow fractionation, electrospray differential mobility analysis, and transmission electron microscopy., *Biotechnol. Bioeng.* 102 (3) (2009) 845–55. doi:10.1002/bit.22085.
- [48] B. a. Andrews, a. S. Schmidt, J. a. Asenjo, Correlation for the partition behavior of proteins in aqueous two-phase systems: effect of surface hydrophobicity and charge., *Biotechnol. Bioeng.* 90 (3) (2005) 380–90. doi:10.1002/bit.20495.
- [49] H. Oka, K. Harada, Y. Ito, Separation of antibiotics by counter-current chromatography., *J. Chromatogr. A* 812 (1-2) (1998) 35–52.
- [50] J. K. Eggersgluess, M. Richter, M. Dieterle, J. Strube, Multi-Stage Aqueous Two-Phase Extraction for the Purification of Monoclonal Antibodies, *Chem. Eng. Technol.* 37 (4) (2014) 675–682. doi:10.1002/ceat.201300604.
- [51] S. Adelman, G. Schembecker, Influence of physical properties and operating parameters on hydrodynamics in Centrifugal Partition Chromatography., *J. Chromatogr. A* 1218 (32) (2011) 5401–13. doi:10.1016/j.chroma.2011.01.064.
- [52] a.R. Paschedag, W. Piarah, M. Kraume, Sensitivity study for the mass transfer at a single droplet, *Int. J. Heat Mass Transf.* 48 (16) (2005) 3402–3410. doi:10.1016/j.ijheatmasstransfer.2005.01.042.
- [53] F. Luechau, T. C. Ling, A. Lyddiatt, A descriptive model and methods for up-scaled process routes for interfacial partition of bioparticles in aqueous two-phase systems, *Biochem. Eng. J.* 50 (3) (2010) 122–130. doi:10.1016/j.bej.2010.04.006.
- [54] P. Jauregi, M. A. Hoeben, R. G. J. M. V. D. Lans, G. Kwant, Recovery of Small Bioparticles by Interfacial Partitioning, *Biotechnol. Bioeng.* 78 (2002) (2002) 355–364. doi:10.1002/bit.10199.
- [55] T. Cunha, R. Aires-Barros, Large-scale extraction of proteins., *Mol. Biotechnol.* 20 (1) (2002) 29–40. doi:10.1385/MB:20:1:029.
- [56] S. Tsoka, O. C. Ciniawskyj, O. R. Thomas, N. J. Titchener-Hooker, M. Hoare, Selective flocculation and precipitation for the improvement of virus-like particle recovery from yeast homogenate., *Biotechnol. Prog.* 16 (4) (2000) 661–7. doi:10.1021/bp0000407.

Modeling and Simulation of Anion-Exchange Membrane Chromatography for Purification of *Sf9* Insect Cell-derived Virus-like Particles.

C. Ladd Effio¹, T. Hahn¹, J. Seiler¹, S. A. Oelmeier^{1,2}, I. Asen³, C. Silberer³,
L. Villain⁴ and J. Hubbuch^{1,*}



¹ : Institute of Process Engineering in Life Sciences, Section IV: Biomolecular Separation Engineering, Karlsruhe Institute of Technology, Engler-Bunte-Ring 1, 76131 Karlsruhe, Germany

² : Boehringer Ingelheim Pharma GmbH & Co. KG, Birkendorfer Str. 65, 88400 Biberach an der Riß, Germany

³ : Diarect AG, Bötzingen Str. 29B, 79111 Freiburg im Breisgau, Germany

⁴ : Sartorius Stedim Biotech, August-Spindler-Str. 11, 37079 Göttingen, Germany

* : Corresponding author. *E-mail address*: juergen.hubbuch@kit.edu (J. Hubbuch)

J. Chrom. A (2015), doi:10.1016/j.chroma.2015.12.006

Abstract

Recombinant protein-based virus-like particles (VLPs) are steadily gaining in importance as innovative vaccines against cancer and infectious diseases. VLPs carry no replicative viral genetic information and are produced as large protein assemblies in recombinant expression systems. Multiple VLPs are currently evaluated in clinical phases requiring a straightforward and rational process design. To date, there is no generic platform process available for the purification of VLPs. Numerous process steps are needed to separate undesired host cell impurities. In order to accelerate and simplify VLP downstream processing, there is a demand for novel development approaches, technologies, and purification tools. Membrane adsorbers have been identified as promising stationary phases for the processing of bionanoparticles due to their large pore sizes. In this work, we present the potential of two strategies for designing VLP processes following the basic tenet of 'quality by design': High-throughput experimentation and process modeling of an anion-exchange membrane capture step. Automated membrane screenings allowed the identification of optimal VLP binding conditions yielding a dynamic binding capacity of 5.7 mg/mL for human B19 parvovirus-like particles derived from *Spodoptera frugiperda* Sf9 insect cells. A mechanistic approach was implemented for radial ion-exchange membrane chromatography using the lumped-rate model and steric mass action model for the *in silico* optimization of a VLP capture step. For the first time, process modeling enabled the *in silico* design of a selective, robust and scalable process with minimal experimental effort for a complex VLP feedstock. The optimized anion-exchange membrane chromatography process resulted in a protein purity of 81.5%, a DNA clearance of 99.2%, and a VLP recovery of 59%.

Keywords: Quality by design, Membrane chromatography, Predictive modeling, Downstream processing, Virus-like particle vaccine, High-throughput process development

1 Introduction

Virus-like particles (VLPs) are highly ordered protein assemblies mimicking the structure of viruses. Recent progress in the development of VLP-based vaccines against highly pathogenic viruses and organisms such as Ebola [1], Malaria [2] or Influenza [3] highlights the importance of this novel molecule class for the global health system. Ensuring a fast and economic availability of VLP vaccines requires a rapid and robust manufacturing process. VLPs are currently produced in recombinant systems such as bacteria, yeast, insect or plant cells necessitating subsequent downstream process steps for the separation of host-cell impurities to minimize the risk of side effects [4]. The most prevalent unit operation for the purification of biopharmaceutical products is ion-exchange chromatography. Traditional chromatography media are based on adsorber particles with pore sizes in the nanometer region causing mass transfer limitations and low binding capacities for bionanoparticles such as viruses or VLPs [5, 4]. Among others, membrane adsorbers have been developed and constantly advanced for the purification of large biomolecules in bind-and-elute mode [6, 7, 8, 9, 10, 11]. Membrane adsorbers are composed of multiple flat sheets of functionalized membranes with pore sizes in the range of micrometers. An increase in the specific surface in such flat sheets can be achieved by grafting hydrogels on membranes to embed ligands [12]. According to Nestola et al. hydrogel-grafted membranes lead to higher recoveries for virus purifications than directly grafted membranes [13]. The geometries of membrane adsorbers are usually either stacked flat sheet or spiral wound modules with axial or radial flow. Regarding separation performance parameters such as resolution, peak width, and dynamic binding capacity, there are no outstanding differences between axial and radial flow geometries [14, 15]. However, radial flow geometries are especially suited for large-scale applications by virtue of lower pressure drops as demonstrated by Besselink et al. [15]: Wide, short axial flow columns can be similarly replaced with low-pressure narrow, tall radial-flow columns without a significant change in performance. The combination of both radial flow geometry and convection-driven mass transport in membrane adsorbers allows high throughputs and productivities for biopharmaceutical products [16, 17].

In recent years, the process development for biologics has been relying predominantly on empirical studies. Minimizing the risks of manufacturing failures and lot-to-lot variations of biological products has been the key motivation for the FDA to forward the approaches 'quality by design' (QbD) and 'process analytical technology' (PAT) [18]. One major contribution to and important tool for process control and design is mechanistic modeling. Multiple thermodynamic and hydrodynamic models have been developed and steadily extended for chromatographic separations of proteins [19, 20, 21, 22, 23, 24, 25]. Recently, novel hydrodynamic models were established for membrane adsorbers including axial and radial flow and validated in various protein case studies [26, 12]. In contrast, there have been only few publications on modeling and simulation of VLP processes. Vicente et al. demonstrated the applicability of the steric mass action model [27] for purified rotavirus-like particles with a mean diameter of 80 nm on stacked flat sheet anion-exchange (AEX) membrane adsorbers [7]. However, the measured and simulated chromatograms for the complex VLP feedstock differed significantly and up to now there has not been any case study reporting on the *in silico* optimization of a VLP separation. The difficulty for *in silico* simulations and optimizations of complex biological feedstocks lies in modeling the mass transfer of components of unknown size and concentration. An approach to dealing with this was previously reported by Hahn et al. [28] and Baumann et al. [29]. In both case studies, UV absorption-based modeling was implemented to simulate the elution profile of complex biological feedstock components using UV peak areas instead of molar concentrations. In this work, we present a case study for the purification of human B19 parvo-VLPs derived from *Spodoptera frugiperda* Sf9 insect cells applying both high-throughput experimentation and

UV absorption-based chromatography modeling. Human B19 parvo-VLPs have a size of 25 to 30 nm and can be assembled in insect cells by expressing the major capsid protein VP2. The particles are currently evaluated in clinical phase studies as vaccine candidates against diseases attributed to parvovirus infections such as fifth disease in children, anaemia, and hydrops fetalis [30, 31]. The developed membrane process allowed the separation of major contaminants such as host cell proteins and DNA in one step and can be predicted and controlled by *in silico* process simulations.

2 Materials & Methods

2.1 Disposables

For screening purposes on a liquid handling station, 1 mL-96 deep well polypropylene plates (Thermo Fisher Scientific Inc., Waltham, Massachusetts, USA) and 96-well half area polystyrene flat-bottom plates by Greiner Bio-One (Kremsmünster, Austria) were used. Fraction collection on a FPLC system was done with 2 mL-96 deep well polypropylene plates (Nalge Nunc International, Rochester, USA). Sterile filtration of buffer solutions was conducted with 0.2 μm cellulose acetate filters (Sartorius AG, Goettingen, Germany). Buffer exchange was performed with PD-10 desalting columns (GE Healthcare, Uppsala, Sweden).

2.2 Chemicals & Buffers

Bis-Tris, Bis-Tris propane and dextran T2000 were purchased from Sigma-Aldrich (St. Louis, USA). Guanidine hydrochloride from AppliChem GmbH (Darmstadt, Germany) and dithiothreitol from Amresco (Solon, USA) were used for the preparation of UHPLC samples. All other chemicals were purchased from Merck KGaA (Darmstadt, Germany). For automated batch membrane chromatography experiments, a low and high pH multicomponent buffer with a buffer capacity of 10 mM, composed of Bis-Tris, Bis-Tris propane and Tris was used to obtain a linear pH gradient between pH 7.5 and pH 9.0. The buffer recipe was calculated according to Kröner and Hubbuch [32]. 10% (v/v) glycerol and 0.5% (v/v) polysorbate 80 were added to all ion-exchange buffers to prevent aggregation and secondary interactions of VLPs [33]. FPLC runs were performed with 20 mM Tris pH 8.5, 0.5% (v/v) polysorbate 80 and 10% (v/v) glycerol (buffer A) and 20 mM Tris pH 8.5, 1 M NaCl, 0.5% (v/v) polysorbate 80 and 10% (v/v) glycerol (buffer B). Membranes were regenerated with 1 M NaOH and 3 M guanidine hydrochloride and stored in 20% (v/v) ethanol in 20 mM Tris pH 8.5.

2.3 Human B19 Parvovirus-like Particles

Human B19 parvo-VLPs composed of the major viral capsid protein VP2 were derived from *Sf9* insect cells. Insect cell pellets were provided by Diarect AG (Freiburg, Germany) and lysed and clarified as described previously by sonication, centrifugation, and filtration [34]. Prior to membrane experiments, buffer exchange was performed using PD-10 desalting columns (GE Healthcare, Uppsala, Sweden).

2.4 Anion-Exchange Membrane Chromatography

All AEX chromatography experiments were performed with Sartobind[®] Q membranes from Sartorius AG (Goettingen, Germany). Binding studies for VLPs were conducted in 96-well

membrane plates on a robotic liquid handling system. Membrane characterization and salt elution studies with clarified VLP feedstocks were done with 3 mL Sartobind[®] nano Q membrane capsules. Experiments with membrane capsules were performed on an ÄKTA-purifier 10 fast protein liquid chromatography (FPLC) equipped with a pump module P-900 (up to 10 mL/min), UV (10 mm path length) monitor (UV-900), a conductivity monitor, and a fraction collector Frac-950 (GE Healthcare, Uppsala, Sweden). The instrument was controlled using the software UNICORN 5.31 (GE Healthcare, Uppsala, Sweden).

2.4.1 Hydrodynamic & Thermodynamic Models

FPLC experiments were conducted with radial spiral-wound membrane adsorbers as displayed in Fig. 1. A general rate model for radial flow chromatography has been developed by Gu et al. [35] considering radial dispersion, convection, and pore diffusion of a component i in radial direction x using differential mass balances. The continuity equation for the component i with a lumped effective mass transfer coefficient $k_{eff,i}$ incorporating film and pore diffusion is given by Eq. (1):

$$\frac{\partial c_i}{\partial t} = \left(\pm u(x) + \frac{D_{ax}}{x} \right) \frac{\partial c_i}{\partial x} + D_{ax} \frac{\partial^2 c_i}{\partial x^2} - \frac{(1 - \varepsilon_{pores})}{\varepsilon_{pores}} k_{eff,i} (c_i - c_{p,i}) \quad i = 1, \dots, N \quad (1)$$

The algebraic sign of the convective transport term $u(x)$ is positive for inward flow which was the case for the membrane capsules used in this work. In Eq.(1), the first term describes the convective transport, the second term the hydrodynamic dispersion, and the last term refers to the transport of component i between bulk and membrane pore volume $c_i - c_{p,i}$ for the membrane porosity ε_{pores} . Danckwerts' boundary conditions [36, 37] can be used to describe the effect of diffusion-dispersion phenomena on the concentration at the column inlet $x = r_a$ (*outer radius*)(Eq.(2)). In contrast, the outlet concentration at $x = r_i$ (*inner radius*) for inward flow is unaffected by these phenomena (Eq.(3)).

$$x = r_a : \quad \frac{\partial c_i}{\partial x}(t, x = r_a) = \frac{u(x = r_a)}{D_{ax}} (c_i(t, x = r_a) - c_{in,i}(t)) \quad (2)$$

$$x = r_i : \quad \frac{\partial c_i}{\partial x}(t, x = r_i) = 0 \quad (3)$$

As described previously by Van Beijeren et al. [12], the frontal area A_{front} for a spiral wound geometry depends on the radial position x and the membrane height H (Eq.(4)):

$$A_{front} = 2\pi x H \quad (4)$$

Thus, for inward flow with the volumetric flow rate F , the linear interstitial velocity u increases towards the center of the membrane adsorber (Eq.(5)):

$$u(x) = \frac{F}{\varepsilon_{pores} 2\pi x H} \quad (5)$$

Most membrane adsorbers include a grafted hydrogel layer with embedded ligands to obtain a higher specific surface area [9]. Such hydrogels may exclude large molecules such as dextran T2000 and viruses [9, 10]. The hydrogel mass transfer can be modeled by incorporating a hydrogel porosity $\varepsilon_{hydrogel}$. Hence, the mass balance for the stationary phase considers accumulation and mass transport inside the membrane pores (Eq.(6)):

$$\frac{\partial c_{p,i}}{\partial t} = \frac{k_{eff,i}}{\varepsilon_{hydrogel}} (c_i - c_{p,i}) - \frac{(1 - \varepsilon_{hydrogel})}{\varepsilon_{hydrogel}} \frac{\partial q_i}{\partial t} \quad i = 1, \dots, N \quad (6)$$

The mass transport of component i in the liquid phase is described by the film transfer coefficient $k_{eff,i}$, the pore concentration $c_{p,i}$, the hydrogel porosity $\varepsilon_{Hydrogel}$, and the concentration bound to the stationary phase q_i . The adsorption term can be described for ion-exchange (IEX) chromatography with the steric mass action (SMA) model developed by Brooks and Cramer [27]. The semi-mechanistic isotherm considers several effects for IEX adsorption and desorption processes:

- Concentration of available binding sites given by the total ionic capacity Λ
- Shielding of ligands by large macromolecules i described by the shielding factor σ_i
- Number of macromolecules' binding sites described by the characteristic charge ν_i
- Ratio of adsorption $k_{ads,i}$ and desorption constant $k_{des,i}$ depicted by the equilibrium term $k_{eq,i} = \frac{k_{ads,i}}{k_{des,i}}$
- Changing salt concentrations $c_{p,salt}$ in the pore volume

The rate of change of the concentration in the stationary phase q_i can be modeled with the kinetic form of the SMA isotherm (Eq.(7)) [24]:

$$\frac{1}{k_{des,i}} \frac{\partial q_i}{\partial t} = k_{eq,i} \left(\Lambda - \sum_{j=1}^N (\nu_j + \sigma_j) q_j \right)^{\nu_i} c_{p,i} - c_{p,salt}^{\nu_i} q_i \quad i = 1, \dots, N \quad (7)$$

Eq. (8) describes the competition of salt ions and other components for binding sites in the stationary phase:

$$q_{salt} = \Lambda - \sum_{j=1}^N \nu_j q_j \quad (8)$$

For estimating SMA and hydrodynamic parameters of complex feedstocks with multiple components of unknown concentration, the absorption coefficient a_i is used. The factor scales the molar concentrations required for modeling mass transport in the stationary phase to absorbance units. Thus, Eq. (7) can be written as (Eq. (9)):

$$\frac{1}{k_{des,i}} \frac{\partial q_i}{\partial t} = k_{eq,i} \left(\Lambda - \sum_{j=1}^N \frac{(\nu_j + \sigma_j)}{a_j} q_j \right)^{\nu_i} c_{p,i} - c_{p,salt}^{\nu_i} q_i \quad i = 1, \dots, N \quad (9)$$

According to Baumann et al. [29], the total ionic capacity predominates, and occupied ligands can be neglected in the case of small sample loadings which do not approach the maximum binding capacity of the stationary phase. This makes it feasible to estimate most SMA and hydrodynamic parameters directly from chromatograms by UV absorption-based modeling as demonstrated previously [29, 25, 28].

Parameter estimation was performed as described previously by chromatogram fitting using a genetic algorithm [38]. Both, parameter estimation and *in silico* optimization of a VLP capture process, were conducted with the chromatography software ChromX [39].

2.4.2 Automated Batch Binding Screenings

Optimal binding conditions for VLPs on the AEX membranes were determined by miniaturized and automated microbatch experiments on a Tecan Freedom EVO[®] 200 system (Tecan, Crailsheim, Germany) using Sartobind[®] Q 96-well plates with a membrane area of 0.7 cm². The high-throughput screening procedure followed the same routine for adsorption isotherms and binding screenings: Equilibration, centrifugation, sample preparation, incubation, loading, centrifugation and preparation of analytical samples. Membranes were equilibrated with 2 mL buffer per well at the desired pH and ionic strength. Centrifugation was performed at 1000 rpm for 10 min. Sample preparation was conducted by mixing stock solutions of buffers and VLP feedstocks at different dilutions in 96-DeepWell plates. Systems were incubated for 10 min on an orbital shaker at 1000 rpm. Subsequently, 300 μ L sample volume was added to each well of the 96-well membrane plate. Thereafter, samples were centrifuged and VLPs in the flow-through were tracked by RP-UHPLC as described below. The adsorption isotherm screening was performed under buffer conditions similar to the initial cell lysis step at 50mM Tris pH 7.4, 50 mM NaCl, 10% (v/v) glycerol and 0.5% (v/v) polysorbate 80. Data was fitted to the Langmuir isotherm. Eq. (10) [40, 41] describes the correlation for the equilibrium concentration in the mobile phase $c_{eq,i}$ and the concentration in the stationary phase q_i assuming a saturation capacity q_S and an equilibrium constant $k_{eq,i}$.

$$q_i = \frac{q_S k_{eq,L,i} c_{eq,i}}{1 + k_{eq,L,i} c_{eq,i}} \quad (10)$$

Subsequent to the determination of VLP adsorption isotherms, the goal was to find optimal buffer conditions for the binding step due to possible displacement effects by other components in the VLP feedstock. Four stock solutions with and without VLP feedstock were prepared at pH 7.5 and pH 9 with 15 and 120 mM NaCl using the multicomponent buffer described under Section 1.1. Buffers were mixed in the appropriate volume ratio to obtain a Design of Experiments (DoE) set-up with four pH values and eight ionic strengths with triplicate determinations. Method and analysis were the same as for the isotherm determination. To obtain optimal binding conditions, the starting VLP concentration in each well was chosen from the non-linear region of the adsorption isotherm.

2.4.3 System & Membrane Characterization

Modeling of hydrodynamic and thermodynamic mass transfer in the membrane capsule and FPLC system requires knowledge of several membrane and system characteristics. The determination of system dead volumes V_d , membrane porosity ε_{pores} and hydrogel porosity $\varepsilon_{hydrogel}$ was done by injecting small and large tracer molecules: 1% v/v acetone, 1 M NaCl, and 10 mg/mL dextran T2000. 100 μ L of the tracer substances were injected via an ÄKTA sample loop with a twofold loop overflow and tracked using UV and conductivity detectors. Acetone and NaCl were used to determine the system dead volume from sample loop to UV and conductivity detector, respectively. Dextran T2000 served as large tracer component for the determination of the interstitial volume V_{int} , the membrane porosity ε_{pores} and the hydrogel porosity $\varepsilon_{hydrogel}$. The ionic capacity of the anion-exchange membrane was obtained by performing a titration with 0.5 M NaOH and 0.01 M HCl according to standard protocols [42, 38] (Eq. (11)) :

$$\Lambda = \frac{c_{HCl} V_{HCl}}{V_M (1 - \varepsilon_t)} \quad (11)$$

All tracer runs and acid-base titrations were performed in at least five copies. Membrane characteristics such as membrane thickness L , membrane height H , outer radius r_a , and inner radius

r_i are illustrated in Fig. 1.

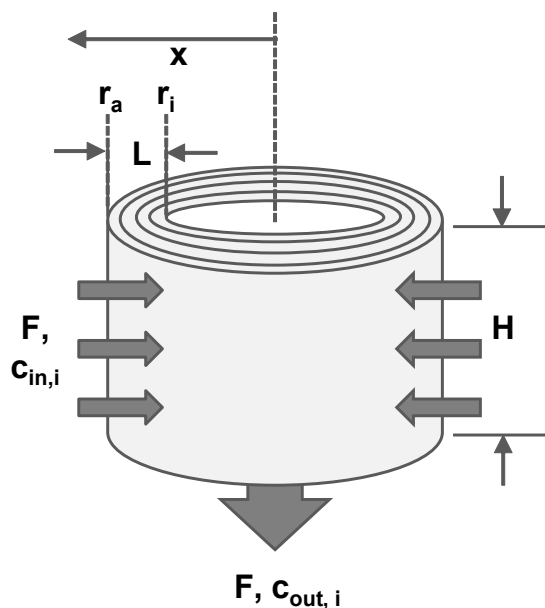


Figure 1 Schematic illustration of a spiral wound membrane adsorber with inward radial flow F , membrane thickness L , membrane height H , outer radius r_a and inner radius r_i .

An overview of all system & membrane parameters is given in Table 1 providing corresponding equations for the calculated values. Chromatograms of dextran T2000 and NaCl pulse experiments were used to estimate the hydrodynamic parameters, i.e. the axial dispersion D_{ax} and the film transfer coefficient $k_{eff,NaCl}$ by chromatogram fitting. All calculated membrane parameters are specified in Table 2.

Table 1 Measured membrane parameters

Parameter	Symbol	Value	Proceeding
Membrane volume	V_M	3 mL	From manufacturer
Membrane thickness	L	8 mm	From manufacturer
Outer radius	r_a	11.25 mm	From manufacturer
Inner radius	r_i	3.25 mm	From manufacturer
Membrane height	H	8 mm	From manufacturer
Total porosity	ε_t	0.798	From manufacturer
Flow rate	F	3 mL/min	Manually controlled
System dead volume	V_d	0.25 mL	Acetone injection without membrane
Retention volume acetone	V_{RetAc}	3.7 mL	Acetone injection with membrane
Retention volume dextran	V_{RetDex}	2.86 mL	Dextran injection with membrane
Retention volume NaCl	V_{NaCl}	3.42 mL	NaCl injection with membrane
Volume of HCl	V_{HCl}	12.8 mL	Acid-base titration
Molarity of HCl	c_{HCl}	0.01 M	Manually controlled

2.4.4 Determination of Dynamic Binding Capacity

An important parameter for selecting and evaluating chromatography media is the dynamic binding capacity (*DBC*). The *DBC* of the AEX membrane adsorbers was determined for VLPs by overloading the membrane with 10 mL VLP feedstock at a VLP concentration $c_{VLP,0}$ of 2.7 mg/mL, and optimum buffer conditions, derived from the batch binding studies (20 mM Tris pH 8.5, 15 mM NaCl, 0.5% (v/v) polysorbate 80, 10% (v/v) glycerol). The breakthrough experiment was conducted at a flow rate of 3 mL/min on the ÄKTApurifier 10 FPLC. Fractions were collected and analysed by reversed-phase (RP)-UHPLC. The *DBC* was calculated determining the applied volume at 10% breakthrough $V_{10\%}$ from the fitted breakthrough curve (Eq. (12)):

$$DBC = c_{VLP,0} \frac{V_{10\%} - V_{RetDex}}{V_M} \quad (12)$$

2.4.5 Calibration of Steric Mass Action Model

For the simulation and *in silico* optimization of an AEX membrane chromatography step, a component-specific calibration of the SMA model was required. Experiments were performed with 3 mL Sartobind[®] Q membrane adsorbers on the ÄKTApurifier 10 FPLC. The composition of buffer A was 20 mM Tris pH 8.5, 0.5% (v/v) polysorbate 80, 10% (v/v) glycerol. For elution, buffer A was supplemented with 1 M NaCl to create buffer B. Regeneration buffer was 1 M NaOH and storage buffer 20% EtOH in 20 mM Tris pH 8.5. Membranes were equilibrated with 5 CV of 1.5% B prior to sample injection. 1 mL VLP feedstock was injected in each run and fractions were collected during the whole run to track the VLP elution. Three salt gradients with gradient slopes of 10 CV, 20 CV and 30 CV from 1.5% to 100% B were performed to generate chromatograms for the SMA parameter estimation. Applying the peak integration tool of the ÄKTA software UNICORN 5.31, the VLP feedstock was divided into multiple subcomponents. Each UV peak was integrated for the 30 CV gradient run and the ratio of peak area and load volume was set as concentration for the UV-based modeling [25] of each component. Estimation of the SMA parameters $k_{eq,i}$, ν_i and the film transfer coefficients $k_{eff,i}$ was done by chromatogram fitting using a genetic algorithm.

2.4.6 Optimization of VLP Purification

Given a defined set of hydrodynamic and thermodynamic parameters, it is possible to simulate chromatograms of a multicomponent system and to optimize the separation of a target component *in silico*. In this work, this was attempted by varying the salt concentrations of a three-step elution process and simulating the effect on purity (P) and yield (Y). Salt concentrations of the first and second salt step were varied between 0.2 and 0.5 M NaCl, while the third salt step elution was at 1 M NaCl. The least-square optimization was performed for an objective fraction volume of 3 CV. The solution of the optimization problem p_{opt} is defined as (Eq. (13)):

$$p_{opt} = \arg \min_p \left(\underbrace{(1 - P(p))}_{\text{impurity}} + \underbrace{(1 - Y(p))}_{\text{loss}} \right) \quad (13)$$

The proposed optimal salt concentrations for the step elution process were evaluated for a loading of 1 and 6.5 mL and flow rates of 1 CV/min, 2 CV/min, and 3 CV/min.

2.5 Size-Exclusion Chromatography

Polishing of VLPs captured by an optimized salt step elution by AEX membrane chromatography was performed on a Superose[®] 6 Increase 10/300 column (GE Healthcare, Uppsala, Sweden). 500 μ L of a 2 mg/mL VLP solution was injected at a flow rate of 0.5 mL/min using PBS pH 7.4 as mobile phase buffer. Fractions were analyzed by RP-UHPLC and capillary gel electrophoresis to evaluate the final purity of the samples.

2.6 Analytical Methods

2.6.1 VLP Quantification

Quantification of VP2-VLPs was conducted as described previously by RP-UHPLC [34]. In brief, a Waters Acquity BEH C4 column was run in acetonitrile gradient elution mode on an UltiMate[®] 3000 RSLC x 2 Dual system (Thermo Fisher Scientific, Waltham, Massachusetts, USA). Samples were pre-denatured with a denaturing buffer containing 8 M guanidine hydrochloride and 60 mM DTT to avoid column blocking by aggregation and carryover. Final concentrations were determined by comparing peak areas with external VLP reference standards of known concentration.

2.6.2 Capillary Gel Electrophoresis

The final protein purity of processed VLPs was assessed by a LabChip[®] GX II capillary gel electrophoresis device separating proteins by size. Sample and chip preparation procedures were performed as described in the manufacturer's protocol for the HT Protein Express Assay [43]. Product quantification was based on peak-baseline integration and the protein purity (P) was determined as the ratio of product concentration c_{VP2} to the total protein concentration c_{Total} (Eq. (14)):

$$P = \frac{c_{VP2}}{c_{Total}} \quad (14)$$

2.6.3 DNA Quantification

DNA quantification was performed using the PicoGreen[®] dsDNA assay kit (Invitrogen, Paisley, United Kingdom) in 96-well plates according to the manufacturer's instructions.

2.6.4 Transmission Electron Microscopy

FPLC fractions and purified VLP samples were further analyzed by transmission electron microscopy to evaluate polydispersity and morphology of VLPs. As described previously [34], samples were applied on carbon grids, washed with ultrapure water, and stained with uranyl acetate prior to analysis on a Philips CM 200 FEG/ST transmission electron microscope at 200 kV.

3 Results & Discussion

3.1 Optimization of VLP Binding by High-Throughput Experimentation

Optimal binding conditions for human B19 parvo-VLPs on AEX membranes were determined by varying pH and ionic strength of the binding buffer in automated high-throughput microbatch

screenings. In a first step, the binding at pH 7.4 and 50 mM NaCl was investigated for increasing VLP concentrations. In Fig. 2 a, the VLP concentration in the stationary phase Q is plotted against the concentration in the mobile phase c_{VLP} with standard deviations illustrated by error bars. The values were fitted using the Langmuir isotherm obtaining a saturation capacity q_S of 5.6 mg VLP per mL membrane volume. The curve shows a similar pattern as usual one-component adsorption isotherms with a linear region for low concentrations and a saturation region for high VLP concentrations. Nevertheless, there is a strong decrease in capacity for higher VLP concentrations such as 1.15 mg/mL. It must be taken into account that the VLP feedstock used for the experiments is a complex multicomponent mixture containing multiple host cell proteins (HCPs), baculoviruses, and nucleic acids (DNA). AEX ligands strongly bind DNA at pH-values higher than pH 4.0, potentially causing the displacement of bound VLPs at high loadings [44]. Besides multicomponent displacement effects, the binding of biomolecules on IEX stationary phases is also influenced by secondary interactions such as hydrophobic adsorption and desorption processes [45, 46]. Therefore, both pH and NaCl concentration were varied using a DoE approach to identify optimum binding conditions for VLPs. For a bind-and-elute procedure, the pH working range was chosen beyond the predicted isoelectric point of the major capsid protein VP2 at pH 6.5 [47]. Moreover, to minimize the risk of VLP disassembly during the IEX process, the pH working range did not exceed a pH of 9.0 [47].

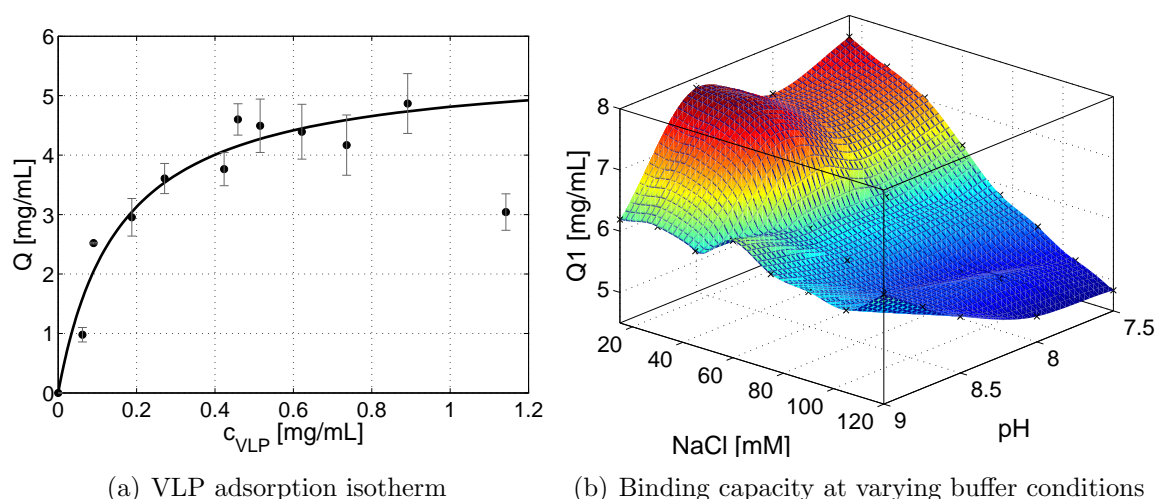


Figure 2 Batch adsorption of human B19 parvo-VLPs on Sartobind[®] Q membranes. Experiments were performed with *Spodoptera frugiperda* Sf9 insect cell lysate containing VLPs composed of the major capsid protein VP2. The VLP concentration in the stationary phase Q at 50 mM Tris pH 7.4, 50 mM NaCl is fitted using the Langmuir isotherm (solid line). The binding screening for varying pH values and NaCl concentrations was conducted with a multicomponent buffer system at a VLP concentration of 1 mg/mL. Each data point represents the mean value of triplicate binding experiments.

Fig 2 b displays the correlation of the VLP concentration in the stationary phase $Q1$ (1 mg/mL VLP in the mobile phase) with both NaCl concentrations and pH. It can be seen that the affinity for VLPs initially increases with pH and the maximum loading concentration is obtained at pH 8.5 and 15 mM NaCl. The bound amount of VLPs at pH 7.5 and 120 mM NaCl is almost 40% lower than at the optimum condition. Interestingly, the highest pH does not come along with the highest $Q1$ -value. At pH 9 and 15 mM NaCl, the loading mass is 19% lower than at pH 8.5. However, $Q1$ at pH 9.0 hardly decreases with increasing salt concentrations in contrast to pH 7.5, 8 and pH 8.5.

In general, there is a clear trend of decreased binding at increasing NaCl concentrations. Low

NaCl concentrations below 15 mM lead to precipitation of VLPs, and datapoints below 15 mM NaCl are therefore not included in Fig. 2 b. The stabilizing effect of NaCl has been reported before for various VLPs [48, 47]. The optimal binding buffer at pH 8.5 and 15 mM NaCl probably incorporates a negative VLP net charge, a low surface hydrophobicity, and a stable VLP conformation [47]. A slight pH increase to pH 9.0 implies a more negative net charge of the capsid protein VP2, but might coincide with conformational changes or even disassembly of VLPs as reported recently for hepatitis B surface antigen VLPs by Yang et al. [49].

3.2 Calibration of Hydrodynamic & Steric Mass Action Model

Subsequent to setting the buffer conditions for the AEX binding step by the DoE approach, elution conditions were optimized by process modeling and simulation. For modeling of the hydrodynamics in the membrane capsule, a dextran pulse was used to determine the axial dispersion coefficient D_{ax} by chromatogram fitting. In Fig. 3a, the UV absorption at a wave length of 215 nm is plotted against the mobile phase volume for a 10 mg/mL dextran T2000 pulse injection on a 3 mL Sartobind[®] Q membrane adsorber. The chromatogram shows an overlay of measured (*dotted line*) and simulated (*solid line*) UV signal. The simulation was possible by estimating the axial dispersion coefficient under consideration of the system and capsule dead volume. All calculated membrane-specific parameters are summarized in Table 2.

Table 2 Calculated membrane parameters

Parameter	Symbol	Value	Proceeding
Fluid volume	V_f	3.4 mL	$V_{RetAc} - V_d$
Void volume capsule	V_{voidC}	1.006 mL	$V_f - \varepsilon_t V_M$
Interstitial volume	V_{int}	2.56 mL	$V_{RetDex} - V_d - V_{voidC}$
Membrane porosity	ε_{pores}	0.518	$\frac{V_{int}}{V_M}$
Hydrogel porosity	$\varepsilon_{hydrogel}$	0.581	$\frac{\varepsilon_t - \varepsilon_{pores}}{1 - \varepsilon_{pores}}$
Axial dispersion	D_{ax}	0.0374 mm ² /s	Chromatogram fitting (dextran)
Film transfer coefficient NaCl	$k_{eff,NaCl}$	0.1829 mm ² /s	Chromatogram fitting (NaCl)
Ionic capacity	Λ	0.211 M	$\frac{c_{HCl} V_{HCl}}{V_M (1 - \varepsilon_t)}$
Volume applied at 10% breakthrough	$V_{10\%}$	9.2 mL	Interpolated from fraction analysis
Dynamic binding capacity for VLPs	DBC	5.7 mg/mL	$c_{VLP,0} \frac{V_{10\%} - V_{RetDex}}{V_M}$

An axial dispersion coefficient D_{ax} of 0.0374 mm²/s was estimated which is quite low in comparison to the dispersion in agarose-based chromatography columns [38]. Thus, the determined D_{ax} -value already implies a small peak-broadening effect by axial dispersion. In order to model the ion-exchange on the membrane surface, the film diffusion coefficient of NaCl was estimated by chromatogram fitting of a 1 M NaCl pulse injection. In Fig. 3b, the conductivity signal is plotted against the mobile phase volume. In contrast to the dextran peak, the measured NaCl peak (*dotted line*) shows a noticeable tailing and a longer retention volume. The NaCl peak was simulated (*solid line*) using the obtained D_{ax} value from the dextran chromatogram fitting and an estimated film transfer coefficient $k_{eff,NaCl}$ of 0.1829 mm/s. The differences in the retention volume of dextran T2000 and NaCl confirm the exclusion effect of large molecules

from hydrogel pores reported by Vicente et al. [10] and Tatarova et al. [9]. Both dispersion and film diffusion could be modeled using the continuity equation for radial flow with a lumped diffusion coefficient and standard tracer molecules for chromatographic stationary phases.

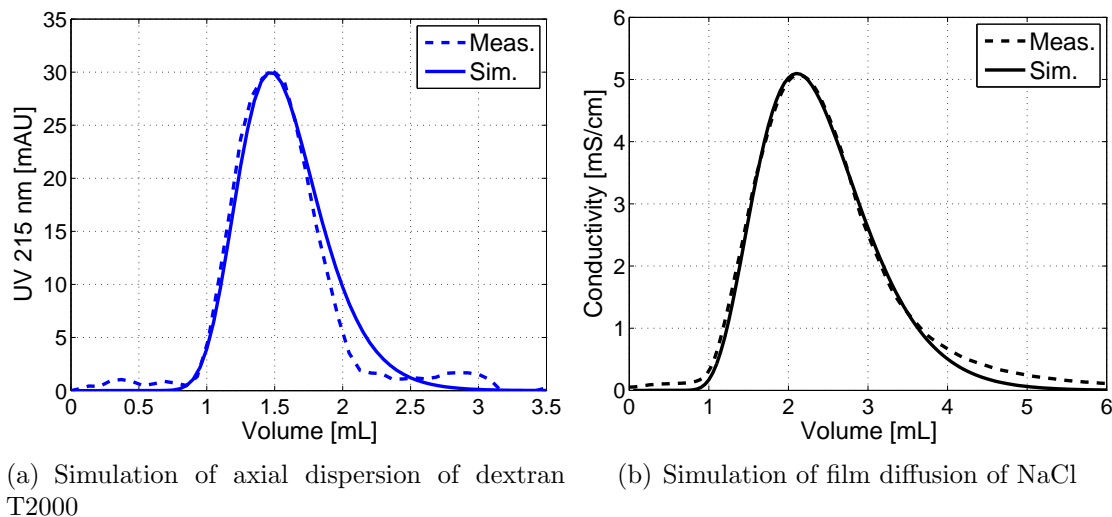


Figure 3 Comparison of measured (dotted lines) and simulated chromatograms (solid lines) for pulse experiments on a 3 mL Sartobind[®] Q membrane capsule with 100 μ L of the tracer molecules dextran T 2000 (10 mg/mL) and NaCl (1 M). System and capsule void volumes are subtracted from each chromatogram.

The SMA model was calibrated by determining the ionic capacity of the membrane (Table 2) and estimating component-specific SMA parameters by chromatogram fitting. In a first step, the dynamic binding of the AEX membrane for VLPs was determined by performing a breakthrough curve with the VLP feedstock. Knowledge of the dynamic binding capacity is essential to assess whether the requirements for UV absorption-based modeling are fulfilled in subsequent calibration runs (see Section 2.4.1). Fig. 4a shows the chromatogram of a breakthrough experiment: The UV absorption at 280 nm is plotted (*black solid line*) against the mobile-phase volume. The ratio of mobile-phase VLP concentration c to initial VLP concentration c_0 is illustrated by green bars with standard deviations for the analytics represented by grey error bars. The VLP breakthrough starts at 8.9 mL mobile-phase volume and the determined dynamic binding capacity at 10% breakthrough is 5.7 mg VLP per mL membrane adsorber (Table 2). The UV signal shows a first increase at about 3.7 min and a saddle point at approximately 9.2 mL followed by the same sharp increase as for the VLP concentration in the analyzed fractions. The sharp breakthrough of VLPs indicates a low dispersion of VLPs through the membrane pores as observed in the dextran T2000 pulse experiments for another large molecule. The achieved *DBC* of 5.7 mg/mL outperforms to the best of our knowledge all so far reported capacities of chromatographic matrices for VLPs [4]. VLP concentrations exceeding the starting concentration c_0 suggest a displacement effect of bound VLPs by other feedstock components with higher ligand affinities. Without the knowledge of the exact feedstock composition, modeling of the breakthrough of each component is not possible [28]. Therefore, model calibration and process simulation was only performed for low loadings with a total volume of 1 mL and a VLP mass of 2 mg corresponding to approximately 11% of the *DBC*. Figs.4b-d show the obtained UV 280 chromatograms for three different salt gradient lengths of 10, 20 and 30 CV from 0.015 M to 1 M NaCl. UV signal and VLP concentrations are again plotted by black solid lines and green bars, respectively. The conductivity is displayed by a dotted grey line. The chromatograms indicate

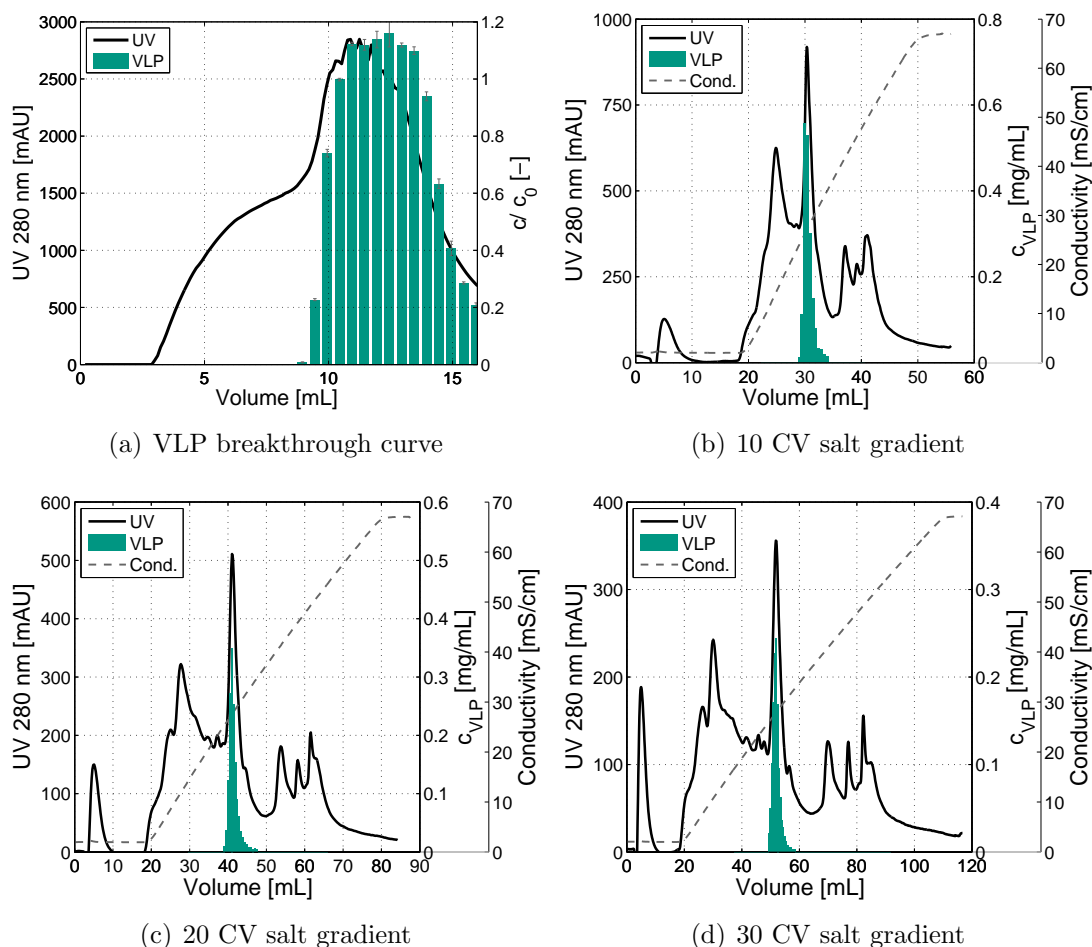
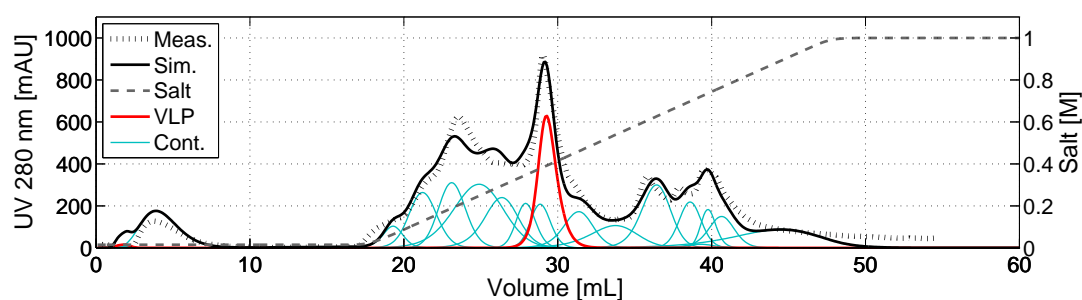


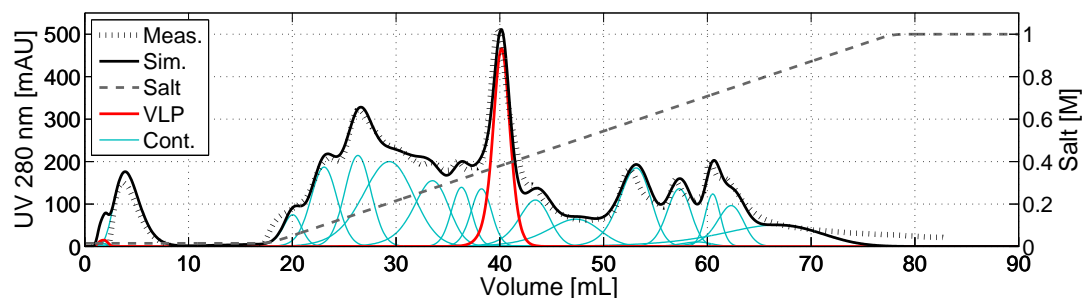
Figure 4 UV chromatograms of bind-and-elute experiments with a clarified human B19 parvo-VLP feedstock on a 3 mL Sartobind[®] Q membrane capsule. The experiments were conducted at a VLP concentration of 2.7 mg/mL (breakthrough experiment) and 2 mg/mL, respectively. The solid lines display the UV absorption signal at 280 nm, the dotted lines show the conductivity signals, and the green bars represent the VLP concentration in all fractions. The sample volumes were 10 mL for the breakthrough experiment and 1 mL for the salt gradient runs. Three different salt gradient slopes were applied with 10, 20 and 30 CV gradients from 15 mM to 1 M NaCl.

the separation of multiple components by the salt gradient elution with increasing resolution for longer gradients. The most outstanding peak with the highest UV absorption at 280 nm elutes at a salt concentration between 0.3 and 0.5 M NaCl in between two other main peak groups. The fraction analysis of all gradient runs demonstrates that VLPs elute exclusively in the region of this major peak. As expected, VLPs get more diluted for lower salt gradient slopes. Although VLPs successfully bind and elute on the anion exchange membrane, the total recovery was only $61 \pm 3\%$ for all experiments. The remaining amount of VLPs can only be washed out of the membrane with 1 M NaOH. Such product loss in an IEX bind-and-elute mode of up to 70% [50, 51] is often observed for VLPs and requires development and evaluation of novel chromatographic matrices and ligands. Conformational changes during adsorption and desorption processes might also elicit the product loss [49]. However, since the VLP recovery was nearly the same for both salt gradient and step elution runs in the evaluated calibration and optimization dataset, all chromatograms could be used for model calibration and process simulation. As described in Section 2.4.5, the UV chromatogram peaks were divided into 17

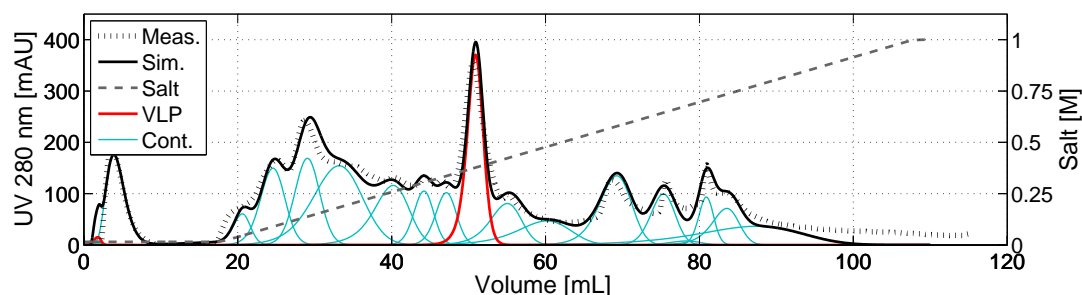
subgroups and used for SMA parameter estimation by chromatogram fitting. Figs. 5a-c illustrate chromatograms of measured (dotted line) and simulated (solid line) elution of VLP feedstock components for the 10, 20 and 30 CV salt gradients. The simulated VLP elution is displayed by a red line, while contaminant peaks are shown as turquoise lines. Estimated SMA parameters, measurement factors, and film diffusion coefficients are provided in Table 3. The simulated chromatograms describe the measured elution with good accordance regarding peak shapes, areas, heights and retention volumes. An even higher accordance of measured and simulated chromatograms might of course be obtained by increasing the number of components for the complex feedstock. On the other side, the number of components strongly affects the modeling effort, provides few information without an extra feedstock characterization procedure, and should thus not be too high.



(a) Simulation of 10 CV salt gradient elution profile



(b) Simulation of 20 CV salt gradient elution profile



(c) Simulation of 30 CV salt gradient elution profile

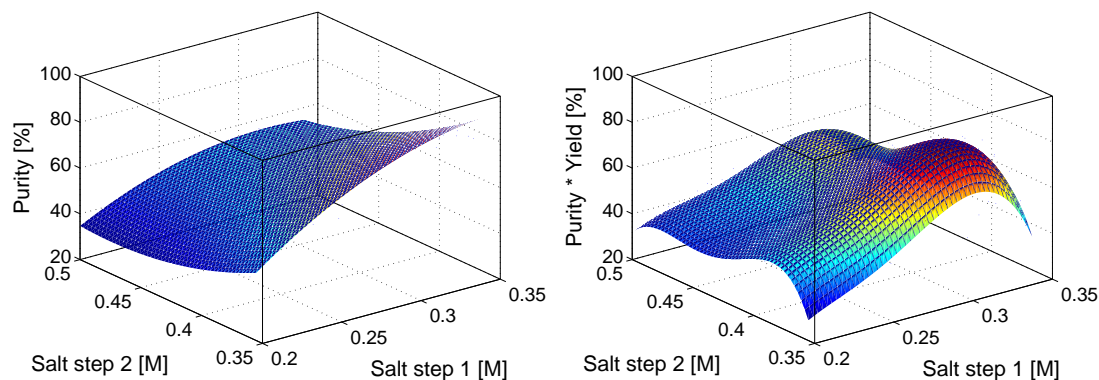
Figure 5 Comparison of measured (dotted lines) and simulated UV chromatograms (solid lines) for the complex VLP feedstock on the AEX membrane capsule. The feedstock was divided into 16 contaminant species (turquoise lines) and the target component (red lines). All component-specific lumped rate and SMA model parameters are provided as supplementary material along with the electronic version of this article. System and capsule void volumes are subtracted in each chromatogram.

Table 3 UV peak areas and converged SMA parameters for a *Spodoptera frugiperda Sf9* insect cell lysate containing human B19 parvovirus-like particles

Component	$Area_{280nm}[mAU * mL]$	k_{eff}	k_{eq}	ν
Contaminant 1	527	0.430	0.300	0.790
Contaminant 2	202	0.662	0.161	2.112
Contaminant 3	606	0.390	0.647	2.245
Contaminant 4	687	0.652	1.827	2.667
Contaminant 5	1260	0.202	4.999	2.742
Contaminant 6	695	0.150	21	7.817
Contaminant 7	339	0.980	90	7.955
Contaminant 8	343	0.820	318	9.000
Target	1111	0.162	6.21E+13	34.320
Contaminant 9	426	0.216	2.65E+04	12.571
Contaminant 10	427	0.161	8.00E+03	8.600
Contaminant 11	722	0.337	4.80E+06	13.548
Contaminant 12	396	0.990	2.80E+07	13,690
Contaminant 13	40	0.280	1.20E+10	18.548
Contaminant 14	228	0.990	2.23E+15	28.260
Contaminant 15	328	0.199	5.43E+15	28.050
Contaminant 16	655	0.140	1.35E+05	7.060

3.3 *In silico* Optimization

Knowledge of hydrodynamic and SMA parameters finally allowed the identification of optimal elution conditions for the investigated separation problem. Using the simulation software ChromX, the salt concentrations of a three-salt step elution process were varied to evaluate the effect on purity and yield. Figs. 6a and 6b illustrate by 3D plots the correlation of VLP purity and purity times yield with the salt concentrations of the first and second salt step.



(a) Prediction of model-based VLP purity for varying salt step elutions
 (b) Prediction of combined model-based VLP purity and yield for varying salt step elutions

Figure 6 *In silico* designed correlations of the model-based VLP purity and yield with regards to salt concentrations in a three-salt step elution process with a Sartobind[®] Q membrane adsorber. The calculations are solely based on the modeled contaminant groups and component-specific SMA parameters.

The first salt step elution is applied to separate impurities with a lower ligand affinity, while the second step elutes both VLPs and impurities with a similar net charge. Thus, purities and yields are only calculated for VLPs eluting in the second salt step for a fraction volume of 3 CV. Fig 6a shows that the purity increases for higher salt concentrations in the first salt step and lower salt concentrations in the second salt step elution. This correlation can be expected since there are sweet spots for the elution of both VLPs and contaminants. The highest and lowest simulated purities obtained were 91% and 30%, respectively. However, the VLP yield shows an opposite trend and increases with lower salt concentrations of salt step 1 and higher salt concentrations of salt step 2, which must be considered for the process design. Fig 6b demonstrates that a high purity and yield can only be reached in a narrow region of salt concentrations. A high salt concentration of salt step 1 causes VLP elution in the first salt step while a lower salt concentration of salt step 2 leads to VLP elution in the third salt step. The sweet spot for an optimized capturing of VLPs is 0.3 ± 0.02 M in salt step 1 and 0.38 ± 0.02 M in salt step 2. It should be noted that given purities are UV-based and calculated exclusively for those contaminant groups included in the model calibration dataset. Moreover, the model-based VLP yield is determined for the eluting fraction and does not account for the product loss caused by irreversible binding or conformational change as described above. The obtained correlations represent a design space for the AEX membrane processing of VLPs that can be used to optimize a capture step, to scale the separation as well as to understand and forecast the effect of process fluctuations following the basic tenet of 'quality by design' (QbD).

To evaluate the feasibility of the proposed salt step process, simulated and measured data were compared and are shown in Fig. 7a-d. The salt concentrations are 0.301 M NaCl (salt step 1), 0.384 M NaCl (salt step 2), and 1 M NaCl (salt step 3) predicting a VLP purity of 88.6% in the second salt step. Fig.7a and Fig. 7c display the measured (dotted lines) and simulated (solid black lines) UV signals of the purification process for a loading of 1 mL and a loading of 6.5 mL with VLPs peaks in red and contaminant peaks in turquoise. Fig. 7b and Fig. 7d show the measured UV absorption (solid black lines) and the VLP concentrations (green bars) in all collected fractions. For both loadings, VLPs eluted exclusively in the second salt step. The total yield of $59\pm 2\%$ was almost the same as in the calibration salt gradient runs indicating that no VLPs were lost by elution in the first or third salt step. The obtained protein purity for the pooled VLP fractions of the second salt step was $81.5\pm 2\%$ as determined by capillary gel electrophoresis (Fig. 9c). The chromatograms illustrate that most contaminants elute in the first and third salt step, although two contaminant groups have similar elution characteristics as the target component and can hardly be separated. Even with longer salt gradients or other salt concentration profiles, a separation of these contaminants cannot be achieved without changing stationary and/ or mobile phase (data not shown). The chromatogram in Fig. 7c shows the same peak elution profile as in Fig. 7a, but with higher peak areas and heights. It must be taken into account that the UV detection limit lies close to 2700 mAU which leads to different peak heights at high loadings for measured and simulated chromatograms. Interestingly, the chromatogram and VLP concentrations in the second salt step demonstrate that the proposed *in silico* optimization procedure can also be used to depict the separation for higher loadings (76% of DBC) than applied in the model calibration dataset. This suggests a quite steep SMA isotherm indicating that in this case, non-linear effects could be neglected for simulating higher loadings of complex feedstocks.

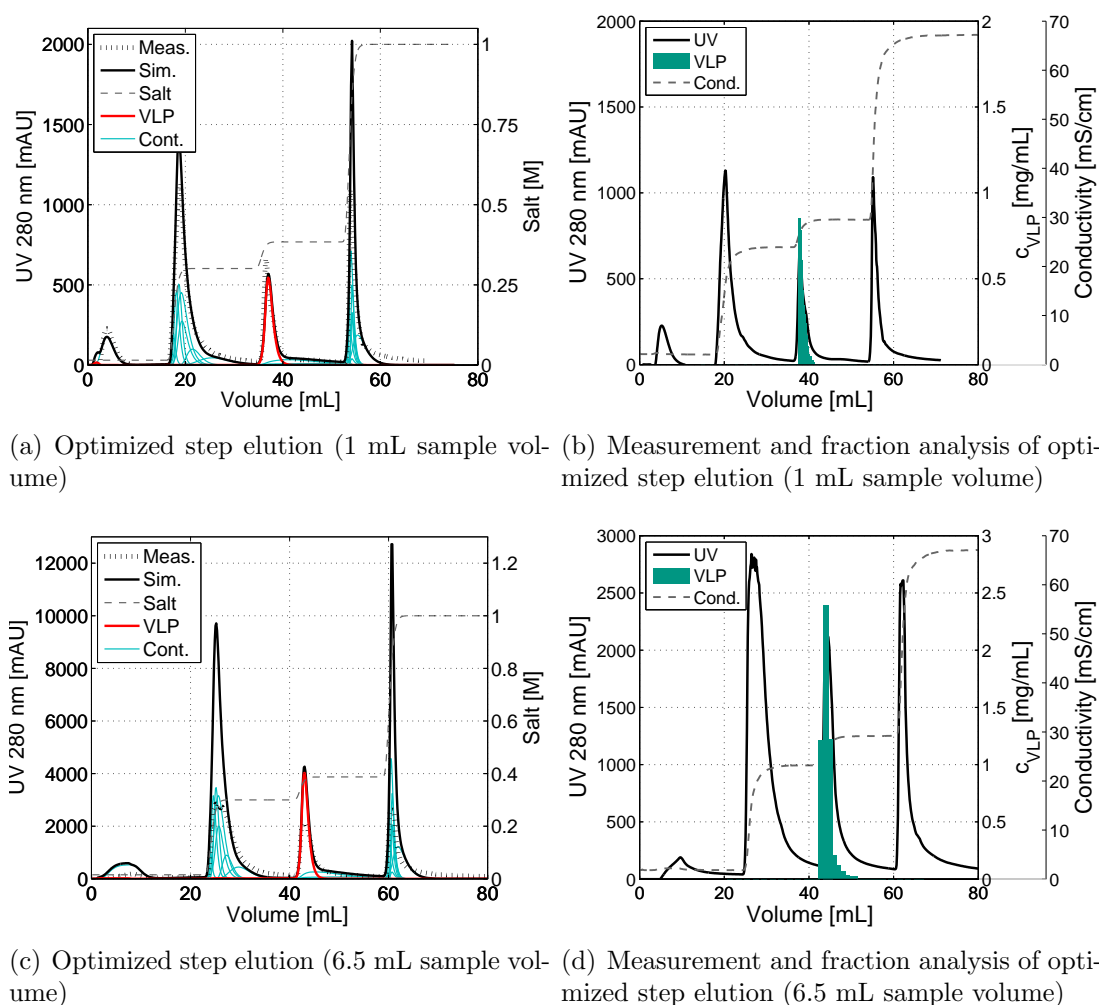


Figure 7 Comparison of measured (dotted lines) and simulated UV chromatograms (solid lines) for the optimized VLP capture process on the AEX membrane capsule at varying load volumes (1 mL and 6.5 mL VLP feedstock). The salt concentrations were 0.301 M NaCl for step 1, 0.384 M NaCl for step 2, and 1 M NaCl for the high-salt step. The upper limit of the UV detector is reached at values between 2500 and 3000 mAU. Product tracking by fraction analysis is shown in figures (b) and (d) displaying VLP concentrations as green bars.

3.4 Impact of Flow Rate

A major advantage of membranes in comparison to conventional chromatography resins is the rapid mass transport lacking intraparticle diffusion limitations [17]. In order to investigate the impact of flow rate on the bind-and-elute VLP process the optimized salt step elution was run at a flow rate of 2 CV/min and 3 CV/min. Fig. 8a and Fig. 8b show the obtained UV chromatograms and tracked VLP concentrations. In contrast to the operation at 1 CV/min, VLPs were not only detected in the second salt elution step, but also in fractions of salt step 1 and for 3 CV/min even in fractions of the flow-through. This demonstrates that an increase in flow rate drastically changes the performance and capacity of the AEX membrane process. The observed variations might be ascribed to kinetic and diffusive limitations of large biomolecules at higher flow rates. Similar phenomena have been reported by Rao [52] for the protein thyroglobulin applied on IEX membranes showing decreased *DBC* at higher flow rates. The findings point out that hydrogel and ligand design on membranes require further optimization by industry

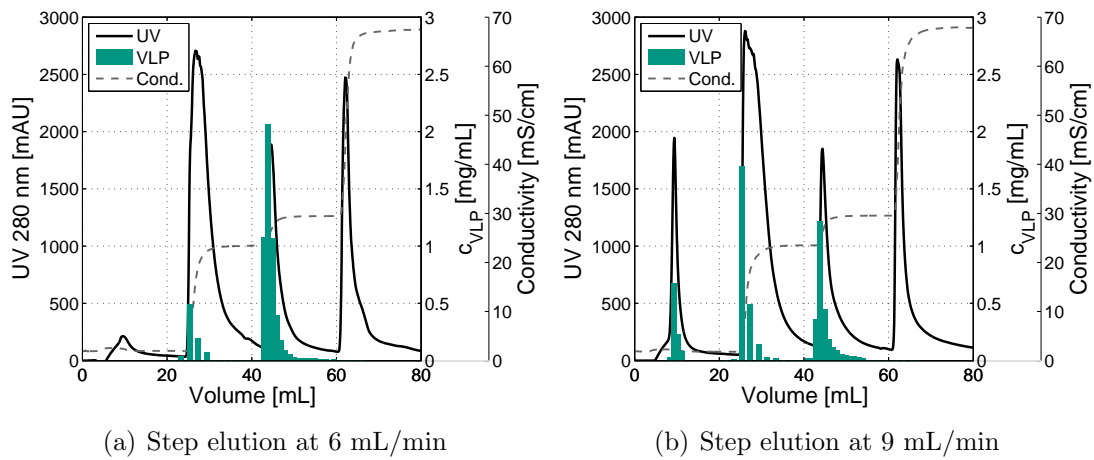


Figure 8 Effect of the flow rate on the performance of the optimized salt step elution procedure of the VLP feedstock for a 3 mL Sartobind[®] Q membrane adsorber and a loading of 6.5 mL VLP feedstock. The solid lines display the UV absorption signal at 280 nm, the dotted lines show the conductivity signals, and the green bars represent the VLP concentration in all fractions.

and academia to obtain higher binding capacities and faster downstream processes for large biomolecules.

3.5 Polishing & Process Evaluation

The designed AEX membrane process yielded a protein purity of $81.5 \pm 2\%$, a DNA concentration of 8 ± 1 ng DNA per $100 \mu\text{g}$ VLP (99.2% clearance), and a VLP recovery of $59 \pm 2\%$. Particle morphology and homogeneity were assessed by TEM analysis (Fig. 9).

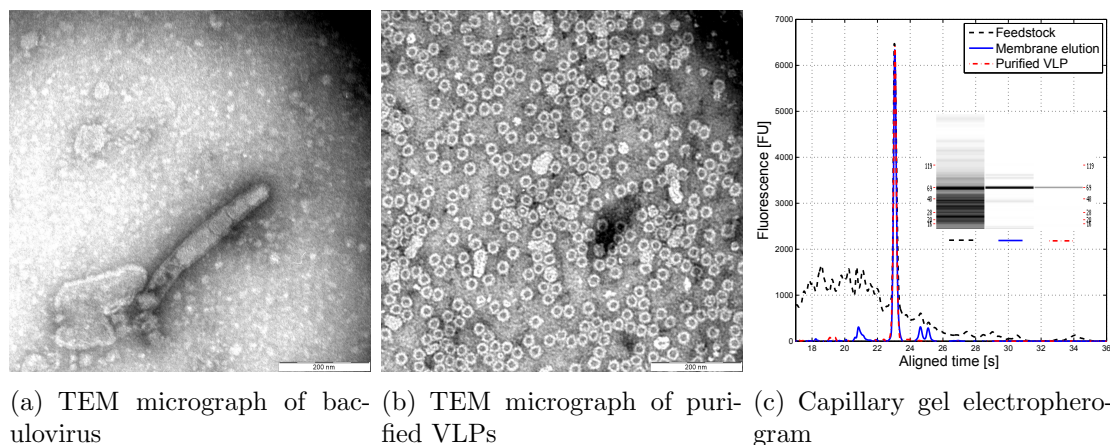


Figure 9 Analysis of process samples by transmission electron microscopy (TEM) and capillary gel electrophoresis. Electropherograms of process samples were normed to the target peak area.

Fig. 9a shows the micrograph of an FPLC fraction collected at a retention volume of 28 mL. A rod-shaped particle is visible with a size of 50×300 nm. Comparing the particles with TEM micrographs from Vicente et al. [8] and Yang et al. [53], both size and morphology indicate the presence of baculoviruses in the first salt step of the optimized elution process. In contrast, there were not any baculoviruses observed on the micrographs of the pooled VLP

fractions. Fig. 9b displays a high number of homogeneous icosahedral particles with a diameter of 25 nm characteristic of human B19 parvo-VLPs [54, 47, 30]. This demonstrates that the VLP structure was not affected by the bind-and-elute membrane process. To further increase the purity of the processed VLPs, pooled fractions from the membrane step were applied on an SEC column. The UV chromatogram of the SEC step is depicted in Fig. 10. The protein purity after the SEC step was $97.9\pm 1\%$ with a step yield of $84\pm 2\%$ separating VLP aggregates and smaller biomolecules. Fig. 9c shows the electropherogram of the VLP feedstock (black dotted line), the membrane-processed VLPs (blue line), and the polished VLPs (red dotted line). The electropherogram underlines that the majority of contaminants is removed by the optimized AEX membrane process with only three residual protein impurity peaks left. Using the AEX membrane capture step and the SEC polishing procedure, all major protein impurities were successfully separated from the target component. The final DNA concentration of the purified VLPs was 0.5 ng DNA per 100 μg VLP (99.9% clearance).

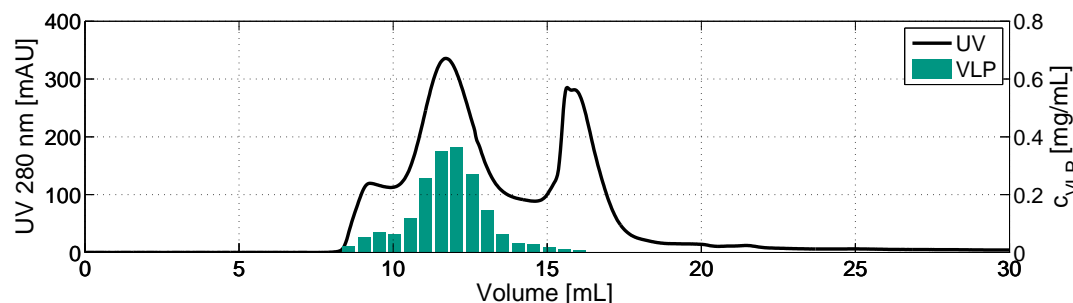


Figure 10 UV chromatogram of a size-exclusion chromatography run with human B19 parvovirus-like particles captured from *Spodoptera frugiperda* Sf9 insect cells by anion-exchange membrane chromatography. 500 μL of a 2 mg/mL VP2-VLP solution were injected on a Superose[®] 6 Increase 10/300 column at a flow rate of 0.5 mL/min. PBS pH 7.4 was used as mobile phase buffer. The solid black line shows the UV absorption at 280 nm while the green bars represent the VLP concentration in the collected fractions.

4 Conclusion & Outlook

The aim of this study was to design a bind-and-elute membrane process for VLPs derived from Sf9 insect cells using rational development tools. For the first time, a proof of concept for simulating and optimizing the chromatographic separation of VLPs with a radial lumped rate model and the SMA isotherm was demonstrated. Automated high-throughput screenings in 96-well format allowed the identification of suitable binding conditions yielding a dynamic binding capacity of 5.7 mg VLP per mL Q membrane. *In silico* process modeling, simulation, and optimization were performed for a radial AEX membrane capsule to control and forecast the elution of VLPs and impurities. Using UV absorption-based modeling, the complex feedstock was divided into 17 subcomponents, and a design space for the elution conditions of the target component was established. An *in silico* optimized process with three salt steps enabled the separation of VLPs from the majority of baculoviruses, HCPs and DNA. The simulated and experimental purities were 88.6% and $81.5\pm 2\%$, respectively. Residual contaminants were cleared by a subsequent SEC polishing procedure. A downside of the developed process was, however, the product loss (60% recovery) and the decrease in performance at increased flow rates. Both effects require a better understanding of the mass transport phenomena on the membrane for a more generic process model incorporating potential conformational VLP changes. Further

membrane optimizations should focus on customizing ligand and stationary phase design for large biomolecules to increase the productivity of membrane-based VLP processes. Both high-through experimentation and chromatography modeling have proven to be valuable rational design tools for process development of VLPs.

Nomenclature

a_i	Absorption coefficient
D_{ax}	Axial dispersion coefficient
ε_{Pores}	Membrane porosity
$\varepsilon_{Hydrogel}$	Stationary phase porosity
ε_t	Total porosity
H	Membrane height
k_{eff}	Effective film/pore transfer coefficient
k_{eq}	Adsorption equilibrium coefficient
$k_{eq,L}$	Adsorption equilibrium coeff. for Langmuir isotherm
L	Membrane thickness
Λ	Stationary phase ionic capacity
ν	Characteristic charge for SMA isotherm
q	Stationary phase concentration of protein
q_s	Single-component saturation conc. for Langmuir isotherm
q_{salt}	Stationary phase concentration of salt
r_a	Outer radius of spiral wound membrane
r_i	Inner radius of spiral wound membrane
σ	Steric shielding coefficient for SMA isotherm
t	Time dimension
u	Interstitial mobile phase velocity
x	Space dimension

Acknowledgements

The authors gratefully acknowledge material supply by **Diarect AG** and **Sartorius Stedim Biotech** and financial support from the **German Federal Ministry of Education and Research** (Grant agreement 0315640B). In addition, we would like to thank Mohammad Fotouhi from the KIT Laboratory for Electron Microscopy for acquisition of transmission electron micrographs and Katrin Töppner and Martin Leuthold (Sartorius Stedim Biotech, Göttingen, Germany) for their support regarding membrane characterization and technology transfer. This research work is part of the project 'Optimization of an industrial process for the production of cell-culture-based seasonal and pandemic influenza vaccines'.

References

- [1] D. Mohammadi, International community ramps up Ebola vaccine effort, *Lancet* 384 (9955) (2014) 1658–1659. doi:10.1016/S0140-6736(14)61788-8.
- [2] R. C. T. Partnership, Efficacy and Safety of the RTS,S/AS01 Malaria Vaccine during 18 Months after Vaccination: A Phase 3 Randomized, Controlled Trial in Children and Young Infants at 11 African Sites, *PLoS Med.* 11. doi:10.1371/journal.pmed.1001685.
- [3] L. F. Fries, G. E. Smith, G. M. Glenn, A recombinant viruslike particle influenza a (h7n9) vaccine, *New England Journal of Medicine* 369 (2013) 2564–2566, pMID: 24224560. doi:10.1056/NEJMc1313186.

- [4] C. Ladd Effio, J. Hubbuch, Next generation vaccines and vectors: Designing downstream processes for recombinant protein-based virus-like particles, *Biotechnology journal* 10 (5) (2015) 715–727. doi:10.1002/biot.201400392.
- [5] N. Willoughby, Too big to bind? Will the purification of large and complex therapeutic targets spell the beginning of the end for column chromatography?, *J. Chem. Technol. Biotechnol.* 84 (2009) 145–150. doi:10.1002/jctb.2020.
- [6] L. Opitz, S. Lehmann, A. Zimmermann, U. Reichl, M. W. Wolff, Impact of adsorbents selection on capture efficiency of cell culture derived human influenza viruses., *J. Biotechnol.* 131 (2007) 309–17. doi:10.1016/j.jbiotec.2007.07.723.
- [7] T. Vicente, M. F. Sousa, C. Peixoto, J. P. Mota, P. M. Alves, M. J. Carrondo, Anion-exchange membrane chromatography for purification of rotavirus-like particles, *J. Memb. Sci.* 311 (2008) 270–283. doi:10.1016/j.memsci.2007.12.021.
- [8] T. Vicente, C. Peixoto, M. J. T. Carrondo, P. M. Alves, Purification of recombinant baculoviruses for gene therapy using membrane processes., *Gene Ther.* 16 (6) (2009) 766–775. doi:10.1038/gt.2009.33.
URL <http://dx.doi.org/10.1038/gt.2009.33>
- [9] I. Tatárová, R. Fáber, R. Denoyel, M. Polakovic, Characterization of pore structure of a strong anion-exchange membrane adsorbent under different buffer and salt concentration conditions., *J. Chromatogr. A* 1216 (2009) 941–7. doi:10.1016/j.chroma.2008.12.018.
- [10] T. Vicente, R. Fáber, P. M. Alves, M. J. T. Carrondo, J. P. B. Mota, Impact of ligand density on the optimization of ion-exchange membrane chromatography for viral vector purification., *Biotechnol. Bioeng.* 108 (2011) 1347–59. doi:10.1002/bit.23058.
- [11] D. J. McNally, D. Darling, F. Farzaneh, P. R. Levison, N. K. H. Slater, Optimised concentration and purification of retroviruses using membrane chromatography., *J. Chromatogr. A* 1340 (2014) 24–32. doi:10.1016/j.chroma.2014.03.023.
- [12] P. van Beijeren, P. Kreis, T. Zeiner, Development of a generic process model for membrane adsorption, *Comput. Chem. Eng.* 53 (2013) 86–101. doi:10.1016/j.compchemeng.2013.03.005.
- [13] P. Nestola, L. Villain, C. Peixoto, D. L. Martins, P. M. Alves, M. J. T. Carrondo, J. P. B. Mota, Impact of grafting on the design of new membrane adsorbers for adenovirus purification, *J. Biotechnol.* 181 (2014) 1–11. doi:10.1016/j.jbiotec.2014.04.003.
- [14] J. Tharakan, M. Belizaire, Ligand efficiency in axial and radial flow immunoaffinity chromatography of factor IX, *J. Chromatogr. A* 702 (1995) 191–196. doi:10.1016/0021-9673(94)01141-Z.
- [15] T. Besselink, A. van der Padt, A. E. M. Janssen, R. M. Boom, Are axial and radial flow chromatography different?, *J. Chromatogr. A* 1271 (2013) 105–114. doi:10.1016/j.chroma.2012.11.027.
- [16] P. van Beijeren, P. Kreis, T. Zeiner, Ion exchange membrane adsorption of bovine serum albumin-Impact of operating and buffer conditions on breakthrough curves, *J. Memb. Sci.* 415–416 (2012) 568–576. doi:10.1016/j.memsci.2012.05.051.

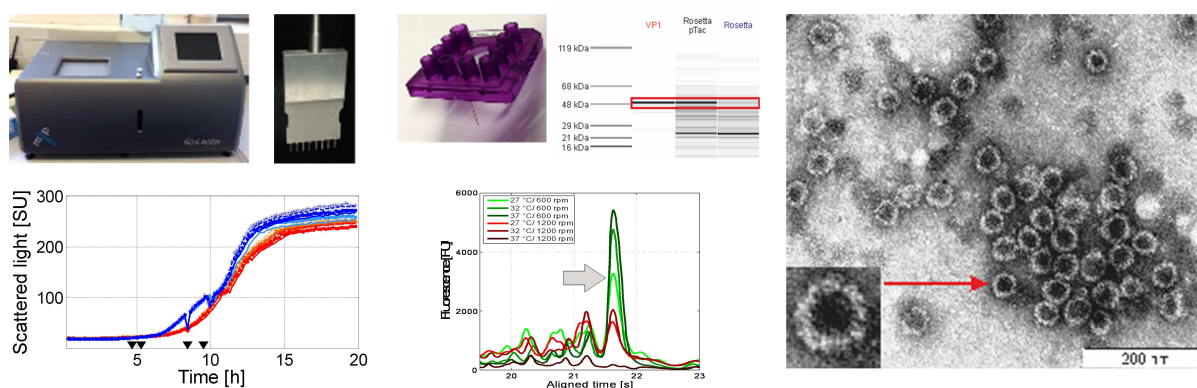
-
- [17] V. Orr, L. Zhong, M. Moo-Young, C. P. Chou, Recent advances in bioprocessing application of membrane chromatography., *Biotechnol. Adv.* 31 (4) (2013) 450–65. doi:10.1016/j.biotechadv.2013.01.007.
- [18] A. S. Rathore, H. Winkle, Quality by design for biopharmaceuticals, *Nature biotechnology* 27 (1) (2009) 26–34.
- [19] J. r. M. Mollerup, T. B. Hansen, S. Kidal, A. Staby, Quality by design-Thermodynamic modelling of chromatographic separation of proteins, *J. Chromatogr. A* 1177 (2008) 200–206. doi:10.1016/j.chroma.2007.08.059.
- [20] S. Gerontas, M. Asplund, R. Hjorth, D. G. Bracewell, Integration of scale-down experimentation and general rate modelling to predict manufacturing scale chromatographic separations, *J. Chromatogr. A* 1217 (2010) 6917–6926. doi:10.1016/j.chroma.2010.08.063.
- [21] S. Gerontas, M. S. Shapiro, D. G. Bracewell, Chromatography modelling to describe protein adsorption at bead level, *J. Chromatogr. A* 1284 (2013) 44–52. doi:10.1016/j.chroma.2013.01.102.
- [22] E. J. Close, J. R. Salm, D. G. Bracewell, E. Sorensen, Modelling of industrial biopharmaceutical multicomponent chromatography, *Chem. Eng. Res. Des.* 92 (2014) 1304–1314. doi:10.1016/j.cherd.2013.10.022.
- [23] A. T. Hanke, M. Ottens, Purifying biopharmaceuticals: Knowledge-based chromatographic process development, *Trends Biotechnol.* 32 (2014) 210–220. doi:10.1016/j.tibtech.2014.02.001.
- [24] T. Hahn, A. Sommer, A. Osberghaus, V. Heuveline, J. Hubbuch, Adjoint-based estimation and optimization for column liquid chromatography models, *Comput. Chem. Eng.* 64 (2014) 41–54. doi:10.1016/j.compchemeng.2014.01.013.
- [25] T. Hahn, P. Baumann, T. Huuk, V. Heuveline, J. Hubbuch, UV absorption-based inverse modeling of protein chromatography, *Eng. Life Sci.* doi:10.1002/elsc.201400247.
- [26] S. Dimartino, C. Boi, G. C. Sarti, A validated model for the simulation of protein purification through affinity membrane chromatography, *J. Chromatogr. A* 1218 (13) (2011) 1677–1690. doi:10.1016/j.chroma.2010.11.056.
- [27] C. a. Brooks, S. M. Cramer, Steric mass-action ion exchange: Displacement profiles and induced salt gradients, *AIChE J.* 38 (1992) 1969–1978. doi:10.1002/aic.690381212.
- [28] T. Hahn, T. Huuk, A. Osberghaus, K. Doninger, S. Nath, S. Hepbildikler, V. Heuveline, J. Hubbuch, Calibration-free inverse modeling of ion-exchange chromatography in industrial antibody purification, *Eng. Life Sci.* doi:10.1002/elsc.201400248.
- [29] P. Baumann, T. Hahn, J. Hubbuch, High-throughput micro-scale cultivations and chromatography modeling: Powerful tools for integrated process development, *Biotechnol. Bioeng.* doi:10.1002/bit.25630.
- [30] S. Chandramouli, A. Medina-Selby, D. Coit, M. Schaefer, T. Spencer, L. a. Brito, P. Zhang, G. Otten, C. W. Mandl, P. W. Mason, P. R. Dormitzer, E. C. Settembre, Generation of a parvovirus B19 vaccine candidate., *Vaccine* 31 (37) (2013) 3872–8. doi:10.1016/j.vaccine.2013.06.062.

- [31] D. I. Bernstein, H. M. El Sahly, W. a. Keitel, M. Wolff, G. Simone, C. Segawa, S. Wong, D. Shelly, N. S. Young, W. Dempsey, Safety and immunogenicity of a candidate parvovirus B19 vaccine., *Vaccine* 29 (2011) 7357–63. doi:10.1016/j.vaccine.2011.07.080.
- [32] F. Kröner, J. Hubbuch, Systematic generation of buffer systems for pH gradient ion exchange chromatography and their application, *J. Chromatogr. A* 1285 (2013) 78–87. doi:10.1016/j.chroma.2013.02.017.
- [33] L. Shi, G. Sanyal, A. Ni, Z. Luo, S. Doshna, B. Wang, T. L. Graham, N. Wang, D. B. Volkin, Stabilization of human papillomavirus virus-like particles by non-ionic surfactants., *J. Pharm. Sci.* 94 (7) (2005) 1538–51. doi:10.1002/jps.20377. URL <http://www.ncbi.nlm.nih.gov/pubmed/15929070>
- [34] C. Ladd Effio, L. Wenger, O. Ötes, S. a. Oelmeier, J. Hubbuch, Downstream processing of virus-like particles: Single-stage and multi-stage aqueous two-phase extraction, *J. Chromatogr. A* 1383 (2015) 35–46. doi:10.1016/j.chroma.2015.01.007.
- [35] T. Gu, G.-J. Tsai, G. T. Tsao, A theoretical study of multicomponent radial flow chromatography, *Chem. Eng. Sci.* 46 (1991) 1279–1288. doi:10.1016/0009-2509(91)85055-3.
- [36] P. Danckwerts, Continuous flow systems. Distribution of residence times, *Chem. Eng. Sci.* 50 (1952) 3857–3866. doi:10.1016/0009-2509(96)81811-2.
- [37] M. T. van Genuchten, J. C. Parker, Boundary Conditions for Displacement Experiments through Short Laboratory Soil Columns1, *Soil Sci. Soc. Am. J.* 48 (1984) 703–708. doi:10.2136/sssaj1984.03615995004800040002x.
- [38] T. C. Huuk, T. Hahn, A. Osberghaus, J. Hubbuch, Model-based integrated optimization and evaluation of a multi-step ion exchange chromatography, *Sep. Purif. Technol.* (2014) 207–222doi:10.1016/j.seppur.2014.09.012.
- [39] T. Hahn, T. Huuk, V. Heuveline, J. Hubbuch, Simulating and Optimizing Preparative Protein Chromatography with ChromX, *J. Chem. Educ.* (2015) 150623161654001doi:10.1021/ed500854a.
- [40] J. Hubbuch, T. Linden, E. Knieps, A. Ljunglöf, J. Thömmes, M. R. Kula, Mechanism and kinetics of protein transport in chromatographic media studied by confocal laser scanning microscopy: Part I. The interplay of sorbent structure and fluid phase conditions, *J. Chromatogr. A* 1021 (2003) 93–104. doi:10.1016/j.chroma.2003.08.112.
- [41] E. J. Close, J. R. Salm, D. G. Bracewell, E. Sorensen, A model based approach for identifying robust operating conditions for industrial chromatography with process variability, *Chem. Eng. Sci.* 116 (2014) 284–295. doi:10.1016/j.ces.2014.03.010.
- [42] A. Osberghaus, S. Hepbildikler, S. Nath, M. Haindl, E. von Lieres, J. Hubbuch, Determination of parameters for the steric mass action model—a comparison between two approaches., *J. Chromatogr. A* 1233 (2012) 54–65. doi:10.1016/j.chroma.2012.02.004.
- [43] Perkin Elmer, HT Protein Express LabChip Kit, Version 2 LabChip GXII User Guide. (2012).
- [44] J. Geigert, The challenge of CMC regulatory compliance for biopharmaceuticals, Springer Science & Business Media, New York, 2014.

-
- [45] W. Y. Chen, Z. C. Liu, P. H. Lin, C. I. Fang, S. Yamamoto, The hydrophobic interactions of the ion-exchanger resin ligands with proteins at high salt concentrations by adsorption isotherms and isothermal titration calorimetry, *Sep. Purif. Technol.* 54 (2007) 212–219. doi:10.1016/j.seppur.2006.09.008.
- [46] O. Shchukina, a.V. Zatirakha, a.D. Smolenkov, P. Nesterenko, O. Shpigun, Anion exchangers with branched functional ion exchange layers of different hydrophilicity for ion chromatography, *J. Chromatogr.* A doi:10.1016/j.chroma.2015.06.039.
- [47] S. P. Sánchez-Rodríguez, L. Münch-Anguiano, O. Echeverría, G. Vázquez-Nin, M. Mora-Pale, J. S. Dordick, I. Bustos-Jaimes, Human parvovirus B19 virus-like particles: In vitro assembly and stability., *Biochimie* 94 (3) (2012) 870–8. doi:10.1016/j.biochi.2011.12.006.
- [48] H. Mach, D. B. Volkin, R. D. Troutman, B. E. I. Wang, Disassembly and Reassembly of Yeast-Derived Recombinant Human Papillomavirus Virus-like Particles (HPV VLPs), *J. Pharm. Sci.* 95 (10) (2006) 2195–2206. doi:10.1002/jps.
- [49] Y. Yang, Mengran Yu, S. Zhang, G. Ma, Z. Su, Adsorption of virus-like particles on ion exchange surface: Conformational changes at different pH detected by dual polarization interferometry, *J. Chromatogr.* A doi:10.1016/j.chroma.2015.07.019.
- [50] L. Urbas, B. L. Jarc, M. Barut, M. Zochowska, J. Chroboczek, B. Pihlar, E. Szolajska, Purification of recombinant adenovirus type 3 dodecahedral virus-like particles for biomedical applications using short monolithic columns., *J. Chromatogr. A* 1218 (2011) 2451–9. doi:10.1016/j.chroma.2011.01.032.
- [51] M. Yu, Y. Li, S. Zhang, X. Li, Y. Yang, Y. Chen, G. Ma, Z. Su, Improving stability of virus-like particles by ion-exchange chromatographic supports with large pore size: advantages of gigaporous media beyond enhanced binding capacity., *J. Chromatogr. A* 1331 (2014) 69–79. doi:10.1016/j.chroma.2014.01.027.
- [52] C. S. Rao, Purification of large proteins using ion-exchange membranes, *Process Biochem.* 37 (3) (2001) 247–256. doi:10.1016/S0032-9592(01)00207-2.
- [53] D.-G. Yang, Y.-C. Chung, Y.-K. Lai, C.-W. Lai, H.-J. Liu, Y.-C. Hu, Avian influenza virus hemagglutinin display on baculovirus envelope: cytoplasmic domain affects virus properties and vaccine potential., *Mol. Ther.* 15 (5) (2007) 989–996. doi:10.1038/sj.mt.6300236.
- [54] L. Gilbert, J. Toivola, D. White, T. Ihalainen, W. Smith, L. Lindholm, M. Vuento, C. Oker-Blom, Molecular and structural characterization of fluorescent human parvovirus B19 virus-like particles., *Biochem. Biophys. Res. Commun.* 331 (2005) 527–35. doi:10.1016/j.bbrc.2005.03.208.

High-throughput Process Development of an Alternative Platform for the Production of Virus-like Particles in *Escherichia coli*

C. Ladd Effio^{1,‡}, P. Baumann^{1,‡}, P. Vormittag¹, C. Weigel¹, A. Middelberg²
and J. Hubbuch^{1,*}



¹ : Institute of Process Engineering in Life Sciences, Section IV: Biomolecular Separation Engineering, Karlsruhe Institute of Technology, Engler-Bunte-Ring 1, 76131 Karlsruhe, Germany
² : Australian Institute for Bioengineering and Nanotechnology, University of Queensland, Brisbane, Australia

[‡] : Contributed equally to this work

* : Corresponding author. *E-mail address*: juergen.hubbuch@kit.edu (J. Hubbuch)

J. Biotechnol. (2016), doi:10.1016/j.jbiotec.2015.12.018

Abstract

The production of safe vaccines against untreatable or new diseases has pushed the research in the field of virus-like particles (VLPs). Currently, a large number of commercial VLP-based human vaccines and vaccine candidates are available or under development. A promising VLP production route is the controlled in vitro assembly of virus proteins into capsids. In the study reported here, a high-throughput screening (HTS) procedure was implemented for the upstream process development of a VLP platform in bacterial cell systems. Miniaturized cultivations were carried out in 48-well format in the BioLector system (m2p-Labs, Germany) using an *Escherichia coli* strain with a tac promoter producing the murine polyomavirus capsid protein (VP1). The screening procedure incorporated micro-scale cultivations, HTS cell disruption by sonication and HTS-compatible analytics by capillary gel electrophoresis. Cultivation temperatures, shaking speeds, induction and medium conditions were varied to optimize the product expression in *E. coli*. The most efficient system was selected based on an evaluation of soluble and insoluble product concentrations as well as on the percentage of product in the total soluble protein fraction. The optimized system was scaled up to cultivation 2.5 L shaker flask scale and purified using an anion exchange chromatography membrane adsorber, followed by a size exclusion chromatography polishing procedure. For proof of concept, purified VP1 capsomeres were assembled under defined buffer conditions into empty capsids and characterized using transmission electron microscopy (TEM). The presented HTS procedure allowed for a fast development of an efficient production process of VLPs in *E. coli*. Under optimized cultivation conditions, the VP1 product totalled up to 43% of the total soluble protein fraction, yielding 1.63 mg VP1 per mL of applied cultivation medium. The developed production process strongly promotes the murine polyoma-VLP platform, moving towards an industrially feasible technology for new chimeric vaccines.

Keywords: Virus-like Particles, *Escherichia coli*, High-throughput Screening, Micro-scale Cultivation, BioLector[®]

1 Introduction

Virus-like particles (VLPs) represent novel molecular means for the containment of infectious diseases and the immunotherapeutic treatment of cancer, Alzheimer’s disease, and autoimmune diseases [1, 2, 3, 4]. A steadily increasing number of VLP-based vaccines is currently undergoing clinical phase studies and several recombinant VLPs have been licensed for prophylactic vaccination against cervical cancer (Gardasil[®], Cervarix[®]), hepatitis B (Recombivax[®], Engerix[®]), and hepatitis E (Hecolin[®]) [5, 6]. Protein-based VLPs are produced by recombinant expression of virus proteins in yeast, insect, or bacteria cells [7]. For the production of homogeneous particles, currently licensed VLP-based vaccines are assembled *in vitro* under defined and controllable buffer conditions. Separate disassembly process steps are needed for *in vivo* assembled VLPs. A promising approach to the rapid and scalable production of VLPs is the expression of virus proteins in *Escherichia coli*. *E. coli* is the recombinant system of choice for multiple biopharmaceutical products, such as human insulin [8], human growth hormones [9], antibody fragments [10], or hepatitis vaccines [11], providing high product titers and total soluble protein values of up to 50% [12].

In recent years, several microbial VLP production systems were developed and tailored to epitope presentations in vaccine formulations, such as the bacteriophage Q β system [4, 13], the human hepatitis B core protein [14, 15, 16], the woodchuck hepadnavirus core protein (WHcAg) [17] or the papaya mosaic virus (PapMV) system [18]. Another well-characterized VLP-based nanocarrier is the murine polyoma virus protein VP1 that is capable of spontaneously self-assembling into capsids and lacking the risk of human pre-existing carrier-specific immunity. *E. coli*-derived VP1 builds pentamer structures that allow processing small protein complexes instead of whole particles and, thus, do not require any additional disassembly steps. Chimeric murine polyoma-VLPs were used in the past for the presentation of influenza antigen epitopes (H190, M2e) [19, 20, 21], group A streptococcus epitopes (J8i) [22, 23], tumor cell epitopes [24, 25], and packaging of small molecules and DNA [26, 27]. However, the current state-of-the-art platform for *E. coli*-derived VP1 is limited by the expression and processing of glutathion-S-transferase (GST)-VP1 fusion tag complexes [28]. These protein tags are widely used for enhancing the solubility of proteins, increasing product titers, and facilitating lab-scale purification by using affinity chromatography for capturing the product of interest with a high selectivity [29, 30, 19]. Major drawbacks of protein tags arise due to multimerization effects, slow and high-priced affinity chromatography media, and the demand for additional downstream procedures for the removal of the fusion tags [28, 31]. Boosting the productivity of the murine polyoma-VLP platform requires an optimization, acceleration, and simplification of both upstream and downstream processing.

An optimization of protein expression in *E. coli* often is time-intensive when performing shaker flask cultivations. Rapid process development can be performed *in silico* using molecular dynamics simulations of the product of interest [32] or by high-throughput experimentation with multiple recently developed tools for miniaturized automated cultivations [33, 34, 35]. However, miniaturization may result in a reduction of accessible process information, leading to difficulties in process control and scale-up [33]. To overcome these shortcomings, more sophisticated systems were developed, e.g. the Advanced Micro-scale Bioreactors (ambr[®]) technology (Sartorius Stedim Biotech, Germany) mimicking lab-scale fermenters on a robotic workstation [36] and the BioLector system (m2p-Labs, Germany) used in this study [37, 38]. For the BioLector system, special 48-well cultivation plates with flower-shaped wells exist for improving mixing and oxygen uptake into the medium [39]. Successful scale-up from the micro-scale to lab-scale can be implemented to gain a large pool of cell broth for subsequent downstream process development [40, 41].

In this paper, we present a high-throughput approach to the design of the upstream process of murine polyoma-VLPs. For proof of concept, we suggest an alternative membrane-based downstream process enabling the rapid large-scale production of future chimeric murine polyoma-VLP-based vaccine candidates.

2 Material & Methods

2.1 Material

2.1.1 Disposables

Cell transformation was carried out in 1 mm polycarbonate electroporation cuvettes (Biozym Scientific GmbH, Germany). Micro-scale cultivation experiments were performed in 48-well FlowerPlates[®] covered with adhesive sterile sealing foil (m2p-Labs, Germany). All pre-cultures were cultivated in 250 mL baffled flasks (Schott, Germany). For scale-up, 2.5 L baffled TUNAIR[™] shake flasks (Sigma Aldrich, Germany) were used. Cell lysis and centrifugation procedures were carried out in 300 μ L polypropylene 96-well plates with a conical bottom (VWR, Germany). Sterile filtration of cell lysates prior to chromatography runs was conducted with 0.45 μ m and 0.1 μ m cellulose acetate filters (Sartorius AG, Germany). 3 mL Slide-A-Lyzer[™] G2 dialysis cassettes with 10 K MWCO cellulose membranes (Life Technologies, USA) were used for the in vitro VLP assembly. For gel electrophoresis (GX) experiments, Novex[®] NuPAGE[®] 4-12% Bis-Tris (1.0 mm, 12 wells) protein gels were purchased from Life Technologies, Sweden. Capillary gel electrophoresis (GX II) was carried out in an HT Protein Express & Pico LabChip[®] (Perkin Elmer, USA). GX II sample preparation was conducted in skirted 96-well twin.tec[®] PCR plates (Eppendorf, Germany). For western blotting, XCell[™] blot sponge pads, filter papers, and a nitrocellulose transfer membrane were purchased from Life Technologies, USA.

2.1.2 Chemicals & Buffers

For the electroporation experiments, super optimal broth (SOB) medium composed of 20 g/L wheat peptone for microbiology (Fluka, Germany), 5 g/L bacteriological yeast extract (Amresco, USA), 10 mM sodium chloride, 2.5 mM potassium chloride (VWR, Germany), and super optimal broth with catabolite repression (SOC) medium, including the ingredients of SOB with additional 10 mM magnesium chloride, 10 mM magnesium sulfate (Merck kGaA, Germany), and 20 mM glucose (VWR, Germany) were used.

For cultivations, a terrific broth (TB) medium was applied, composed of 12 g/L wheat peptone, 24 g/L bacteriological yeast extract, 5 g/L glycerol bidistilled 99.5% (VWR, Germany), and 89 mM potassium dihydrogen phosphate (VWR, Germany). For the selection of transformed cells, antibiotics were added to a final concentration of 100 μ g/mL carbenicillin and 34 μ g/mL chloramphenicol (AppliChem GmbH, Germany). The TB medium was adjusted to pH 6 or pH 7 using potassium hydroxide and for experiments including magnesium, magnesium sulfate heptahydrate (Merck kGaA, Germany) was added to a final concentration of 2 mM. The induction procedure of the pTac promoter was realized with isopropyl- β -D-thiogalactopyranosid (IPTG) from a 1 M stock solution (VWR, Germany).

As a lysis buffer for native protein release (compatible with the GX II system), a 20 mM Tris buffer (Merck KGaA, Germany) adjusted to pH 8 with hydrochloric acid (Merck KGaA, Germany), including 1X SigmaFAST[™] protease inhibitor and 5 mM dithiothreitol (DTT) (Sigma Aldrich, Germany), was used. The lysis buffer for purification experiments consisted of 20 mM Tris-HCl (VWR, Germany), 1 mM EDTA disodium dihydrate (Fluka Chemie GmbH,

Switzerland), 5% (v/v) glycerol, 1X SigmaFASTTM protease inhibitor, and 5 mM DTT (Sigma Aldrich, Germany). Total protein extraction under denaturing conditions was carried out using trichloroacetic acid (TCA) BioChemica (AppliChem, Germany) and acetone for liquid chromatography (Merck KGaA, Germany).

The compositions of the binding and elution buffer for anion-exchange chromatography were 20 mM Tris (pH 8), 5 mM DTT, 1 mM EDTA, and 5% (v/v) glycerol, with an additional 1 M NaCl (Merck KGaA, Germany) in the elution buffer. 20 mM Tris (pH 8), 5 mM DTT, 1 mM EDTA, 5% (v/v) glycerol, and 250 mM NaCl were used as running buffer for purification by size-exclusion chromatography. The VLP assembly buffer developed by Middelberg et al. [19] was used, which consists of 0.5 M ammonium sulfate, 20 mM Tris (pH 7.4), 5% (v/v) glycerol, and 1 mM calcium chloride (VWR, Germany).

Gel electrophoresis (GX) was carried out using 20X Bolt[®] MES SDS running buffer, NuPAGE[®] 4X LDS sample buffer, and the Novex[®] Sharp unstained protein standard (Life Technologies, Sweden). DTT was prepared as a 1 M stock solution. For protein staining, a 'blue silver' staining solution, consisting of 10% (v/v) phosphoric acid of 85% purity (Roth, Germany), 100 g/L ammonium sulfate BioChemica (AppliChem, Germany), 1.2 g/L Coomassie Brilliant Blue G-250 (Merck, Germany), and 20% (v/v) methanol (Sigma Aldrich, Germany), was used. For capillary gel electrophoresis (GX II) experiments, an HT protein express reagent kit was purchased from Perkin Elmer, USA. A 1 mg/mL lysozyme solution (Hampton research, USA) served as an internal concentration standard.

The transfer buffer for western blotting was composed of 192 mM glycine, 20% (v/v) methanol (Sigma Aldrich, Germany), and 25 mM Tris(hydroxymethyl)-aminomethane (Merck KGaA, Germany) and was adjusted to pH 8.3. As further buffers, Tris-buffered saline (TBS), including 500 mM chloride and 20 mM Tris adjusted to pH 7.5, and TBS-T with additional 0.05% (v/v) of Tween 20 were applied. The solution for color development (AP color development reagent kit) was purchased from BioRad Laboratories, USA.

2.1.3 Instrumentation

Transformations were conducted using a MicroPulserTM Electroporator (Bio-Rad Laboratories, USA). High-throughput micro-scale cultivation experiments were carried out in a BioLector[®] MB micro-scale fermentation system (m2p-Labs, Germany). Shake flask cultivations were conducted in a MaxQTM 6000 incubator (Thermo Fisher Scientific, USA). A 5810 R centrifuge (Eppendorf, Germany) was used for liquid-solid separation procedures, including cell harvest. Release of the intracellular product was realized using a Model 120 Sonic Dismembrator equipped with an eight-tip horn positioner (Thermo Fisher Scientific, USA) for high-throughput micro-scale cell disruption and with a Digital Sonifier[®] 450 (Branson Ultrasonic Corporation, USA) for the scale-up cell lysis procedure. Product purification experiments were carried out in an ÄKTATM Purifier system (GE Healthcare Life Sciences, Sweden), equipped with a pump P-900, mixer M-925, UV detector UV-900, motor valve INV-907, pH and conductivity monitoring unit pH/C-900, and a fraction collector Frac-950 unit. For pH adjustment of all buffers, an HI-3220 pH meter (Hanna Instruments, USA) was used. Gel electrophoresis was carried out in an Xcell SureLockTM Novex[®] MiniCell gel chamber equipped with a PowerEase[®] 500 power supply (Life Technologies, USA). Capillary gel electrophoresis (GX II) was carried out in a Caliper LabChip[®] GX II (Perkin Elmer, USA). Sample denaturation for both the GX and GX II system was realized in a MUR 13 thermo-shaker with additional lid heating (HLC BioTech, Germany). Assembled virus-like particles were inspected by transmission electron microscopy (TEM) on a CM 200 FEG/ST electron microscope (Philips, Netherlands).

2.2 Upstream Process Development

2.2.1 Plasmid Construction & Host Strain

The plasmid pALVP1TAC [42] was generously provided by Prof. Robert Garcea (University of Colorado, USA) and sequenced by JenaGen GmbH, Germany. The plasmid pTacVP1 was constructed by inserting the nucleic acid sequence of murine polyoma virus capsid protein VP1 (sequence M34958) with optimized codon usage (Fig. 1) between the NdeI and HindIII sites of a pTac-MAT-Tag-1 expression vector (Sigma-Aldrich, USA). A stop codon was inserted in front of HindIII to prevent the translation of the N-terminal metal affinity tag. The plasmid was designed and synthesized by Centic Biotec, Germany. *E. coli* Rosetta(DE3)pLysS cells (Merck KGaA, Germany) were prepared for electroporation by the standard procedure: Growth in SOB medium (250 mL shaker flasks, 37°C, 180 rpm), harvest at an OD_{600 nm}-value of 0.3 by centrifugation (4°C, 18,000 x g), followed by several cooling and washing steps with sterile bi-distilled water. Transformation was carried out in a MicroPulserTM Electroporator at 1.8 kV with 100 μ L cells and 100 ng DNA. Transformed cells containing pTacVP1 with the ampicillin resistance gene were selected on carbenicillin agar plates.

2.2.2 Micro-scale Cultivations

The pre-cultures for the micro-scale cultivations were prepared as 80 mL cultures in TB medium using *E. coli* Rosetta pTacVP1 from a cryo culture in the MaxQTM 6000 incubator (180 rpm - 37 °C). 4 different pre-cultures were employed, applying TB medium of variable composition (pH 6 - w or w/o 2 mM magnesium sulfate and pH 7 - w or w/o 2 mM magnesium sulfate). After 16 h (late exponential phase), the cells were diluted to a final OD_{600 nm} of 0.1 AU using the different TB media (equally treated pre-culture for all experiments). The working volume of the 48-well FlowerPlate[®] was set to 1 mL for all cultivation experiments. The cultivation plate was sealed with an adhesive gas-permeable sterile membrane.

The micro-scale cultivation experiments were performed at shaking speeds of 600 rpm or 1200 rpm, covering a temperature set of 27, 32, and 37 °C. According to the FlowerPlate[®] product sheet [43], 600 rpm shaking speed at 1 mL filling volume represents oxygen limited conditions ($K_La = 85.9$ 1/h) whereas 1200 rpm shaking speed at 1 mL filling volume ($K_La = 371.6$ 1/h) is in a range of a bench scale stirred tank reactor [44]. Per 48-well FlowerPlate[®], each cultivation experiment was performed in triplicate, allowing for a total of 16 conditions to be screened (combined with all shaking speeds and temperatures, this adds up to $16 \cdot 6 = 96$ conditions). These 16 conditions covered 2 different pH values (pH 6 and pH 7), 2 different additive setups (w and w/o 2 mM magnesium sulfate), 2 different induction times (OD_{600 nm} of 0.5 AU and 4 AU), as well as 2 different inducer concentrations (0.1 mM and 0.5 mM of IPTG) as a full factorial experimental design. The respective induction times, being in scattered light units in the BioLector[®] system, were calculated using scattered light - OD_{600 nm} correlation functions (600 rpm: Scattered light = $11.69 \cdot OD_{600\ nm} + 17.59$; 1200 rpm: Scattered light = $11.36 \cdot OD_{600\ nm} + 16.14$). After 20 h, the cultivation procedure was stopped. 50 μ L of each well of the FlowerPlate[®] were transferred to 300 μ L polypropylene 96-well plates with a conical bottom for TCA total protein extraction under denaturing conditions. Additionally, 150 μ L of cell broth were transferred to another 300 μ L polypropylene 96-well plate for native cell disruption by sonication. All plates for protein release were centrifuged at 3200 x g and 10 °C for 30 min and the supernatant was discarded.

2.2.3 High-throughput Cell Disruption

For total protein extraction under denaturing conditions using a TCA protocol, the cell pellets were resuspended in 200 μL of ultrapure water. Then, 10 μL of 100% (w/v) TCA solution were added to each well and the plate was shaken for 20 s and subsequently stored on ice for 10 min. The plate was then centrifuged at 3200 x g and 4 $^{\circ}\text{C}$ for 10 min and the supernatant was discarded. The pellet was washed twice with 200 μL of cold pure acetone, followed by another centrifugation cycle after each washing step. In a final step the supernatant was removed, the pellet was dried for 3-4 h and stored at -20 $^{\circ}\text{C}$ until analysis.

For HTS sonication experiments using the Model 120 Sonic Dismembrator (Fisher Scientific), the cell pellets were resuspended in 150 μL of lysis buffer for native protein release (compatible with the GX II system). The sonication device was operated with an amplitude of 70%, applying 6 cycles of 20 s pulse duration. Between the pulses, 30 s chilling on ice followed. After the final sonication cycle, the plates were centrifuged twice at 4 $^{\circ}\text{C}$ and 3200 x g for 30 min. The supernatant was transferred to another 96-well plate and stored at -20 $^{\circ}\text{C}$ until analysis in the GX II system.

2.2.4 Scale-up Culture

A scale-up culture from the 1 mL micro-scale cultivation yielding highest VP1 titers to a 2.5 L shake flask culture was realized by keeping the oxygen transfer rate constant, as shown by Hermann et al. [45]. The corresponding shaking frequency for scale-up (180 rpm) was taken from Baumann et al. [41]. The TB medium at pH 6 included 2 mM magnesium sulfate and the induction was carried out at $\text{OD}_{600\text{ nm}}$ of 0.5 AU with 0.5 mM IPTG. 20 h after inoculation, the cells were centrifuged at 3200 x g and 4 $^{\circ}\text{C}$ for 30 min. Product release under native conditions was performed by sonication using a Digital Sonifier[®] 450 equipped with a 1/2" extension cylindrical sonication probe. The cell pellets from 400 mL culture were suspended in 20 mL native lysis buffer for purification experiments. The sonication procedure was carried out at an amplitude of 70% applying 8 cycles of 15 s pulse duration (each cycle followed by 30 s chilling on ice). The lysates were centrifuged twice at 10 $^{\circ}\text{C}$ and 18,000 x g for 30 min, followed by a 0.45 μm filtration step using PES filters by Sartorius, Germany.

2.3 Downstream Process Development

VP1 expressed in *E. coli* Rosetta cells was purified by anion-exchange (AEX) membrane chromatography and size-exclusion chromatography (SEC). A clarified *E. coli* lysate (1 mL) was loaded onto a 3 mL Sartobind[®] Q Nano Membrane Capsule (Sartorius Stedim Biotech GmbH, Goettingen, Germany) at 3 mL/min and purified by applying a salt step elution with NaCl. Pooled VP1 fractions of the AEX eluate were further processed on a Superose 6[®] Increase 10/300 GL column (Ge Healthcare, Uppsala, Sweden) at a flow rate of 0.5 mL/min. Purified VP1 was finally assembled into VLPs by dialysis into the assembly buffer, followed by dialysis against PBS for 16 h prior to analysis by transmission electron microscopy (TEM).

2.4 Analytical Methods

2.4.1 SDS-PAGE & Western Blot

For gel electrophoresis, the TCA pellet from the total protein extraction protocol was dissolved in 1X NuPAGE[®] LDS sample buffer, including 12.5 mM DTT for gel electrophoresis ($\text{OD}_{600\text{ nm}} \cdot 200 \mu\text{L}$), for 2 h in an overhead shaker. For native samples in solution, the sample preparation was performed according to the Novex[®] NuPAGE[®] 4-12% Bis-Tris protein gel

manual [46]. Purified VP1 derived from the GST-tag process developed by Middelberg et al. [19] served as reference standard. All samples were denatured at 100 °C and 300 rpm for 15 min on a plate shaker with lid heating. All following steps were carried out as described in the user manual. For each set of samples, two distinct gels were created, one for western blotting without staining and another stained with 'blue silver' staining solution.

Proteins were transferred from SDS-PAGE gels to a nitrocellulose membrane at 30 kV for 1 h using the XCell IITM blot module from Life Technologies, USA. Washing, blocking with 5% BSA, and incubation with primary and secondary antibodies were performed according to the user manual [47]. Rabbit-derived anti-VP1 antibody was a gift of Prof. Robert Garcea [42] and was used as primary antibody. Alkaline phosphatase affinity-purified donkey anti-rabbit IgG (Jackson ImmunoResearch Laboratories, USA) served as secondary antibody. Product detection was carried out using alkaline phosphatase color reagents (BioRad Laboratories, USA). All gels and membranes were analyzed in a Bio-5000 gel scanner.

2.4.2 Capillary Gel Electrophoresis

For quantitative determination of purities and VP1 concentrations, all samples were analyzed in a LabChip[®] GX II capillary gel electrophoresis device as duplicates with an HT Protein Express LabChip[®] kit. Purified VP1 derived from the GST-VP1 process developed by Middelberg et al. [19] served as reference standard. The sample and chip preparation procedures for liquid samples were performed as described in the manufacturer's protocol for the HT Protein Express Assay [48]. In contrast to this, the dried samples from the TCA extraction were dissolved in 100 μ L HT Protein Express sample buffer, including 34 mM of DTT. All further steps followed the above-mentioned protocol for liquid samples. Sample analysis was carried out using the HT Protein Express 200 assay in the LabChip[®] GX 3.1 software. Product quantification was based on peak-baseline integration of the product peak and comparison to a lysozyme standard of 1 mg/mL.

2.4.3 DNA Quantification

PicoGreen[®] dsDNA assay kit (Invitrogen, Paisley, United Kingdom) was used to quantify DNA according to the manufacturer's instructions. Samples were diluted ten fold with TE buffer prior to measurement.

2.4.4 Transmission Electron Microscopy

Visualization and characterization of assembled virus-like particles were carried out by transmission electron microscopy (TEM) on a CM 200 FEG/ST electron microscope. Sample preparation was performed as described previously by Ladd Effio et al. [49].

3 Results & Discussion

3.1 Codon Optimization & Product Detection

The expression of virus proteins in *E. coli* depends on various parameters, such as strain and vector design, promoter, cultivation and induction conditions, as well as on codon usage. First cultures with *E. coli* Rosetta(DE3)pLysS cells and the pALVP1TAC [42] plasmid showed very poor yields below 1% of total soluble protein (TSP) (data not shown) following cultivation protocols by Chuan et al. [30]. Chuan et al. [30] demonstrated the presence of several rare codons in the pALVP1TAC-derived insert of pGexVP1. Hence, we sequenced pALVP1TAC and looked

for under-represented codons in the *E. coli* genome. According to Henaut et al. [50], Chen et al. [51], and Nakamura et al. [52], codons which are considered rare in *E. coli* are AGG, AGA, CGG, and CGA encoding for arginine, GGA encoding for glycine, ATA encoding for isoleucine, CTA encoding for leucine, and CCC encoding for proline. As shown in Fig. 1, seven of these rare codons are represented in the insert of the VP1 sequence.

Aiming at a higher protein expression, the sequence was codon-optimized for *E. coli* by Centic Biotec (Heidelberg, Germany), obtaining a modified insert sequence than Chuan et al. [30] (85% identity). Subsequently, the codon-optimized DNA sequence was inserted into a vector with a tac promoter and transformed into *E. coli* Rosetta cells (see section 2.2.1). For the proof of concept, expression of the product of interest on the shaker flask scale was evaluated by several analytical methods: SDS-PAGE, western blot, capillary gel electrophoresis, and reversed-phase ultra-high-performance liquid chromatography (data not shown). Fig. 2 shows an overview of the different procedures for the detection of VP1 in *E. coli* cell lysates with and without the constructed pTacVP1 plasmid. A protein ladder and a VP1 standard are included in each of the analytical technologies. Fig. 2A illustrates the VP1 identification using capillary gel electrophoresis, showing virtual gels with VP1 highlighted as a red box. The VP1 standard (red) was detected at 49 kDa (aligned time of 21.7 s inside the capillary). Accordingly, the transformed *E. coli* Rosetta pTacVP1 strain (black) revealed a pronounced peak at the same molecular weight as the VP1 standard, whereas the *E. coli* Rosetta wild type (blue) shows low fluorescence at 49 kDa only. In Fig. 2B the product-specific western blot is illustrated with VP1 highlighted as a red box. Lane 1 represents the VP1 standard, lane 2 and 3 include the total protein extracts of *E. coli* Rosetta pTacVP1 and the Rosetta wild type respectively. The VP1 standard (lane 1) revealed an identical band pattern in the western plot as as the total protein extract of *E. coli* Rosetta pTacVP1 (lane 2). The gel bands of the total protein extract of the *E. coli* Rosetta wild type (lane 3), by contrast, were insensitive to the product-specific antibody.

Different orthogonal analytical methodologies, namely, capillary gel electrophoresis, SDS-PAGE, western blot, as well as reversed-phase chromatography (data not shown), indicated the presence of VP1 in the codon-optimized *E. coli* Rosetta pTacVP1 strain. As shown in the *E. coli* Rosetta wild type lysate, a minor amount of impurities was detected with the same molecular weight as VP1. The weak bands of the *E. coli* Rosetta wild type lysate (Fig. 2B, lane 3) is explained by cross reactivity of the proteins to the primary antibody for VP1, as reported by Leavitt et al. [42].

3.2 High-throughput Cultivations

3.2.1 Growth Curves

The high-throughput cultivation experiments covered shaking speeds of 600 rpm and 1200 rpm, temperatures of 27, 32, and 37 °C, two medium pH values of pH 6 and pH 7, two additive setups (w and w/o 2 mM magnesium sulfate), two induction times of $OD_{600\text{ nm}} = 0.5$ AU and 4 AU, as well as two inducer concentrations of 0.1 mM and 0.5 mM IPTG. The growth curves for all conditions investigated are illustrated in Fig. 3 with separated plots for the different combinations of temperature and shaking speeds. In each individual plot, cultivations performed at pH 6 are marked in red and at pH 7 in blue (dark colored conditions include 2 mM magnesium sulfate). Conditions induced at an $OD_{600\text{ nm}}$ of 0.5 AU are illustrated as lines (dashed lines for induction using 0.1 mM IPTG, solid lines for 0.5 mM IPTG), whereas inductions at $OD_{600\text{ nm}}$ of 4 AU are shown as markers (asterisk for induction using 0.1 mM IPTG, circles for 0.5 mM

3 PUBLICATIONS & MANUSCRIPTS

VP1	1	ATG GCC CCC AAA AGA AAA AGC GGC GTC TCT AAA TGC GAG ACA AAA TGT ACA AAG GCC TGT
VP1*	1	ATG GCA CCT AAG CGT AAG AGC GGT GTC TCT AAG TGC GAG ACT AAG TGC ACC AAG GCA TGC
VP1	61	CCA AGA CCC GCA CCC GTT CCC AAA CTG CTT ATT AAA GGG GGT ATG GAG GTG CTG GAC CTT
VP1*	61	CCA CGT CCG GCA CCA GTT CCA AAA CTG CTG ATT AAG GGT GGT ATG GAG GTA CTG GAT CTG
VP1	121	GTG ACA GGG CCA GAC AGT GTG ACA GAA ATA GAA GCT TTT CTG AAC CCC AGA ATG GGG CAG
VP1*	121	GTA ACG GGT CCG GAT TCT GTA ACT GAG ATC GAG GCT TTT CTG AAC CCA CGT ATG GGT CAG
VP1	181	CCA CCC ACC CCT GAA AGC CTA ACA GAG GGA GGG CAA TAC TAT GGT TGG AGC AGA GGG ATT
VP1*	181	CCG CCG ACT CCG GAA TCT CTG ACT GAA GGT GGT CAG TAC TAC GGT TGG TCT CGT GGT ATT
VP1	241	AAT TTG GCT ACA TCA GAT ACA GAG GAT TCC CCA GGA AAT AAT ACA CTT CCC ACA TGG AGT
VP1*	241	AAC CTG GCT ACT AGC GAT ACC GAG GAT TCC CCA GGT AAC AAT ACC CTG CCG ACT TGG TCT
VP1	301	ATG GCA AAG CTC CAG CTT CCC ATG CTC AAT GAG GAC CTC ACC TGT GAC ACC CTA CAA ATG
VP1*	301	ATG GCT AAA CTG CAG CTG CCG ATG CTG AAC GAG GAT CTG ACT TGC GAC ACT CTG CAG ATG
VP1	361	TGG GAG GCA GTC TCA GTG AAA ACC GAG GTG GTG GGC TCT GGC TCA CTG TTA GAT GTG CAT
VP1*	361	TGG GAA GCG GTT TCT GTA AAA ACC GAA GTG GTG GGC TCT GGT TCC CTG CTG GAT GTA CAC
VP1	421	GGG TTC AAC AAA CCC ACA GAT ACA GTA AAC ACA AAA GGA ATT TCC ACT CCA GTG GAA GGC
VP1*	421	GGT TTC AAC AAA CCG ACC GAC ACT GTG AAC ACC AAA GGC ATC TCC ACC CCG GTA GAA GGT
VP1	481	AGC CAA TAT CAT GTG TTT GCT GTG GGC GGG GAA CCG CTT GAC CTC CAG GGA CTT GTG ACA
VP1*	481	AGC CAG TAC CAC GTA TTC GCC GTT GGT GGC GAA CCT CTG GAC CTG CAA GGT CTG GTT ACC
VP1	541	GAT GCC AGA ACA AAA TAC AAG GAA GAA GGG GTA GTA ACA ATC AAA ACA ATC ACA AAG AAG
VP1*	541	GAT GCG CGT ACC AAA TAC AAA GAA GAA GGT GTT GTG ACC ATC AAA ACC ATC ACC AAA AAA
VP1	601	GAC ATG GTC AAC AAA GAC CAA GTC CTG AAT CCA ATT AGC AAG GCC AAG CTG GAT AAG GAC
VP1*	601	GAC ATG GTC AAC AAA GAC CAG GTC CTG AAC CCG ATC AGC AAA GCG AAA CTG GAC AAA GAC
VP1	661	GGA ATG TAT CCA GTT GAA ATC TGG CAT CCA GAT CCA GCA AAA AAT GAG AAC ACA AGG TAC
VP1*	661	GGC ATG TAC CCG GTG GAA ATC TGG CAC CCG GAC CCT GCC AAA AAC GAA AAC ACG CGT TAC
VP1	721	TTT GGC AAT TAC ACT GGA GGC ACA ACA ACT CCA CCC GTC CTG CAG TTC ACA AAC ACC CTG
VP1*	721	TTC GGC AAC TAC ACG GGC GGC ACC ACC ACC CCG CCG GTT CTG CAG TTC ACT AAC ACT CTG
VP1	781	ACA ACT GTG CTC CTA GAT GAA AAT GGA GTT GGG CCC CTC TGT AAA GGA GAG GGC CTA TAC
VP1*	781	ACT ACC GTG CTG CTG GAC GAA AAC GGC GTT GGT CCG CTG TGT AAA GGT GAA GGC CTG TAT
VP1	841	CTC TCC TGT GTA GAT ATA ATG GGC TGG AGA GTT ACA AGA AAC TAT GAT GTC CAT CAC TGG
VP1*	841	CTG TCC TGT GTT GAT ATC ATG GGC TGG CGT GTT ACC CGT AAC TAC GAC GTC CAT CAT TGG
VP1	901	AGA GGG CTT CCC AGA TAT TTC AAA ATC ACC CTG AGA AAA AGA TGG GTC AAA AAT CCC TAT
VP1*	901	CGT GGC CTG CCG CGT TAT TTC AAA ATT ACC CTG CGC AAA CGC TGG GTT AAA AAC CCG TAT
VP1	961	CCC ATG GCC TCC CTC ATA AGT TCC CTT TTC AAC AAC ATG CTC CCC CAA GTG CAG GGC CAA
VP1*	961	CCG ATG GCG TCC CTG ATT AGC TCC CTG TTC AAC AAC ATG CTG CCG CAG GTG CAA GGC CAG
VP1	1021	CCC ATG GAA GGG GAG AAC ACC CAG GTA GAG GAG GTT AGA GTG TAT GAT GGG ACT GAA CCT
VP1*	1021	CCT ATG GAA GGT GAA AAT ACC CAG GTG GAA GAA GTT CGC GTT TAT GAC GGC ACC GAA CCG
VP1	1081	GTA CCG GGG GAC CCT GAT ATG ACG CGC TAT GTT GAC CGC TTT GGA AAA ACA AAG ACT GTA
VP1*	1081	GTG CCG GGC GAT CCG GAT ATG ACG CGC TAT GTT GAC CGC TTT GGC AAA ACC AAA ACG GTT
VP1	1141	TTT CCT GGA AAT TAA 1155
VP1*	1141	TTT CCG GGC AAT TAA 1155

Figure 1 Codon optimization of the VP1 sequence for recombinant protein expression in *E. coli*. The original DNA sequence of VP1 is illustrated above the sequence after codon optimization (VP1*) with rare codons highlighted in red. Unchanged sequences in the VP1 genetic code are indicated by lines.

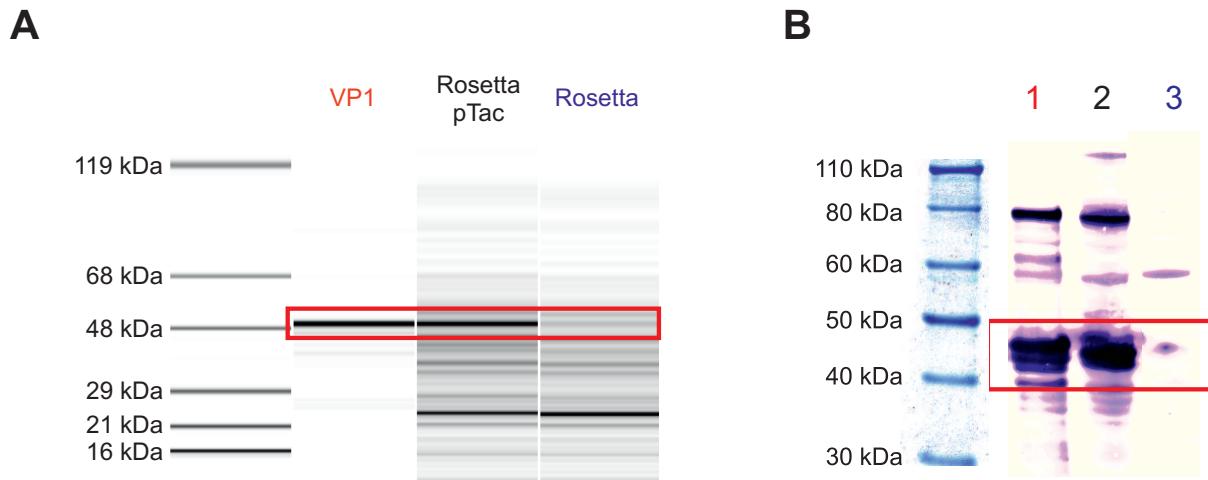


Figure 2 Product (VP1) identification out of a crude feedstock of transformed *E. coli* Rosetta pTacVP1. A: Capillary gel electrophoresis of a purified VP1 standard, an *E. coli* Rosetta pTacVP1 lysate, and an *E. coli* Rosetta wild type lysate. VP1 is detected at 49 kDa in the virtual gel. B: Western blot of a purified VP1 standard (lane 1), an *E. coli* Rosetta pTacVP1 lysate (lane 2), and an *E. coli* Rosetta wild type lysate (lane 3). The relevant product-related bands are highlighted in red at a molecular weight of 45 kDa.

IPTG).

The lag phase of the *E. coli* Rosetta pTacVP1 cells decreases steadily from 27 °C (6 to 7 h) up to 37 °C (3 h), shifting the induction times (downward triangles) closer to the time of inoculation (0 h). All other factors show negligible impact on the lag phase, with the medium pH being the only exception. In all setups the lag phase of cells cultivated at pH 6 is elongated compared to those grown at pH 7, most pronounced for the cells cultivated at 27 °C. The increased time until starting the exponential phase for cultivations at lower temperatures is intuitive due to the decrease in metabolic activity of *E. coli* cells at a temperature other than the optimum of 37 °C. The negative effect of acidic pH on the lag phase is due to *E. coli* having its pH optimum in the neutral region.

The shape of the exponential growth shows highest variations when comparing conditions of different shaking speeds. All cells cultivated at 1200 rpm (right graphs, Fig. 3) display an ideal exponential growth until the stationary phase. In contrast to this, all cultivations performed at 600 rpm result in multiple varying slopes of the exponential growth separated by intermediate plateaus. This effect is pronounced for cells cultivated at pH 7. Such behavior was also described by Funke et al. [53] for *E. coli* when accumulating acidic metabolites under fermenting conditions. Lower shaking frequencies (600 rpm - $K_{La} = 85.9$ 1/h) result in poor mixing and low oxygen uptake into the medium inducing such fermenting conditions. Cultivations performed at pH 6 are less influenced as cells grow under 'pseudo-fermenting' conditions starting from inoculation due to the acidic environment.

The final plateaus of the stationary phase are elevated for all conditions at a shaking speed of 1200 rpm compared to those at 600 rpm, yielding a maximal scattered light plateau of 285 SU at 27 °C. In comparison, the maximal scattered light signal for the same temperature at 600 rpm is about 40% lower (180 SU). With an increase in temperature up to 37 °C, this effect is less pronounced. Whereas the stationary phase plateaus vary significantly for different shaker speeds and temperatures, all other cultivation factors investigated are negligible. As discussed above, higher shaking speeds result in a better oxygen uptake into the medium (1200 rpm - $K_{La} = 371.6$ 1/h) and, thus, enhance growth under aerobic conditions.

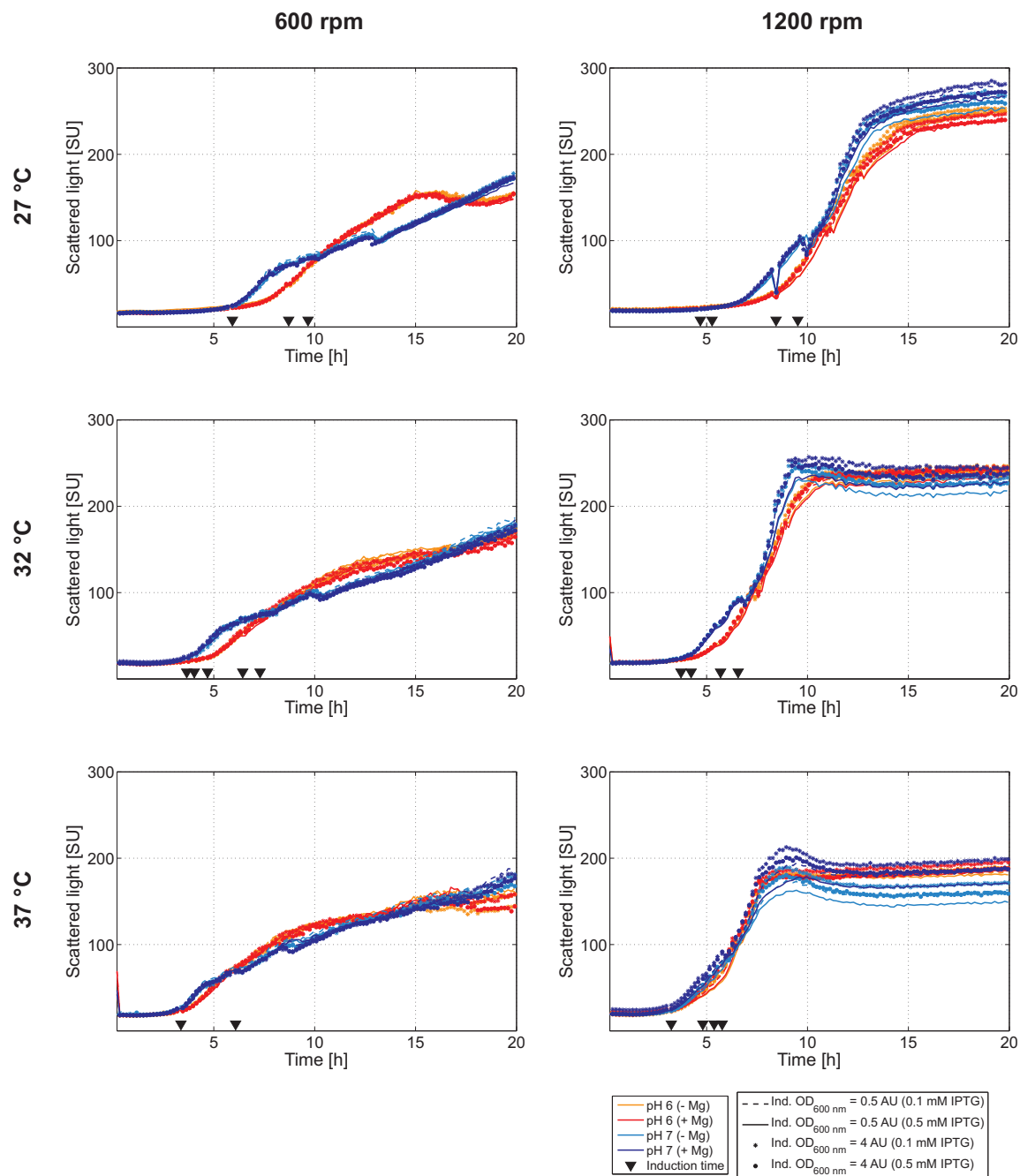


Figure 3 BioLector[®] growth curves of *E. coli* Rosetta pTacVP1 under different cultivation conditions: Temperatures of 27, 32, and 37 °C and two shaking speeds of 600 and 1200 rpm were investigated. For each setup, four distinct media compositions were examined, being two pH values of pH 6 (red curves) and pH 7 (blue curves) with (dark colored) and without (light colored) addition of 2 mM magnesium sulfate. As a final factor, four different induction setups were investigated, being the induction times $OD_{600\text{ nm}}$ of 0.5 (lines) and 4 (markers) using 0.1 mM (dashed line/ asterisk) or 0.5 mM IPTG (solid line/ circle), respectively.

3.2.2 Soluble VP1 Fraction

The soluble protein fraction of cells after sonication and lysate clarification for all conditions investigated is shown in Fig. 4 as 3D bar plots. Again, plots are separated for different combinations of shaking speeds and temperatures. All VP1 concentrations c_{VP1} are normalized to the maximal concentration attained under all conditions $c_{VP1,max}$ of $1.63 \text{ mg/mL} \pm 0.13 \text{ mg/mL}$ (37°C , 600 rpm, pH 6, including 2 mM magnesium sulfate, induced at $OD_{600 \text{ nm}}$ of 0.5 AU using 0.5 mM IPTG).

All cultivations performed at 1200 rpm (right) resulted in lower VP1 titers compared to those at shaker speeds of 600 rpm (left), with the highest value $38.8\% \pm 4.5\%$ at 27°C and 1200 rpm compared to the overall maximum $c_{VP1,max}$. A decrease in temperature is beneficial for the formation of soluble VP1 at 1200 rpm, shifting $c_{VP1}/c_{VP1,max}$ from up to $16.4\% \pm 1.9\%$ at 37°C to $38.8\% \pm 4.5\%$ at 27°C . Nevertheless, the maximal VP1 concentration investigated at 1200 rpm was below that of most conditions examined for 600 rpm shaking speed, ranging from $c_{VP1}/c_{VP1,max}$ of $30.8\% \pm 4.2\%$ to $100\% \pm 8.2\%$. For experiments performed at 600 rpm, the VP1 concentration in the soluble protein fraction follows an inverse trend towards cultivation temperature, shifting $c_{VP1}/c_{VP1,max}$ from up to $49.2\% \pm 4.9\%$ at 27°C to $100\% \pm 8.2\%$ at 37°C . For 32°C and 37°C , additional pH effects become apparent, showing a positive effect for cells cultivated under acidic conditions (pH 6) compared to experiments performed in a medium of pH 7. The addition of 2 mM magnesium sulfate did not show pronounced effects in all setups investigated. Also the induction time and inducer concentration were determined to be factors of minor importance.

These findings of high native protein production under fermenting conditions with low oxygen supply and increased temperature agree with the findings of Baumann et al. [41] for glutathione-S-transferase and Losen et al. [54] for benzoylformate decarboxylase. However, they contradict the experiments of Chuan et al. [30], who found an optimal production of 0.18 mg/mL VP1 at a decreased temperature of 26°C . Note that the maximal VP1 concentration in this study of $1.63 \text{ mg/mL} \pm 0.13 \text{ mg/mL}$ corresponds to an increase of approximately a factor of 10 compared to Chuan et al. [30]. Nevertheless, both Chuan et al. [30] and Liew et al. [55] conclude that growth limiting cultivation conditions lead to increased product titers of VP1 or GST-VP1, respectively. Finally, the pH of the cultivation medium was found to be an important factor for enhancing native VP1 production. The effect of increased soluble protein production under acidic conditions was also reported by Kopetzki et al. [56] for α -glucosidase produced in *E. coli*. As fermenting conditions with acidic by-products have a positive impact on soluble VP1 formation, the decreased pH after inoculation can enhance this effect. Whereas the negligible influence of the inducer concentration on the product formation agrees with Baumann et al. [41], the low impact of the induction time investigated in this study is in contradiction, as was also reported by Galloway et al. [57].

When comparing the trends of the growth curves to the soluble VP1 titers, there is a clear correlation of increased productivity of *E. coli* cells under non-optimal growth conditions. All experiments performed at high shaker speed (1200 rpm) resulted in unlimited growth (Fig. 2, right) and, consequently, yielded low titers on soluble VP1 (Fig. 3, right). Fermenting conditions at 600 rpm shaker speed, by contrast, resulted in varying slopes of the exponential growth separated by intermediate plateaus and were found beneficial for soluble VP1 formation with product concentrations of up to $1.63 \text{ mg/mL} \pm 0.13 \text{ mg/mL}$ (Fig. 3, left). Note that excess stress on cell growth, as shown for fermenting conditions (600 rpm) and low cultivation temperatures (27°C), reduced this effect, which might be due to product degradation as a consequence of cell starvation.

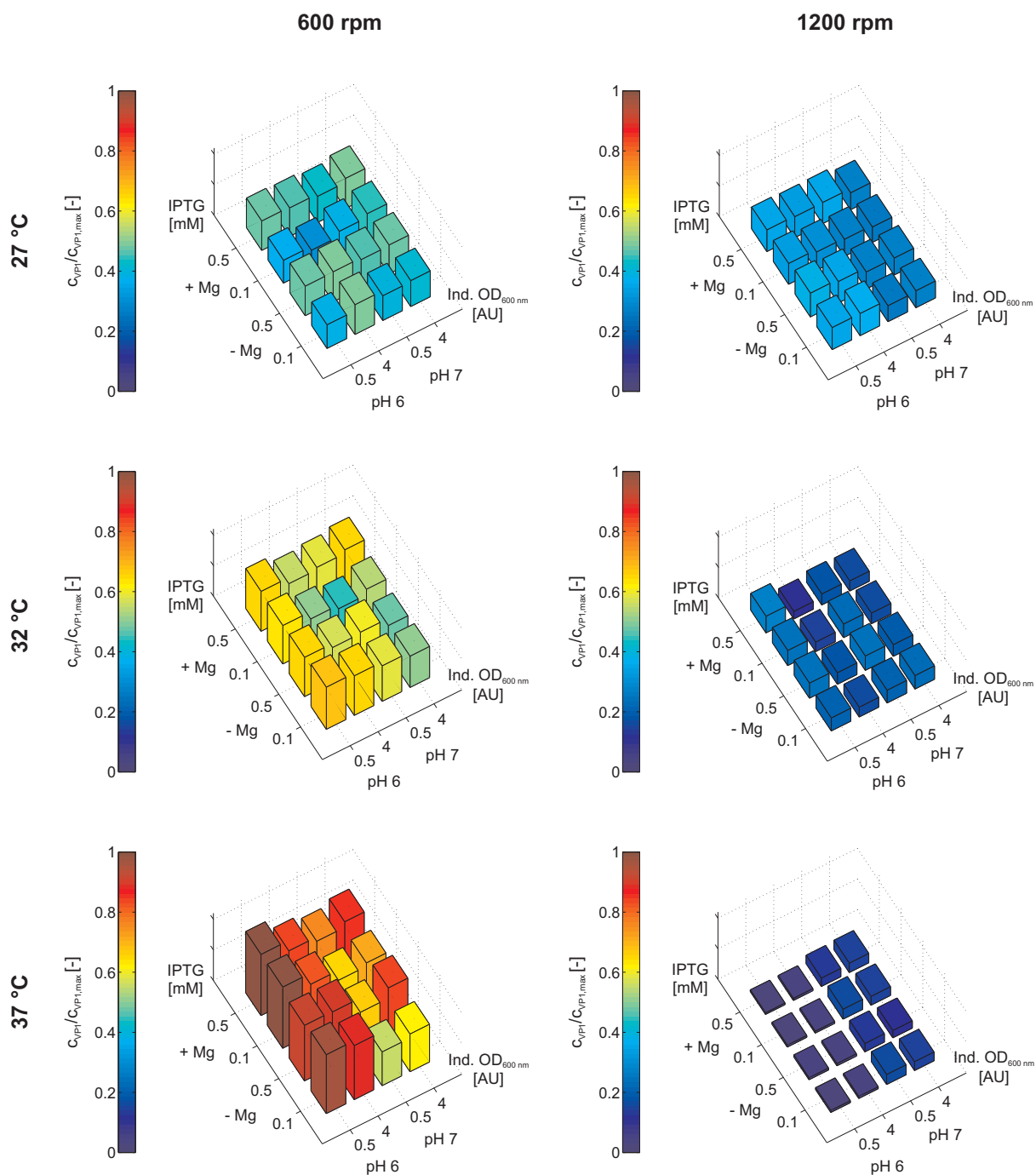


Figure 4 Soluble protein fraction of lysed cells shown in 3D bar plots. Separated plots are shown for different combinations of shaking speeds (600 rpm and 1200 rpm) and temperatures (27, 32, and 37 °C). Results for different media compositions (pH and magnesium sulfate concentrations), induction times, and inducer concentrations are shown for each individual sub-plot. All VP1 concentrations c_{VP1} are normalized to the maximal concentration attained under all conditions $c_{VP1,max}$ being $1.63 \text{ mg/mL} \pm 0.13 \text{ mg/mL}$.

3.2.3 Ratio of VP1 to Total Soluble Protein

Besides the overall product titer of soluble VP1, also the initial purity of the sample (ratio of VP1 to total soluble protein) is an important factor for subsequent purification processes. A comparison of soluble VP1 titers and total soluble protein (TSP) is shown in Fig. 5A. The different combinations of temperature and shaker speeds are indicated as different markers, whereas different media compositions are highlighted as colors. All data points were fitted with a linear regression function yielding a coefficient of determination R^2 of 85.6%, indicating that the purity of the samples increased linearly with the amount of produced soluble VP1. All cell lysates derived from cultivations at 1200 rpm are found in the bottom left corner of Fig. 5A (circles, upward triangles, diamonds). 600 rpm cultures, by contrast, are found at higher soluble VP1 and TSP values in Fig. 5A (asterisks, downward triangles, hexagrams) with the overall best result found for the 37 °C cultivations (hexagrams), as was discussed earlier. The linear increase of TSP with soluble VP1 indicates a product enrichment without causing additional upward regulation of impurity levels. Fig. 5B illustrates this effect of shaker speed and temperature on the VP1 titer and the TSP for lysates from cultivations equivalent to the optimal system point (1.63 mg/mL \pm 0.13 mg/mL VP1) by capillary gel electrophoresis runs. In the electropherograms the VP1 peak is highlighted at an aligned time of 21.7 s (49 kDa). Green lines illustrate analyzed lysates from cultivations performed at 600 rpm (27, 32, and 37 °C) whereas red lines represent lysates from 1200 rpm cultivations. Whereas impurity levels are constant, VP1 levels vary strongly, most pronounced when comparing 37 °C - 600 rpm as the maximum VP1 concentration and 37 °C - 1200 rpm as the condition of low expression levels. The overall optimal system point for both soluble VP1 and TSP was found for the optimum identified in the 'Soluble VP1 fraction' section, resulting in a TSP of 42.6% with a concentration of 1.63 mg/mL \pm 0.13 mg/mL soluble VP1 (arrow in Fig. 5A). Hence, the system point of 37 °C, 600 rpm, pH 6, including 2 mM magnesium sulfate, induced at OD_{600 nm} of 0.5 AU using 0.5 mM IPTG was selected for scale-up and downstream process development, as both initial purity and product levels were optimal under the investigated upstream conditions.

3.2.4 Ratio of Soluble to Total Expressed VP1

Apart from the soluble VP1 fraction, also the total product fraction, including insoluble species, was determined using a TCA protocol for total protein extraction under denaturing conditions (Fig. 6). Fig. 7 illustrates the ratio of soluble to total expressed VP1 for each setup. For cultivations performed at 1200 rpm, the fraction of soluble VP1 is low, ranging from 4.6% to 39.1% compared to experiments at 600 rpm, where the fraction ranges from 20.9% to 106.1%. The optimal ratio of soluble to total VP1 was obtained for cells grown at 600 rpm and 27 °C, the range being 67.4% to 106.1%. Under these conditions, the neutral medium condition of pH 7 was beneficial compared to pH 6. The same trend was found for cultivations at 600 rpm under 32 °C as well as 37 °C. 32 °C was found to be the condition of the lowest soluble to insoluble VP1 ratio for cells cultivated at 600 rpm.

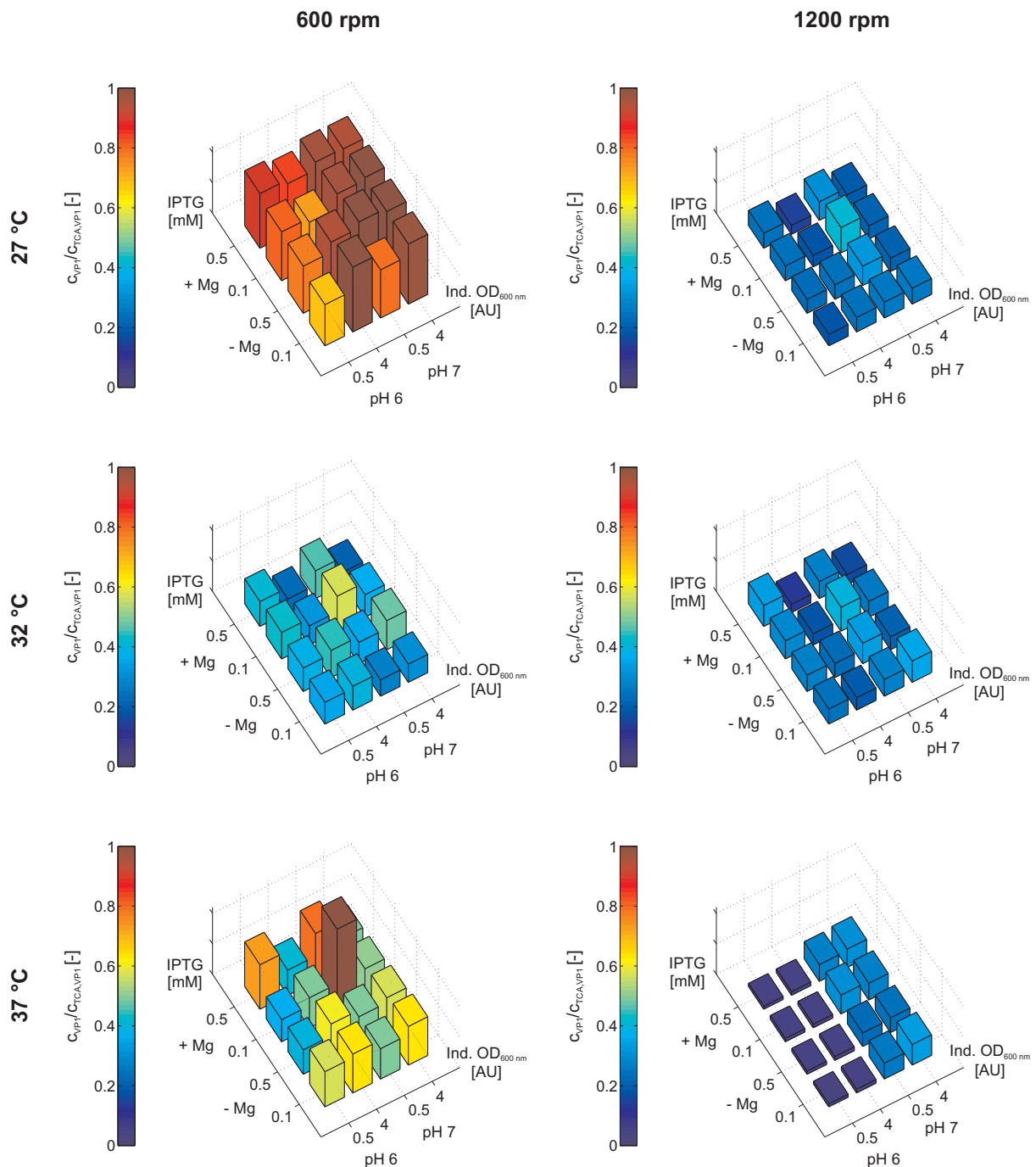


Figure 5 Impurity levels of the different lysates investigated in the BioLector[®] screening. A: Ratio of VP1 to total soluble protein, including a linear regression of data points. The different combinations of temperature and shaker speeds are indicated as different markers and different media compositions are highlighted as colors. B: Comparison of the impact of shaker speed and temperature on the VP1 titer and the impurity levels shown for the media conditions of the overall optimal system point (pH 6, including 2 mM magnesium sulfate, induced at $OD_{600\text{ nm}}$ of 0.5 AU using 0.5 mM IPTG). Electropherograms of these 6 combinations of temperature and shaking speed, with green lines representing cultivations at 600 rpm (27, 32, and 37 °C) and red lines at 1200 rpm (27, 32, and 37 °C) and the VP1 peak at an aligned time of 21.7 s (49 kDa).

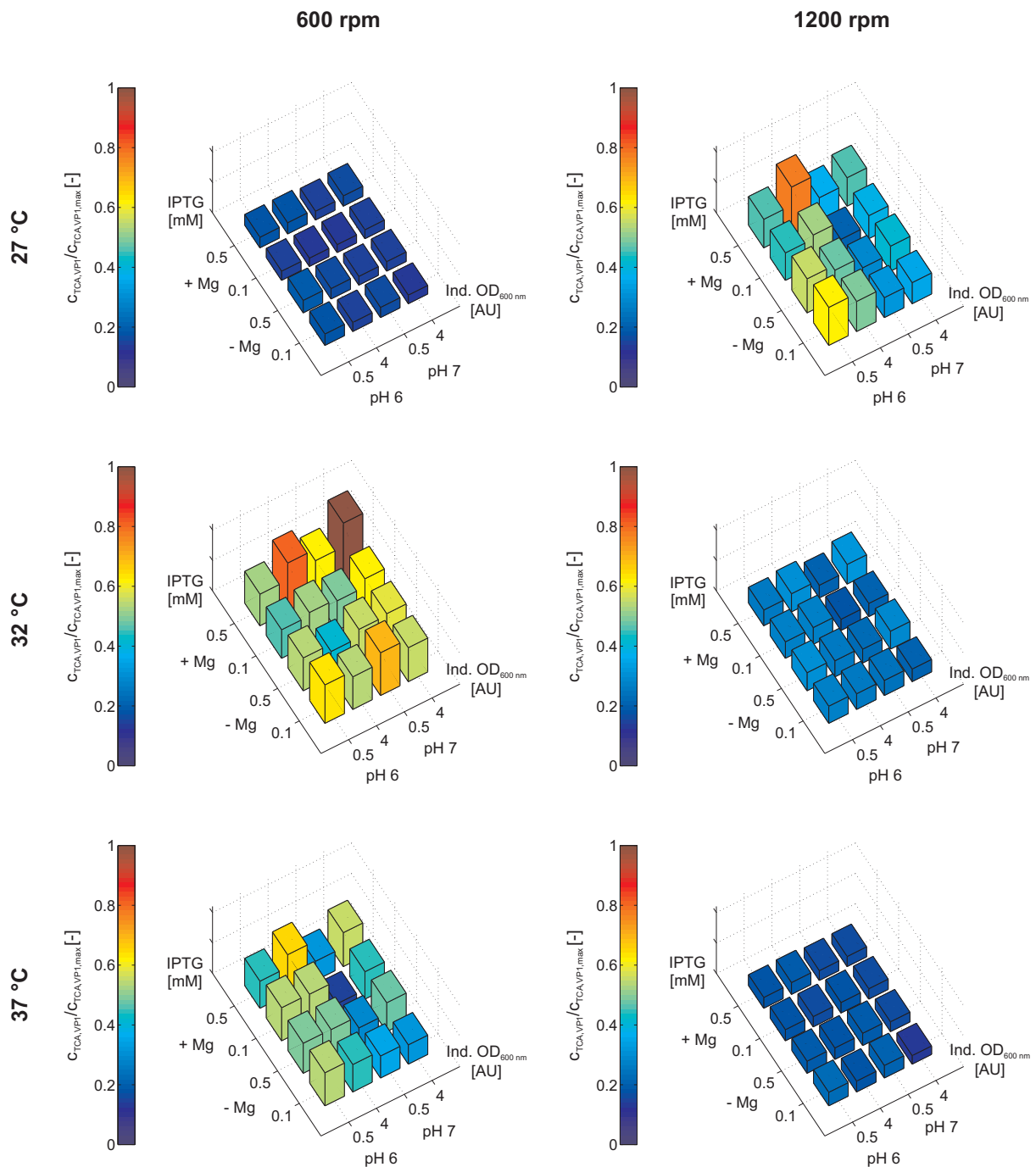


Figure 6 Total (soluble and insoluble) VP1 fraction shown in 3D bar plots. Separated plots are shown for different combinations of shaking speeds (600 rpm and 1200 rpm) and temperatures (27, 32, and 37 °C). Results for different media compositions (pH and magnesium sulfate concentrations), induction times and inducer concentrations are shown for each individual sub plot. All VP1 concentrations $C_{TCA,VP1}$ are normalized to the maximal concentration attained in all conditions $C_{TCA,VP1,max}$.

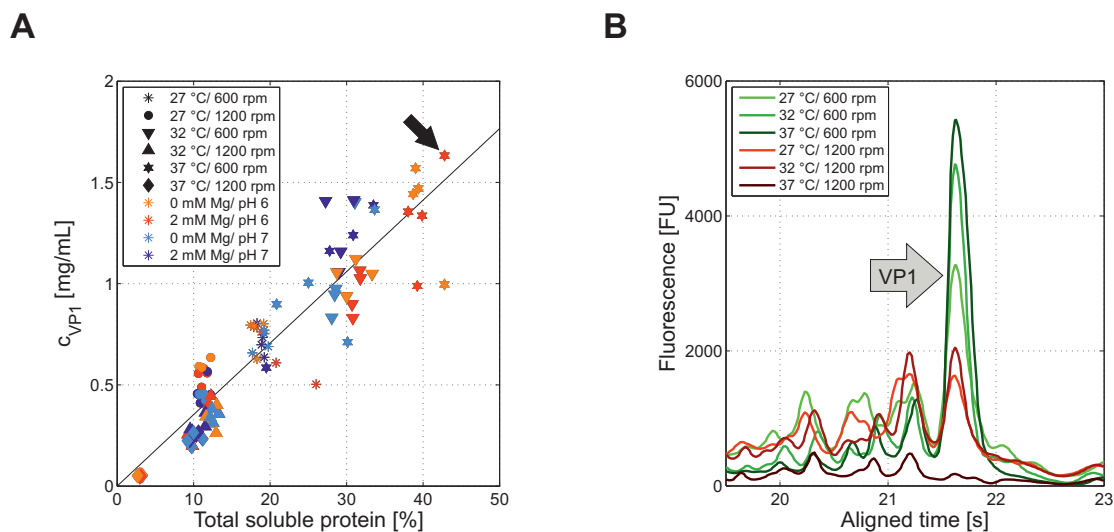


Figure 7 Ratio of soluble to total expressed VP1 of lysed cells shown in 3D bar plots. Separated plots are shown for different combinations of shaking speeds (600 rpm and 1200 rpm) and temperatures (27, 32, and 37 °C). Results for different media compositions (pH and magnesium sulfate concentrations), induction times, and inducer concentrations are shown for each individual sub-plot.

It was shown that a good mixing and oxygen uptake at 1200 rpm do not only result in low soluble VP1 titers as discussed earlier, but also in the formation of aggregates and inclusion bodies. Poor shaking at 600 rpm shaker speed, by contrast, resulted in ratios of soluble VP1 of up to 100%, mostly for conditions of reduced temperature, as was reported by other research groups [55, 58, 59, 56]. Note that a factor of 100% does not imply optimal conditions for yielding high overall product titers (compare Fig. 3), but conditions of non-soluble VP1 formation. For the condition of highest productivity of $1.63 \text{ mg/mL} \pm 0.13 \text{ mg/mL}$ VP1, the ratio of soluble product was determined to be 72.8%, indicating an economic system point for scale-up, as was discussed earlier.

3.3 VP1 Purification & Assembly of Virus-like Particles

The development of an alternative production pathway for murine polyoma VLPs without an affinity protein tag entails the establishment of a novel downstream process. Fig. 8 summarizes the outcome of the purification procedure with chromatograms for the capture and polishing step, electropherograms of VP1 process samples, and a TEM micrograph of assembled murine polyoma VLPs.

Capturing of VP1 from clarified *E. coli* cell lysate was performed by anion-exchange membrane chromatography. The chromatogram of the optimized salt step elution is shown in Fig. 8A. UV absorption (blue line), conductivity signals (dashed gray line), and VP1 concentration (green bars) are plotted against the mobile phase volume. Virtual gels for all fractions are plotted below the chromatogram to track the elution of VP1 and HCPs. As shown in the chromatogram of Fig. 8A, VP1 eluted mainly in the second salt step removing weaker and stronger charged molecules in a low salt step at 0.09 M NaCl and a high salt step at 1 M NaCl, respectively. $69 \pm 4 \%$ VP1 were recovered in the second salt step with a protein purity of $61 \pm 0.9 \%$ in the

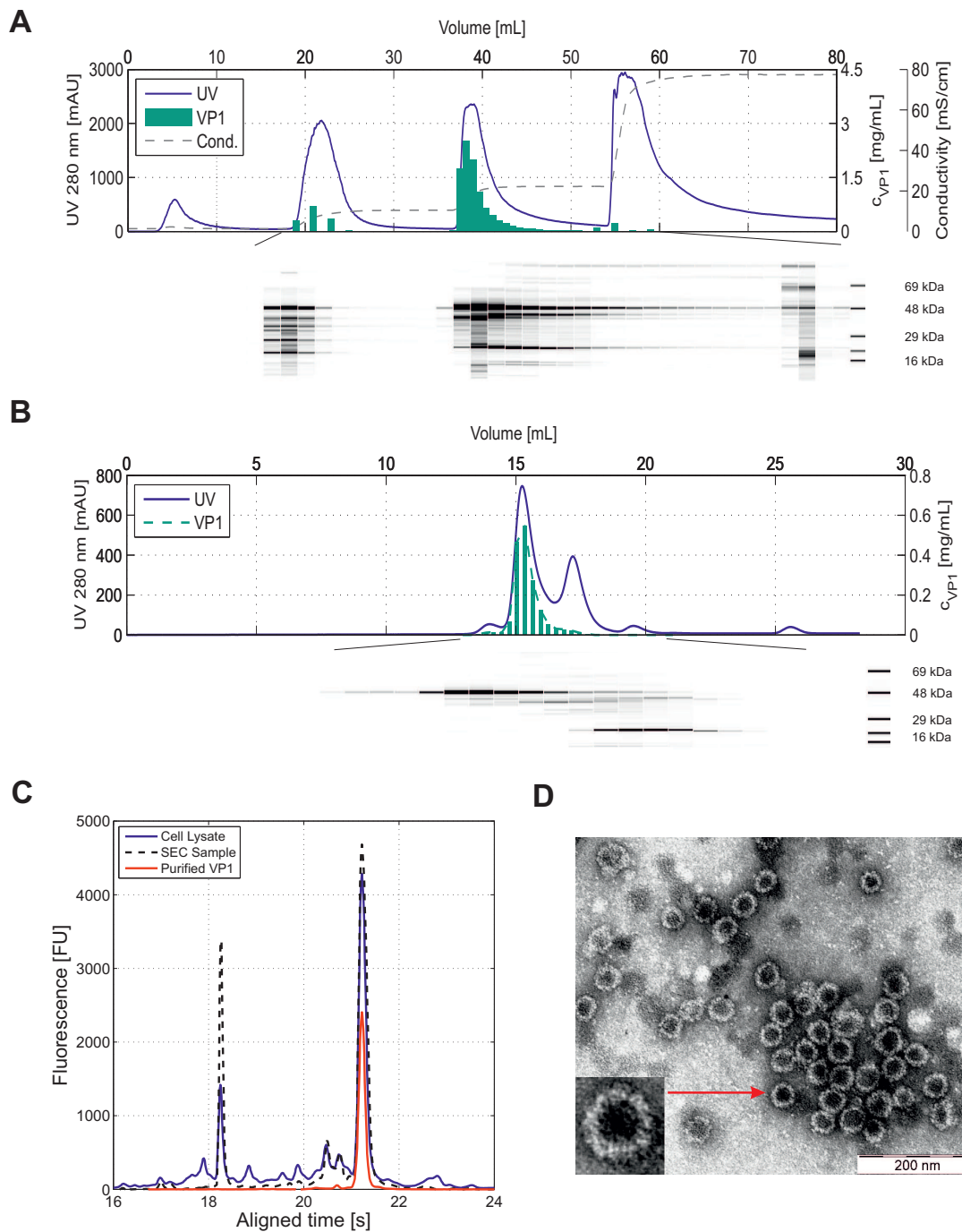


Figure 8 VP1 purification and VLP assembly procedure. **A:** Chromatogram of the AEX step for VP1 capturing. The UV signal is illustrated as a blue line, the conductivity is shown as a dashed line, and the VP1 concentrations are marked as green bars. The product-containing fractions are magnified in virtual gels of the capillary gel electrophoresis procedure, with the VP1 fraction shown at 49 kDa. **B:** Chromatogram of the SEC step for VP1 polishing. The UV signal is illustrated as a blue line and the VP1 concentrations are marked as green bars. The product-containing fractions are magnified in virtual gels of the capillary gel electrophoresis procedure with the VP1 fraction shown at 49 kDa. **C:** Electropherograms of the cell lysate (blue solid line), the pooled elution fraction after AEX (black dashed line), and the purified product after SEC polishing (red solid line). The VP1 peak is detected at 21.6 s of aligned time. **D:** TEM micrographs of the generated VLP sample after VLP assembly, showing spherical homogeneous particles (diameter of 40-50 nm).

pooled fractions. Fig 8B shows the chromatogram of the polishing step by size-exclusion chromatography for VP1 captured by anion-exchange membrane chromatography. The UV signal (blue line) reveals four major peaks. VP1 (green bars) elutes in the major peak at a retention volume of 15 mL, separating smaller host cell impurities (10 to 40 kDa) as displayed in the virtual gels of the FPLC fractions. The final protein purity of the pooled VP1 fractions was 92 ± 2 % with 6 ± 1 ng DNA per 100 μ g VP1, recovering 58 ± 1.5 % of VP1. In Fig. 8C capillary gel electrophoresis analysis of clarified cell lysate (dashed black line), captured VP1 (blue line), and polished VP1 (red line) is compared in an electropherogram. The comparison reveals the high purity achieved at the end of the two-step downstream process with only one minor impurity left. The cell lysate obtained from the 2.5 L shaker flask-scale fermentation showed almost the same VP1 concentration of 1.5 ± 0.2 mg/mL as in the 1 mL micro-scale cultivation and a similar TSP value of 42 ± 2 %.

Purified VP1 at a concentration of 0.3 mg/mL was finally assembled to VLPs, as described earlier by Middelberg et al. [19]. Fig. 8D shows the TEM micrographs of the generated VLP sample, revealing spherical homogeneous particles with diameters of 40-50 nm. The empty particles can hardly be distinguished from those murine polyoma VLPs produced by Middelberg et al. [19, 27] or Ewers et al. [60]. While the overall recovery of the downstream process should still be optimized, the concept was proven by purifying non GST-tagged VP1 with a rapid and scalable two-step purification procedure, yielding a protein and DNA purity close to threshold values in licensed VLP-based vaccine formulations [6]. Both anion-exchange chromatography and size-exclusion chromatography currently are the methods of choice for the purification of numerous viral or VLP-based vaccines and vaccine candidates [61, 62, 63, 64]. Thus, an industrially common downstream process setup was developed for the processing of VP1 capsomeres.

4 Conclusion

Generating high numbers of vaccine doses in short time and at low cost remains the main challenge for the vaccine industry, especially in the light of pandemic threats and arising pathogens. VLPs represent promising nanocarriers for antigen epitopes of pathogens, but still lack straightforward and easily controllable upstream and downstream procedures.

In this study, we aimed at optimizing both expression and purification methods of the murine polyoma VLP platform by using a high-throughput screening procedure for micro-scale upstream process development and product analysis. A novel insert and expression system was designed and used to produce up to 1.63 mg/mL \pm 0.13 mg/mL VP1. The highest product titers were obtained at a high temperature (37 °C), a low oxygen supply at 600 rpm shaker speed, and a acid pH of 6. To the best of our knowledge, this exceeds all reported VLP yields achieved in shaker flask cultivations so far. In general, the micro-scale cultivations suggested that induced stress during cell growth and product formation (e.g. by oxygen limitation or acidic pH) is beneficial for high titers of soluble product. The main parameter was identified to be the oxygen supply that needed to be low to ensure fermenting conditions.

For proof of concept, VP1 derived from 2.5 L shaker flask cultivations was purified by a simple two-step downstream process and finally assembled into homogeneous, spherical particles. The produced VLPs constitute an ideal potential carrier platform for the presentation of antigen epitopes, packaging of small molecules, DNA or as a model nanoparticle or viral system. The microbial murine polyoma VLP platform has been advanced significantly towards an industrially feasible option for tailored vaccines. Future research should now focus on applying the optimized process conditions to the production and clinical evaluation of novel chimeric VLP constructs.

Acknowledgments

The authors would like to acknowledge the financial support by the German Federal Ministry of Education and Research (BMBF) - funding codes 0316071B & 0315640B- and general support by Kimberly D. Erickson and Professor Robert Garcea (University of Colorado, Boulder, CO, USA), Centic Biotec (Germany) and m2p-Labs (Germany). This research work is part of the projects 'Optimization of an industrial process for the production of cell-culture-based seasonal and pandemic influenza vaccines' and 'ERA Net Euro Trans Bio - 6: Development of an integrated strategy for a high-throughput process development platform on a micro-scale format - FORECAST'. The authors bear the complete responsibility for the content of this publication. The authors declare no conflict of interest.

References

- [1] R. L. Garcea, L. Gissmann, Virus-like particles as vaccines and vessels for the delivery of small molecules., *Curr. Opin. Biotechnol.* 15 (6) (2004) 513–7.
- [2] G. T. Jennings, M. F. Bachmann, The coming age of virus-like particle vaccines., *Biol. Chem.* 389 (5) (2008) 521–536.
- [3] N. Kushnir, S. J. Streatfield, V. Yusibov, Virus-like particles as a highly efficient vaccine platform: diversity of targets and production systems and advances in clinical development., *Vaccine* 31 (1) (2012) 58–83.
- [4] M. F. Bachmann, P. Whitehead, Active immunotherapy for chronic diseases., *Vaccine* 31 (14) (2013) 1777–84.
- [5] World Health Organization, Guidelines on the quality, safety and efficacy of recombinant malaria vaccines targeting the pre-erythrocytic and blood stages of *Plasmodium falciparum*. (2014).
- [6] C. Ladd Effio, J. Hubbuch, Next generation vaccines and vectors: Designing downstream processes for recombinant protein based virus-like particles., *Biotechnol. J.* 10 (5) (2015) 715–27.
- [7] L. H. L. Lua, N. K. Connors, F. Sainsbury, Y. P. Chuan, N. Wibowo, A. P. J. Middelberg, Bioengineering virus-like particles as vaccines., *Biotechnol. Bioeng.* 111 (3) (2014) 425–40.
- [8] J. R. Swartz, Advances in *Escherichia coli* production of therapeutic proteins., *Curr. Opin. Biotechnol.* 12 (2001) 195–201.
- [9] T. K. Joergensen, L. H. Bagger, J. Christiansen, G. H. Johnsen, J. R. Faarbaek, L. Joergensen, B. S. Welinder, Quantifying biosynthetic human growth hormone in *Escherichia coli* with capillary electrophoresis under hydrophobic conditions., *J. Chromatogr. A* 817 (1998) 205–214.
- [10] D. C. Andersen, L. Krummen, Recombinant protein expression for therapeutic applications., *Curr. Opin. Biotechnol.* 13 (2002) 117–123.
- [11] X. Zhang, M. Wei, H. Pan, Z. Lin, K. Wang, Z. Weng, Y. Zhu, L. Xin, J. Zhang, S. Li, N. Xia, Q. Zhao, Energetic changes caused by antigenic module insertion in a virus-like particle revealed by experiment and molecular dynamics simulations., *Vaccine* 32 (2014) 4039–50.

- [12] V. I. Tishkov, A. G. Galkin, V. V. Fedorchuk, P. A. Savitsky, A. M. Rojkova, H. Gieren, M. R. Kula, Pilot scale production and isolation of recombinant NAD⁺- and NADP⁺-specific formate dehydrogenases., *Biotechnol. Bioeng.* (1999) 187–193.
- [13] M.-E. Riviere, A. Caputo, N. Laurent, I. Vostiar, N. Andreasen, S. Cohen, R. W. Kressig, J. M. Ryan, A. Graf, Active Ab Immunotherapy Cad106 Phase II Dose-Adjuvant Finding Study: Immune Response., *Alzheimers Dement* 10 (2014) 447–448.
- [14] W. Fiers, M. De Filette, K. El Bakkouri, B. Schepens, K. Roose, M. Schotsaert, A. Birkett, X. Saelens, M2e-based universal influenza A vaccine., *Vaccine* 27 (2009) 6280–3.
- [15] J. Vekemans, A. Leach, J. Cohen, Development of the RTS,S/AS malaria candidate vaccine., *Vaccine* 27 Suppl 6 (2009) G67–71.
- [16] A. Bouchie, GSK plows ahead with EMA malaria vaccine submission., *Nat. Biotechnol.* 31 (2013) 1066.
- [17] D. C. Whitacre, B. O. Lee, D. R. Milich, Use of hepadnavirus core proteins as vaccine platforms., *Expert Rev Vaccines* 8 (11) (2010) 1565–1573.
- [18] M. Baz, Y. Abed, C. Savard, C. Pare, C. Lopez, G. Boivin, D. Leclerc, Development of a universal influenza A vaccine based on the M2e peptide fused to the papaya mosaic virus (PapMV) vaccine platform., *Vaccine* 26 (2008) 3395–3403.
- [19] A. P. J. Middelberg, T. Rivera-Hernandez, N. Wibowo, L. H. L. Lua, Y. Fan, G. Magor, C. Chang, Y. P. Chuan, M. F. Good, M. R. Batzloff, A microbial platform for rapid and low-cost virus-like particle and capsomere vaccines., *Vaccine* 29 (41) (2011) 7154–62.
- [20] N. Wibowo, Y. P. Chuan, L. H. Lua, A. P. Middelberg, Modular engineering of a microbially-produced viral capsomere vaccine for influenza., *Chem. Eng. Sci.* 103 (2013) 12–20.
- [21] M. R. Anggraeni, N. K. Connors, Y. Wu, Y. P. Chuan, L. H. L. Lua, A. P. J. Middelberg, Sensitivity of immune response quality to influenza helix 190 antigen structure displayed on a modular virus-like particle., *Vaccine* 31 (2013) 4428–35.
- [22] T. Rivera-Hernandez, J. Hartas, Y. Wu, Y. P. Chuan, L. H. L. Lua, M. Good, M. R. Batzloff, A. P. J. Middelberg, Self-adjuvanting modular virus-like particles for mucosal vaccination against group A streptococcus (GAS)., *Vaccine* 31 (2013) 1950–5.
- [23] Y. P. Chuan, T. Rivera-Hernandez, N. Wibowo, N. K. Connors, Y. Wu, F. K. Hughes, L. H. L. Lua, A. P. J. Middelberg, Effects of pre-existing anti-carrier immunity and antigenic element multiplicity on efficacy of a modular virus-like particle vaccine., *Biotechnol. Bioeng.* 110 (2013) 2343–51.
- [24] K. Tegerstedt, A. Franzén, T. Ramqvist, T. Dalianis, Dendritic cells loaded with polyomavirus VP1/VP2Her2 virus-like particles efficiently prevent outgrowth of a Her2 / neu expressing tumor., *Cancer Immunol Immunother* 56 (2007) 1335–1344.
- [25] M. Eriksson, K. Andreasson, J. Weidmann, K. Lundberg, K. Tegerstedt, Murine Polyomavirus Virus-Like Particles Carrying Full- Length Human PSA Protect BALB / c Mice from Outgrowth of a PSA Expressing Tumor., *PLoS One* 6 (8).

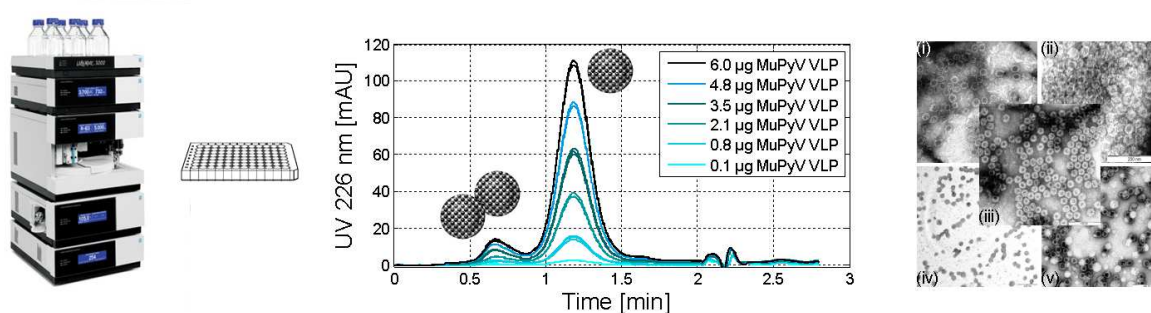
-
- [26] K. Tegerstedt, A. V. Franzén, K. Andreasson, J. Joneberg, S. Heidari, T. Ramqvist, T. Dalianis, Murine polyomavirus virus-like particles (VLPs) as vectors for gene and immune therapy and vaccines against viral infections and cancer., *Anticancer Res.* 25 (2005) 2601–8.
- [27] D. I. Lipin, Y. P. Chuan, L. H. L. Lua, A. P. J. Middelberg, Encapsulation of DNA and non-viral protein changes the structure of murine polyomavirus virus-like particles., *Arch. Virol.* 153 (2008) 2027–39.
- [28] D. I. Lipin, L. H. L. Lua, A. P. J. Middelberg, Quaternary size distribution of soluble aggregates of glutathione-S-transferase-purified viral protein as determined by asymmetrical flow field flow fractionation and dynamic light scattering., *J. Chromatogr. A* 1190 (2008) 204–14.
- [29] M. E. Kimple, J. Sondek, Overview of affinity tags for protein purification., *Curr Protoc Protein Sci* (2004) 9–9.
- [30] Y. P. Chuan, L. H. L. Lua, A. P. J. Middelberg, High-level expression of soluble viral structural protein in *Escherichia coli*., *J. Biotechnol.* 134 (1-2) (2008) 64–71.
- [31] N. K. Connors, Y. Wu, L. H. Lua, A. P. Middelberg, Improved fusion tag cleavage strategies in the downstream processing of self-assembling virus-like particle vaccines., *Food Bioprod. Process.* 92 (2014) 143–151.
- [32] A. Schaller, N. K. Connors, S. A. Oelmeier, J. Hubbuch, A. P. Middelberg, Predicting recombinant protein expression Experiments using molecular Dynamics simulation., *Chem. Eng. Sci.* 121 (2014) 340–350.
- [33] J. I. Betts, F. Baganz, Miniature bioreactors: current practices and future opportunities., *Microb. Cell Fact.* 5 (21) (2006) 1–14.
- [34] J. Altenbach-Rehm, C. Nell, M. Arnold, D. Weuster-Botz, Parallel Bubble Columns with Fed-Batch Technique for Microbial Process Development on a Small Scale., *Chem Eng Technol* 22 (12) (1999) 1051–1058.
- [35] R. Puskeiler, K. Kaufmann, D. Weuster-Botz, Development, parallelization, and automation of a gas-inducing milliliter-scale bioreactor for high-throughput bioprocess design (HTBD)., *Biotechnol. Bioeng.* 89 (5) (2005) 512–23.
- [36] S. Rameez, S. S. Mostafa, C. Miller, A. A. Shukla, High-Throughput Miniaturized Bioreactors for Cell Culture Process Development: Reproducibility, Scalability, and Control., *Biotechnol. Prog.* 30 (2011) 497–505.
- [37] K. Kottmeiner, J. Weber, C. Mueller, T. Bley, J. Buechs, Asymmetric Division of *Hansenula polymorpha* Reflected by a Drop of Light Scatter Intensity Measured in Batch Microtiter Plate Cultivations at Phosphate Limitation., *Biotechnol. Bioeng.* 104 (2009) 554–561.
- [38] R. Huber, S. Roth, N. Rahmen, J. Buechs, Utilizing highthroughput experimentation to enhance specific productivity of an *E.coli* T7 expression system by phosphate limitation., *BMC Biotechnol.* 22 (2011) 1–11.
- [39] M. Funke, S. Diederichs, F. Kensy, C. Mueller, J. Buechs, The Baffled Microtiter Plate : Increased Oxygen Transfer and Improved Online Monitoring in Small Scale Fermentations., *Biotechnol. Bioeng.* 103 (6) (2009) 1118–1128.

- [40] F. Kensy, C. Engelbrecht, J. Buechs, Scale-up from microtiter plate to laboratory fermenter: evaluation by online monitoring techniques of growth and protein expression in *Escherichia coli* and *Hansenula polymorpha* fermentations., *Microb. Cell Fact.* 68 (8) (2009) 1–15.
- [41] P. Baumann, N. Bluthardt, S. Renner, H. Burghardt, A. Osberhaus, J. Hubbuch, Integrated development of up- and downstream processes supported by the Cherry-Tag for real-time tracking of stability and solubility of proteins., *J. Biotechnol.* 200 (2015) 27–37.
- [42] A. D. Leavitt, T. M. Roberts, R. L. Garcea, Polyoma Virus Major Capsid Protein, VP1 - purification after high-level expression in *Escherichia coli*., *J. Biol. Chem.* 260 (23) (1985) 12803–12809.
- [43] m2p-Labs, Flower plate data sheet. (2013).
- [44] T. V. Kirk, N. Szita, Oxygen Transfer Characteristics of Miniaturized Bioreactor Systems., *Biotechnol. Bioeng.* 110 (4) (2013) 1005–1019.
- [45] R. Hermann, M. Lehmann, J. Büchs, Characterization of gas-liquid mass transfer phenomena in microtiter plates., *Biotechnol. Bioeng.* 81 (2) (2003) 178–86.
- [46] Life Technologies, NuPAGE Technical Guide. (2010).
- [47] Life Technologies, XCell II Blot Module - User Manual. (2009).
- [48] Perkin Elmer, HT Protein Express LabChip Kit, Version 2 LabChip GXII User Guide. (2012).
- [49] C. Ladd Effio, L. Wenger, O. Ötes, S. A. Oelmeier, J. Hubbuch, Downstream processing of virus-like particles: Single-stage and multi-stage aqueous two-phase extraction., *J. Chromatogr. A* 1383 (2015) 35–46.
- [50] A. Henaut, A. Danchin, Analysis and predictions from *Escherichia coli* sequences., American Society for Microbiology, Washington D.C., 1996, pp. 2047–2066.
- [51] D. Chen, D. E. Texada, Low-usage codons and rare codons of *Escherichia coli* Mini Review., *Gene Ther. Mol. Biol.* 10 (2006) 1–12.
- [52] Y. Nakamura, T. Gojobori, T. Ikemura, Codon usage tabulated from the international DNA sequence databases: status for the year 2000., *Nucleic Acids Res.* 27 (1999) 292.
- [53] M. Funke, A. Buchenauer, U. Schnakenberg, W. Mokwa, S. Diederichs, A. Mertens, C. Mueller, F. Kensy, J. Buechs, Microfluidic BioLector - Microfluidic Bioprocess Control in Microtiter Plates., *Biotechnol. Bioeng.* 107 (3) (2010) 497–505.
- [54] M. Losen, B. Frölich, M. Pohl, J. Büchs, Effect of oxygen limitation and medium composition on *Escherichia coli* fermentation in shake-flask cultures., *Biotechnol. Prog.* 20 (4) (2004) 1062–8.
- [55] M. W. O. Liew, A. Rajendran, A. P. J. Middelberg, Microbial production of virus-like particle vaccine protein at gram-per-litre levels., *J. Biotechnol.* 150 (2) (2010) 224–31.
- [56] E. Kopetzki, G. Schumacher, P. Buckel, Control of formation of active soluble or inactive insoluble baker’s yeast alpha-glucosidase PI in *Escherichia coli* by induction and growth conditions., *Mol. Gen. Genet.* 216 (1989) 149–155.

-
- [57] C. A. Galloway, M. P. Sowden, H. C. Smith, Increasing the yield of soluble recombinant protein expressed in *E. coli* by induction during late log phase., *Biotechniques* 34 (3) (2003) 524–526.
- [58] Y. Shirano, D. Shibata, Low temperature cultivation of *Escherichia coli* carrying a rice lipoxygenase L-2 cDNA produces a soluble and active enzyme at a high level., *FEBS Letters* 271 (1990) 128–130.
- [59] C. H. Schein, M. H. M. Noteborn, Formation of soluble recombinant proteins in *Escherichia coli* is favored by lower growth temperature., *Nat. Biotechnol.* 6 (1988) 291–294.
- [60] H. Ewers, A. E. Smith, I. F. Sbalzarini, H. Lilie, P. Koumoutsakos, A. Helenius, Single-particle tracking of murine polyoma virus-like particles on live cells and artificial membranes., *Proc. Natl. Acad. Sci. U. S. A.* 102 (2005) 1–6.
- [61] C. Peixoto, M. F. Q. Sousa, A. C. Silva, M. J. T. Carrondo, P. M. Alves, Downstream processing of triple layered rotavirus like particles., *J. Biotechnol.* 127 (2007) 452–61.
- [62] B. T. J. Hahn, D. Courbron, M. Hamer, M. Masoud, J. Wong, K. Taylor, J. Hatch, M. Sowers, E. Shane, M. Nathan, H. Jiang, Z. Wei, J. Higgins, K.-H. Roh, J. Burd, D. Chinchilla-Olszar, M. Malou-Williams, D. P. Baskind, G. E. Smith, Rapid Manufacture and Release of a GMP Batch of Avian Influenza A(H7N9) Virus-Like Particle Vaccine Made Using Recombinant Baculovirus-Sf9 Insect Cell Culture Technology., *Bioprocess. J.* 12 (2013) 1–10.
- [63] T. Kröber, M. W. Wolff, B. Hundt, A. Seidel-Morgenstern, U. Reichl, Continuous purification of influenza virus using simulated moving bed chromatography., *J. Chromatogr. A* 1307 (2013) 99–110.
- [64] J. M. Wagner, J. D. Pajerowski, C. L. Daniels, P. M. McHugh, J. A. Flynn, J. W. Balliet, D. R. Casimiro, S. Subramanian, Enhanced production of Chikungunya virus-like particles using a high-pH adapted *Spodoptera frugiperda* insect cell line., *PLoS One* 9.

High-throughput Characterization of Virus-like Particles by Interlaced Size-Exclusion Chromatography.

C. Ladd Effio¹, S. A. Oelmeier^{1,2} and J. Hubbuch^{1,*}



¹ : Institute of Process Engineering in Life Sciences, Section IV: Biomolecular Separation Engineering, Karlsruhe Institute of Technology, Engler-Bunte-Ring 1, 76131 Karlsruhe, Germany

² : Boehringer Ingelheim Pharma GmbH & Co. KG, Birkendorfer Str. 65, 88400 Biberach an der Riß, Germany

* : Corresponding author. *E-mail address:* juergen.hubbuch@kit.edu (J. Hubbuch)

Vaccine (2016), doi:10.1016/j.vaccine.2016.01.035

Abstract

The development and manufacturing of safe and effective vaccines relies essentially on the availability of robust and precise analytical techniques. Virus-like particles (VLPs) have emerged as an important and valuable class of vaccines for the containment of infectious diseases. VLPs are produced by recombinant protein expression followed by purification procedures to minimize the levels of process- and product-related impurities. Monitoring of these impurities is mandatory during process development and manufacturing. Especially the characterization and control of the VLP structure and dispersity are crucial issues for a safe and effective vaccine. Currently used methods require long analysis times and tailor-made assays. In this work, we present a size-exclusion ultra-high performance liquid chromatography (SE-UHPLC) method to characterize VLPs and quantify aggregates within 3.1 min per sample applying interlaced injections. Four analytical SEC columns were evaluated for the analysis of human B19 parvo-VLPs and murine polyoma-VLPs. The optimized method was successfully used for the characterization of five recombinant protein-based VLPs including human papillomavirus (HPV) VLPs, human enterovirus 71 (EV71) VLPs, and chimeric hepatitis B core antigen (HBcAg) VLPs pointing out the generic applicability of the assay. Measurements were supported by transmission electron microscopy and dynamic light scattering. It was demonstrated that the iSE-UHPLC method provides a rapid, precise and robust tool for the characterization of VLPs. Two case studies on purification tools for VLP aggregates and storage conditions of HPV VLPs highlight the relevance of the analytical method for high-throughput process development and process monitoring of virus-like particles.

Keywords: Virus-like particle vaccines, Size-exclusion HPLC, Papillomavirus, Aggregates, High-throughput analytics, Process Analytical Technology

1 Introduction

Control, prevention, and therapy of infectious diseases, cancer, and chronic diseases remain major challenges for our global health system. In recent years, novel promising vaccination and immunotherapy prospects for public health threats have been arising from the development of virus-like particles (VLPs). VLPs are protein assemblages which are produced by recombinant expression of viral structural proteins in prokaryotic or eukaryotic cells [1, 2]. Thus, the structure and morphology of highly pathogenic viruses such as HIV [3], Influenza, [4] and Ebola [5] can be mimicked or tailor-made nanocarriers for antigen epitopes can be designed. Such chimeric VLPs are especially interesting for the development of generic vaccine platforms [6], the prevention of malaria (RTS,S vaccine) [7], and the immunotherapy of cancer [8], chronic diseases [9], and Alzheimer's disease [10].

Due to the production in genetically modified expression hosts, the analysis of product-related and process-related impurities is crucial during development and manufacturing of VLP vaccines [11, 12]. Process-related impurities such as host cell proteins (HCPs), DNA, and endotoxins can be rapidly detected and assessed by methods standardized in the biopharmaceutical industry for therapeutic proteins and antibodies such as capillary electrophoresis, ELISA, real-time PCR, etc. [13]. In contrast, quantitative analysis of product-related impurities such as aggregates is more challenging and mostly tailor-made for each vaccine due to the large size and complexity of VLPs. Traditionally, VLP characterization is often done by transmission electron microscopy (TEM) requiring high investment costs, extensive sample and instrument preparation work, and specialized staff. In addition, sample preparations such as staining, coating on carbon grids, and drying might affect the VLP structure and dispersity. A faster and widely used technology for VLP characterization is dynamic light scattering (DLS) [14, 15, 16]. The method allows the determination of hydrodynamic particle diameters and particle dispersity by measuring the fluctuations of light scattering from particles in solution. However, DLS is less sensitive in resolving aggregates and VLPs [17]. Hence, quantitative VLP characterization is difficult to realize by both TEM and DLS. Currently used quantitative methods for VLP aggregates are asymmetrical flow field-flow fractionation (AF4) [18, 19, 17], disc centrifugation particle size analysis [20], electrospray differential mobility analysis [19], and size-exclusion chromatography (SEC) [21]. However, these techniques are very time-consuming with typical analysis times ranging from 30 to 60 min per sample [18, 19, 17, 21].

SEC is probably the most widely used technique for aggregate quantification in the biopharmaceutical industry [22]. SEC methods have been successfully applied for process monitoring during development phases of capsomere vaccines [23], recombinant fusion protein vaccines [16], human hepatitis B virus core antigen (HBcAg) VLPs [21], and human hepatitis B virus surface antigen (HBsAg) VLPs [24, 25, 26, 27]. In recent years, SEC columns and periphery equipment have been constantly developed moving towards smaller adsorber particle sizes and low-dispersion ultra-high performance liquid chromatography (UHPLC) instrumentation [28]. Rapid SE-UHPLC methods have been realized for monoclonal antibodies by performing interlaced sample injections instead of single injections with analysis times of 2-6 min [29, 30]. Fig.1 shows a schematic drawing of the principle of interlaced SEC (iSEC) methods. The 'information phase' (*green*) in a SEC run is the time range including the elution of relevant species (aggregates, monomer). The longest phase in a classical SEC method run (single injection) is the 'lag phase' (*blue*) in the beginning, which is the time range from injection to elution of the first species. The 'hold-up' (*blue*) phase refers to the time from the end of the information phase to the column's void time defined by the elution of small molecules such as salts. In order to reduce the total analysis time of SEC methods without changing the performance of 'information phases' the 'lag phase' can be eliminated by injecting subsequent samples prior to

the complete elution of previous sample components. This operation is referred to as interlaced injection mode.

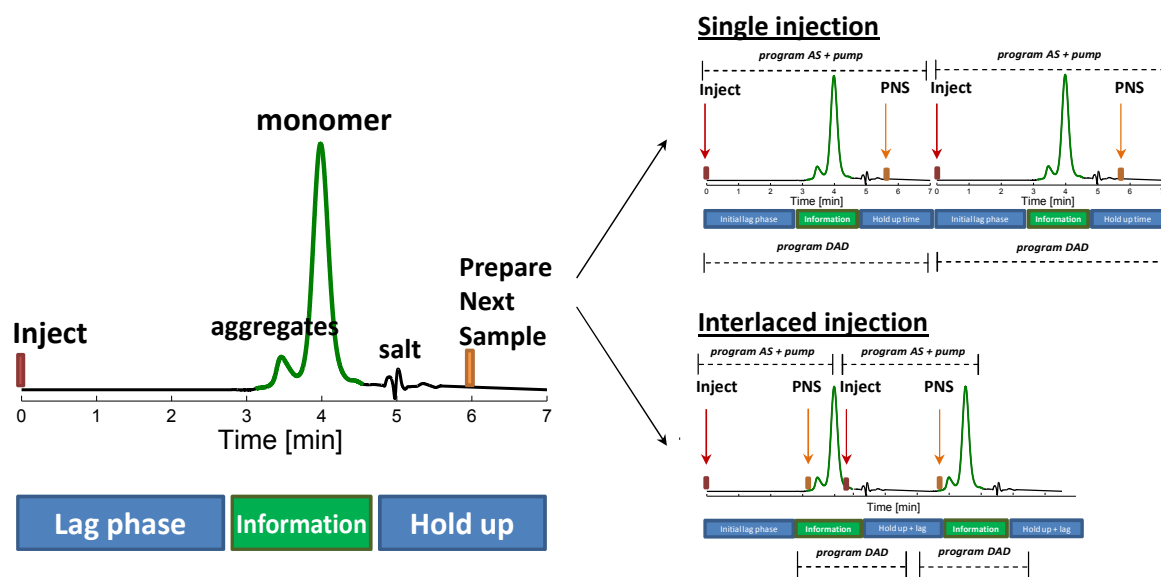


Figure 1 Schematic illustration of SEC chromatograms for single- and interlaced-injection mode of an analyte containing aggregates and monomer. Information phases are marked by green colored bars, lag and hold-up phases by blue colored bars. Timelines for the program of the autosampler (AS) and pump and the diode array detector (DAD) are presented for two sequent injections in single- and interlaced-injection mode.

In this work, we present the development and application of an iSE-UHPLC method for recombinant protein-based VLPs. The feasibility of the assay was evaluated for human papilloma (HPV) VLPs [31], human enterovirus 71 (EV71) VLPs [32], murine polyomavirus (MuPyV) VLPs [6], human B19 parvo (B19 VP1/VP2) VLPs [33], and chimeric HBcAg VLPs [8]. Two case studies are presented for the application of the iSE-UHPLC during downstream process development and stability studies. The designed method allows a rapid assessment of VLP dispersity and is well-suited for high-throughput pharmaceutical process development and process monitoring of VLPs in preclinical, clinical and postlicensing phases.

2 Materials & Methods

2.1 Disposables

For precipitation screenings, sample storage, fractionation by FPLC and UHPLC, 350 μ L-polypropylene plates (Greiner Bio-One, Kremsmünster, Austria) were used. Stability studies with HPV VLPs were performed in 1.5 mL-polypropylene Eppendorf[®] Safe-Lock Tubes (Eppendorf, Hamburg, Germany). Frozen VLPs were thawed and centrifuged in the same tubes at 18,000 x g and 4°C for 10 min. All buffer solutions were sterile filtered with 0.2 μ m cellulose acetate filters (Sartorius AG, Göttingen, Germany). Buffer exchange was performed with PD-10 desalting columns (GE Healthcare, Uppsala, Sweden).

2.2 Chemicals & Buffers

For the SE-UHPLC method, K_2HPO_4 was obtained from VWR BDH Prolabo (Radnor, Pennsylvania, USA). MOPS was purchased from Carl Roth GmbH& Co. KG (Karlsruhe, Germany). The SEC standard proteins thyroglobulin from bovine thyroid and uracil were purchased from Sigma-Aldrich (St. Louis, MO, USA) and Alfa Aesar (Ward Hill, MA, USA), respectively. All other chemicals were obtained from Merck KGaA (Darmstadt, Germany). All buffer solutions were prepared with ultra pure water drawn from a water purification system provided by Sartorius (Goettingen, Germany). UHPLC analysis was conducted with buffers composed of 0.2 M K_2HPO_4 and 0.25 M KCl. The pH value was set at pH 7.0 for characterization studies with HPV VLPs and pH 7.4 for the SEC analysis of other VLPs. Semi-preparative purifications of B19 VP1/VP2 VLPs were performed by aqueous two-phase extraction and precipitation with PEG 4000 as described previously [34] and by anion-exchange membrane chromatography [35]. PBS buffer at pH 7.4 was used as mobile-phase buffer for chromatography experiments with a semi-preparative SEC column. 0.2 M K_2HPO_4 pH 7 with 0-0.5 M KCl and 0.2 M MOPS pH 7 with 0-0.5 M NaCl were used to evaluate the stability of HPV VLPs at varying ionic strengths.

2.3 Virus-like Particles

The general applicability of an interlaced SE-UHPLC method for VLP characterization was evaluated with several purified VLPs differing in size, morphology, expression hosts, and number of viral proteins. An overview of analyzed VLPs is given in Table 1.

Table 1 Overview of evaluated virus-like particles. BEVS/IC: baculovirus expression vector/ insect cell system; EV: enterovirus; HBV: hepatitis B virus; HPV: human papilloma virus; MuPyV: murine polyomavirus.

Virus	Family	Expression system	Recombinant protein	Diameter	Ref.
HPV	Papillomaviridae	<i>S. cerevisiae</i>	L1 (55 kDa)	40-60 nm	[42, 15]
MuPyV	Polyomaviridae	<i>E. coli</i>	VP1 (42 kDa)	40-50 nm	[6]
HBV	Hepadnaviridae	<i>E. coli</i>	core antigen (21 kDa)	30-34 nm	[50]
EV 71	Picornaviridae	BEVS/IC	VP1 (33 kDa), VP2 (28 kDa), VP3 (27 kDa), VP4 (8 kDa)	25-35 nm	[44, 51]
Parvovirus B19	Parvoviridae	BEVS/IC	VP1 (83 kDa), VP2 (58 kDa)	25-30 nm	[52, 33, 34]

HPV VLPs (HPV type 33 [31]) derived from yeast cells were kindly provided by Merck & Co (Kenilworth, NJ, USA) at a concentration of 0.8 mg/mL in a formulation buffer containing histidine and polysorbate 80 (pH 6.2). HPV VLPs were purified by several chromatography and filtration steps as reported by Cook et al. [36]. MuPyV VLPs were produced at shaker flask scale in *Escherichia coli* cells, purified using the GST affinity tag process published by Middelberg et al. [6], and dialyzed into PBS (pH 7.4) yielding a final concentration of 0.3 mg/mL. Human enterovirus 71 (EV71) VLPs derived from *Spodoptera frugiperda* Sf9 insect cells were

kindly supplied by Sentinext Therapeutics (Penang, Malaysia) in a Tris buffer (pH 7.5) at a concentration of 0.1 mg/mL. Chimeric HBcAg VLPs with fused tumor epitopes were expressed in *E.coli* and generously provided by BioNTech Protein Therapeutics (Mainz, Germany) in a Tris buffer (pH 7.2) at a concentration of 2.18 mg/mL. B19 VP1/VP2 VLPs were kindly provided by Diarect AG (Freiburg, Germany) at a concentration of 0.5 mg/mL. VLPs were produced in *Sf9* insect cells, purified by several ultracentrifugation steps and dialyzed into a phosphate buffer (pH 7.4). In general, VLPs were stored at -80°C and centrifuged ($18,000 \times g$, 4°C , 10 min) prior to analysis by SE-UHPLC, DLS or TEM. VLP concentrations were provided by the project partners or, in the case of MuPyV VLPs, were determined by measuring UV absorption at 280 nm and using the theoretical extinction coefficient for MuPyV VLP VP1 ($1.36 \text{ mL}/(\text{mg}\cdot\text{cm})$ [37]).

2.4 Size-Exclusion Ultra-High Performance Liquid Chromatography

SE-UHPLC analysis was performed on an UltiMate[®] 3000 RSLC x 2 Dual system provided by Thermo Fisher Scientific (Waltham, MA, USA). The UHPLC consisted of a HPG-3400RS pump module, a WPS-3000 autosampler, a TCC-3200 column oven, and a DAD3000 detector. System control and peak integration was done with the software Chromeleon[®] 6.80 (Thermo Fisher Scientific, Waltham, MA, USA). Sample injection was done by full-loop injection with a $20 \mu\text{L}$ sample loop, a $15 \mu\text{L}$ injection needle, and a $250 \mu\text{L}$ syringe. Samples were cooled in the autosampler at 8°C prior to column experiments which were performed at 25°C . UHPLC measurements were conducted in triplicates. The feasibility of a VLP aggregate separation by SEC was evaluated with B19 VP1/VP2 VLPs and MuPyV VLPs comparing four different columns: TSKGel G5000 PWxl [17] (Tosoh Bioscience, Stuttgart, Germany), TSKGel G6000 PWxl (Tosoh Bioscience, Stuttgart, Germany), ACQUITY UPLC Protein BEH450 (Waters Corporation, Milford, MA, USA), and SRT SEC-1000 (Sepax Technologies, Newark, DE, USA). An overview of column characteristics and applied flow rates is given in Table 2.

Table 2 Applied analytical size-exclusion chromatography columns for large biomolecules.

Column	Dimension	Particle size	Pore size	p_{max}	Flow rate
TSKGel G5000 PWxl	7.8 x 300 mm	$10\mu\text{m}$	1000 \AA	20 bar	100 cm/h (0.8 mL/min)
TSKGel G6000 PWxl	7.8 x 300 mm	$13\mu\text{m}$	$>1000 \text{ \AA}$	20 bar	100 cm/h (0.8 mL/min)
ACQUITY UPLC BEH450	4.6 x 150 mm	$2.5\mu\text{m}$	450 \AA	310 bar	144 cm/h (0.4 mL/min)
SRT SEC-1000	4.6 x 300 mm	$5\mu\text{m}$	1000 \AA	241 bar	217-361 cm/h (0.6-1 mL/min)

Interlaced SEC (iSEC) experiments were realized using the SRT SEC-1000 column at a flow rate of 0.8 mL/min by shifting the 'PrepareNextSample' ('PNS') and the 'Inject' commands of subsequent samples to earlier points in time (Fig.1). As explained in detail by Diederich et al. [30], the system was split in two virtual parts in order to record the information phase of each sample separately. In timebase I, settings for pump, autosampler, and column compartment were controlled, while timebase II controlled the DAD (Fig.1).

2.5 Dynamic Light Scattering

For comparison of iSE-UHPLC results, VLP samples were analyzed by dynamic light scattering (DLS) to determine the hydrodynamic diameter and the polydispersity index (PdI) of VLPs. DLS measurements were performed using a Malvern Zetasizer Nano ZSP (Malvern Instruments, Worcestershire, UK). The DLS-based aggregate content was determined by the volume distribution which assumes the presence of spherical particles. Measurements were performed in triplicates.

2.6 Transmission Electron Microscopy

Transmission electron microscopy (TEM) micrographs were taken on a Philips CM 200 FEG/ST transmission electron microscope at 200 kV from all VLP samples to visualize the VLP structure, dispersity, and morphology. The sample preparation procedure has been described earlier [34]. VLPs were coated onto carbon-coated grids, washed with ultra-pure water, and stained using 1% [w/w] uranyl acetate.

2.7 Purification Methods for Aggregate Removal

Size-exclusion chromatography and precipitation with polyethylene glycol (PEG) were evaluated as potential unit operations for the separation of B19 VP1/VP2 VLPs and VLP aggregates. An ÄKTA-purifier 10 fast protein liquid chromatography (FPLC) equipped with a pump module P-900, UV monitor (UV-900), a conductivity monitor, and a fraction collector Frac-950 (GE Healthcare, Uppsala, Sweden) was used for semi-preparative purifications of B19 VP1/VP2-VLPs. The software UNICORN 5.31 (GE Healthcare, Uppsala, Sweden) allowed the control of FPLC methods. B19 VP1/VP2 VLPs were isolated from *Sf9* insect cells by sonication and subsequent solid-liquid separation steps as described previously [34]. Initial purification was performed by anion-exchange (AEX) membrane chromatography using 3 mL Sartobind[®] Q membrane adsorbers provided by Sartorius AG (Goettingen, Germany). The method has recently been described by our group [35]. The majority of HCPs, baculoviruses, and DNA were separated by a bind-and-elute process with three salt steps (0.3 M NaCl (step I), 0.38 M NaCl (step II), and 1 M NaCl (step III)). 1 mL pre-purified VLPs (pooled fractions from AEX membrane step II) were finally injected on a Superose[®] 6 Increase 10/300 column (GE Healthcare, Uppsala, Sweden) at a flow rate of 38 cm/h (0.5 mL/min) to investigate the separation of VLP aggregates. Fractions were collected in 300 μ L 96-well plates and analyzed by iSE-UHPLC. Precipitation studies with polyethylene glycol (PEG) 4000 were conducted on a robotic liquid handling station. A Tecan Freedom EVO[®]200 system (Tecan, Crailsheim, Germany) was used as liquid handling platform and controlled using the software Evoware 2.3 (Tecan, Crailsheim, Germany). Liquid handling calibration, set-up, and the precipitation screening method were described earlier [38, 39]. In brief, 300 μ L systems with different PEG concentrations and constant VLP concentrations were prepared in 96-well plates in triplicates by mixing ultra pure water, a 40% [w/w] PEG 4000 stock solution, and pre-purified B19 VP1/VP2-VLPs. Systems were mixed on an orbital shaker, centrifuged, and supernatant samples were diluted four fold with PBS prior to analysis by iSE-UHPLC.

2.8 Stability Studies with HPV VLPs

The dispersity of HPV VLPs was assessed under several stress conditions to identify critical parameters which might trigger the formation of VLP aggregates. Chemical stress was applied by exchanging the buffer from the formulation buffer containing stabilizing agents to phosphate

and MOPS buffers with varying ionic strengths. Subsequently, buffer-exchanged VLPs were stored for 3 d at 8°C prior to analysis. Thermal stress was applied by incubating VLP samples on an orbital shaker at 300 rpm for 1-5 h at 40°C. Incubation at 1400 rpm, 15°C in 1.5 mL-polypropylene Eppendorf® Safe-Lock Tubes with a sample volume of 300 μ L was performed to trigger mechanical stress on VLPs. Freeze-thaw stress was applied by freezing the samples in 1.5 mL-polypropylene Eppendorf® Safe-Lock Tubes in liquid nitrogen and thawing them at 25°C. Prior to analysis, all VLP samples were centrifuged as described above.

3 Results & Discussion

3.1 Development of an Interlaced SEC-UHPLC Method

In the International Conference on Harmonization (ICH) guideline Q2 [40] on the validation of analytical procedures, it is suggested to verify among others the specificity, precision, linearity, and robustness of novel methods for biopharmaceutical products. The initial objective was therefore to identify an analytical column separating VLPs and VLP aggregates in order to develop a specific analytical method. A pre-selection of columns was done based on pore sizes (>300 Å) and published SEC studies with VLPs [24, 25, 26, 27]. Subsequently, column performances were compared by injecting B19 VP1/VP2 VLP and MuPyV VLP samples on the columns in single-injection mode. Fig. 2a shows an overlay of UV chromatograms derived from the analysis of 8 μ g B19 VP1/VP2 VLPs, while Fig. 2b displays the overlay of UV chromatograms for SEC runs with 3 μ g MuPyV VLPs. In each chromatogram, the UV absorption at 226 nm is plotted against the mobile-phase volume. Due to different column void volumes, the elution volumes of VLP components differ between the columns. The void volumes are 2.1 mL for the Acquity BEH 450 column (black solid line), 3.9 mL for the SRT 1000 column (blue solid line), 12.1 mL for the TSKgel G5000 PWxl column (black dotted line), and 12.3 mL for the TSKgel G6000 PWxl column (red dotted line). This implies a lower buffer consumption for SEC runs with Acquity and SRT columns than with TSKgel columns. Neglecting the UV peaks close to the void volumes, only the SRT 1000 column shows multiple peaks for the VLP samples: The elution of B19 VP1/VP2 VLPs is split into three peak groups with two minor and one major peak, while the elution of MuPyV VLPs reveals one minor and one major peak. Peak fractionation and analysis by SDS-PAGE evidenced the presence of major viral proteins in all three UV peaks of the B19 VP1/VP2 VLP sample and in the two UV peaks of MuPyV VLPs (data not shown). Moreover, the total peak areas in the SEC chromatograms generated with the SRT 1000 column are higher than in those generated with other columns. This suggests a higher recovery and less secondary interactions of VLP components with the SRT 1000 column matrix. The weaker performance of other evaluated columns was attributed to different base materials (methacrylate vs. silica) and pore sizes (450 Å vs. 1000 Å). It must be noted that both peak resolution and recovery might have been higher for all columns at lower flow rates. However, the main goal of this work was to develop a rapid analytical procedure for VLP aggregates.

In Fig. 2c, the elution of MuPyV VLPs is compared with the elution of a protein standard composed of thyroglobulin and uracil. The UV chromatogram of the MuPyV VLPs demonstrates that the major peak at 3.09 mL elutes prior to thyroglobulin (3.38 mL, 17 d.nm [41]) and thyroglobulin aggregates (3.22 mL) indicating a larger size for the MuPyV VLPs and B19 VP1/VP2 VLPs. Due to the highest selectivity and recovery, the SRT 1000 column was selected for all subsequent experiments. In the following, the impact of the mobile-phase flow was evaluated to test the robustness and to accelerate the method. Fig 2c shows the overlay of chromatograms generated with 2.1 μ g MuPyV VLPs at flow rates ranging from 217 to 361 cm/h

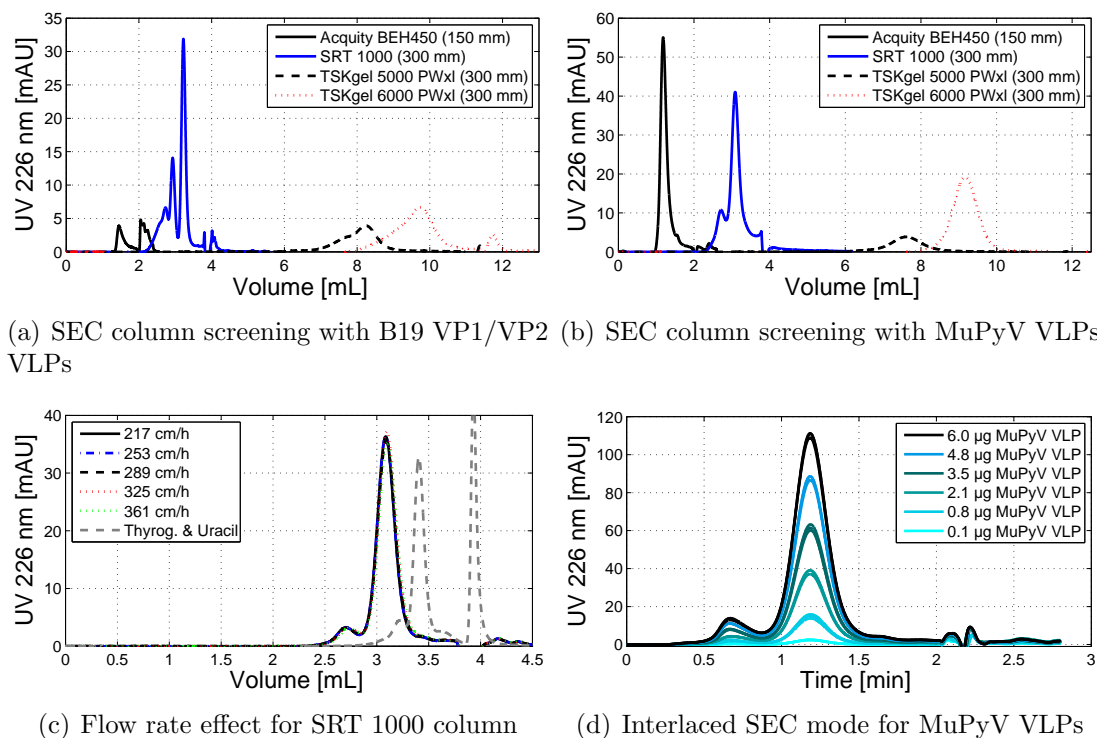


Figure 2 Development steps of an interlaced SE-UHPLC method for VLPs. Chromatograms represent the mean of triplicate determinations. a) Overlaid chromatograms of 8 μg human B19 parvo (B19 VP1/VP2) VLPs injected on an Acquity BEH450 (black solid line), SRT 1000 (blue solid line), TSKgel G5000 PWxl (black dotted line), and TSKgel G6000 PWxl column (red dotted line). b) Overlaid chromatograms of 3 μg murine polyomavirus (MuPyV) VLPs injected on an Acquity BEH450 (black solid line), SRT 1000 (blue solid line), TSKgel G5000 PWxl (black dotted line) and TSKgel G6000 PWxl column (red dotted line). c) Overlay of chromatograms of 2.1 μg MuPyV VLPs for an SRT 1000 column at varying flow rates. The elution profile of a protein standard composed of thyroglobulin and uracil is plotted as gray dotted line. d) Chromatogram of MuPyV VLPs injected on an SRT 1000 column in interlaced-injection mode at a flow rate of 0.8 mL/min. Increasing VLP masses were loaded on the column and are plotted in triplicates.

(0.6-1 mL/min). Chromatograms were hardly influenced by the flow rate in the examined range. This allows a high-throughput of samples even in single-injection mode. For the implementation of an iSEC method, an operating flow rate of 289 cm/h (0.8 mL/min) was chosen. The analysis time at this flow rate was 6.0 min with an initial lag phase of 3.1 min for MuPyV VLP aggregates and 2.7 min for B19 VP1/VP2 VLP aggregates. In the iSEC method, the start of timebase II (DAD) was triggered at 2.66 min of timebase I (autosampler and pump). At 0.34 min of timebase II, the injection of the next sample in timebase I was triggered. The 'PrepareNextSample' was set at 1.7 min of timebase I to ensure a total analysis time of 3.1 min per sample. Fig. 2d shows the chromatogram of overlaid triplicate injections of varying MuPyV VLP concentrations. The elution profile with two major peaks steadily increasing for higher loadings does not differ at all from the chromatograms generated by the single-injection mode. This underlines both repeatability and linearity of the iSEC method for the analysis of MuPyV VLPs. Furthermore, it is shown that the presence and ratio of the two major peaks do not depend on the injected VLP mass in the investigated range.

3.2 Characterization of Virus-like Particles by iSE-UHPLC, TEM & DLS

The developed iSEC method was evaluated for several VLPs in order to test the general applicability of the method. Moreover, an important issue was whether different peaks in iSEC chromatograms were created by VLPs of varying sizes or by VLPs of the same size forming VLP dimers or trimers. Therefore, samples were analyzed by iSE-UHPLC, TEM, and DLS. Fig. 3 shows an overview of iSE-UHPLC and TEM measurements for five different VLPs, while Table 3 lists the results obtained from DLS measurements.

Table 3 Summary of VLP characterization by dynamic light scattering (DLS) and interlaced SEC (iSEC) UHPLC. Retention times according to iSE-UHPLC are given for the elution of VLP monomers.

VLP/ Protein	Average size [d.nm]	PdI (DLS)	Aggregates (DLS) [% v/v]	Aggregates (iSEC) [%]	Retention time (iSEC) [min]
HPV VLP	60.8	0.134	0	5.8±0.2	0.93
MuPyV VLP	65.1	0.216	0	8.2±0.4	1.19
EV 71	55.9	0.204	0	14±3.0	1.2
HBcAg VLP	40.3	0.123	0	1.4±0.2	1.33
B19 VP1/VP2 VLP	211.1	0.467	51.5	55.8±0.5	1.42

The UV chromatograms in Fig. 3 are plotted against the measurement time of timebase II. In the following, only UV peaks with retention times below the iSEC retention time of thyroglobulin (1.56 min) are discussed. The chromatogram in Fig. 3a reveals two UV peaks for a sample containing 16 μg HPV VLPs, while the TEM micrograph displays spherical particles with pentamer structures and a total particle size of 45-60 nm. Similar particle diameters and structures were observed by Zhao et al. [42, 15] for HPV VLPs derived from yeast cells. In the TEM micrographs, there were not any VLPs detected with a size larger than 65 nm, while DLS analysis determined a mean particle size of 60.8 d.nm for HPV VLPs (Table 3). Hence, the first peak in the iSEC chromatogram (0.52 min) is probably attributed to the formation of VLP aggregates as reported by Deschuyteneer et al. [20]. The aggregate level in the HPV VLP sample was 5.8±0.2% according to the iSEC method, while no aggregates were detected by DLS measurements (Table 3). For MuPyV VLPs, the iSEC chromatogram in Fig. 3b looks similar as for HPV VLPs with one minor (0.68 min) and one major UV peak (1.19 min). Again, TEM micrographs display spherical particles with a similar morphology as HPV VLPs and particle sizes of 40-50 nm. The VLP aggregate level was 8.2±0.4% according to iSE-UHPLC. The presence of aggregates in MuPyV VLP preparations has also been reported by Pease et al. [19] and Mohr et al. [43]. Fig. 3c shows the iSEC chromatogram of 2.0 μg EV71 VLPs. The major peak elutes at 1.2 min. The UV absorption signal is noisy and very low with a maximum at 1.2 mAU demonstrating that observed peaks are close to the detection limit of the DAD. This impedes the exact quantification of VLP aggregates. Despite a low concentration, the presence of spherical particles in the EV71 VLP sample is demonstrated by the TEM micrograph. In contrast to other analyzed VLPs revealing empty particles, EV71 VLPs appeared as solid particles with diameters of 35-50 nm. A similar particle structure and morphology of EV71 VLPs was observed by Liu et al. [44]. According to DLS measurements, the average particle size for EV71 VLPs was 55.9 nm and no aggregates were detected. In Fig. 3d, the iSEC chromatogram and TEM micrograph of 50 μg chimeric HBcAg VLPs are displayed. The chromatogram shows

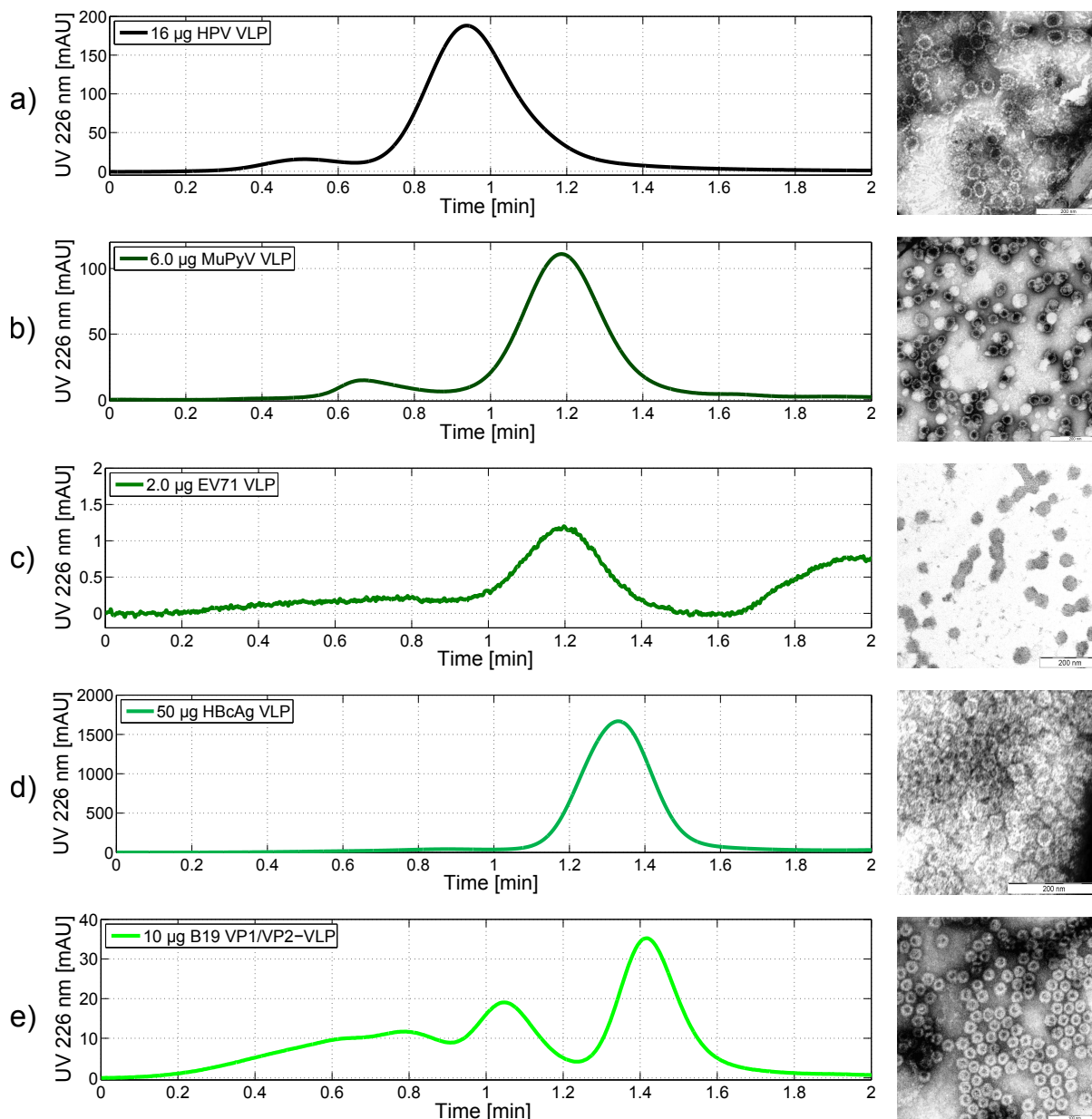


Figure 3 Characterization of virus-like particles by interlaced SE-UHPLC and transmission electron microscopy (TEM). Chromatograms and TEM micrographs are arranged according to decreasing particle sizes: a) 16 μg human papilloma (HPV) VLPs, b) 6.0 μg murine polyomavirus (MuPyV) VLPs, c) 2.0 μg human enterovirus 71 (EV71) VLPs, 50 μg chimeric HBcAg VLPs, and e) 10 μg human B19 parvo (B19 VP1/VP2) VLPs.

a uniform dispersity with one major peak eluting at 1.33 min. The TEM micrograph illustrates a high number of empty particles with diameters ranging from 35 to 40 nm. The mean particle diameter determined by DLS was 40.3 nm. The aggregate level according to the iSE-UHPLC method was $1.4 \pm 0.2\%$, while no aggregates were detected by DLS measurements. Fig. 3e displays the chromatogram of a sample containing 10 μg B19 VP1/VP2 VLPs. Three UV peaks eluting at 0.6 min, 1.04 min, and 1.42 min indicate a polydisperse distribution. In contrast, the TEM micrograph shows homogeneous icosahedral empty particles with a size of 25-30 nm. Con-

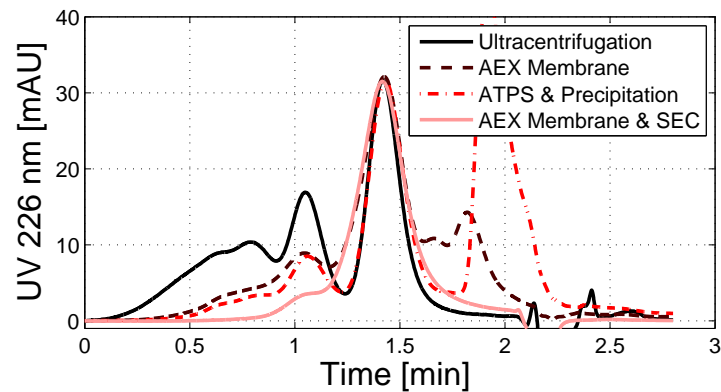
sidering the elution times of thyroglobulin (1.56 min, 17 d.nm [41]) and HPV VLPs (0.93 min, 60 d.nm), the UV peak at 1.42 min shows probably the elution of B19 VP1/VP2 VLPs while the other two peaks are attributed to VLP dimers (1.04 min) and larger VLP aggregates (0.6 min). Both DLS and iSE-UHPLC analysis evidence an aggregate level above 50% (Table 3). Such an unusually high amount of aggregates in B19 VP1/VP2 VLP samples has not yet been reported elsewhere. Since B19 VP1/VP2 VLPs are evaluated as human vaccine candidates against diseases attributed to parvovirus infections [33], the impact of aggregates on safety, immunogenicity and reactogenicity of a VLP vaccine should be carefully evaluated in the future. Skin reactions reported in a clinical phase study with a B19 VP1/VP2 VLP vaccine candidate [45] might have been attributed to increased levels of VLP aggregates.

Summarizing the VLP characterization by the developed iSE-UHPLC method, it could be demonstrated that a resolution of VLPs and VLP aggregates in the size range of 20-120 nm is feasible. Although the DLS results listed in Table 3 indicated the presence of aggregates in the B19 VP1/VP2 VLP sample, no aggregates were detected by the method for other VLP samples. Nevertheless, the polydispersity index (PdI) given by the DLS instrument correlates with the aggregate level determined by the iSEC method. The lowest PdI of 0.123 was determined for HBcAg VLPs containing 1.4% aggregates, while the highest PdI of 0.467 was identified for B19 VP1/VP2 VLPs containing 55.8% aggregates. Comparing results from DLS, TEM and iSE-UHPLC analysis, the iSEC method provides a precise and robust high-throughput analytical technique for VLPs.

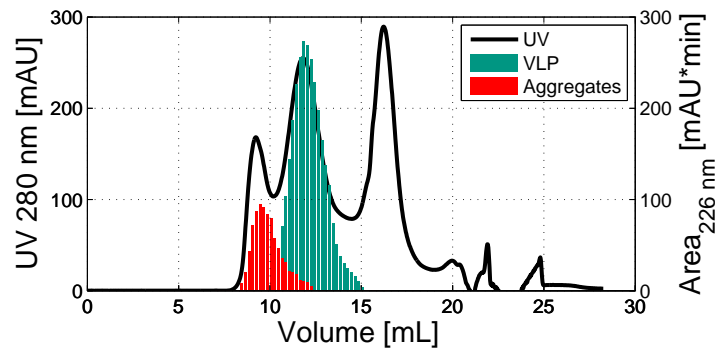
3.3 Purification Tools for the Separation of VLP Aggregates

In the following, the developed iSE-UHPLC method was applied for the assessment of VLP purification procedures. The characterization of VLPs has revealed the presence of aggregates in all measured VLP samples. The propensity of aggregate formation during VLP processing can be manipulated by adding stabilizers such as detergents, sugars or polyols into buffer solutions of purification and storage process chains [43, 46]. However, irreversible aggregates also form during expression in cell culture, and apart from stabilization procedures, there is a demand for separation techniques for VLP aggregates. In this work, the highest aggregate level was determined for B19 VP1/VP2 VLPs making these particles attractive to evaluate the effect of downstream processing on the aggregate level. Fig. 4a shows the iSEC chromatogram of the same VLP insect cell feedstock purified by different purification procedures. Chromatograms are normalized to the VLP monomer peak at 1.42 min to highlight varying aggregate levels. The residual DNA levels were below 20 ng/mL, and protein purities varied between 81% (AEX membrane sample [35]) and 99% (ultracentrifugation sample) according to measurements by picogreen assay and capillary gel electrophoresis (data not shown). The elution profiles demonstrate that peaks eluting between 0 and 1.2 min show the highest UV areas for VLPs purified by ultracentrifugation ($55.8\pm 0.5\%$) and the lowest for VLPs purified by a combination of AEX membrane chromatography and SEC [35] ($5.9\pm 0.4\%$). Moreover, VLP samples purified by an ATPS and precipitation procedure revealed a lower aggregate level ($27.5\pm 0.4\%$) than VLPs purified by AEX membrane chromatography ($30.7\pm 0.7\%$). These findings suggest that a separation of aggregates might be feasible by both chromatographic and non-chromatographic unit operations.

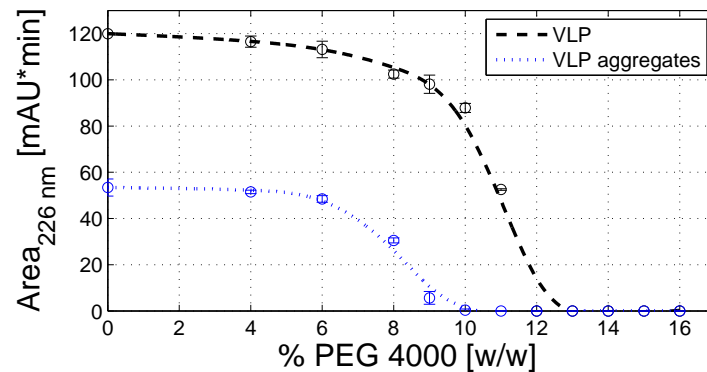
Fig. 4b shows the chromatogram of a VLP aggregate separation by size-exclusion chromatography on an FPLC system. 1500 μg B19 VP1/VP2 VLPs purified by AEX membrane chromatography were injected on a Superose[®] 6 Increase 10/300 column. VLP monomers (*green bars*) and VLP aggregates (*red bars*) were tracked by the iSE-UHPLC method. The elution profile displays three major peaks for the VLP sample: VLP aggregates (9.1 mL), VLP monomers



(a) UHPLC chromatograms for VLPs purified by different downstream processes



(b) Separation of VLP aggregates by SEC



(c) Separation of VLP aggregates by SEC

Figure 4 Comparison of purification tools for the separation of VLP aggregates from human B19 parvo (B19 VP1/VP2) VLPs. a) UHPLC chromatograms for VLPs purified by ultracentrifugation (black solid line), anion-exchange (AEX) membrane chromatography (purple dotted line), aqueous two-phase extraction (ATPS) and precipitation (red dotted line), and AEX membrane chromatography and SEC (rose solid line). b) Chromatogram of a B19 VP1/VP2 VLP polishing step on a Superose® 6 Increase column tracking VLPs (green bars) and VLP aggregates (red bars). c) Solubility curves for 0.5 mg/mL B19 VP1/VP2 VLPs tracking VLPs (black) and VLP aggregates (blue) at increasing concentrations of polyethylene glycol 4000.

(11.5 mL), and residual HCPs (16.4 mL). Hence, a separation of VLP aggregates was also rendered with a preparative SEC resin. In Fig. 4c, iSEC UV peak areas of VLP monomers (*black*

dotted line) and VLP aggregates (*blue spotted line*) are plotted against increasing concentrations of PEG 4000. Data points are interpolated with lines to guide the eye and represent the soluble fraction of each component at a certain PEG concentration. A decrease of solubility is observed at different PEG concentrations for VLP monomers and VLP aggregates. While VLP aggregates precipitated thoroughly at 10% [w/w] PEG 4000, about $81\pm 2\%$ VLP monomers were detected in the soluble fraction at this concentration. Thus, a separation of irreversible VLP aggregates might be realized by adding PEG to a VLP sample, performing a solid-liquid separation and finally formulating VLPs in a stabilizing buffer to prevent the formation of new aggregates. A similar approach has, for instance, been used for the separation of IgG aggregates by Giese et al. [47].

3.4 Effect of Process Conditions on the Stability of HPV VLPs

The propensity to form aggregates varies for each VLP depending on structural characteristics and process conditions such as pH, ionic strength, temperature, shear forces, freeze-thaw cycles or interactions with equipment surfaces. The developed iSEC-UHPLC method is a rapid assay to evaluate the effect of such process conditions on VLPs. In a case study, HPV VLPs with a comparably low level of aggregates ($5.8\pm 0.2\%$) were exposed to different stress conditions. Fig. 5 gives an overview of iSEC chromatograms for HPV VLPs subjected to chemical, thermal, mechanical and freeze-thaw stress conditions. Chromatograms were normalized to the VLP monomer peak to highlight changes in aggregate levels.

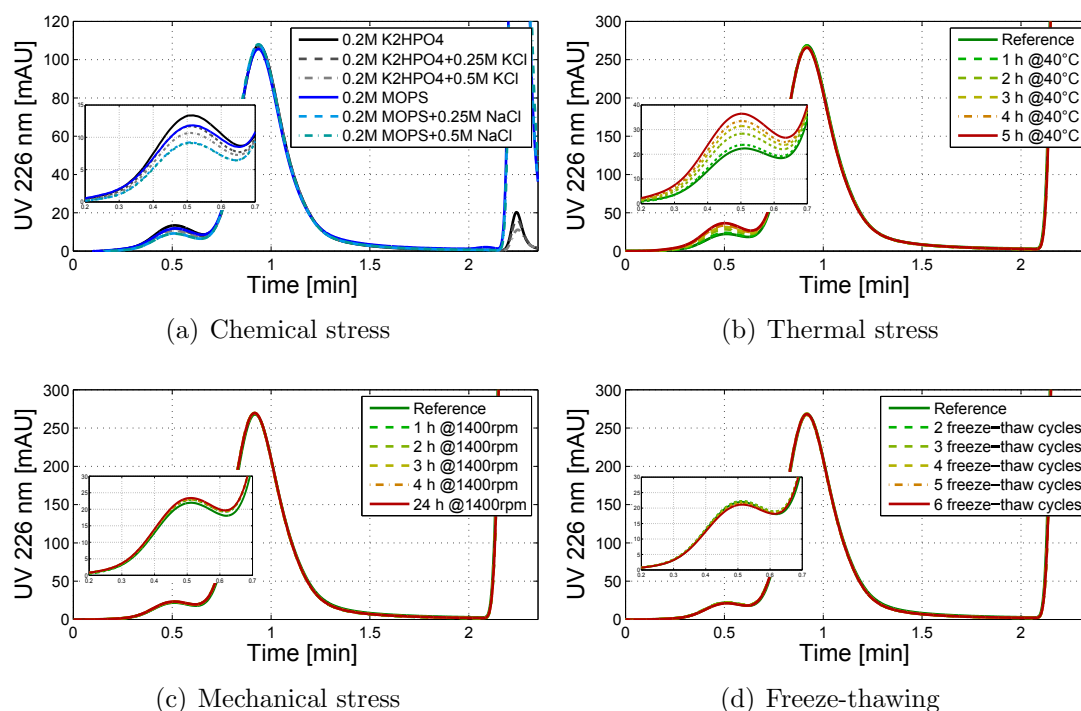


Figure 5 Characterization of human papilloma (HPV) VLPs under different stress conditions. a) The impact of ionic strength on the formation of aggregates was assessed by storing 0.4 mg/mL VLPs in different buffer solutions for 3 d at 8°C. b) Thermal stress was applied by heating 0.8 mg/mL VLPs at 40°C for 1-5 h. c) Mechanical stress was applied by incubating 0.8 mg/mL VLPs on an orbital shaker at 1400 rpm for 1-24 h. d) Stress by freeze-thawing was applied by 2-6 cycles of freezing in liquid nitrogen with subsequent thawing at room temperature at a VLP concentration of 0.8 mg/mL. VLPs underwent the first freeze-thaw cycle upon sample preparation.

Fig. 5a depicts the impact of ionic strength and buffer components on the VLP aggregate level. VLPs that were buffer-exchanged and stored for three days in a phosphate buffer without additional neutral salt revealed the highest level of aggregates ($9.6\pm 0.2\%$), while the lowest aggregate level was observed for VLPs stored in 0.2 M MOPS with 0.5 M NaCl ($6.7\pm 0.2\%$). In general, there was a clear trend of a decrease in aggregate levels with increasing salt concentrations and with MOPS buffers instead of phosphate buffers. Both buffer components are usually used during purification of HPV VLPs by cation-exchange (CEX) chromatography and mixed-mode (MM) chromatography [36]. Fig. 5b shows the effect of exposure to an elevated temperature (40°C) on the formation of VLP aggregates. An increase in aggregate levels from $5.8\pm 0.2\%$ to $10.4\pm 0.3\%$ was observed after sample incubation for five hours at 40°C . Aggregate levels steadily increased with increasing heat exposure time. Thermal stability studies are especially important to assess risks arising due to interrupted cold chains or inadequate storage conditions. The obtained results demonstrate that the investigated stabilized and formulated HPV VLPs are prone to form aggregates when exposed to 40°C for more than one hour. In contrast, Fig. 5c and Fig. 5d indicate that mechanical stress such as intense mixing for up to 24 hours and numerous freeze-thaw cycles hardly change the dispersity of HPV VLPs in the used formulation buffer. Aggregate levels vary between $5.8\pm 0.2\%$ and $6.7\pm 0.2\%$. This confirms the findings of Shi et al. [14] identifying the non-ionic surfactant polysorbate 80 as stabilizer for HPV VLPs during freezing and reconstitution as well as mechanical stress conditions.

4 Conclusion & Outlook

In this work, we report the development and application of a high-throughput analytical tool for the characterization of virus-like particles. Recently, the relevance of SE-HPLC methods for viral vaccines has been highlighted by Yang et al. [21]. Using a low-dispersion UHPLC system, we identified an SRT 1000 column as optimal SEC column for quantification of VLP aggregates at low buffer consumption and high flow rates. The implementation of an interlaced SE-UHPLC procedure allowed the characterization of VLPs within 3.1 min. To the best of our knowledge, this represents the fastest so far reported method for the quantification of VLP aggregates. The feasibility of the assay was proven for a variety of VLPs with total particle sizes ranging from 20 to 120 d.nm. The VLP characterization by the iSEC method was supported and complemented by TEM and DLS measurements. In two case studies applying the assay, we demonstrated how aggregate levels are manipulated by both downstream processing and storage of VLPs. Promising conditions for aggregate removal by precipitation with polyethylene glycol were determined applying high-throughput experimentation on a robotic liquid-handling station. The developed analytical method enables rapid assessment of suitable purification and formulation procedures for VLPs. Future studies should focus on evaluating the impact of VLP aggregates on product quality attributes. In order to ensure both safety and immunogenicity of VLP vaccines, it will be important to specify acceptable and alarm limits for VLP aggregates, identify critical process parameters (ICH Q7 [48]), and define design spaces for production processes (ICH Q8 [49]). A well-suited process analytical technique for this purpose has been presented herein.

Acknowledgements

The authors gratefully acknowledge material supply by **Diarect AG**, **Merck & Co**, **Sentinx Therapeutics**, **BioNTech Protein Therapeutics**, **Tosoh Bioscience** and financial support from the **German Federal Ministry of Education and Research** (Grant agreement

0315640B). In addition, we would like to thank Mohammad Fotouhi from the KIT Laboratory for Electron Microscopy for acquisition of TEM micrographs, Thiemo Huuk for his support regarding UHPLC methods, Ozan Ötes for performing part of the experimental work, and Mike Kosinski (Merck & Co), Fiona K. Hughes, Nani Wibowo and Anton Middelberg (The University of Queensland) for their support regarding VLP handling and technology transfer. This research work is part of the project 'Optimization of an industrial process for the production of cell-culture-based seasonal and pandemic influenza vaccines'. The authors declare no conflict of interest.

References

- [1] A. Zeltins, Construction and characterization of virus-like particles: a review., *Mol. Biotechnol.* 53 (1) (2013) 92–107. doi:10.1007/s12033-012-9598-4.
- [2] L. H. L. Lua, N. K. Connors, F. Sainsbury, Y. P. Chuan, N. Wibowo, A. P. J. Middelberg, Bioengineering virus-like particles as vaccines., *Biotechnol. Bioeng.* 111 (3) (2014) 425–40. doi:10.1002/bit.25159.
- [3] L. Buonaguro, M. Tagliamonte, M. L. Visciano, H. Andersen, M. Lewis, R. Pal, M. L. Tornesello, U. Schroeder, J. Hinkula, B. Wahren, F. M. Buonaguro, Immunogenicity of HIV virus-like particles in rhesus macaques by intranasal administration., *Clin. Vaccine Immunol.* 19 (6) (2012) 970–3. doi:10.1128/CVI.00068-12.
- [4] J. G. H. Low, L. S. Lee, E. E. Ooi, K. Ethirajulu, P. Yeo, A. Matter, J. E. Connolly, D. a. G. Skibinski, P. Saudan, M. Bachmann, B. J. Hanson, Q. Lu, S. Maurer-Stroh, S. Lim, V. Novotny-Diermayr, Safety and immunogenicity of a virus-like particle pandemic influenza A (H1N1) 2009 vaccine: results from a double-blinded, randomized Phase I clinical trial in healthy Asian volunteers., *Vaccine* 32 (39) (2014) 5041–8. doi:10.1016/j.vaccine.2014.07.011.
- [5] Y. Sun, R. Carrion, L. Ye, Z. Wen, Y.-T. Ro, K. Brasky, A. E. Ticer, E. E. Schwegler, J. L. Patterson, R. W. Compans, C. Yang, Protection against lethal challenge by Ebola virus-like particles produced in insect cells., *Virology* 383 (2009) 12–21. doi:10.1016/j.virol.2008.09.020.
- [6] A. P. J. Middelberg, T. Rivera-Hernandez, N. Wibowo, L. H. L. Lua, Y. Fan, G. Magor, C. Chang, Y. P. Chuan, M. F. Good, M. R. Batzloff, A microbial platform for rapid and low-cost virus-like particle and capsomere vaccines., *Vaccine* 29 (41) (2011) 7154–62. doi:10.1016/j.vaccine.2011.05.075.
- [7] J. Vekemans, A. Leach, J. Cohen, Development of the RTS,S/AS malaria candidate vaccine., *Vaccine* 27 Suppl 6 (2009) G67–71. doi:10.1016/j.vaccine.2009.10.013.
- [8] T. Klamp, J. Schumacher, G. Huber, C. Kühne, U. Meissner, A. Selmi, T. Hiller, S. Kreiter, J. Markl, O. Türeci, U. Sahin, Highly specific auto-antibodies against claudin-18 isoform 2 induced by a chimeric HBcAg virus-like particle vaccine kill tumor cells and inhibit the growth of lung metastases., *Cancer Res.* 71 (2) (2011) 516–27. doi:10.1158/0008-5472.CAN-10-2292.
- [9] M. F. Bachmann, P. Whitehead, Active immunotherapy for chronic diseases., *Vaccine* 31 (14) (2013) 1777–84. doi:10.1016/j.vaccine.2013.02.001.

-
- [10] B. Chackerian, Virus-like particle based vaccines for Alzheimer disease, *Hum. Vaccin.* 6 (11) (2010) 926–930. doi:10.4161/hv.6.11.12655.
- [11] B. Metz, G. van den Dobbelsteen, C. van Els, J. van der Gun, L. Levels, L. van der Pol, N. Rots, G. Kersten, Quality-control issues and approaches in vaccine development., *Expert Rev. Vaccines* 8 (2009) 227–238. doi:10.1586/14760584.8.2.227.
- [12] C. Ladd Effio, J. Hubbuch, Next generation vaccines and vectors: Designing downstream processes for recombinant protein-based virus-like particles, *Biotechnol. J.* 10 (2015) 715–727. doi:10.1002/biot.201400392.
- [13] M. J. T. Carrondo, P. M. Alves, N. Carinhas, J. Glassey, F. Hesse, O. W. Merten, M. Micheletti, T. Noll, R. Oliveira, U. Reichl, A. Staby, A. P. Teixeira, H. Weichert, C. F. Mandenius, How can measurement, monitoring, modeling and control advance cell culture in industrial biotechnology?, *Biotechnol. J.* 7 (2012) 1522–1529. doi:10.1002/biot.201200226.
- [14] L. Shi, G. Sanyal, A. Ni, Z. Luo, S. Doshna, B. Wang, T. L. Graham, N. Wang, D. B. Volkin, Stabilization of human papillomavirus virus-like particles by non-ionic surfactants., *J. Pharm. Sci.* 94 (7) (2005) 1538–51. doi:10.1002/jps.20377.
- [15] Q. Zhao, M. J. Allen, Y. Wang, B. Wang, N. Wang, L. Shi, R. D. Sitrin, Disassembly and reassembly improves morphology and thermal stability of human papillomavirus type 16 virus-like particles., *Nanomedicine* 8 (2012) 1182–9. doi:10.1016/j.nano.2012.01.007.
- [16] Z. Yu, J. C. Reid, Y.-P. Yang, Utilizing dynamic light scattering as a process analytical technology for protein folding and aggregation monitoring in vaccine manufacturing., *J. Pharm. Sci.* 102 (2013) 4284–90. doi:10.1002/jps.23746.
- [17] R. Lang, G. Winter, L. Vogt, a. Zurcher, B. Dorigo, B. Schimmele, Rational design of a stable, freeze-dried virus-like particle-based vaccine formulation., *Drug Dev. Ind. Pharm.* 35 (2009) 83–97. doi:10.1080/03639040802192806.
- [18] A. Citkowicz, H. Petry, R. N. Harkins, O. Ast, L. Cashion, C. Goldmann, P. Bringmann, K. Plummer, B. R. Larsen, Characterization of virus-like particle assembly for DNA delivery using asymmetrical flow field-flow fractionation and light scattering, *Anal. Biochem.* 376 (2008) 163–172. doi:10.1016/j.ab.2008.02.011.
- [19] L. F. Pease, D. I. Lipin, D.-H. Tsai, M. R. Zachariah, L. H. L. Lua, M. J. Tarlov, A. P. J. Middelberg, Quantitative characterization of virus-like particles by asymmetrical flow field flow fractionation, electrospray differential mobility analysis, and transmission electron microscopy., *Biotechnol. Bioeng.* 102 (2009) 845–55. doi:10.1002/bit.22085.
- [20] M. Deschuyteneer, A. Elouahabi, D. Plainchamp, M. Plisnier, D. Soete, Y. Corazza, L. Lockman, S. Giannini, M. Deschamps, Molecular and structural characterization of the L1 virus-like particles that are used as vaccine antigens in CervarixTM, the AS04- adjuvanted HPV-16 and -18 cervical cancer vaccine, *Hum. Vaccin.* 6 (2010) 407–419. doi:10.4161/hv.6.5.11023.
- [21] Y. Yang, H. Li, Z. Li, Y. Zhang, S. Zhang, Y. Chen, M. Yu, G. Ma, Z. Su, Size-exclusion HPLC provides a simple, rapid, and versatile alternative method for quality control of vaccines by characterizing the assembly of antigens, *Vaccine* 33 (2015) 1143–1150. doi:10.1016/j.vaccine.2015.01.031.

- [22] S. Fekete, A. Beck, J.-L. Veuthey, D. Guillaume, Theory and practice of size exclusion chromatography for the analysis of protein aggregates., *J. Pharm. Biomed. Anal.* 101 (2014) 161–173. doi:10.1016/j.jpba.2014.04.011.
- [23] A. Tekewe, N. K. Connors, F. Sainsbury, N. Wibowo, L. H. Lua, A. P. Middelberg, A Rapid and Simple Screening Method to Identify Conditions for Enhanced Stability of Modular Vaccine Candidates, *Biochem. Eng. J.* 100 (2015) 50–58. doi:10.1016/j.bej.2015.04.004.
- [24] U. Schmidt, R. Rudolph, G. Böhm, Mechanism of assembly of recombinant murine polyomavirus-like particles., *J. Virol.* 74 (2000) 1658–62.
- [25] Y. Li, J. Bi, W. Zhou, Y. Huang, L. Sun, A.-P. Zeng, G. Ma, Z. Su, Characterization of the large size aggregation of Hepatitis B virus surface antigen (HBsAg) formed in ultrafiltration process, *Process Biochem.* 42 (3) (2007) 315–319. doi:10.1016/j.procbio.2006.08.016.
- [26] Y. Huang, J. Bi, Y. Zhang, W. Zhou, Y. Li, L. Zhao, Z. Su, A highly efficient integrated chromatographic procedure for the purification of recombinant hepatitis B surface antigen from *Hansenula polymorpha.*, *Protein Expr. Purif.* 56 (2007) 301–10. doi:10.1016/j.pep.2007.08.009.
- [27] M. Yu, S. Zhang, Y. Zhang, Y. Yang, G. Ma, Z. Su, Microcalorimetric study of adsorption and disassembling of virus-like particles on anion exchange chromatography media, *J. Chromatogr. A* 1388 (2015) 195–206. doi:10.1016/j.chroma.2015.02.048.
- [28] P. Hong, S. Koza, E. S. P. Bouvier, Size-Exclusion Chromatography for the Analysis of Protein Biotherapeutics and their Aggregates., *J. Liq. Chromatogr. Relat. Technol.* 35 (2012) 2923–2950. doi:10.1080/10826076.2012.743724.
- [29] D. Farnan, G. T. Moreno, J. Stults, A. Becker, G. Tremintin, M. van Gils, Interlaced size exclusion liquid chromatography of monoclonal antibodies, *J. Chromatogr. A* 1216 (2009) 8904–8909. doi:10.1016/j.chroma.2009.10.045.
- [30] P. Diederich, S. K. Hansen, S. a. Oelmeier, B. Stolzenberger, J. Hubbuch, A sub-two minutes method for monoclonal antibody-aggregate quantification using parallel interlaced size exclusion high performance liquid chromatography., *J. Chromatogr. A* 1218 (2011) 9010–8. doi:10.1016/j.chroma.2011.09.086.
- [31] K. Kim, S. Park, K. Ko, Current status of human papillomavirus vaccines, *Clin. Exp. Vaccine Res.* 3 (2014) 168–175. doi:10.7774/cevr.2014.3.2.168.
- [32] P.-Y. Lim, A. C. Hickey, M. F. Jamiluddin, S. Hamid, J. Kramer, R. Santos, K. N. Bossart, M. J. Cardoso, Immunogenicity and performance of an enterovirus 71 virus-like-particle vaccine in nonhuman primates, *Vaccine* (2015) 1–8doi:10.1016/j.vaccine.2015.05.108.
- [33] S. Chandramouli, A. Medina-Selby, D. Coit, M. Schaefer, T. Spencer, L. a. Brito, P. Zhang, G. Otten, C. W. Mandl, P. W. Mason, P. R. Dormitzer, E. C. Settembre, Generation of a parvovirus B19 vaccine candidate., *Vaccine* 31 (37) (2013) 3872–8. doi:10.1016/j.vaccine.2013.06.062.
- [34] C. Ladd Effio, L. Wenger, O. Ötes, S. a. Oelmeier, J. Hubbuch, Downstream processing of virus-like particles: Single-stage and multi-stage aqueous two-phase extraction, *J. Chromatogr. A* 1383 (2015) 35–46. doi:10.1016/j.chroma.2015.01.007.

-
- [35] C. Ladd Effio, T. Hahn, J. Seiler, S. A. Oelmeier, I. Asen, C. Silberer, L. Villain, J. Hubbuch, Modeling and simulation of anion-exchange membrane chromatography for purification of *Sf9* insect cell-derived virus-like particles., Manuscript submitted to J. Chromatogr. A.
- [36] J. C. Cook III, Process for purifying human papillomavirus virus-like particles, uS Patent 6,602,697 (Aug. 5 2003).
- [37] D. I. Lipin, Y. P. Chuan, L. H. L. Lua, a. P. J. Middelberg, Encapsulation of DNA and non-viral protein changes the structure of murine polyomavirus virus-like particles., Arch. Virol. 153 (11) (2008) 2027–39. doi:10.1007/s00705-008-0220-9.
- [38] M. Wiendahl, C. Völker, I. Husemann, J. Krarup, A. Staby, S. Scholl, J. Hubbuch, A novel method to evaluate protein solubility using a high throughput screening approach, Chem. Eng. Sci. 64 (2009) 3778–3788. doi:10.1016/j.ces.2009.05.029.
- [39] S. Oelmeier, C. Ladd-Effio, J. Hubbuch, Alternative separation steps for monoclonal antibody purification: Combination of centrifugal partitioning chromatography and precipitation, J. Chromatogr. A 1319 (2013) 118–126.
- [40] ICH Guideline Q2. Validation of analytical procedures: Text and methodology (1994).
- [41] H. P. Erickson, Size and shape of protein molecules at the nanometer level determined by sedimentation, gel filtration, and electron microscopy, Biol. Proced. Online 11 (1) (2009) 32–51. doi:10.1007/s12575-009-9008-x.
- [42] Q. Zhao, H. H. Guo, Y. Wang, M. W. Washabaugh, R. D. Sitrin, Visualization of discrete L1 oligomers in human papillomavirus 16 virus-like particles by gel electrophoresis with Coomassie staining., J. Virol. Methods 127 (2005) 133–40. doi:10.1016/j.jviromet.2005.03.015.
- [43] J. Mohr, Y. P. Chuan, Y. Wu, L. H. L. Lua, A. P. J. Middelberg, Virus-like particle formulation optimization by miniaturized high-throughput screening., Methods 60 (3) (2013) 248–56. doi:10.1016/j.ymeth.2013.04.019.
- [44] C.-C. Liu, M.-S. Guo, F. H.-Y. Lin, K.-N. Hsiao, K. H.-W. Chang, A.-H. Chou, Y.-C. Wang, Y.-C. Chen, C.-S. Yang, P. C.-S. Chong, Purification and characterization of enterovirus 71 viral particles produced from vero cells grown in a serum-free microcarrier bioreactor system., PLoS One 6. doi:10.1371/journal.pone.0020005.
- [45] D. I. Bernstein, H. M. El Sahly, W. a. Keitel, M. Wolff, G. Simone, C. Segawa, S. Wong, D. Shelly, N. S. Young, W. Dempsey, Safety and immunogenicity of a candidate parvovirus B19 vaccine., Vaccine 29 (43) (2011) 7357–63. doi:10.1016/j.vaccine.2011.07.080.
- [46] N. K. Jain, N. Sahni, O. S. Kumru, S. B. Joshi, D. B. Volkin, C. Russell Middaugh, Formulation and stabilization of recombinant protein based virus-like particle vaccines, Adv. Drug Deliv. Rev. doi:10.1016/j.addr.2014.10.023.
- [47] G. Giese, A. Myrold, J. Gorrell, J. Persson, Purification of antibodies by precipitating impurities using Polyethylene Glycol to enable a two chromatography step process., J. Chromatogr. B. Analyt. Technol. Biomed. Life Sci. 938 (2013) 14–21. doi:10.1016/j.jchromb.2013.08.029.
- [48] ICH Guideline Q7. Good manufacturing practice for active pharmaceutical ingredients. (2000).

3 PUBLICATIONS & MANUSCRIPTS

- [49] ICH Guideline Q8. Pharmaceutical development. (2006).
- [50] L. I. Karpenko, V. A. Ivanisenko, I. A. Pika, N. A. Chikaev, A. M. Eroshkin, T. A. Veremeiko, A. A. Ilyichev, Insertion of foreign epitopes in HBcAg : how to make the chimeric, *Amino Acids* 18 (2000) 329–337.
- [51] S.-Y. Lin, H.-Y. Chiu, B.-L. Chiang, Y.-C. Hu, Development of EV71 virus-like particle purification processes, *Vaccine* (2015) 1–8doi:10.1016/j.vaccine.2015.04.077.
- [52] B. Kaufmann, A. a. Simpson, M. G. Rossmann, The structure of human parvovirus B19., *Proc. Natl. Acad. Sci. U. S. A.* 101 (32) (2004) 11628–33. doi:10.1073/pnas.0402992101.

4 Conclusion & Outlook

Improving global access to biopharmaceutical drugs and vaccines and accelerating manufacturing processes in the light of pandemic threats represent major challenges for current technologies. This doctoral thesis was centered on developing economic, innovative and rapid process solutions for a novel molecular entity of vaccine, gene therapy and diagnostic products: virus-like particles (VLPs). Prospects, production routes and process bottlenecks of this class of large biomolecules were described. Based on these findings, different strategies were applied for development and optimization of VLP processes.

A key aspect of this thesis was the method development of aqueous two-phase extraction (ATPE) processes for purification of large biomolecules. For miniaturized process development a high-throughput screening (HTS) procedure combining ATPE and precipitation was designed. The novel HTS tool incorporated automated precipitation, solid-liquid separation and resolubilization steps on a robotic liquid handling station. Downstream processes for monoclonal antibodies (mAbs) and VLPs were successfully developed with the non-chromatographic HTS purification tool obtaining a high product recovery, capacity and purity. The HTS approach allowed the generation of a large dataset of ATPS phase diagrams and partitioning patterns that were effectively correlated with solubility curves of both target and contaminant components. Critical process parameters and optimal design spaces for ATPS partitioning of VLPs and mAbs were identified. Future studies should focus on transferring the results obtained in miniaturized batch systems to multi-stage and larger scale instruments. First experiments on multi-stage ATPE of mAbs and VLPs by centrifugal partition chromatography (CPC) revealed promising results regarding separation efficiency and product stability. However, for an industrially relevant process alternative, future work should focus on automating and miniaturizing multi-stage ATPE and modeling the mass transfer with hydrodynamic and thermodynamic approaches. Especially the establishment of a robust thermodynamic model will determine the industrial feasibility of ATPE complying with regulatory guidelines on deeper process understanding ('Quality by Design (QbD)'). The generation of ATPS data bases and further HTS systematization to user-friendly screening formats as in chromatography would additionally accelerate the ongoing trend towards industrial applications.

The relevance of HTS approaches for process development was also underlined in this thesis by the design of an alternative production process for VLPs. Application of HTS tools such as micro-scale cultivations, capillary gel electrophoresis and micro-scale cell lysis allowed a rapid optimization of the expression of the murine polyoma virus protein VP1 in *Escherichia coli*. The microbial upstream process allows a highly economic production of murine polyomavirus (MuPyV) VLPs. These VLPs have proved to be effective as chimeric vaccine platforms in multiple preclinical studies. Future research should focus on the development and clinical evaluation of tailored MuPyV VLP vaccine candidates based on the novel production process. Potential process deviations caused by fused antigenic epitopes will be rapidly adaptable by the developed HTS methods. In general, the applied HTS approaches for upstream and downstream processing were especially valuable for designing processes where no physical models exist.

In order to design a more chromatographic-like purification procedure for VLPs, an anion-exchange membrane process was developed using a hybrid approach of HTS methods and mechanistic modeling. Mass transfer in spiral wound membrane modules was simulated

by implementing a hydrodynamic model for radial flow. Modeling of electrostatic interactions during a VLP capture step from a complex insect cell lysate was realized by UV absorption-based modeling with scaled component specific parameters of the steric mass action (SMA) model. Therefore, the feedstock was divided into 17 component groups differing in AEX membrane elution behaviour. Subsequent to parameter estimation with automated algorithms, a design space for controlling and forecasting the elution of VLPs and impurities was developed. The *in silico* optimized process resulted in a high VLP purity and demonstrated the high convenience of the novel model approach for complex industrial feedstocks. However, drawbacks of the designed membrane process were the high product loss due to irreversible binding and the reduced process performance at higher flow rates. Future studies should consider the evaluation of novel membrane designs and ligands as well as tracking of conformational VLP changes during processing. Concerning VLP characterization, a novel HTS method based on size-exclusion ultra-high performance liquid chromatography (UHPLC) was established. The developed method allowed analysis of 20 samples per hour applying interlaced injections. Five different VLP vaccine candidates were successfully characterized with the method. The relevance of the novel tool as process analytical technique was highlighted by HTS case studies on the separation of VLPs and aggregates and the stability of human papilloma VLPs at varying stress conditions. The analytical procedure has the potential to become a novel, rapid and robust quality control assay for viral or VLP-based vaccines.

In conclusion, this doctoral thesis has enlarged the purification and process development toolbox for VLPs. The advanced methodologies for HTS- and model-based approaches will facilitate manufacturing of current and future VLP products. Prospective studies should focus on evaluating ATPE, precipitation and membrane chromatography for VLPs with varying epitopes and lipid envelopes. Both VLP structures will be highly important for future applications in gene therapy, cancer immunotherapy and vaccination.

References

- ADELMANN, S. and SCHEMBECKER, G. (2011). *Influence of physical properties and operating parameters on hydrodynamics in Centrifugal Partition Chromatography*. J. Chromatogr. A, 1218:5401.
- AL-MAHTAB, M., AKBAR, S. M. F., AGUILAR, J. C., UDDIN, M. H., KHAN, M. S. I. and RAHMAN, S. (2013). *Therapeutic potential of a combined hepatitis B virus surface and core antigen vaccine in patients with chronic hepatitis B*. Hepatol. Int., 7:981.
- ALBERTSSON, P. (1971). *Partition of cell particles and macromolecules: distribution and fractionation of cells, mitochondria, chloroplasts, viruses, proteins, nucleic acids, and antigen-antibody complexes in aqueous polymer two-phase systems*. Wiley-Interscience.
- ANDRE, F. (2002). *How the research-based industry approaches vaccine development and establishes priorities*. Developments in biologicals, 110:25.
- ANDREWS, B. A. and ASENJO, J. A. (2010). *Theoretical and Experimental Evaluation of Hydrophobicity of Proteins to Predict their Partitioning Behavior in Aqueous Two Phase Systems: A Review*. Sep. Sci. Technol., 45:2165.
- ANDREWS, B. A., SCHMIDT, A. S. and ASENJO, J. A. (2005). *Correlation for the partition behavior of proteins in aqueous two-phase systems: effect of surface hydrophobicity and charge*. Biotechnol. Bioeng., 90:380.
- ANGGRAENI, M. R., CONNORS, N. K., WU, Y., CHUAN, Y. P., LUA, L. H. L. and MIDDELBERG, A. P. J. (2013). *Sensitivity of immune response quality to influenza helix 190 antigen structure displayed on a modular virus-like particle*. Vaccine, 31:4428.
- ASENJO, J. A. (1994). *Model for predicting the partition behaviour of proteins in aqueous two-phase systems*. J. Chromatogr. A, 668:47.
- AZEVEDO, A. M., ROSA, P. A. J., FERREIRA, I. F. and AIRES-BARROS, M. R. (2008). *Integrated process for the purification of antibodies combining aqueous two-phase extraction, hydrophobic interaction chromatography and size-exclusion chromatography*. J. Chromatogr. A, 1213:154.
- BACHMANN, M. F. and WHITEHEAD, P. (2013). *Active immunotherapy for chronic diseases*. Vaccine, 31:1777.
- BAZ, M., ABED, Y., SAVARD, C., PARE, C., LOPEZ, C., BOIVIN, G. and LECLERC, D. (2008). *Development of a universal influenza A vaccine based on the M2e peptide fused to the papaya mosaic virus (PapMV) vaccine platform*. Vaccine, 26:3395.
- BERG, A., OELMEIER, S. A., KITTELMANN, J., DISMER, F. and HUBBUCH, J. (2012). *Development and characterization of an automated high throughput screening method for optimization of protein refolding processes*. J. Sep. Sci., 35:3149.

REFERENCES

- BERNSTEIN, D. I., EL SAHLY, H. M., KEITEL, W. A., WOLFF, M., SIMONE, G., SEGAWA, C., WONG, S., SHELLY, D., YOUNG, N. S. and DEMPSEY, W. (2011). *Safety and immunogenicity of a candidate parvovirus B19 vaccine*. *Vaccine*, 29:7357.
- BEZOLD, F., GOLL, J. and MINCEVA, M. (2015). *Study of the applicability of non-conventional aqueous two-phase systems in counter-current and centrifugal partition chromatography*. *J. Chromatogr. A*, 1388.
- BHAMBURE, R., KUMAR, K. and RATHORE, A. S. (2011). *High-throughput process development for biopharmaceutical drug substances*. *Trends Biotechnol.*, 29:127.
- BILLAUD, J.-N., PETERSON, D., BARR, M., SALLBERG, M., GARDUNO, F., GOLDSTEIN, P., MCDOWELL, W., HUGHES, J., JONES, J., CHEN, A. and MILICH, D. (2005). *Combinatorial Approach to Hepadnavirus-Like Particle Vaccine Design*. *J. Virol.*, 79:13656.
- BOUCHIE, A. (2013). *GSK plows ahead with EMA malaria vaccine submission*. *Nat. Biotechnol.*, 31:1066.
- BROOKS, C. A. and CRAMER, S. M. (1992). *Steric mass-action ion exchange: Displacement profiles and induced salt gradients*. *AIChE J.*, 38:1969.
- BRUNAUER, S., EMMETT, P. H. and TELLER, E. (1938). *Adsorption of gases in multimolecular layers*. *Journal of the American chemical society*, 60:309.
- BUILDER, S., HART, R., LESTER, P., OGEZ, J. and REIFSNYDER, D. (1995). *Aqueous multiple-phase isolation of polypeptide*. US Patent 5,407,810.
- CANTIN, G. T., RESNICK, S., JIN, H., O'HANLON, R., ESPINOSA, O., STEVENS, A., PAYNE, J., GLENN, N. R., RASOCHOVA, L. and ALLEN, J. R. (2011). *Comparison of Methods for Chemical Conjugation of an Influenza Peptide to Wild-Type and Cysteine-Mutant Virus-Like Particles Expressed in Pseudomonas fluorescens*. *Int. J. Pept. Res. Ther.*, 17:217.
- CERVERA, L., GUTIÉRREZ-GRANADOS, S., MARTÍNEZ, M., BLANCO, J., GÒDIA, F. and SEGURA, M. M. (2013). *Generation of HIV-1 Gag VLPs by transient transfection of HEK 293 suspension cell cultures using an optimized animal-derived component free medium*. *J. Biotechnol.*, 166:152.
- CHACKERIAN, B. (2010). *Virus-like particle based vaccines for Alzheimer disease*. *Hum. Vaccin.*, 6:926.
- CHANDRAMOULI, S., MEDINA-SELBY, A., COIT, D., SCHAEFER, M., SPENCER, T., BRITO, L. A., ZHANG, P., OTTEN, G., MANDL, C. W., MASON, P. W., DORMITZER, P. R. and SETTEMBRE, E. C. (2013). *Generation of a parvovirus B19 vaccine candidate*. *Vaccine*, 31:3872.
- CHEN, J., MA, G. X. and LI, D. Q. (1999). *Preparative Biochemistry and Biotechnology HPCPC Separation of Proteins using Polyethylene Glycol- Potassium Phosphate Aqueous Two-Phase*. *Prep. Biochem. Biotechnol.*, 29:371.

- CLOSE, E. J., SALM, J. R., BRACEWELL, D. G. and SORENSSEN, E. (2014). *Modelling of industrial biopharmaceutical multicomponent chromatography*. Chem. Eng. Res. Des., 92:1304.
- COFFMAN, J. L., KRAMARCZYK, J. F. and KELLEY, B. D. (2008). *High-throughput screening of chromatographic separations: I. Method development and column modeling*. Biotechnol. Bioeng., 100:605.
- COOK, J. C. (2003). *Process for purifying human papillomavirus virus-like particles*. US Patent 6,602,697.
- COOPER, M. R., STEWART, D. C., KAHL, F. R., BROWN, W. M. and CORDELL, A. R. (2002). *Medicine at the medical center then and now: one hundred years of progress*. South. Med. J., 95:1113.
- CROWELL, K. (1997). *Pharmaceutical applications of liquid-liquid extraction*. In GOLDBERG, E. (editor), *Handbook of Downstream Processing*, pages 48–69. Springer Netherlands.
- DE FOLTER, J. and SUTHERLAND, I. A. (2009). *Universal counter-current chromatography modelling based on counter-current distribution*. J. Chromatogr. A, 1216:4218.
- DIEDERICH, P., HOFFMANN, M. and HUBBUCH, J. (2015). *High-throughput process development of purification alternatives for the protein avidin*. Biotechnology Progress, 31:957.
- DiMASI, J. A., HANSEN, R. W. and GRABOWSKI, H. G. (2003). *The price of innovation: New estimates of drug development costs*. J. Health Econ., 22:151.
- DISMER, F., ALEXANDER OELMEIER, S. and HUBBUCH, J. (2013). *Molecular dynamics simulations of aqueous two-phase systems: Understanding phase formation and protein partitioning*. Chem. Eng. Sci., 96:142.
- DOCHEZ, C., BOGERS, J. J., VERHELST, R. and REES, H. (2014). *HPV vaccines to prevent cervical cancer and genital warts: an update*. Vaccine, 32:1595.
- ESPITIA-SALOMA, E., VÁZQUEZ-VILLEGAS, P., AGUILAR, O. and RITO-PALOMARES, M. (2014). *Continuous aqueous two-phase systems devices for the recovery of biological products*. Food Bioprod. Process., 92:101.
- FARLOW, M. R., ANDREASEN, N., RIVIERE, M.-E., VOSTIAR, I., VITALITI, A., SOVAGO, J., CAPUTO, A., WINBLAD, B. and GRAF, A. (2015). *Long-term treatment with active A β immunotherapy with CAD106 in mild Alzheimer's disease*. Alzheimers. Res. Ther., 7:1.
- FIERS, W., DE FILETTE, M., EL BAKKOURI, K., SCHEPENS, B., ROOSE, K., SCHOTSAERT, M., BIRKETT, A. and SAELENS, X. (2009). *M2e-based universal influenza A vaccine*. Vaccine, 27:6280.

REFERENCES

- FISCHER, I., HSU, C.-C., GÄRTNER, M., MÜLLER, C., OVERTON, T. W., THOMAS, O. R. T. and FRANZREB, M. (2013). *Continuous protein purification using functionalized magnetic nanoparticles in aqueous micellar two-phase systems*. J. Chromatogr. A, 1305:7.
- FREUNDLICH, H. (1906). *Over the adsorption in solution*. J. Phys. Chem, 57:385.
- GARCEA, R. L. and GISSMANN, L. (2004). *Virus-like particles as vaccines and vessels for the delivery of small molecules*. Curr. Opin. Biotechnol., 15:513.
- GHOSH, R. (2002). *Protein separation using membrane chromatography : opportunities and challenges*. J. Chromatogr. A, 952:13.
- GIBSON, T. J., MCCARTY, K., MCFADYEN, I. J., CASH, E., DALMONTE, P., HINDS, K. D., DINERMAN, A. A., ALVAREZ, J. C. and VOLKIN, D. B. (2011). *Application of a High-Throughput Screening Procedure with PEG-Induced Precipitation to Compare Relative Protein Solubility During Formulation Development with IgG1 Monoclonal Antibodies*. J. Pharm. Sci., 100:1009.
- GRABHERR, R. and REICHL, U. (2015). *Editorial: Can modern vaccine technology pursue the success of traditional vaccine manufacturing?* Biotechnol. J., 10(5):657.
- GROSS, J. and SADOWSKI, G. (2001). *Perturbed-Chain SAFT: An Equation of State Based on a Perturbation Theory for Chain Molecules*. Ind. Eng. Chem. Res., 40(4):1244.
- GRUDZIEN, L., LAND MADEIRA, FISHER, D., MA, J. and GARRARD, I. (2013). *Phase system selection with fractional factorial design for purification of recombinant cyanovirin-N from a hydroponic culture medium using centrifugal partition chromatography*. J. Chromatogr. A, 1285:57.
- GU, T., TSAI, G.-J. and TSAO, G. T. (1991). *A theoretical study of multicomponent radial flow chromatography*. Chem. Eng. Sci., 46:1279.
- GUO, P., EL-GOHARY, Y., PRASADAN, K., SHIOTA, C., XIAO, X., WIERSCH, J., PAREDES, J., TULACHAN, S. and GITTES, G. K. (2012). *Rapid and simplified purification of recombinant adeno-associated virus*. J. Virol. Methods, 183:139.
- HAHN, B. T. J., COURBRON, D., HAMER, M., MASOUD, M., WONG, J., TAYLOR, K., HATCH, J., SOWERS, M., SHANE, E., NATHAN, M., JIANG, H. U. A., WEI, Z., HIGGINS, J., ROH, K.-H., BURD, J., CHINCHILLA-OLSZAR, D., MALOU-WILLIAMS, M., BASKIND, D. P. and SMITH, G. E. (2013). *Rapid Manufacture and Release of a GMP Batch of Avian Influenza A(H7N9) Virus-Like Particle Vaccine Made Using Recombinant Baculovirus-Sf9 Insect Cell Culture Technology*. Bioprocess. J., 12(2):1.
- HAHN, T., HUUK, T., HEUVELINE, V. and HUBBUCH, J. (2015a). *Simulating and Optimizing Preparative Protein Chromatography with ChromX*. J. Chem. Educ.
- HAHN, T., HUUK, T., OSBERGHAUS, A., DONINGER, K., NATH, S., HEPBILDIKLER, S., HEUVELINE, V. and HUBBUCH, J. (2015b). *Calibration-free inverse modeling of ion-exchange chromatography in industrial antibody purification*. Eng. Life Sci., pages n/a–n/a.

- HAHN, T., SOMMER, A., OSBERGHAUS, A., HEUVELINE, V. and HUBBUCH, J. (2014). *Adjoint-based estimation and optimization for column liquid chromatography models*. *Comput. Chem. Eng.*, 64:41.
- HANSEN, S. K. and OELMEIER, S. A. (2012). *Meeting report: High-throughput process development - HTPD 2012*. *Biotechnol. J.*, 7:1189.
- HANSON, C. (2013). *Recent advances in liquid-liquid extraction*. Elsevier.
- HATTI-KAUL, R. (2000). *Aqueous Two-phase Systems: Methods and Protocols*. *Methods in biotechnology*. Humana Press.
- HAYENGA, K. and VALEX, P. (2002). *Methods for protein purification using aqueous two-phase extraction*. US Patent 6,437,101.
- HERWIG, C., GARCIA-APONTE, O. F., GOLABGIR, A. and RATHORE, A. S. (2015). *Knowledge management in the QbD paradigm: manufacturing of biotech therapeutics*. *Trends Biotechnol.*, 33:381.
- HOLMES, K., SHEPHERD, D. A., ASHCROFT, A. E., WHELAN, M., ROWLANDS, D. J. and STONEHOUSE, N. J. (2015). *Assembly pathway of hepatitis B core virus-like particles from genetically fused dimers*. *J. Biol. Chem.*, 290:16238.
- HOPMANN, E. and MINCEVA, M. (2012). *Separation of a binary mixture by sequential centrifugal partition chromatography*. *J. Chromatogr. A*, 1229:140.
- HUBBUCH, J. (2012). *Editorial: High-throughput process development*. *Biotechnol. J.*, 7:1185.
- HUUK, T. C., HAHN, T., OSBERGHAUS, A. and HUBBUCH, J. (2014). *Model-based integrated optimization and evaluation of a multi-step ion exchange chromatography*. *Sep. Purif. Technol.*, 136:207.
- ITO, Y. and BOWMAN, R. L. (1977). *Horizontal Flow-Through Coil Planet Centrifuge without Rotating Seals*. *Anal. Biochem.*, 83:63.
- ITO, Y., WEINSTEIN, M., AOKI, I., HARADA, R., KIMURA, E. and NUNOGAKI, K. (1966). *The Coil Planet Centrifuge*. *Nature*, 212:985.
- JOSEFSBERG, J. O. and BUCKLAND, B. (2012). *Vaccine process technology*. *Biotechnol. Bioeng.*, 109:1443.
- JUE, E., YAMANISHI, C. D., CHIU, R. Y. T., WU, B. M. and KAMEI, D. T. (2014). *Using an aqueous two-phase polymer-salt system to rapidly concentrate viruses for improving the detection limit of the lateral-flow immunoassay*. *Biotechnol. Bioeng.*, 111:2499.
- KACZMARCZYK, S. J., SITARAMAN, K., YOUNG, H. A., HUGHES, S. H. and CHATTERJEE, D. K. (2011). *Protein delivery using engineered virus-like particles*. *Proc. Natl. Acad. Sci. U. S. A.*, 108:16998.

REFERENCES

- KARPENKO, L. I., IVANISENKO, V. A., PIKA, I. A., CHIKAEV, N. A., EROSHKIN, A. M., VEREMEIKO, T. A. and ILYICHEV, A. A. (2000). *Insertion of foreign epitopes in HBcAg : how to make the chimeric*. Amino Acids, 18:329.
- KEPKA, C., EDSÖ, J. and TJERNELD, F. (2009). *Recovery of plasmids in an aqueous two-phase system*. US Patent 7,553,658.
- KESWANI, R. K., LAZEBNIK, M. and PACK, D. W. (2015). *Intracellular trafficking of hybrid gene delivery vectors*. J. Control. Release, 207:120.
- KESWANI, R. K., POZDOL, I. M. and PACK, D. W. (2013). *Design of hybrid lipid/retroviral-like particle gene delivery vectors*. Mol. Pharm., 10:1725.
- KLAMP, T., SCHUMACHER, J., HUBER, G., KÜHNE, C., MEISSNER, U., SELMI, A., HILLER, T., KREITER, S., MARKL, J., TÜRECI, O. and SAHIN, U. (2011). *Highly specific auto-antibodies against claudin-18 isoform 2 induced by a chimeric HBcAg virus-like particle vaccine kill tumor cells and inhibit the growth of lung metastases*. Cancer Res., 71:516.
- LACSON, E., TENG, M., ONG, J., VIENNEAU, L., OFSTHUN, N. and LAZARUS, J. M. (2005). *Antibody response to Engerix-B s and Recombivax-HB s hepatitis B vaccination in end-stage renal disease*. Hemodial. Int., 9:367.
- LADIWALA, A., REGE, K., BRENNEMAN, C. M. and CRAMER, S. M. (2005). *A priori prediction of adsorption isotherm parameters and chromatographic behavior in ion-exchange systems*. Proc. Natl. Acad. Sci. U. S. A., 102:11710.
- LANGMUIR, I. (1916). *The constitution and fundamental properties of solids and liquids*. Journal of the American Chemical Society, 38:2221.
- LEE, C.-K., WANG, N.-H. and JU, Y.-H. (1995). *Purification of Aspartase by Aqueous Two-Phase System and Affinity Membrane Chromatography in Sequence*. Sep. Sci. Technol., 30:509.
- LIN, S.-Y., YEH, C.-T., LI, W.-H., YU, C.-P., LIN, W.-C., YANG, J.-Y., WU, H.-L. and HU, Y.-C. (2015). *Enhanced enterovirus 71 virus-like particle yield from a new baculovirus design*. Biotechnol. Bioeng., 112:2005.
- LINK, A., ZABEL, F., SCHNETZLER, Y., TITZ, A., BROMBACHER, F. and BACHMANN, M. F. (2012). *Innate immunity mediates follicular transport of particulate but not soluble protein antigen*. J. Immunol., 188:3724.
- LOVE, J. C., LOVE, K. R. and BARONE, P. W. (2013). *Enabling global access to high-quality biopharmaceuticals*. Curr. Opin. Chem. Eng., 2:383.
- LOW, J. G. H., LEE, L. S., OOI, E. E., ETHIRAJULU, K., YEO, P., MATTER, A., CONNOLLY, J. E., SKIBINSKI, D. A. G., SAUDAN, P., BACHMANN, M., HANSON, B. J., LU, Q., MAURER-STROH, S., LIM, S. and NOVOTNY-DIERMAYR, V. (2014). *Safety and immunogenicity of a virus-like particle pandemic influenza A (H1N1) 2009 vaccine: results from a double-blinded, randomized Phase I clinical trial in healthy Asian volunteers*. Vaccine, 32:5041.

- LU, Y., CHAN, W., KO, B. Y., VANLANG, C. C. and SWARTZ, J. R. (2015). *Assessing sequence plasticity of a virus-like nanoparticle by evolution toward a versatile scaffold for vaccines and drug delivery*. Proc. Natl. Acad. Sci., pages 1–6.
- LUA, L. H. L., CONNORS, N. K., SAINSBURY, F., CHUAN, Y. P., WIBOWO, N. and MIDDELBERG, A. P. J. (2014). *Bioengineering virus-like particles as vaccines*. Biotechnol. Bioeng., 111:425.
- LUECHAU, F., LING, T. C. and LYDDIATT, A. (2010). *A descriptive model and methods for up-scaled process routes for interfacial partition of bioparticles in aqueous two-phase systems*. Biochem. Eng. J., 50:122.
- MADEIRA, P. P., BESSA, A., DE BARROS, D. P. C., TEIXEIRA, M. A., ÁLVARES RIBEIRO, L., AIRES-BARROS, M. R., RODRIGUES, A. E., CHAIT, A. and ZASLAVSKY, B. Y. (2013). *Solvatochromic relationship: Prediction of distribution of ionic solutes in aqueous two-phase systems*. J. Chromatogr. A, 1271:10.
- MARSHALL, V. and BAYLOR, N. W. (2011). *Food and Drug Administration regulation and evaluation of vaccines*. Pediatrics, 127 Suppl:23.
- MCNALLY, D. J., DARLING, D., FARZANEH, F., LEVISON, P. R. and SLATER, N. K. H. (2014). *Optimised concentration and purification of retroviruses using membrane chromatography*. J. Chromatogr. A, 1340:24.
- MEHAY, A. and GU, T. (2014). *A General Rate Model of Ion-Exchange Chromatography for Investigating Ion-Exchange Behavior and Scale-up*. J. Microb. Biochem. Technol., 06:216.
- MIDDELBERG, A. P. J., RIVERA-HERNANDEZ, T., WIBOWO, N., LUA, L. H. L., FAN, Y., MAGOR, G., CHANG, C., CHUAN, Y. P., GOOD, M. F. and BATZLOFF, M. R. (2011). *A microbial platform for rapid and low-cost virus-like particle and capsomere vaccines*. Vaccine, 29:7154.
- MOLLERUP, J. M. (2008). *A Review of the Thermodynamics of Protein Association to Ligands, Protein Adsorption, and Adsorption Isotherms*. Chem. Eng. Technol., 31:864.
- MOLLERUP, J. R. M., HANSEN, T. B., KIDAL, S. and STABY, A. (2008). *Quality by design-Thermodynamic modelling of chromatographic separation of proteins*. J. Chromatogr. A, 1177:200.
- NEEPER, M., HOFMANN, K. and JANSEN, K. (1996). *Expression of the major capsid protein of human papillomavirus type 11 in Saccharomyces cerevisiae*. Gene, 180:1.
- NESTOLA, P., PEIXOTO, C., SILVA, R. R. J. S., ALVES, P. M., MOTA, J. P. B. and CARRONDO, M. J. T. (2015). *Improved virus purification processes for vaccines and gene therapy*. Biotechnol. Bioeng., 112:843.
- NESTOLA, P., VILLAIN, L., PEIXOTO, C., MARTINS, D. L., ALVES, P. M., CARRONDO, M. J. T. and MOTA, J. P. B. (2014). *Impact of grafting on the design of new membrane adsorbers for adenovirus purification*. J. Biotechnol., 181:1.

REFERENCES

- NFOR, B. K., VERHAERT, P. D. E. M., VAN DER WIELEN, L. A. M., HUBBUCH, J. and OTTENS, M. (2009). *Rational and systematic protein purification process development: the next generation*. Trends Biotechnol., 27:673.
- NUNO, R., FERREIRA, L. A., MADEIRA, P. P., TEIXEIRA, J. A., UVERSKY, V. N. and ZASLAVSKY, B. Y. (2015). *Analysis of partitioning of organic compounds and proteins in aqueous polyethylene glycol-sodium sulfate aqueous two-phase systems in terms of solute - solvent interactions*. J. Chromatogr. A, 1415:1.
- OELMEIER, S. A., DISMER, F. and HUBBUCH, J. (2012a). *Molecular dynamics simulations on aqueous two-phase systems - Single PEG-molecules in solution*. BMC Biophys., 5:1.
- OELMEIER, S. A., LADD EFFIO, C. and HUBBUCH, J. (2012b). *High throughput screening based selection of phases for aqueous two-phase system-centrifugal partitioning chromatography of monoclonal antibodies*. J. Chromatogr. A, 1252:104.
- OPITZ, L., LEHMANN, S., ZIMMERMANN, A., REICHL, U. and WOLFF, M. W. (2007). *Impact of adsorbents selection on capture efficiency of cell culture derived human influenza viruses*. J. Biotechnol., 131:309.
- ORR, V., ZHONG, L., MOO-YOUNG, M. and CHOU, C. P. (2013). *Recent advances in bioprocessing application of membrane chromatography*. Biotechnol. Adv., 31:450.
- OSBERGHAUS, A., HEPBILDIKLER, S., NATH, S., HAINDL, M., VON LIERES, E. and HUBBUCH, J. (2012). *Determination of parameters for the steric mass action model—a comparison between two approaches*. J. Chromatogr. A, 1233:54.
- PALOMARES, L. A. and RAMÍREZ, O. T. (2009). *Challenges for the production of virus-like particles in insect cells: The case of rotavirus-like particles*. Biochem. Eng. J., 45:158.
- PRONKER, E., WEENEN, T., COMMANDEUR, H., A.D.M.E. OSTERHAUS and CLAASSEN, H. (2011). *The gold industry standard for risk and cost of drug and vaccine development revisited*. Vaccine, 29:5846.
- PUSHKO, P., PEARCE, M. B., AHMAD, A., TRETYAKOVA, I., SMITH, G., BELSER, J. A. and TUMPEY, T. M. (2011). *Influenza virus-like particle can accommodate multiple subtypes of hemagglutinin and protect from multiple influenza types and subtypes*. Vaccine, 29:5911.
- RATHORE, A. S. and WINKLE, H. (2009). *Quality by design for biopharmaceuticals*. Nat. Biotechnol., 27(1).
- RESCHKE, T., BRANDENBUSCH, C. and SADOWSKI, G. (2014). *Modeling aqueous two-phase systems: I. Polyethylene glycol and inorganic salts as ATPS former*. Fluid Phase Equilib., 368:91.
- RICHTER, M., DIETERLE, M. and RUDOLPH, F. (2014). *Protein purification by means of aqueous two-phase centrifugal extraction*. WO Patent App. PCT/EP2014/053,768.

- RITO-PALOMARES, M. and LYDDIATT, A. (2002). *Process integration using aqueous two-phase partition for the recovery of intracellular proteins*. Chem. Eng. J., 87:313.
- RIVERA-HERNANDEZ, T., HARTAS, J., WU, Y., CHUAN, Y. P., LUA, L. H. L., GOOD, M., BATZLOFF, M. R. and MIDDELBERG, A. P. J. (2013). *Self-adjuvanting modular virus-like particles for mucosal vaccination against group A streptococcus (GAS)*. Vaccine, 31:1950.
- RIVIERE, M.-E., CAPUTO, A., LAURENT, N., VOSTIAR, I., ANDREASEN, N., COHEN, S., KRESSIG, R. W., RYAN, J. M. and GRAF, A. (2014). *Active Ab Immunotherapy Cad106 Phase Ii Dose-Adjuvant Finding Study: Immune Response*. Alzheimer's Dement., 10:P447.
- ROSA, P. A. J., AZEVEDO, A. M., SOMMERFELD, S., BÄCKER, W. and AIRES-BARROS, M. R. (2013a). *Aqueous two-phase extraction as a platform in the biomanufacturing industry: economical and environmental sustainability*. Biotechnol. Adv., 29:559.
- ROSA, P. A. J., AZEVEDO, A. M., SOMMERFELD, S., MUTTER, M., BÄCKER, W. and AIRES-BARROS, M. R. (2013b). *Continuous purification of antibodies from cell culture supernatant with aqueous two-phase systems: from concept to process*. Biotechnol. J., 8:352.
- SCHALLER, A., CONNORS, N. K., OELMEIER, S. A., HUBBUCH, J. and MIDDELBERG, A. P. (2014). *Predicting recombinant protein expression Experiments using molecular Dynamics simulation*. Chem. Eng. Sci., pages 1–11.
- SCHWIENHEER, C., MERZ, J. and SCHEMBECKER, G. (2014). *Selection and Use of Poly Ethylene Glycol and Phosphate Based Aqueous Two-Phase Systems for the Separation of Proteins by Centrifugal Partition Chromatography*. J. Liq. Chromatogr. Relat. Technol., 38:929.
- SELVAKUMAR, P., LING, T. C., WALKER, S. and LYDDIATT, A. (2010). *A practical implementation and exploitation of ATPS for intensive processing of biological feedstock: A novel approach for heavily biological feedstock loaded ATPS*. Sep. Purif. Technol., 75:323.
- SHARMA, S., WHALLEY, A., MCCLAUGHLI, J., BRELLO, F., BISHOP, B. and BANERJEE, A. (2011). *Fermentation process technology transfer for production of a recombinant vaccine component*. BioPharm International, 24:30.
- SMITH, M. T., HAWES, A. K. and BUNDY, B. C. (2013). *Reengineering viruses and virus-like particles through chemical functionalization strategies*. Curr. Opin. Biotechnol., 24:620.
- SPOHN, G., SCHORI, C., KELLER, I., SLADKO, K., SINA, C., GULER, R., SCHWARZ, K., JOHANSEN, P. L., JENNINGS, G. T. and BACHMANN, M. F. (2014). *Preclinical efficacy and safety of an anti-IL-1 β vaccine for the treatment of type 2 diabetes*. Mol. Ther. - Methods Clin. Dev., 1:1.

REFERENCES

- SUEN, S. Y., LIU, Y. C. and CHANG, C. S. (2003). *Exploiting immobilized metal affinity membranes for the isolation or purification of therapeutically relevant species*. J. Chromatogr. B Anal. Technol. Biomed. Life Sci., 797:305.
- SUMNER, N. (2011). *Developing counter current chromatography to meet the needs of pharmaceutical discovery*. J. Chromatogr. A, 1218:6107.
- SUN, Y., CARRION, R., YE, L., WEN, Z., RO, Y.-T., BRASKY, K., TICER, A. E., SCHWEGLER, E. E., PATTERSON, J. L., COMPANS, R. W. and YANG, C. (2009). *Protection against lethal challenge by Ebola virus-like particles produced in insect cells*. Virology, 383:12.
- SUTHERLAND, I., HEWITSON, P., SIEBERS, R., VAN DEN HEUVEL, R., ARBENZ, L., KINKEL, J. and FISHER, D. (2011). *Scale-up of protein purifications using aqueous two-phase systems: comparing multilayer toroidal coil chromatography with centrifugal partition chromatography*. J. Chromatogr. A, 1218:5527.
- SUTHERLAND, I. A. (2007). *Recent progress on the industrial scale-up of counter-current chromatography*. J. Chromatogr. A, 1151:6.
- SUTHERLAND, I. A., AUDO, G., BOURTON, E., COUILLARD, F., FISHER, D., GARRARD, I., HEWITSON, P. and INTES, O. (2008). *Rapid linear scale-up of a protein separation by centrifugal partition chromatography*. J. Chromatogr. A, 1190:57.
- TARGOVNIK, A., CASCONI, O. and MIRANDA, M. (2012). *Extractive purification of recombinant peroxidase isozyme c from insect larvae in aqueous two-phase systems*. Sep. Purif. Technol., 98:199.
- TEGERSTEDT, K., FRANZÉN, A., RAMQVIST, T. and DALIANIS, T. (2007). *Dendritic cells loaded with polyomavirus VP1/VP2Her2 virus-like particles efficiently prevent out-growth of a Her2 / neu expressing tumor*. Cancer Immunol Immunother, 56:1335.
- TEGERSTEDT, K., FRANZÉN, A. V., ANDREASSON, K., JONEBERG, J., HEIDARI, S., RAMQVIST, T. and DALIANIS, T. (2005). *Murine polyomavirus virus-like particles (VLPs) as vectors for gene and immune therapy and vaccines against viral infections and cancer*. Anticancer Res., 25:2601.
- TRAN, R., TITCHENER-HOOKER, N. and LACKI, K. (2011). *Aqueous two phase extraction augmented precipitation process for purification of therapeutic proteins*. US Patent App. 13/131,034.
- TREIER, K., HANSEN, S., RICHTER, C., DIEDERICH, P., HUBBUCH, J. and LESTER, P. (2012). *High-throughput methods for miniaturization and automation of monoclonal antibody purification processes*. Biotechnology Progress, 28:723.
- TSUKAMOTO, M., TAIRA, S., YAMAMURA, S., MORITA, Y., NAGATANI, N., TAKAMURA, Y. and TAMIYA, E. (2009). *Cell separation by an aqueous two-phase system in a microfluidic device*. Analyst, 134:1994.

- UMEH, R., OGUCHE, S., OGUONU, T., PITMANG, S., SHU, E., ONYIA, J.-T., DANIAM, C. A., SHWE, D., AHMAD, A., JONGERT, E., CATTEAU, G., LIEVENS, M., OFORI-ANYINAM, O. and LEACH, A. (2014). *Immunogenicity and safety of the candidate RTS,S/AS01 vaccine in young Nigerian children: A randomized, double-blind, lot-to-lot consistency trial*. *Vaccine*, 32:6556.
- VALENZULA, P., MEDINA, A., RUTTER, W. J., AMMERER, G. and HALL, B. D. (1982). *Synthesis and assembly of hepatitis B virus surface antigen particles in yeast*. *Nature*, 298(22):347.
- VAN, A., SHANAGAR, J., HJORTH, R., HALL, M. and ESTMER, N. (2011). *Separation method using single polymer phase systems*. EP Patent App. EP20,100,729,364.
- VAN BEIJEREN, P., KREIS, P. and ZEINER, T. (2013). *Development of a generic process model for membrane adsorption*. *Comput. Chem. Eng.*, 53:86.
- VARGAS, M., SEGURA, A., WU, Y.-W., HERRERA, M., CHOU, M.-L., VILLALTA, M., LEON, G. and BURNOUF, T. (2015). *Human plasma-derived immunoglobulin G fractionated by an aqueous two-phase system, caprylic acid precipitation, and membrane chromatography has a high purity level and is free of detectable in vitro thrombogenic activity*. *Vox Sanguinis*, 108:169.
- VEKEMANS, J., LEACH, A. and COHEN, J. (2009). *Development of the RTS,S/AS malaria candidate vaccine*. *Vaccine*, 27S:67.
- VICENTE, T., ROLDÃO, A., PEIXOTO, C., CARRONDO, M. J. T. and ALVES, P. M. (2011). *Large-scale production and purification of VLP-based vaccines*. *J. Invertebr. Pathol.*, 107:42.
- VICENTE, T., SOUSA, M. F., PEIXOTO, C., MOTA, J. P., ALVES, P. M. and CARRONDO, M. J. (2008). *Anion-exchange membrane chromatography for purification of rotavirus-like particles*. *J. Memb. Sci.*, 311:270.
- VIJAYARAGAVAN, K. S., ZAHID, A., YOUNG, J. W. and HELDT, C. L. (2014). *Separation of porcine parvovirus from bovine serum albumin using PEG-salt aqueous two-phase system*. *J. Chromatogr. B. Analyt. Technol. Biomed. Life Sci.*, 967:118.
- VOESTE, T., WEBER, K., HISKEY, B. and BRUNNER, G. (2012). *Liquid-Liquid Extraction*. *Ullmann's Encycl. Ind. Chem. Vo. 21*, 21:250.
- WELLNITZ, S., JOHN, C. and SCHAUB, C. (2014). *Recombinant particle based vaccines against human cytomegalovirus infection*. WO Patent App. PCT/EP2013/072,717.
- WERNER, R. G. (2004). *Economic aspects of commercial manufacture of biopharmaceuticals*. *J. Biotechnol.*, 113:171.
- WHITACRE, D. C., LEE, B. O. and MILICH, D. R. (2010). *Use of hepadnavirus core proteins as vaccine platforms*. *Expert Rev Vaccines*, 8(11):1565.

REFERENCES

- WIENDAHL, M., SCHULZE WIERLING, P., NIELSEN, J., FOMSGAARD CHRISTENSEN, D., KRARUP, J., STABY, A. and HUBBUCH, J. (2008). *High Throughput Screening for the Design and Optimization of Chromatographic Processes - Miniaturization, Automation and Parallelization of Breakthrough and Elution Studies*. Chem. Eng. Technol., 31:893.
- WIENDAHL, M., SELBACH, B. and HUBBUCH, J. (2007). *High throughput screening techniques in downstream processing: Preparation, characterization and optimization of aqueous two-phase systems*. Chem. Eng. Sci., 62:2011.
- WIENDAHL, M., VÖLKER, C., HUSEMANN, I., KRARUP, J., STABY, A., SCHOLL, S. and HUBBUCH, J. (2009). *A novel method to evaluate protein solubility using a high throughput screening approach*. Chem. Eng. Sci., 64:3778.
- WILLOUGHBY, N. (2009). *Too big to bind? Will the purification of large and complex therapeutic targets spell the beginning of the end for column chromatography?* J. Chem. Technol. Biotechnol., 84:145.
- WOLFF, M. W. and REICHL, U. (2008). *Downstream Processing: From Egg to Cell Culture-Derived Influenza Virus Particles*. Chem. Eng. Technol., 31:846.
- WOLFF, M. W., SIEWERT, C., HANSEN, S. P., FABER, R. and REICHL, U. (2010). *Purification of cell culture-derived modified vaccinia ankara virus by pseudo-affinity membrane adsorbers and hydrophobic interaction chromatography*. Biotechnol. Bioeng., 107:312.
- YU, L. X. (2008). *Pharmaceutical Quality by Design: Product and Process Development, Understanding, and Control*. Pharm. Res., 25:781.
- ZHANG, L. and SUN, Y. (2010). *Molecular simulation of adsorption and its implications to protein chromatography: A review*. Biochem. Eng. J., 48:408.
- ZHAO, Q., GUO, H. H., WANG, Y., WASHABAUGH, M. W. and SITRIN, R. D. (2005). *Visualization of discrete L1 oligomers in human papillomavirus 16 virus-like particles by gel electrophoresis with Coomassie staining*. J. Virol. Methods, 127:133.
- ZHAO, Q., MODIS, Y., HIGH, K., TOWNE, V., MENG, Y., WANG, Y., ALEXANDROFF, J., BROWN, M., CARRAGHER, B., POTTER, C. S., ABRAHAM, D., WOHLPART, D., KOSINSKI, M., WASHABAUGH, M. W. and SITRIN, R. D. (2012). *Disassembly and reassembly of human papillomavirus virus-like particles produces more virion-like antibody reactivity*. Virol. J., 9:1.

Christopher Ladd Effio

KIT Campus South, Institute of Process Engineering in Life Sciences, Section IV: Biomolecular Separation Engineering, Engler-Bunte-Ring 3, 76131 Karlsruhe, Christopher.Ladd@kit.edu, +49 721 608-47529

Curriculum vitae

PERSON

Name	Christopher Ladd Effio
Date/place of birth	03/23/1987 in Lima, Peru
Nationality	German
Marital status	Married



EDUCATION

08/2012 - 10/2015	PhD student at the chair of Biomolecular Separation Engineering, Karlsruhe Institute of Technology (KIT) Research project: 'Process development for virus-like particles'
10/2006 - 03/2012	Studies of Chemical Engineering (Dipl.-Ing.), Karlsruhe Institute of Technology (KIT)
09/2011 - 03/2012	Diploma thesis at Karlsruhe Institute of Technology (KIT) Project title: 'Evaluation of alternative separation steps for processing of monoclonal antibodies'
11/2009 - 04/2010	Student research project at Karlsruhe Institute of Technology (KIT) Project title: 'Optimization of culture media and dynamic cross-flow filtration for microalgae'
09/1997 - 03/2006	Gutenberg secondary school, Mainz, Final degree: Abitur

WORK EXPERIENCE

Since 05/2012	Research Associate/ PhD student at Karlsruhe Institute of Technology (KIT)
10/ 2010 - 03/ 2011	Merck KGaA, Darmstadt Internship in Advanced Technologies - Process Development Project title: 'Mobile Energy - Development of a purification process for lithium-ion battery electrolytes'
08/2010 - 09/2010	CEAMSA, Vigo, Spanien Internship in R&D Project title: 'Process development for carrageenans and pectins'
05/2010 - 07/2010	Scientific Member at Karlsruhe Institute of Technology (KIT) Project title: 'Protein analytics for magnetic bioseparation project'
08/2006 - 09/2006	Schott AG, Mainz Temporary job in product divisions for glass ceramics
07/2005	Boehringer Ingelheim Pharma GmbH & Co. KG, Ingelheim Temporary job in filling & packing department (GMP zone)

AWARDS

07/2014	Young Scientist Award (Crafty Chromatographer) 8th International Conference on Countercurrent Chromatography (CCC), London, UK
---------	--

Christopher Ladd Effio

KIT Campus South, Institute of Process Engineering in Life Sciences, Section IV: Biomolecular Separation Engineering, Engler-Bunte-Ring 3, 76131 Karlsruhe, Christopher.Ladd@kit.edu, +49 721 608-47529

PUBLICATIONS – PEER REVIEWED ARTICLES

- Vaccine 2016 C. Ladd Effio, S. Oelmeier, J. Hubbuch
High-throughput characterization of virus-like particles by interlaced size-exclusion chromatography
Vaccine, 2016, 10.1016/j.vaccine.2016.01.035
- Journal of Chromatography A 2016 C. Ladd Effio, T. Hahn, J. Seiler, S. Oelmeier, I. Asen, C. Silberer, L. Villain, J. Hubbuch
Modeling and simulation of anion-exchange membrane chromatography for purification of Sf9 insect cell-derived virus-like particles
J. Chromatogr. A, 1429 (2016), 142-154
- Journal of Biotechnology 2016 C. Ladd Effio, P. Baumann, C. Weigel, P. Vormittag, A. Middelberg, J. Hubbuch
High-throughput process development of an alternative platform for the production of virus-like particles in Escherichia coli
J. Biotechnol., 219 (2016), 7-19
- Biotechnology Journal 2015 C. Ladd Effio and J. Hubbuch
Next generation vaccines and vectors: Designing downstream processes for recombinant protein-based virus-like particles
Biotechnol. J., 10 (2015), 715–727
- Journal of Chromatography A 2015 C. Ladd Effio, L. Wenger, O. Ötes, S. Oelmeier, R. Kneusel, J. Hubbuch
Downstream processing of virus-like particles: Single-stage and multi-stage aqueous two-phase extraction
J. Chromatogr. A, 1383 (2015), 35–46
- Human Vaccines & Immunotherapeutics 2014 C. Ladd Effio and J. Hubbuch
Meeting Report VLPNPV: Session 10: Virus-like particle and nano-particle vaccines
Hum. Vaccin. Immunother., 10 (2014), 3080–3082
- Journal of Chromatography A 2013 S. Oelmeier, C. Ladd Effio, J. Hubbuch
Alternative separation steps for monoclonal antibody purification: Combination of centrifugal partitioning chromatography and precipitation
J. Chromatogr. A, 1319 (2013), 118–126
- Journal of Chromatography A 2012 S. Oelmeier, C. Ladd Effio, J. Hubbuch
High throughput screening based selection of phases for aqueous two-phase system-centrifugal partitioning chromatography of monoclonal antibodies
J. Chromatogr. A, 1252 (2012), 104–114

Christopher Ladd Effio

KIT Campus South, Institute of Process Engineering in Life Sciences, Section IV: Biomolecular Separation Engineering, Engler-Bunte-Ring 3, 76131 Karlsruhe, Christopher.Ladd@kit.edu, +49 721 608-47529

PUBLICATIONS – CONFERENCE CONTRIBUTIONS

Talks

- | | |
|---|---|
| International Symposium on Preparative and Process Chromatography (PREP), Philadelphia, 07/2015 | P. Baumann, C. Ladd Effio, C. Weigel, P. Vormittag, A. Middelberg, J. Hubbuch
Establishment of a high-throughput platform for the production of virus-like particles in E. coli |
| Biopartitioning & Purification Conference (BPP), Vienna, 06/2015 | C. Ladd Effio, S. Oelmeier, J. Hubbuch
Centrifugal partition chromatography - multistage aqueous two-phase extraction of biopharmaceutical products |
| The Future of Biologics, Singapore, 03/2015 | C. Ladd Effio, S. Oelmeier, J. Hubbuch
Novel development strategies for the downstream processing of virus-like particles |
| International Solvent Extraction Conference (ISEC), Würzburg, 09/2014 | C. Ladd Effio, S. Oelmeier, J. Hubbuch
Centrifugal partition chromatography - multistage aqueous two-phase extraction of biopharmaceutical products |
| Countercurrent Chromatography (CCC), London, 07/2014 | C. Ladd Effio, S. Oelmeier, J. Hubbuch
Evaluation of centrifugal partition chromatography for the purification of virus-like particles |
| VLP & Nano-Particle Vaccines Conference, San Diego, 06/2014 | C. Ladd Effio, L. Wenger, O. Ötes, S. Oelmeier, J. Hubbuch
Development of alternative purification steps for virus-like particles using high-throughput experimentation |
| European Network on Viral Vaccine Processes (ENVVP), Frankfurt a. M., 11/2013 | C. Ladd Effio, L. Wenger, S. Oelmeier, J. Hubbuch
High-throughput process development for the purification of virus-like particles |

Posters

- | | |
|---|---|
| International Symposium on Preparative and Process Chromatography (PREP), Philadelphia, 07/2015 | P. Baumann, C. Ladd Effio, C. Weigel, P. Vormittag, A. Middelberg, J. Hubbuch
Establishment of a high-throughput platform for the production of virus-like particles in E. coli |
| Biopartitioning & Purification Conference (BPP), Vienna, 06/2015 | C. Ladd Effio, S. Oelmeier, J. Hubbuch
Towards a generic capture process for virus-like particles: Aqueous two-phase extraction and precipitation |
| Recovery of Biological Products XVI, Rostock, 07/2014 | C. Ladd Effio, J. Seiler, T. Hahn, S. Oelmeier, R. Kneusel, L. Villain, J. Hubbuch
Evaluation of alternative unit operations for the purification of virus-like particles |